# Shaking Table Testing of Geotechnical Response of Densified Fine-Grained Soils to Cyclic Loadings: Application to Highly Densified Tailings

**Fahad Abdulaziz Alshawmar**

A thesis submitted in partial fulfilment of the requirements for the
Doctorate in Philosophy degree in Civil Engineering

under the supervision of

**Prof. Mamadou Fall**

Department of Civil Engineering
Faculty of Engineering
University of Ottawa

## Abstract

Liquefaction is a major challenge in geotechnical engineering in which soil strength and stiffness are compromised due to earthquake activity. Understanding and predicting the behaviour and liquefaction susceptibility of soils under cyclic loading is a critical issue in civil engineering, mining and protective engineering. Numerous earthquake-induced ground failure events (e.g., substantial ground deformation, reduced bearing capacity) or liquefaction in natural fine-grained soils or manmade fine-grained soils (i.e., fine tailings) produced by mining activities have been observed and reported in the literature. Tailings are manmade soils that remain following the extraction of metals and minerals from mined ore in a mine processing plant. Traditionally, such tailings are stored in surface tailings impoundments at the mine's surface. However, geotechnical and environmental risks and consequences related to conventional tailings impoundments have attracted the attention of the engineering community to develop novel methods of tailings disposal and management to minimize geotechnical and environmental risks. Thus, engineers have introduced and implemented innovative tailings technologies—thickened tailings and paste tailings—as cost-effective means for tailings management in mining operations. As both thickened tailings and paste tailings have lower water content and higher solid content than tailings in conventional impoundments, these tailings may be more resistant to liquefaction. However, it should be noted that the seismic or cyclic behaviour of these thickened and paste tailings, with and without heavy rainfall effects, are not fully understood. There is little technical information or data about the behaviour and liquefaction of thickened and paste tailings under seismic or cyclic loading conditions.

The objective of the present PhD research is to investigate the response of layered thickened and paste tailings deposits, with and without heavy rainfall effects, to cyclic loads by conducting shaking table tests. To simulate the field deposition of thickened and paste tailings, tailings were deposited in three thin layers in a flexible laminar shear box (FLSB) attached to the shaking table equipment. A sinusoidal seismic loading at a frequency of 1 Hz and peak horizontal acceleration of 0.13g was applied at the bottom of the layered tailings deposits. Acceleration, displacement and pore water pressure responses to the cyclic loading were monitored at the middle depth of each layer of the tailings deposits. Regarding the acceleration response of these thickened and paste tailings deposits (without the effect of heavy rainfall), there was no difference between the middle of the bottom and middle layers or at the base of the shaking table. However, the acceleration at the middle of the top layer differed from the acceleration at the base of the shaking table. Throughout shaking, the layered tailings deposits (with and without the effect of heavy rainfall) exhibited contraction and dilation responses. The excess pore water pressure ratios of the layered thickened tailings deposit that was not exposed to heavy rainfall prior to shaking were found to exceed 1.0 during shaking. However, for the layered paste tailings deposit that was not exposed to the effect of heavy rainfall prior to shaking, the excess pore water pressure ratios were found to be lower than 0.85 during shaking. This reveals that without the effect of heavy rainfall, the layered thickened tailings deposit was susceptible to liquefaction, whereas the layered paste tailings deposit was resistant to liquefaction during shaking. The excess pore water ratios of the layered thickened and the paste tailings deposits that were exposed to heavy rainfall prior to shaking were found to be lower than 0.8 during shaking. This reveals that with the effect of heavy rainfall, the layered thickened and paste tailings deposits were resistant to liquefaction during shaking. The results and findings of this PhD research thus provide valuable information for the implementation of tailings in earthquake-prone areas.

## Acknowledgments

First and foremost, all thanks are due to Allah (God, the Merciful Creator and Cherisher) for granting me the health, strength, patience and determination to undertake this PhD thesis.

I would like to express my deepest gratitude and sincere thanks to my supervisor, Professor Mamadou Fall, for providing enduring guidance, encouragement and academic support to help me overcome difficulties and challenges at all stages of this PhD thesis. These words are but a small gesture of my gratitude to him.

I would also like to extend my gratitude and thanks to the members of my PhD thesis committee, Professor Shahid Azam (University of Regina), Professor Mohammad Rayhani (Carleton University), Professor Ahmad Jrade (University of Ottawa) and Professor Son Nguyen (University of Ottawa), for their invaluable suggestions and comments on my thesis.

I would also like to thank Dr. Muslim Majeed, Dr. Gamal Elnabelsya and Mr. Jean Claude Célestin, technical officers at the Department of Civil Engineering, University of Ottawa, for their technical assistance and support during the course of laboratory work. As well, I am thankful to Mr. Leo Denner, technical officer at the Department of Mechanical Engineering, University of Ottawa, for his assistance during the course of laboratory work. I am indebted to my colleagues, Mr. Shuai Guo and Mr. Sadah Haruna, at the University of Ottawa for their appreciated assistance in the laboratory work.

I would also like to express my thanks to the Ministry of Higher Education in Saudi Arabia, represented by Qassim University, for the scholarship and financial support for my studies.

Most of all, I would like to express my profound gratitude from the deepest part of my heart to the members of my beloved family. I owe much to my wonderful parents, Abdulaziz and Nourah. This achievement would not have been possible without their encouragement, prayers and continuous support. I would also like to express my sincere gratitude to my beloved wife, Khawlah, for her enduring moral support and patience throughout the journey of my studies. I would also like to extend my gratitude to my wonderful children, Lateen, Abdulaziz and Aous, who bring joy and happiness to their parents' lives. Special thanks also go to my brothers and sisters, Mona, Dr. Ahmad, Abdullah, Hailah, Oroob and Mohammad, for their support and encouragement during my studies.

**Dedication**

***This thesis is dedicated to***

***My role models, My parents, Abdulaziz and Nourah***

# Table of Contents

## List of Figures

## List of Tables

## List of Symbols and Abbreviations

| | |
|---|---|
| TTs | Thickened tailings |
| PTs | Paste tailings |
| g | Gravity due to acceleration |
| GDP | Gross domestic product |
| WISE | World information service on energy |
| FLSB | Flexible laminar shear box |
| L | Length of flexible laminar shear box |
| W | Width of flexible laminar shear box |
| H | Height of flexible laminar shear box |
| $G_s$ | Specific gravity |
| PI | Plasticity index |
| $D_{10}$ | Effective diameter or size (grain diameter corresponding to 10% finer in the grain size distribution) |
| $D_{30}$ | Grain diameter corresponding to 30% finer in the grain size distribution |
| $D_{50}$ | Grain diameter corresponding to 50% finer in the grain size distribution |
| $D_{60}$ | Grain diameter corresponding to 60% finer in the grain size distribution |
| $C_u$ | Coefficient of uniformity |
| $C_c$ | Coefficient of curvature |
| USCS | Unified soil classification system |
| SM | Silty sands |
| ML | Sandy silts of low plasticity |
| CL | Sandy clays of low plasticity |
| CPB | Cemented paste backfill |

| | |
|---|---|
| $\boldsymbol{K_o}$ | Coefficient of lateral earth pressure at rest |
| OCR | Overconsolidation ratio |
| $\boldsymbol{\tau_h}$ | Horizontal cyclic shear stress |
| $\boldsymbol{\sigma'_o}$ | Initial effective overburden pressure |
| $\boldsymbol{\sigma_{dc}}$ | Cyclic deviator stress |
| $\boldsymbol{\sigma'_{1C}}$ | Effective major confining stress |
| $\boldsymbol{\sigma'_{3C}}$; $\boldsymbol{\sigma'_3}$ | Effective minor confining stress |
| $\boldsymbol{\sigma_d}$ | Deviator stress |
| NGI | Norwegian geotechnical institute |
| $\boldsymbol{\tau_h/\sigma'_o}$; $\boldsymbol{\pm\sigma_{dc}/2\sigma'_o}$; $\boldsymbol{\pm\sigma_d/2\sigma'_{1C}}$; $\boldsymbol{\tau/\sigma'_o}$; $\boldsymbol{\sigma_d/2\sigma'_3}$; CSR | Cyclic stress ratio |
| $N_c$; N | Number of cycles |
| $D_r$ | Relative density |
| $N_L$ | Number of cycles to liquefaction |
| $\boldsymbol{u}$ | Pore water pressure |
| SPT | Standard penetration test |
| CPT | Cone penetration test |
| $V_s$ | Shear wave velocity |
| BPT | Becker penetration test |
| MSF | Magnitude scaling factor |
| CRR | Cyclic resistance ratio |
| $\boldsymbol{a_{max}}$ | Peak horizontal acceleration at the ground surface |
| $\boldsymbol{g}$ | Gravity acceleration; Acceleration |
| $\boldsymbol{\sigma_{vo}}$ | Total vertical overburden stress |
| $\boldsymbol{\sigma'_{vo}}$ | Effective vertical overburden stress; Initial effective vertical stress; Initial vertical effective stress |

| | |
|---|---|
| $r_d$ | Stress reduction coefficient |
| $z$ | Depth below the ground surface |
| $(N_1)_{60}$ | Corrected standard penetration blow count |
| $N_m$ | Measured standard penetration resistance |
| $C_N$ | Standard penetration test blow count correction factor for the effective overburden stress |
| $C_E$ | Standard penetration test blow count correction factor for the hammer energy ratio |
| $C_B$ | Standard penetration test blow count correction factor for the borehole diameter |
| $C_R$ | Standard penetration test blow count correction factor for the rod length |
| $C_S$ | Standard penetration test blow count correction factor for the samplers with or without liners |
| $q_{c1N}$ | Corrected cone penetration test tip resistance |
| $C_Q$ | Normalizing factor for cone penetration resistance |
| $P_a$ | Atmospheric pressure |
| $q_c$ | Field cone penetration resistance measured at the tip |
| $V_{s1}$ | Overburden stress-corrected shear wave velocity |
| FS | Factor of safety |
| $w_c$ | Water content |
| LL | Liquid limit |
| U.S. | United States |
| CL-ML | Silty clay |
| CH | Clays of high plasticity |

| | |
|---|---|
| MH | Silt of high plasticity, elastic silts |
| FC | Fine content |
| SA | Single amplitude |
| $\boldsymbol{r_u}$ | Excess pore water pressure ratio |
| DA | Double amplitude |
| $\boldsymbol{\gamma}$ | Shear strain |
| $OCR_D$ | Overconsolidation ratio due to desiccation |
| $OCR_M$ | Mechanical overconsolidation ratio |
| NTs | Natural tailings |
| STs | Silica tailings |
| $SiO_2$ | Silicon dioxide |
| ASTM | American standard testing material |
| wt | Weight |
| pH | A measure of the acidity or alkalinity of the tailings |
| SP | Poorly graded sand |
| A1, A2, A3 and A4 | Accelerometers to measure the accelerations |
| P1, P2 and P3 | Pore pressure transducers to measure the pore water pressures |
| HD1, HD2 and HD3 | Cable displacement transducers to measure the horizontal displacements |
| VD1, VD2 and VD3 | Cable displacement transducers to measure the vertical displacements |
| 5TE1, 5TE2 and 5TE3 | Sensors to measure the volumetric water contents |
| N | Geometric scaling factor |
| EI | Flexural rigidity |

| | |
|---|---|
| $\Delta \boldsymbol{u}$ | Excess pore water pressure |
| VWC | Volumetric water content |
| ICOLD | International commission on large dams |
| XRD | X-Ray diffraction analysis |
| 1-D | One dimension of horizontal movement |

# 1 Chapter 1: General Introduction

## 1.1. Introduction

The demand for the products of the extractive mining industries continually increases worldwide. The mining industries offer many materials that people depend on to construct infrastructure and everyday-use instruments, to gain large quantities of energy and to provide fertilisers for the agriculture sector (Carvalho, 2017). In addition, the mining industry contributes significantly to the economies of several countries around the world. For instance, the mining industry contributed 3.4% to the gross domestic product (GDP) of Canada in 2015 and employs over 373,000 workers across the country (Marshall, 2016). However, one of the shortcomings of the mining industry/operations is that it produces enormous volumes of tailings every year. In Canada, the mining industry produced 217 million tonnes of mine tailings in 2008 (Statistics Canada, 2012). Tailings are wastes that mostly consist of silt-sized particles and have properties comparable to those of natural silt or silty sand, with low plasticity (Bussière, 2007; Ali et al. 2021; Fang et al. 2021).

Tailings are conventionally deposited hydraulically in the form of slurry in a disposal area, which is retained by a structure known as the tailings dam. Tailings dams are among the largest earth structures built by geotechnical engineers (Azam and Li, 2010; Aldhafeeri and Fall, 2021), and there are more than 3,500 tailings dams around the world (Davies, 2002). In general, liquefaction can be defined as a phenomenon in which saturated natural soils and tailings (man-made soils) undergo excessive deformation as a result of the development of excess pore water pressure ($r_u$) when they are subjected to static or dynamic loading under undrained conditions (James et al., 2011). The deposited conventional slurry tailings, which have high water content ($w_c$), can be susceptible to liquefaction as they are cohesionless and saturated and as their volume contracts (James et al., 2011; Alainachi and Fall, 2020).

During the last century, numerous failures of the conventional slurry tailings dams due to earthquake-induced liquefaction have been reported in many places around the world. The liquefaction failure of the Barahona copper tailings dam during the earthquake in Chile in October 1928 was considered the first case of tailings dam failure that had been recorded (Ishihara et al., 1980). This failure caused the flow of 4 million tonnes of liquefied tailings, killing 54 people (Dobry and Alvarez, 1967; Ishihara et al., 1980). The earthquake that hit the town of El Cobre in Chile in March 1965 caused the liquefaction failure of the two copper tailings dams in the town. This resulted in the release of 2.25 million $m^3$ of liquefied tailings, killing more than 200 people (Dobry and Alvarez, 1967; Highter and Vallee, 1980; Ishihara et al., 1980; WISE, 2017). The Mochikoshi tailings dam in Japan failed due to liquefaction during the January 1978 Izu-Ohshima earthquake, releasing 80,000 $m^3$ liquefied tailings and killing one person (Ishihara et al., 1980; WISE, 2017). The recent disastrous failure of the Las Palmas tailings dams in Chile during the February 2010 Maule earthquake is considered one of the latest examples of earthquake-induced liquefaction failure in Chile. It resulted in the flow of over 100,000 $m^3$ liquefied tailings up to an approximately 0.5 km distance, contaminating the region and killing four people (Verdugo et al., 2012; Verdugo and González, 2015). Most recently, the Fundaõ tailings dam failed due to liquefaction following the earthquake that occurred in Brazil in November 2015. It resulted in the release of more than 50 million $m^3$ liquefied tailings, killing 19 people, displacing many other people, contaminating the rivers in the area, and leaving hundreds of thousands of people without access to clean water and food (Miranda and Marques, 2016; Gomes et al., 2017; WISE, 2017).

To prevent or minimise the potential disastrous risks associated with the aforementioned liquefaction failures of tailings dams due to earthquakes, mining or geotechnical engineers have been looking for alternatives to the conventional dams used for slurry tailings. These alternatives involve dewatering the mine tailings through the use of densification technologies prior to deposition on the earth surface. The densification technologies involve thickened tailings, paste tailings and dry-stack tailings. The surface disposal of thickened and paste tailings is currently increasingly being implemented in mining operations worldwide. Examples of facilities that have implemented the surface disposal of thickened tailings are the Kidd Creek and Musselwhite mines in Canada, the Cerro Negro Norte and Esperanza (Centinela) mines in Chile and the Sunrise Dam mine in Australia (Robinsky et al., 1991; Kam et al., 2011; Barrera et al., 2015; Seddon and Albee, 2015). Compared to the facilities that deposit thickened tailings on the earth surface, there are very limited facilities (maybe only two or three) that deposit paste tailings (Fourie, 2012). An example of a mine that implemented the surface paste tailings technology is the Bulyanhulu mine in Kahama, Tanzania (Theriault et al., 2003; Fall et al., 2009).

Thickened and paste tailings are generated from the significant dewatering of the slurry tailings produced in the mine processing plant. These two types of densification technology do not involve grain segregation and display a yield stress; as such, a gentle slope will be formed (Daliri et al., 2016). The range of solid content for thickened tailings is generally 50−70%, and that for paste tailings is generally 70−85% (Bussière, 2007). In addition, the use of the thickened and paste tailings technologies offers benefits in terms of avoiding or reducing the dependency on the conventional tailings dams, which are associated with catastrophic geotechnical and environmental failures, and allowing water recovery prior to deposition, which offers a significant benefit to the economic sector particularly in regions with dry climates, in which the water cost is considerably high (Simms, 2017).

## 1.2. **Problem statement**

The behaviour and the liquefaction susceptibility of man-made fine-grained soils (i.e. fine tailings) under seismic or cyclic loading is a crucial theme in geotechnical and mining engineering. The considerable number of earthquake-induced ground failure or liquefaction cases involving man-made fine-grained soils (i.e. fine-grained tailings) has led the researchers to conduct several laboratory experiments on tailings materials mostly by using small-scale equipment such as cyclic simple shear or cyclic triaxial equipment (Ishihara et al., 1981; Poulos et al., 1985; Crowder, 2004; Wijewickreme et al., 2005; Al-Tarhouni, 2008; Verdugo and Santos, 2009; Kim et al., 2011; James et al., 2011; Geremew and Yanful, 2012; Dilari, 2013; Seidalinova, 2014; Suazo et al., 2016; Hu et al., 2017). Furthermore, a large-scale equipment known as a shaking table has recently been used specifically to study the cyclic behaviour of the 'conventional' tailings (i.e. hard-rock tailings) (Pepin et al., 2012a, 2012b). However, no investigation has been conducted to date for evaluating the seismic- or cyclic-loading-induced liquefaction susceptibility of the highly densified fine-grained tailings (i.e. thickened and paste tailings) using the shaking table. As mining or geotechnical engineers are concerned about the liquefaction susceptibility of such materials in regions that are prone to earthquakes, it is very important to address this research gap by performing a shaking-table testing program.

## 1.3. **Research Objectives**

The main objective of this study was to simulate the in-situ scenario in terms of the deposition of layered highly densified fine-grained tailings, thickened and paste tailings, as well as the shaking conditions. This would significantly expand the understanding of the cyclic behaviour and liquefaction susceptibility of the layered highly densified fine-grained tailings and would permit mining or geotechnical engineers/regulators to have insight into such technologies before they implement these in regions with frequent seismic activities. Below are the sub-objectives of this study.

1. To provide background information on mine tailings, tailings impoundments, highly densified tailings technologies, and the cyclic liquefaction behaviour of natural and man-made fine-grained soils (mine tailings).

2. To perform shaking-table testing for evaluating the geotechnical response of highly densified tailings to cyclic loading, which involves:
    2.1. evaluating the geotechnical response of thickened tailings under cyclic loading conditions using a shaking table and
    2.2. evaluating the geotechnical response of paste tailings under cyclic-loading conditions using a shaking table.
3. To perform shaking-table testing to evaluate the rainfall-induced changes in the geotechnical responses of highly densified tailings to cyclic loadings.

### 1.4. Research approach and methods

The approach and methods that were used by this study to attain its objectives are schematically presented in Figure 1.1. First, the problem was defined and an alternative solution to it was devised. Then comprehensive theoretical and technical background information on the problem was gathered, and a literature review was conducted. Experimental work was then carried out, in which the geotechnical response and cyclic loading-induced liquefaction susceptibility of layered thickened and paste tailings were evaluated using a shaking table, after which the effect of rainfall on the geotechnical response and liquefaction susceptibility of layered highly densified tailings was evaluated through a shaking-table test. The experimental works are briefly discussed below.

Fine-grained tailings consisting of a mixture of synthetic silica tailings and natural tailings were tested. The physical properties of these tailings will be presented in the pertinent chapters of the technical papers. Tap water was used as mixing water; it was mixed with the aforementioned tailings to produce highly densified tailings (thickened and paste tailings) with the desired consistency for surface disposal, as in the field.

A 750 mm × 750 mm × 750 mm (L × W × H) flexible laminar shear box (FLSB) mounted on a 1000 mm × 1000 mm (L × W) shaking table was used to examine the layered thickened and paste tailings under one-dimensional cyclic shaking. The characteristics of both the FLSB and the shaking table will be presented in detail in the pertinent chapters of the technical papers.

The surface deposition strategy used in the field was then simulated by depositing the highly densified tailings (thickened and paste tailings) in three thin layers (each only 150 mm thick) in the FLSB to form a 5.6% slope, where the deposition cycling would be separated by a period of 2–3 days. These deposited highly densified tailings (thickened and paste tailings) were then subjected to sinusoidal dynamic loading with a 1 Hz frequency and a 0.13g peak horizontal acceleration. It should be emphasised that the loading conditions that were selected in this testing program were not meant to represent the identical conditions that occur during a natural earthquake because these loading conditions had a one-dimensional signal, a uniform amplitude, a constant frequency and a long duration. Rather, these conditions were selected due to the facility limitations and to gain a more profound insight into the cyclic behaviour of highly densified tailings and provide the key information needed for the future development of a model for describing the seismic behaviour of such tailings. To monitor the properties and responses of such highly densified tailings (thickened and paste tailings) during and after shaking application, several types of instruments or sensors were installed at different depths of the tailings. These instruments had pore pressure transducers for measuring the pore water pressure changes, cable displacement transducers for measuring the settlement and horizontal deformation changes, 5TE sensors for measuring the volumetric water content changes and accelerometers for measuring the acceleration changes.

A general explanation will then be given in the third technical paper (Chapter 5), where the effect of heavy rainfall following a drying period on the behaviour and liquefaction susceptibility of the layered highly densified tailings in the shaking table will be discussed. The obtained experimental test results provide fundamental knowledge and information about the liquefaction behaviour of layered highly densified tailings (thickened and paste tailings) technologies subjected to cyclic loadings. Furthermore, a better understanding of the behaviour of these technologies during cyclic loadings will help the professionals in the mining or geotechnical sector select the safest and most appropriate disposal tailings technologies.

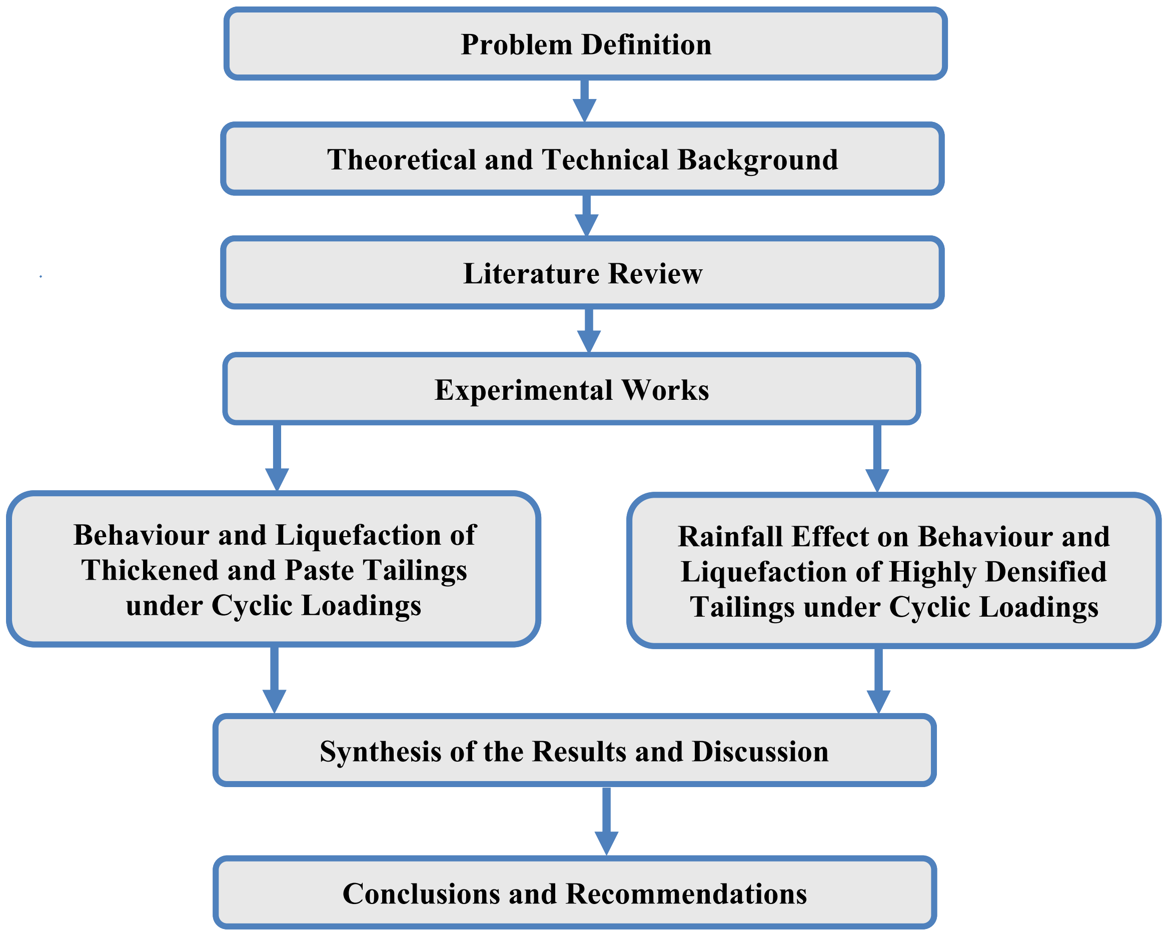


Figure 1.1. Research and study approach

## 1.5. Tasks and organization of the thesis

This thesis is divided into seven chapters discussing the objectives of the study and the tasks that were carried out in connection to it. The main tasks that were carried out in the study are illustrated in Figure 1.2.

**Chapter One** of this thesis gives a general introduction of the research that was done. It also presents the problem statement, the study objectives and the research methods that were used.

**Chapter Two** provides background information on the tailings, tailings impoundments and highly densified tailings technologies (i.e. thickened, paste and dry-stack tailings).

**Chapter Three** presents a comprehensive literature review on the phenomenon of seismic liquefaction, the factors that can affect the liquefaction susceptibility of soils and the liquefaction criteria for soils and presents a review of the previous studies on the seismic liquefaction behaviour of natural and man-made fine-grained soils (mine tailings).

**Chapters Four and Five** have a research-paper-based thesis format including three technical papers. Each of these technical papers contains a section on each of the following: introduction, the materials and equipment that were used in the experiment, the testing program and procedure, the study results and their discussion, the conclusion of the paper and the references. It should be noted that because the main results of these chapters are presented as technical papers, some information is repeated in these papers. This is due to the fact that each paper is independently written (i.e. without taking into account the content of the other papers or the rest of the document) and in accordance with the manuscript preparation instructions of the corresponding publication medium.

**Chapter Four** contains two research manuscripts (**Technical Papers 1 and 2**). These two technical papers are based on the experimental investigation that was conducted (i.e. the shaking-table testing). **Technical Paper 1** in **Section 4.2** deals with the geotechnical response of the layered thickened tailings that were subjected to shaking conditions. The objective of **Technical Paper 2** in **Section 4.3** is similar to that of **Technical Paper 1** except that the tailings in the former are layered paste tailings whereas those in the latter are layered thickened tailings.

**Chapter Five** contains one research manuscript **(Technical Paper 3; Section 5.2)**, which studies the effect of rainfall on the geotechnical response of layered highly densified tailings subjected to shaking conditions.

**Chapter Six** synthesizes the results obtained from the experimental testing in order to provide valuable insight into the response of highly densified tailings technologies (thickened and paste tailings) to seismic or cyclic loadings, which can help mining or geotechnical engineers deal with such technologies specifically in regions with frequent seismic activities.

**Chapter Seven** presents a summary of the study's conduct, findings and conclusions as well as the recommendations for future studies.

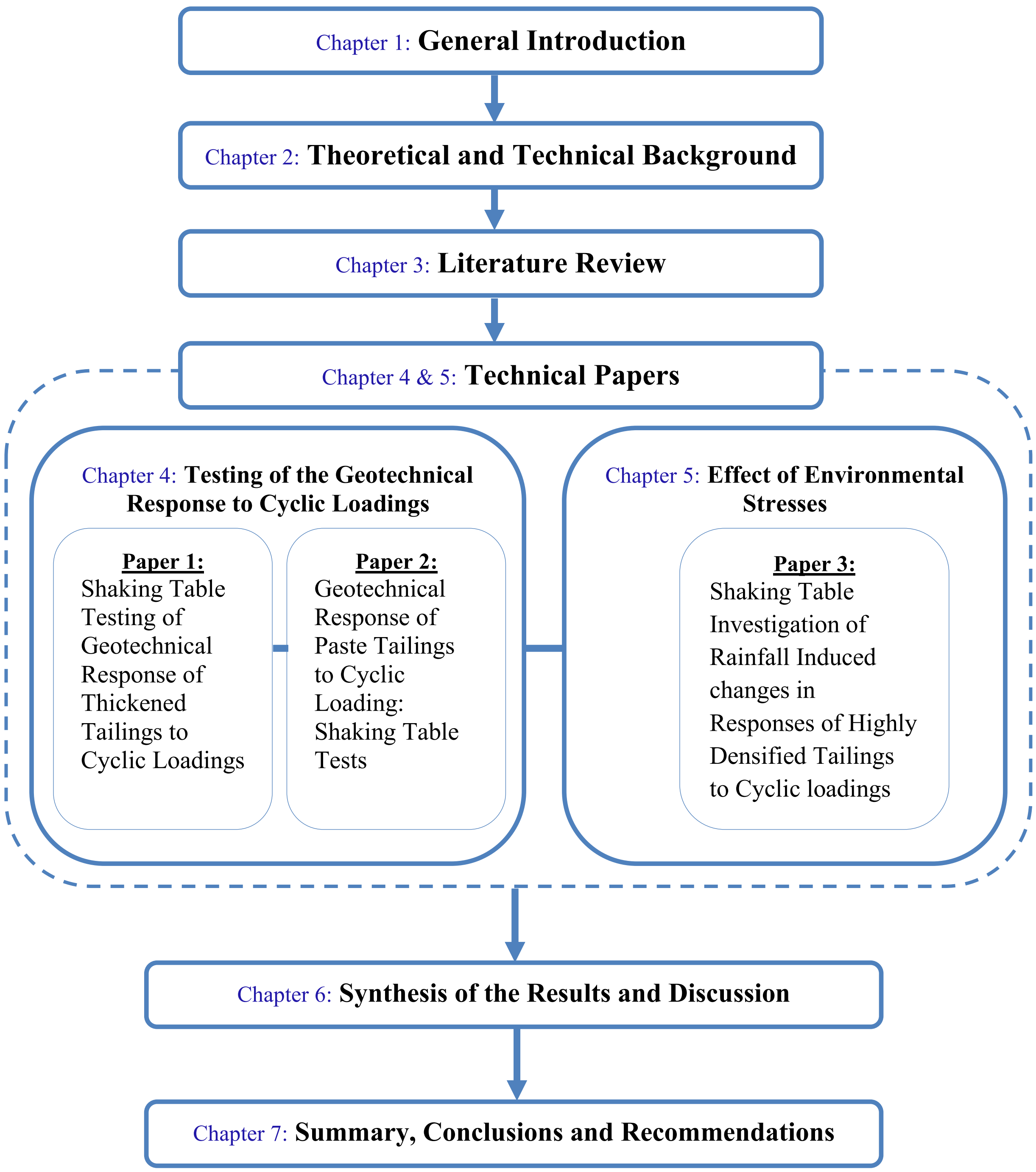


Figure 1.2. Tasks and organization of the thesis

## 1.6. **References**


Alainachi, I, Fall, M. (20.20). Chemically induced changes in the geotechnical response of cementing paste backfill in shaking table test. Journal of Rock Mechanics and Geotechnical Engineering, https://doi.org/10.1016/j.jrmge.2020.11.002.

Aldhafeeri, Z., Fall, M. (2021). Coupled effect of sulphate and temperature on the reactivity of cemented tailings backfill. International Journal of Mining, Reclamation and Environment 35 (2), 80-94.

Ali, G., Fall, M., Alainachi, I. (2021). Time-and temperature-dependence of rheological properties of cemented tailings backfill with sodium silicate. Journal of Materials in Civil Engineering 33 (3), 04020498.

Al-Tarhouni, M.A. (2008). Liquefaction and post-liquefaction behaviour of gold mine tailings under simple shear loading. Master thesis, Department of Civil and Environmental Engineering, Carleton University, Ottawa, Ontario, Canada.

Azam, S., and Li, Q. (2010). Tailings dam failures: a review of the last one hundred years. Geotechnical News, 28(4): 50-53.

Barrera, S., Cacciuttolo, C., and Caldwell, J. (2015). Reassessment of best available tailings management practices. In Proceedings of Tailings and Mine Waste Conference, 26-28 October 2015, Vancouver, British Columbia, Canada.

Bussière, B. (2007). Colloquium 2004: hydrogeotechnical properties of hard rock tailings from metal mines and emerging geoenvironmental disposal approaches. Canadian Geotechnical Journal, 44(9): 1019-1052.

Carvalho, F.P. (2017). Mining industry and sustainable development: time for change. Food and Energy Security, 6(2): 61-77.

Crowder, J.J. (2004). Deposition, consolidation, and strength of a non-plastic tailings paste for surface disposal. PhD thesis, Department of Civil Engineering, University of Toronto, Toronto, Ontario, Canada.

Daliri, F. (2013). The influence of desiccation and stress history on monotonic and cyclic shear response of thickened gold tailings. PhD thesis, Department of Civil and Environmental Engineering, Carleton University, Ottawa, Ontario, Canada.

Daliri, F., Simms, P., and Sivathayalan, S. (2016). Shear and dewatering behaviour of densified gold tailings in a laboratory simulation of multi-layer deposition. Canadian Geotechnical Journal, 53(8): 1246-1257.

Davies, M.P. (2002). Tailings impoundment failures: are geotechnical engineers listening? Geotechnical News, 20(3): 31-36.

Dobry, R., and Alvarez, L. (1967). Seismic failure of Chilean tailings dams. Journal of the Soil Mechanics and Foundations Division, ASCE, 93(SM6): 237-260.

Fall, M., Célestin, J.C., and Han, F.S. (2009). Suitability of bentonite-paste tailings mixtures as engineering barrier material for mine waste containment facilities. Minerals Engineering 22 (9-10): 840-848.

Fang, K., Fall, M., Cui, L (2021). Thermo-chemo-mechanical cohesive zone model for cemented paste backfill-rock interface. Engineering Fracture Mechanics 244, 107546.

Fourie, A.B. (2012). Perceived and realised benefits of paste and thickened tailings for surface deposition. In Proceedings of the 15th International Seminar on Paste and Thickened Tailings (Paste2012), 16-19 April 2012, Sun City, South Africa, pp. 53-64.

Geremew, A.M., and Yanful, E.K. (2012). Laboratory investigation of the resistance of tailings and natural sediments to cyclic loading. Geotechnical Geological Engineering, 30(2): 431-447.

Gomes, L.E.O, Correa L.B., Sá, F., Neto, R.R., and Bernardino, A.F. (2017). The impacts of the Samarco mine tailing spill on the Rio Doce estuary, Eastern Brazil. Marine Pollution Bulletin, 120(1-2): 28-36.

Highter, W.H., and Vallee, R.P. (1980). The liquefaction of different mine tailings under stress-controlled loading. Engineering Geology, 16(1-2): 147-150.

Hu, L., Wu, H., Zhang, L., Zhang, P., and Wen, Q. (2017). Geotechnical properties of mine tailings. Journal of Materials in Civil Engineering, ASCE, 29(2): 04016220.

Ishihara, K., Troncoso, J., Kawase, Y., and Takahashi, Y. (1980). Cyclic strength characteristics of tailings materials. Soils and Foundations, 20(4): 127-142.

Ishihara, K., Yasuda, S., and Yokota, K. (1981). Cyclic strength of undisturbed mine tailings. In Proceedings of the First International Conference on Recent Advances in Geotechnical Earthquake Engineering and Soil Dynamics, 26 April - 3 May 1981, St. Louis, Missouri, USA, Vol. 1, pp. 53-58.

James, M., Aubertin, M., Wijewickreme, D., and Wilson, G.W. (2011). A laboratory investigation of the dynamic properties of tailings. Canadian Geotechnical Journal, 48(11): 1587-1600.

Kam, S., Girard, J., Hmidi, N., Mao, Y., and Longo, S. (2011). Thickened tailings disposal at Musselwhite Mine. In Proceedings of the 14th International Conference on Paste and Thickened Tailings (Paste2011), 1-7 April 2011, Perth, Australia, pp. 225-236.

Kim, H., Daliri, F., Simms, P., and Sivathayalan, S. (2011). The influence of desiccation and overconsolidation on monotonic and cyclic shear response of thickened gold tailings. In Proceedings of the 64th Canadian Geotechnical Conference (2011 Pan-Am CGS), 2-6 October 2011, Toronto, Ontario, Canada.

Marshall, B. (2016). Facts and figures of the Canadian mining industry. The Mining Association of Canada (MAC), Ottawa, Ontario, Canada, pp. 1-119.

Miranda, L.S., and Marques, A.C. (2016). Hidden impacts of the Samarco mining waste dam collapse to Brazilian marine fauna–an example from the staurozoans (Cnidaria). Biota Neotropica, 16(2): 1-4.

Pépin, N., Aubertin, M., and James, M. (2012a). Seismic table investigation of the effect of inclusions on the cyclic behaviour of tailings. Canadian Geotechnical Journal, 49(4): 416-426.

Pépin, N., Aubertin, M., James, M., and Leclerc, M. (2012b). Seismic simulator testing to investigate the cyclic behaviour of tailings in an instrumented rigid box. Geotechnical Testing Journal, 35(3): 469-479.

Poulos, S.J., Robinsky, E.I., and Keller, T.O. (1985). Liquefaction resistance of thickened tailings. Journal of Geotechnical Engineering, 111(12): 1380-1394.

Robinsky, E., Barbour, S.L., Wilson, G.W., Bordin, D., and Fredlund, D.G. (1991). Thickened sloped tailings disposal-an evaluation of seepage and abatement of acid drainage. In Proceedings of the Second International Conference on the Abatement of Acidic Drainage, Invited Lecture, 16-18 September 1991, Montreal, Quebec, Canada, pp. 529-549.

Seddon, K.D., and Albee, J.K. (2015). Characterization of a thickened tailings beach. In Proceedings of the 18th International Seminar on Paste and Thickened Tailings (Paste2015), 5-7 May 2015, Cairns, Australia, pp. 493-504.

Seidalinova, A. (2014). Monotonic and cyclic shear loading response of fine-grained gold tailings. Master thesis, The University of British Columbia, Vancouver, British Columbia, Canada.

Simms, P. (2017). 2013 Colloquium of the Canadian Geotechnical Society: geotechnical and geoenvironmental behaviour of high-density tailings. Canadian Geotechnical Journal, 54(4): 455-468.

Statistics Canada. (2012). Human activity and the environment: waste management in Canada, 1-46.

Suazo, G., Fourie, A., Doherty, J., and Hasan, A. (2016). Effects of confining stress, density and initial static shear stress on the cyclic shear response of fine-grained unclassified tailings. Géotechnique, 66(5): 401-12.

Theriault, J., Frostiak, J., and Welch, D. (2003). Surface disposal of paste tailings at the Bulyanhulu gold mine, Tanzania. In Proceedings of Mining and the Environment Conference III, 25-28 May 2003, Sudbury, Ontario, Canada, pp. 1-8.

Verdugo, R., and González, J. (2015). Liquefaction-induced ground damages during the 2010 Chile earthquake. Soil Dynamics and Earthquake Engineering, 79: 280-295.

Verdugo, R., and Santos, E. (2009). Liquefaction resistance of thickened tailings of copper mines. In Proceedings of the 17th International Conference on Soil Mechanics and Geotechnical Engineering (ICSMGE), 5-9 October 2009, Alexandria, Egypt, pp. 295-298.

Verdugo, R., Sitar, N., Frost, J.D., Bray, J.D., Candia, G., Eldridge, T., Hashash, Y., Olson, S., and Urzua, A. (2012). Seismic performance of earth structures during the February 2010 Maule, Chile, earthquake: dams, levees, tailings dams, and retaining walls. Earthquake Spectra, 28(S1): S75-S96.

Wijewickreme, D., Sanin, M.V., and Greenaway, G.R. (2005). Cyclic shear response of fine-grained mine tailings. Canadian Geotechnical Journal, 42(5): 1408-1421.

World Information Service on Energy (WISE). (2017). Chronology of major tailings dam failures. See https://www.wise-uranium.org/mdaf.html [accessed December 10, 2017].

# 2 Chapter 2: Theoretical and Technical Background

## 2.1. Introduction

In this chapter, a review of the fundamental theoretical and technical background information on man-made soils (tailings) and their storage and deposition technologies is provided. Particularly, Section 2.2 provides background information on mine tailings, tailings impoundments and the highly densified tailings technology. In mine tailings section (Section 2.2.1), a brief review of the generation of tailings from mineral processing and of their general engineering characteristics is provided. Then in tailings impoundments section (Section 2.2.2), the main types of surface tailings dam or impoundment according to their construction (i.e. water-retention-type dams and raised embankment dams) are discussed. Finally, a general review of the three main types of highly densified tailings technology (i.e. thickened tailings, paste tailings and dry-stack tailings) is provided in Section 2.2.3.

## 2.2. Man-made fine-grained soils from mining operations

### 2.2.1. Mine tailings

Mine waste is a by-product of mining operation and mineral extraction. Such mine waste mainly involves two types of waste: waste rock and tailings. Waste rock (particle size ranging from fine sands to boulders) is excavated to reach the ore, which presents economic benefits, whereas tailings (particle size ranging from colloids to fine sands, with the silty fraction predominating) consist of particles of crushed rock from the mine processing (James et al., 2013; Daliri, 2013; Cui and Fall, 2018; Roshani et al., 2018; Fang and Fall, 2020). In general, waste rock is stored in piles on the earth surface while tailings are stored in slurry form in an impoundment on the earth surface (James et al., 2013). As the subject of the current study is related to tailings, this section will focus only thereon.

The term *tailings* refers to the waste materials that remain after the extraction of valuable minerals from the ore. Generally, tailings are generated in slurry form made up of particles of rock and process water (Fall and Samb, 2009; James et al., 2013; Ghirian and Fall, 2016; Bull and Fall, 2020). The generation of tailings from mineral processing passes through several main stages: crushing, grinding, concentration, dewatering and tailing slurry disposal (Vick, 1983; Fall et al. 2009; Xiao et al., 2020). In addition, optional processes containing leaching or heating may follow or replace the concentration process (Vick, 1983). Figure 2.1 shows the processes involved in the generation of tailings. In the crushing process, the rock fragments are reduced from mine-run size to a size that can be fed to the grinder. Then the grinding process performs further size reduction of the fragments resulting from the previous process using rod mills and a ball. As the concentrations of the particles resulting from the grinding process are different, the concentration process separates the particles with high concentrations from those with lower concentrations (tailings). For the leaching process, the minerals are removed from the ground particles often using a strong acid or an alkaline solution. The heating process is mainly used for the extraction of oil from oil sands (Roshani et al., 2017). The last process is the dewatering of the tailings using thickeners or vacuum suction techniques, and then the disposal of the slurry tailings in an impoundment (see Figure 2.2). The tailings are either pumped or gravity fed through pipelines or open flumes from the mine processing plant to the storage facility (Heidarian, 2012). Following the deposition of such tailings, their coarse particles settle near the point of deposition while the fine particles settle farther away therefrom (Vick, 1983).

The physical characteristics of tailings significantly differ depending on the site, type of ore and the milling process and deposition approach used (Chryss, 2017). The behaviour of tailings can be determined through the grain size distribution, water content and plasticity (James et al., 2013). The sizes of the tailings particles may range from those of sand to clay, and 40–70% of the tailings resulting from the most common and inexpensive metals are made to pass through a 0.074 mm (No. 200) sieve, but 90% or more of the tailings resulting from precious metals such as gold are made to pass through a 0.074 mm (No. 200) sieve (Davies et al., 2002). The grain size distributions and some physical properties of different types of tailings are presented in Figures 2.3-2.5 and in Table 2.1, respectively.

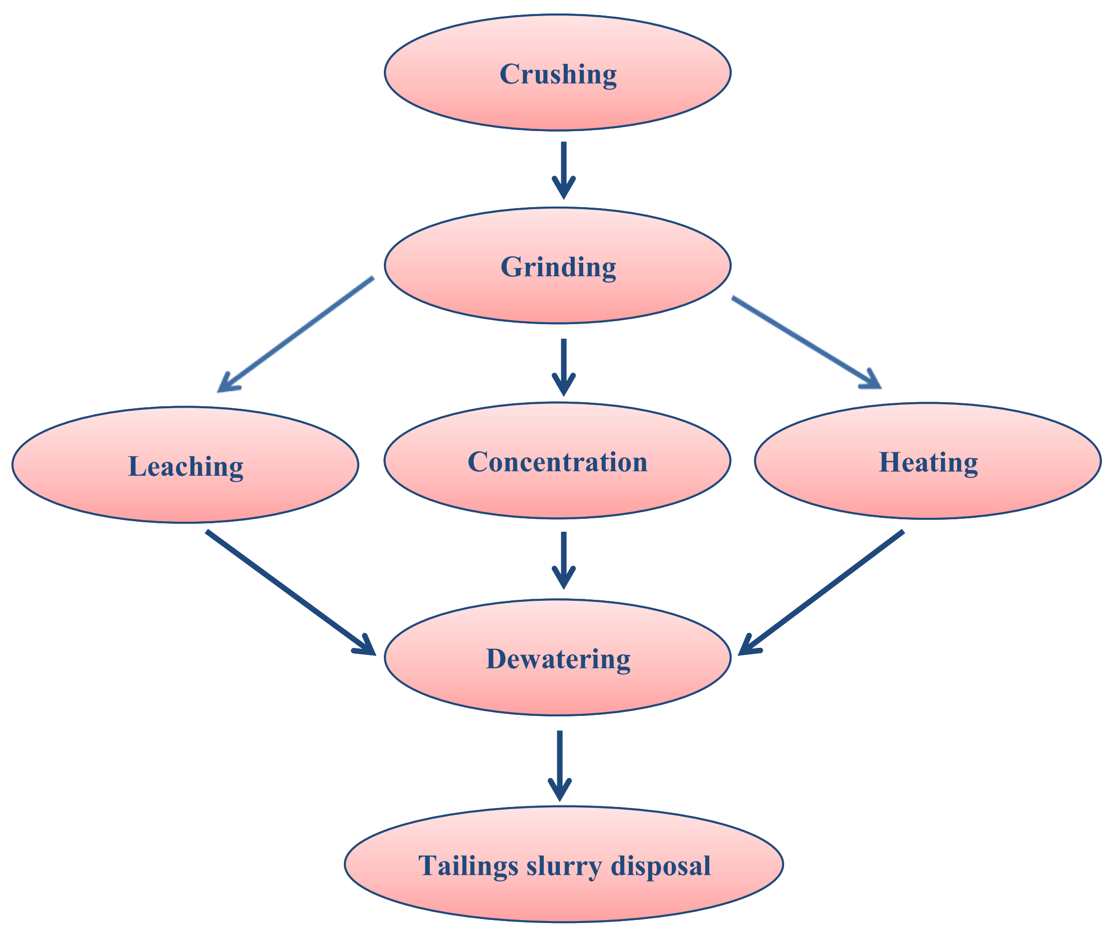


Figure 2.1. Processes involved in tailings generation (Vick, 1983)

Figure 2.2. Discharging slurry tailings in a tailings impoundment (Bussière, 2007)

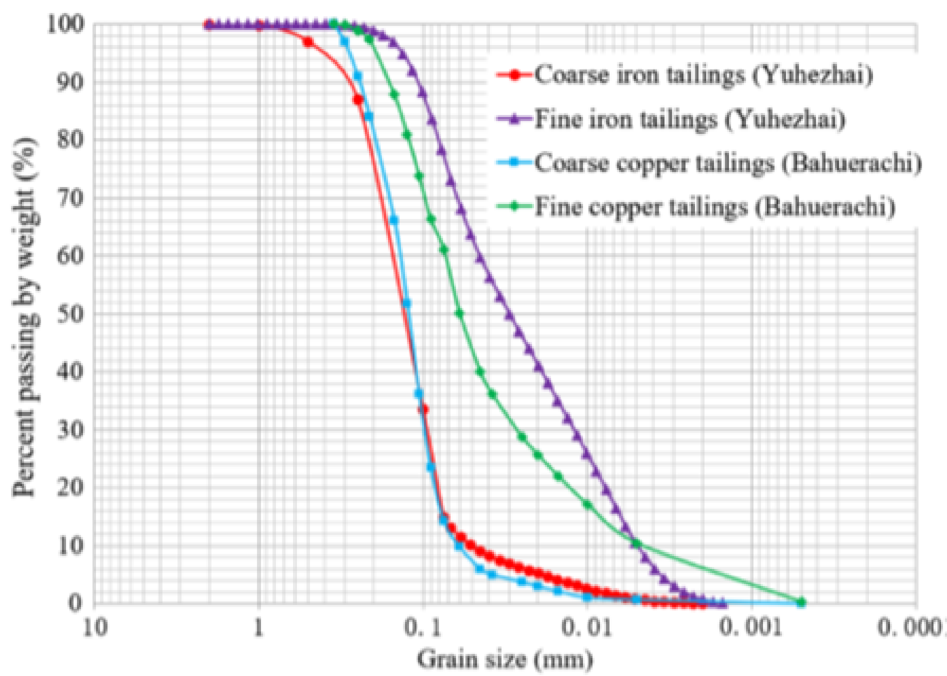


Figure 2.3. Grain size distributions of coarse and fine iron and copper tailings (Hu et al., 2017)

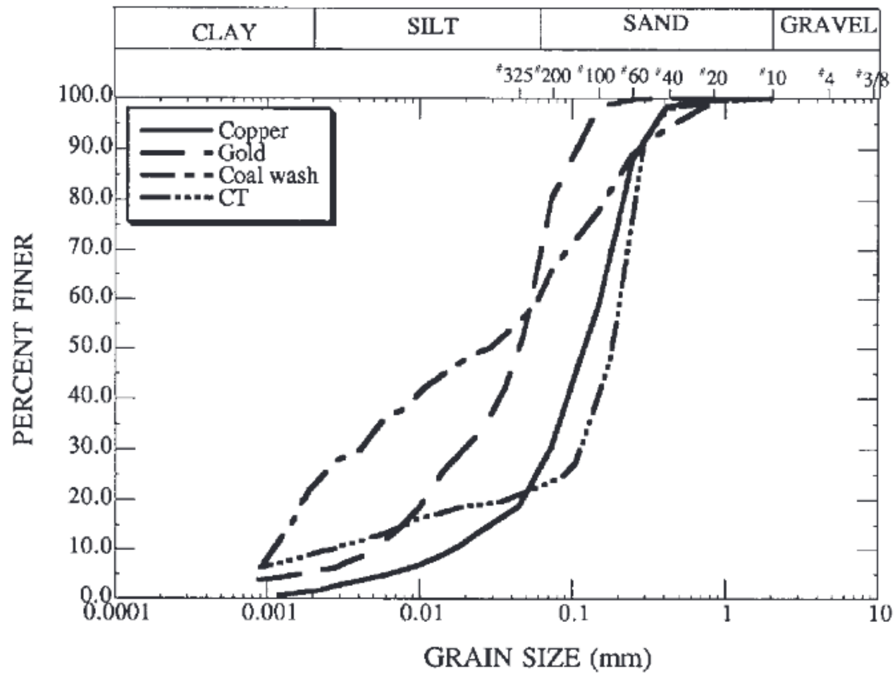


Figure 2.4. Grain size distributions of copper, gold, coal and oil sand (CT) tailings (Qiu and Sego, 2001)

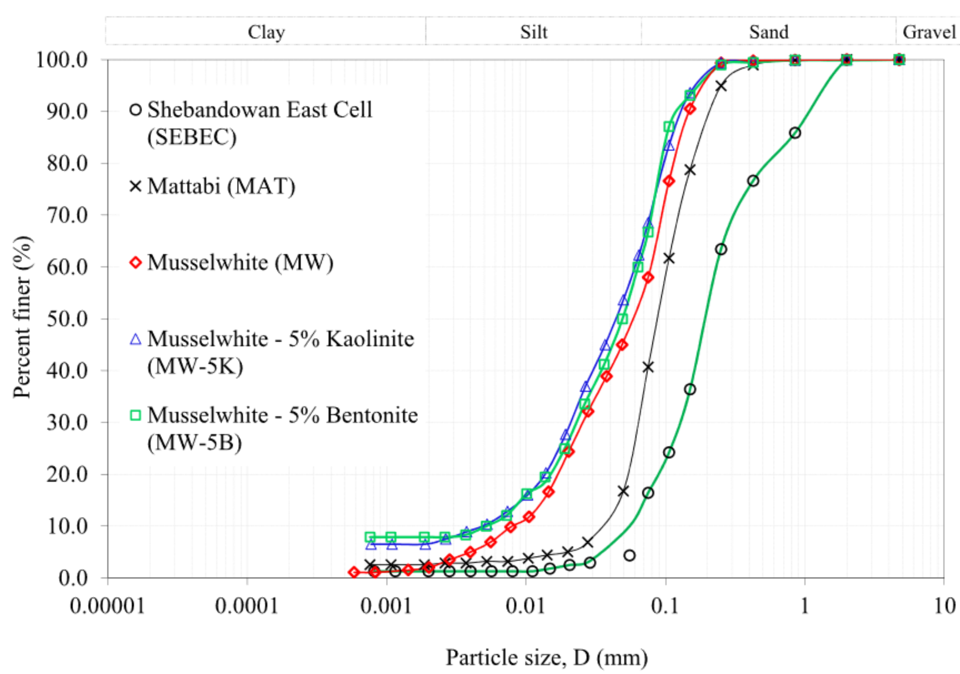


Figure 2.5. Grain size distributions of the Shebandowan nickel mine, Mattabi copper-zinc mine and Musselwhite gold mine tailings (Geremew and Yanful, 2013)

Table 2.1. Some physical properties of different types of tailings

| Tailings type | $G_s$ | PI (%) | $D_{10}$ (μm) | $D_{30}$ (μm) | $D_{50}$ (μm) | $D_{60}$ (μm) | $C_u$ | $C_c$ | Classification (USCS) | Reference |
|---|---|---|---|---|---|---|---|---|---|---|
| Copper | 2.75 | - | 16.28 | 72.25 | 120.6 | 153.5 | 9.43 | 2.09 | SM | Qiu and Sego (2001) |
| Gold | 3.17 | - | 5.00 | 19.00 | 44.8 | 54.0 | 10.80 | 1.34 | ML | |
| Coal | 1.94 | 16.0 | 1.31 | 4.13 | 29.2 | 60.0 | 45.80 | 0.22 | CL | |
| Oil sand (CT) | 2.60 | - | 2.70 | 11.20 | 182.0 | 204 | 75.56 | 0.23 | SM | |
| Copper-gold-zinc | 3.36-4.42 | 2.0 | NA | NA | NA | NA | NA | NA | ML | Wijewickreme et al. (2005) |
| Copper-gold | 2.78 | - | NA | NA | NA | NA | NA | NA | ML | |
| Copper-zinc | 3.29 | 12.6 | 37.00 | 65.00 | 88.0 | 101.0 | 2.73 | 1.13 | CL | Geremew and Yanful (2013) |
| Nickel | 3.22 | 1.0 | 56.50 | 140.0 | 200.0 | 245.0 | 4.34 | 1.42 | ML | |
| Gold | 3.32 | 4.3 | 10.20 | 28.70 | 68.1 | 79.0 | 7.75 | 1.02 | ML | |
| Coarse copper | 2.77 | - | 65.00 | 90.00 | 120.0 | 140.0 | 2.15 | 0.89 | SM | Hu et al. (2017) |
| Fine copper | 2.76 | 15.0 | 5.00 | 28.00 | 60.0 | 78.0 | 14.80 | 2.12 | CL | |
| Coarse iron | 3.23 | - | 51.00 | 93.00 | 120.0 | 160.0 | 3.11 | 1.05 | SM | |
| Fine iron | 3.08 | 9.0 | 5.00 | 12.00 | 30.0 | 45.0 | 8.82 | 0.59 | CL | |

### 2.2.2. **Tailings impoundments**

The term *tailings impoundment* has been defined by many researchers. For instance, Bjelkevik (2005) has defined tailings impoundment as “the storage space/volume that is created by the tailings dams where the tailings are deposited and stored”. In addition, Heidarian (2012) provided another definition in which the conventional impoundment is defined as “a ground surface with a constructed embankment dam on it to store water and tailings”. The objective of the construction of tailings impoundments is to dispose of tailings in an economical way while ensuring both impoundment stability and environment preservation (Heidarian, 2012). Surface tailings impoundments can be classified into two types according to their construction: water-retention-type dams and raised embankment dams (Vick, 1983). Raised embankment dams can be further classified into three types according to their construction method: upstream, downstream and centreline dams (Vick, 1983). Failures of both water-retention-type dams and raised embankment dams have occurred in numerous countries, as shown in Figure 2.6. Such failures are usually attributed to several factors, such as seepage, foundation failure, overtopping, earthquake, mine subsidence, structural, erosions and slope instability (Lyu et al., 2019). Figure 2.7 shows the number of incidents for each cause of failure globally and in Europe. In addition, tailings impoundments have been reported to be associated with liquefaction-induced failure and reclamation problems (Wickland and Wilson, 2005).

Water-retention-type dams, as shown in Figure 2.8, are constructed entirely to their complete height prior to discharging the tailings in the impoundment on the earth surface. This type of dam includes the following: impervious core, drainage zones, filters and upstream riprap. In addition, these dams are considered more appropriate for tailings impoundments when storage places for large volumes of water are needed.

Unlike water-retention-type dams, raised embankment dams (upstream, downstream and centreline) are constructed in stages throughout the impoundment lifetime. Also, compared with water-retention-type dams, the initial cost of raised embankment dams is lower. Raised embankment dams thus lead to a lower cash flow compared to water-retention-type dams because they can be constructed over a longer period. Furthermore, raised embankment dams offer considerably greater flexibility in the selection of the materials to be used.

The first method of constructing raised embankment dams is the upstream method, as illustrated in Figure 2.9, which begins with the construction of a starter dike. Then the tailings from the crest of this starter dike are discharged to create a beach, which serves as the foundation for the following dike. This process continues as the height of the embankment increases. In this method, as a general rule, the percentage of sand in the discharged tailings should not be below 40−60%. Using the upstream raised embankment construction method offers two crucial advantages. Firstly, it costs less than the two other methods (the downstream and centreline methods) do because it does not need a large amount of material for the construction of the perimeter dikes. Secondly, it is considered the simplest raised embankment construction method in terms of the construction of the perimeter dikes. The use of the upstream raised embankment construction method also has several disadvantages, however, such as poor control of the phreatic surface, low water storage capacity, susceptibility to seismic liquefaction and raising rate restriction. Davies et al. (2002) reported that most of the failures of upstream dams have occurred because of one or a combination of the following factors: earthquake, high level of saturation, sharp slope, poor control of the water in the pond, poor method of construction for the existing fine materials in the dam shell, static liquefaction and failure of the embedded decant structures. Therefore, the construction method of upstream dams has been improved as follows: finger or blanket drains are added to reduce the phreatic level, the beaches are compacted to provide stability and the slopes are designed to be 3 horizontal to 1 vertical, or even flatter.

The second construction method of raised embankment dams is the downstream method, as illustrated in Figure 2.10, which starts with the discharge of the tailings at the back of a starter dike. Then the embankment fill is placed on the downstream slope of the prior height increase to realize the subsequent height increases. The use of the downstream method offers numerous advantages, such as a greater water storage capacity, greater resistance to liquefaction than the two other methods and a non-restricted raising rate. However, the use of the downstream method presents one significant disadvantage: a high cost compared with the two other methods (the upstream and centreline methods) because it needs a large amount of embankment fill.

The third construction method of raised embankment dams is the centreline method, as illustrated in Figure 2.11, which starts with the construction of a starter dike, followed by the discharge of the tailings from the crest of the starter dike to create a beach. To realize the subsequent height increases, fill material is placed on both the beach and the downstream slope of the prior height increase. The centreline method has the advantages of both the upstream and downstream methods but does not have their disadvantages. That is, in the centreline method the raising rate is not restricted by the dissipation of the pore water pressure. Also, the centreline method normally provides acceptable resistance to liquefaction. As for the cost of construction using such method, it is situated between those of the upstream and downstream methods because the amount of fill material needed is also situated between those of such methods. The centreline method, however, is not ideal for the permanent storage of large amounts of water, but it can store flood water for a short time without having a negative impact on the embankment stability.

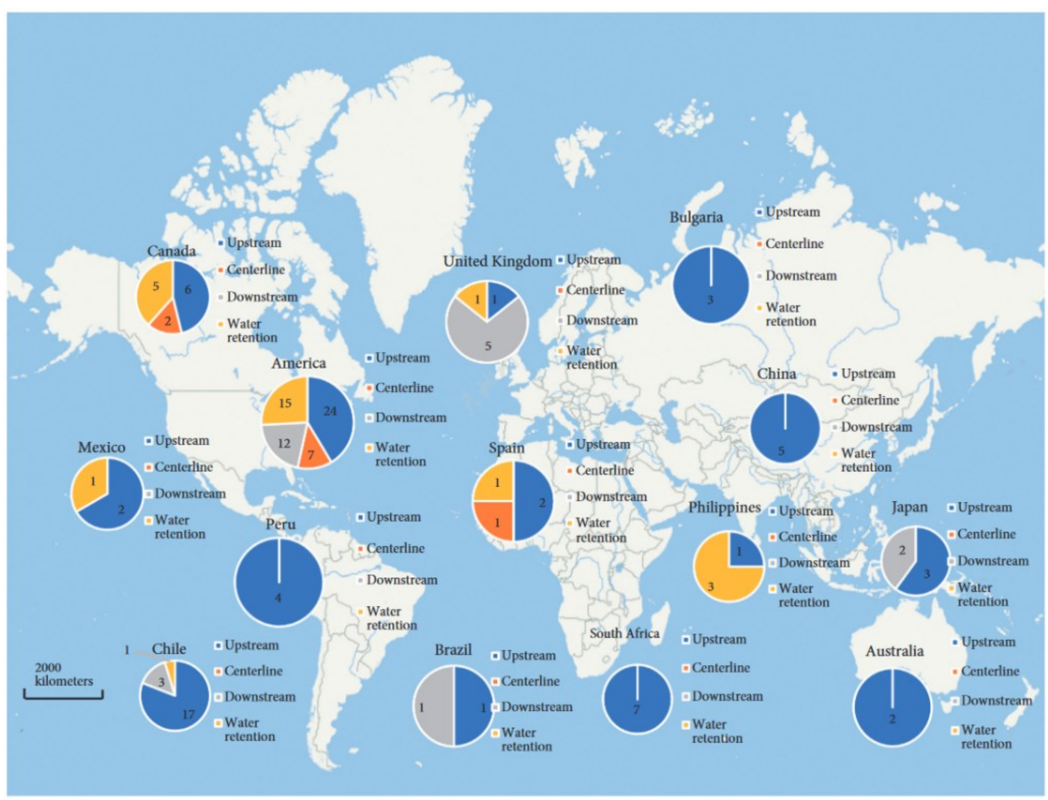


Figure 2.6. Tailings dam failures in many countries (Lyu et al., 2019)

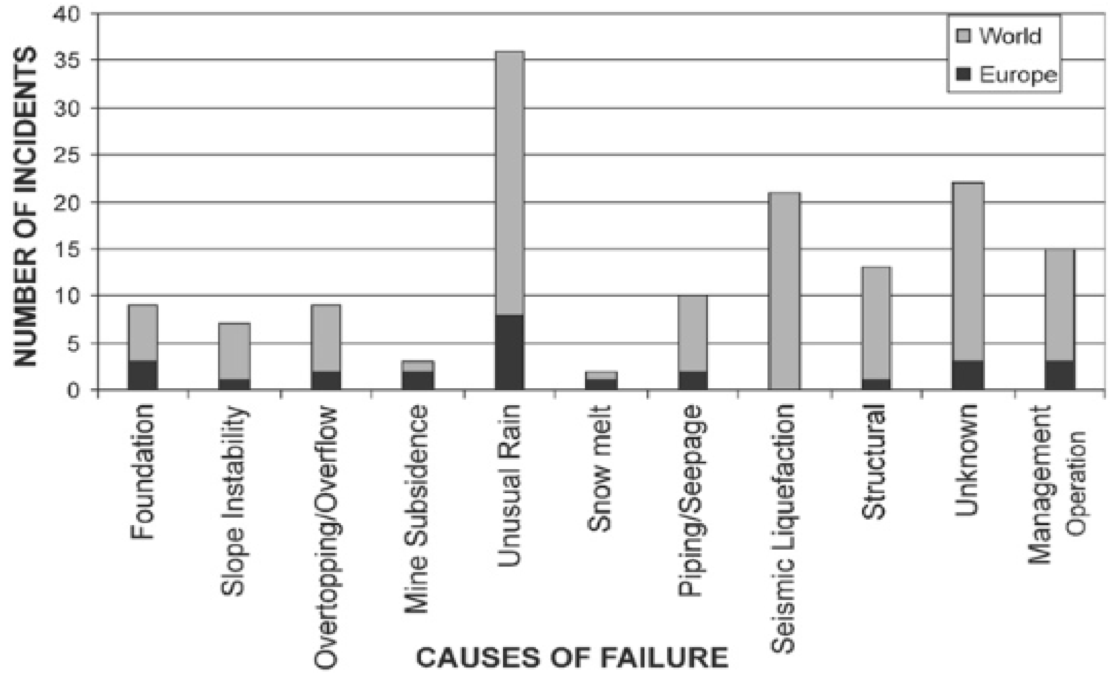


Figure 2.7. Incidents for each cause of tailings dam failure in the world and in Europe (Rico et al., 2007)

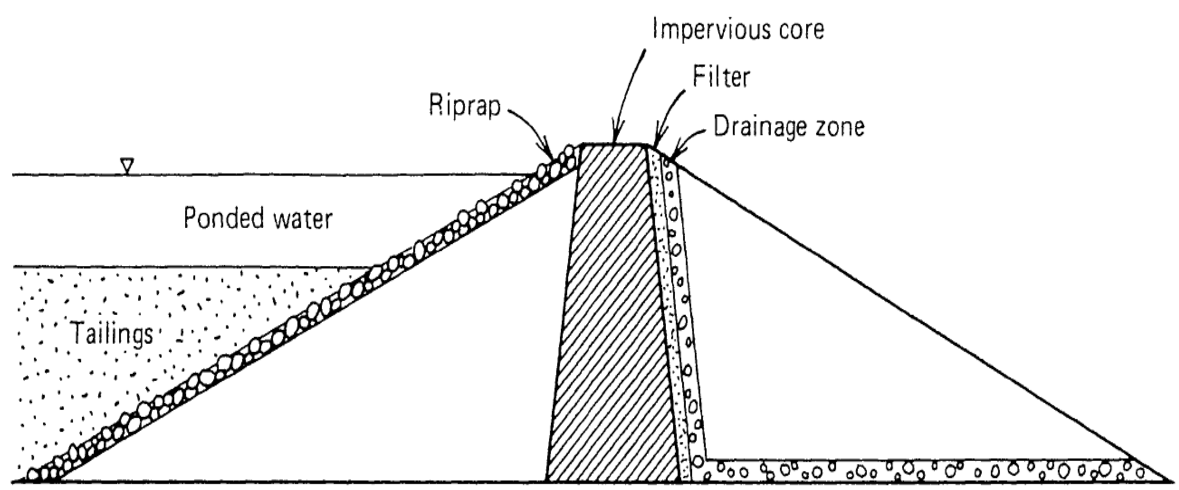


Figure 2.8. Water-retention-type dam for tailings storage (Vick, 1983)

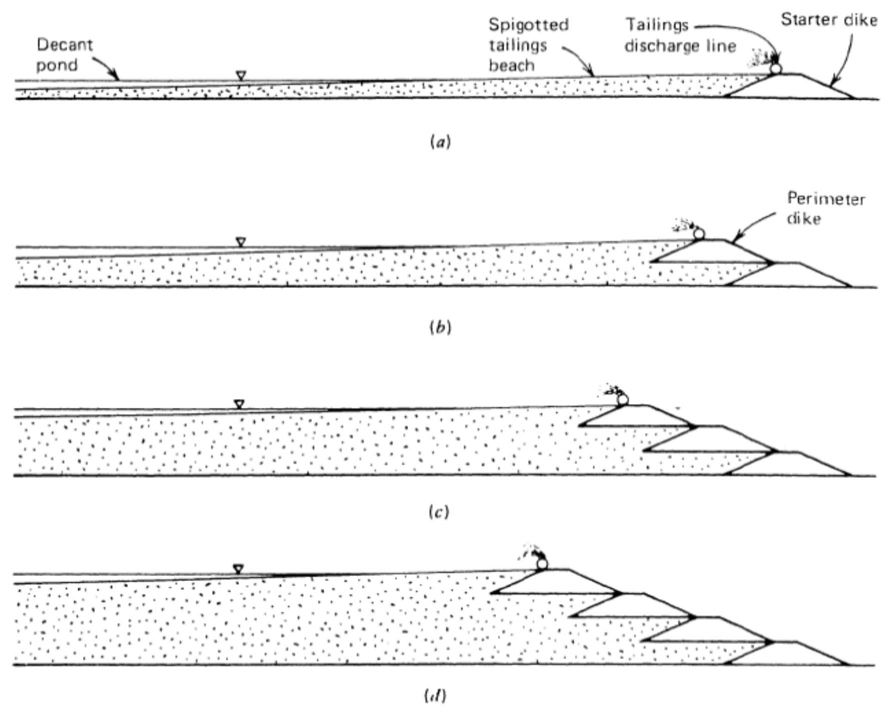


Figure 2.9. Sequential raising using the upstream raised embankment dam construction method (Vick, 1983)

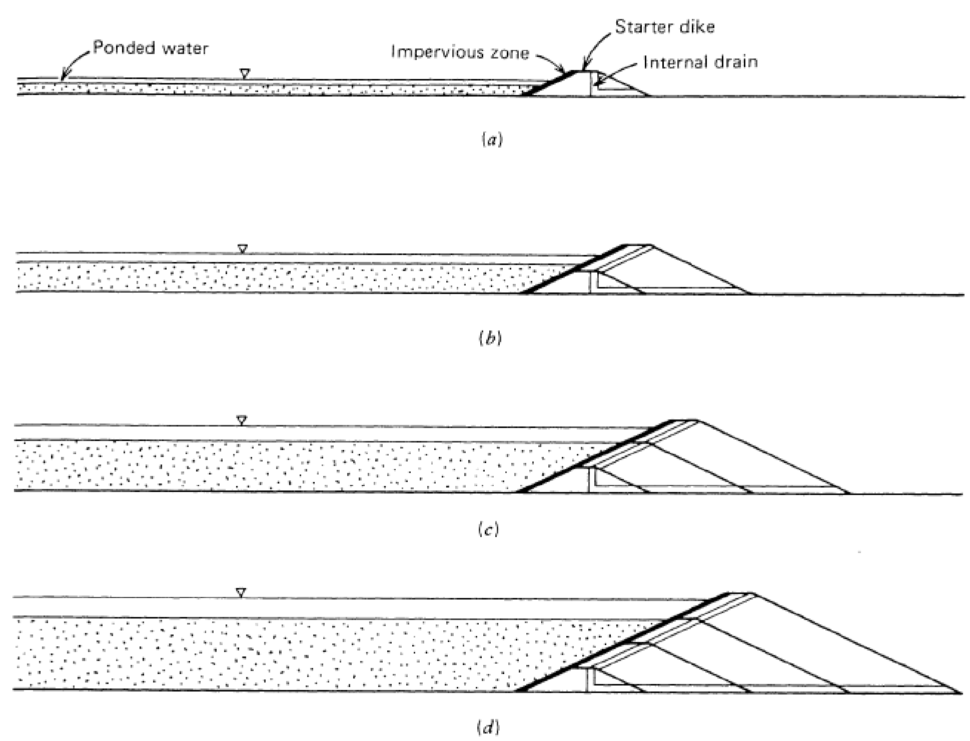


Figure 2.10. Sequential raising using the downstream raised embankment dam construction method (Vick, 1983)

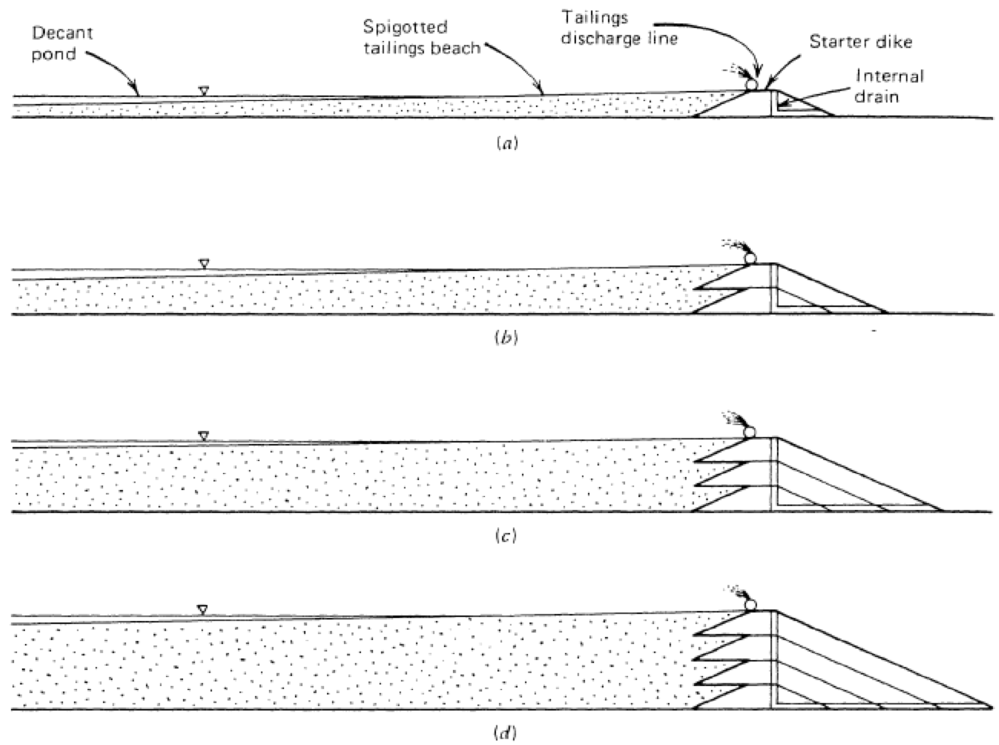


Figure 2.11. Sequential raising using the centerline raised embankment dam construction method (Vick, 1983)

### 2.2.3. **Highly densified tailings**

#### 2.2.3.1. **Thickened tailings**

Thickened tailings are dense, viscous mixtures of tailings and water and are not fully subjected to the dewatering process (Davies and Rice, 2001; Edraki et al., 2014). The pioneer of the thickened tailings technology is Robinsky (1975), and the Kidd Creek Mine facility in Ontario, Canada is considered the first mine that employed such technology. Figure 2.12 shows a summary of the relative number of dewatered mine tailings facilities, including thickened tailings, in the world. Typically, compression thickeners or a combination of thickeners and filter presses is used to attain thickened tailings behaviour (Engels, 2002). With regard to thickened tailings, they are dewatered until the amount of solid contents already ranges from 50 to 70% and until the solid contents no longer segregate upon deposition (as the conventional slurry tailings do) due to the homogenous behaviour of thickened tailings with low permeability (Robinsky et al., 1991; Bussière, 2007). In the mining industry, unlike slurry tailings, thickened tailings are usually known to generally have a yield stress higher than 20 Pa but not higher than 100 Pa, and are discharged from the spigot to form stacks at a gentle slope ranging from 2 to 6% (Robinsky et al., 1991; Engels, 2002). The thickened tailings discharge is shown in Figure 2.13. By using the thickened tailings technology, the risk related to the geotechnical instability of dams can be significantly diminished as no dam construction is required and no pond of water is formed (Bussière, 2007). In addition, Bussière (2007) pointed out that deposition in thin layers enhances the geotechnical properties of this form of technology. The strength gain of thickened tailings increases through self-weight consolidation and desiccation when these tailings are subjected to the natural climate (Bussière, 2007). Boger (2013) compares the characteristics of slurry, thickened and paste tailings in the storage area, as shown in Table 2.2.

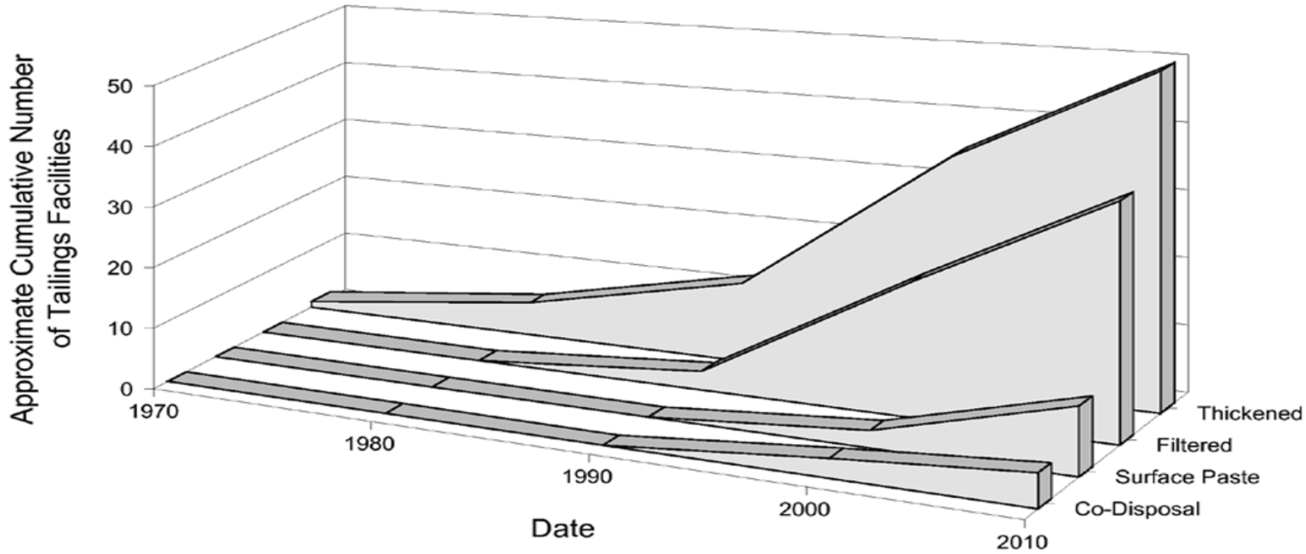


Figure 2.12. Trends in the use of dewatered mine tailings in mining (Davies et al., 2010)

Figure 2.13. Thickened tailings discharge at Kidd Creek, ON, Canada (left) and at Mt. Keith, Western Australia (right) (Engels, 2002)

Table 2.2. Comparison of the characteristics of slurry, thickened and paste tailings (Boger, 2013)

| | Slurry Tailings | Thickened tailings | Paste tailings |
|---|---|---|---|
| **Final density** | Low | Medium/high | High |
| **Segregation** | High | Slight | None |
| **Supernatant water** | High | Some | None |
| **Post-placement shrinkage** | High | Some | Insignificant |
| **Seepage** | High | Some | Insignificant |
| **Rehabilitation** | Delayed | Immediate | Immediate |
| **Permeability** | Medium/low | Low | Very low |
| **Application** | Above ground | Above ground | Above and under ground |
| **Footprint** | Medium | High | Low |
| **Water consumption** | High | Medium | Low |
| **Reagent recovery** | Low | Medium | High |

2.2.3.2. **Paste tailings**

The term *paste tailings* refers to dewatered slurry tailings that once pumped will not have a critical flow velocity, after deposition will not undergo grain size segregation and once discharged into the earth surface will not generate a substantial amount of bleed water (Theriault et al., 2003; Alshawmar and Fall, 2020). The Bulyanhulu gold mine in Tanzania is considered the first facility in the world that implemented the paste tailings technology on the earth surface (Theriault et al., 2003). A summary of the relative number of dewatered mine tailings facilities (including paste tailings facilities) in the world is shown in Figure 2.12. Paste tailings behave as a dense, viscous mixture of tailings and water, has a consistency comparable to that of wet concrete, must contain at least 15% by weight passing a 20 μm to obtain a flowable paste material and should keep enough colloidal water to form a mixture with no grain size segregation (Verburg, 2001; Haruna and Fall, 2020). Such technology can be generated by sending the conventional slurry tailings to high-density thickeners and/or filters, but as a result, the solid contents of this generated paste range from 70 to 85% (Meggyes and Debreczeni, 2006; Bussière, 2007). As the dewatering process increases the viscosity of the paste tailings, positive displacement pumps are needed for transporting the tailings to the storage facility (Theriault et al., 2003). Paste tailings have a yield stress that ranges from 100 to 1000 Pa, with a slump value of 200−275 mm (Bussière, 2007). The flow of the paste tailings rests at the slope, which usually ranges from 3° to 10°, when the underlying material has stabilised (Theriault et al., 2003). The risks related to dam failures can be largely reduced through the use of the paste tailings technology, where the need for dam construction is eliminated (Bussière, 2007). The thin-layer deposition process of paste tailings is cycled to help in the desiccation of surface tailings (Theriault et al., 2003). This process makes paste tailings gain strength in addition to the strength gained from self-weight consolidation (Theriault et al., 2003). The deposition of fresh paste tailings layers is shown in Figure 2.14. The characteristics of paste tailings in the storage area are presented in Table 2.2 and are compared with those of slurry and thickened tailings.


Figure 2.14. Deposition of fresh paste tailings layers at the Bulyanhulu gold mine in Tanzania (Engels, 2002; Theriault et al., 2003)

2.2.3.3. **Dry-stack tailings**

Dry-stack tailings, also known as filtered tailings, are produced by dewatering tailings until there is no longer any pumpable water therefrom using vacuum and pressure filters (Davies and Rice, 2001). Such technology was first employed in the coal mining industry (Bussière, 2007). A summary of the relative number of dewatered mine dry-stack tailings facilities in the world is shown in Figure 2.12. The degree of saturation of dry-stack tailings ranges from 70% to 85%, and their solid contents are higher than 85% (Davies and Rice, 2001; Bussière, 2007). Dry-stack tailings can be transported to the tailings storage facility either by a conveyor or a truck, and are then placed, spread and compacted to create an unsaturated, dense and stable tailings stack (Davies and Rice, 2001), as shown in Figure 2.15. Like thickened and paste tailings, dry-stack tailings significantly reduce the stability risks associated with the failures of tailings dams as the need for dam construction is eliminated (Bussière, 2007). According to Davies (2011), the dry-stack tailings technology is the ideal management option for the recovery of water for process water supply, which is specifically vital in arid environments, and when the topography/foundation conditions contraindicate the implementation of the conventional tailings impoundments.

Figure 2.15. Transport of dry-stack tailings using a conveyor (left) and a truck (right) (Engels, 2002; Anglo, 2004)

## 2.3. **Conclusion**

Theoretical and technical background information related to man-made soils or tailings has been summarised in this chapter. The generation of tailings from mineral processing passes through numerous main stages: crushing, grinding, concentration, dewatering and tailing slurry disposal. Furthermore, optional processes (i.e. leaching or heating) may follow or substitute for the process of concentration. Significantly, there is a difference in the physical characteristics of tailings, which can be attributed to the site, type of ore or the milling process or deposition approach used. Traditionally, tailings are deposited in slurry form and are stored in surface impoundments. Two types of impoundments according to the construction method used are known worldwide: water-retention-type dams and raised embankment dams. There are three forms of raised embankment dams according to the construction method used: upstream, downstream and centreline dams. Although the upstream method costs less than the downstream and centreline methods, it has been reported to be more susceptible to liquefaction. Earthquake-induced liquefaction failure of tailings impoundments is a common issue specifically in highly seismic areas. With the development of the dewatering or densification technology, tailings can be deposited on the earth surface in one of the following forms: thickened, paste and dry-stack tailings. Generally, these forms of tailings provide an important benefit in terms of reducing the geotechnical risks associated with the failure of tailings dams as no dams need to be constructed. The high solid contents in such highly densified or dewatered tailings lead to increased strength of the tailings, which consequently increases their resistance to liquefaction.

## 2.4. **References**


Anglo. (2004). Debswana Diamond Company: Orapa and Lethlhakane Mines-Orapa Mine No.1 Plant Slimes Dam Operating Manual. Report NO. CED/002/2004. Geoflux, Gabarone, Botswana and Anglo & American Technical Division, Johannesburg, South Africa.

Alshawmar, F, Fall M (2020). Earthquake induced liquefaction potential of paste tailings: shaking table results. Proceedings of the 5rd International Conference on Civil Structural and Transportation Engineering (ICCSTE'20), Paper No. 159, DOI: 10.11159/iccste20.159

Bjelkevik, A. (2005). Water cover closure design for tailings dams: state of the art report. Department of Civil and Environmental Engineering, Division of Geotechnology, Lulea˚University of Technology, Sweden.

Boger, D.V. (2013). Rheology of slurries and environmental impacts in the mining industry. Annual review of chemical and biomolecular engineering, 4: 239-257.

Bull, A.J., Fall, M. (2020). Thermally induced changes in metalloid leachability of cemented paste backfill that contains blast furnace slag. Minerals Engineering 156, 106520.

Bussière, B. (2007). Colloquium 2004: hydrogeotechnical properties of hard rock tailings from metal mines and emerging geoenvironmental disposal approaches. Canadian Geotechnical Journal, 44(9): 1019-1052.

Chryss, A. (2017). Effects of clay in tailings handling and storage. Clays in the Mineral Processing Value Chain, Gräfe, M., Klauber, C., McFarlane, A.J., and Robinson, D.J., Eds., Cambridge University Press, Cambridge, UK, pp. 381-399.

Daliri, F. (2013). The influence of desiccation and stress history on monotonic and cyclic shear response of thickened gold tailings. PhD thesis, Department of Civil and Environmental Engineering, Carleton University, Ottawa, Ontario, Canada.

Davies, M. (2011). Filtered dry stacked tailings-the fundamentals. In Proceedings of the 15th International Conference on Tailings and Mine waste '11, 6-9 November 2011, Vancouver, British Colombia, Canada, pp. 1-10.

Davies, M.P., and Rice, S. (2001). An alternative to conventional tailings management- "dry stack" filtered tailings. In Proceedings of the 8th International Conference on Tailings and Mine Waste '01, 15-18 January 2001, Fort Collins, Colorado, USA, pp. 411-420.

Davies, M.P., Lighthall, P.C., Rice, S., and Martin, T.E. (2002). Design of tailings dams and impoundments. Keynote address, Tailings and Mine Waste Practices SME, AGM Phoenix, pp. 1-18.

Davies, M.P., Lupo, J., Martin, T., McRoberts, E., Musse, M., and Ritchie, D. (2010). Dewatered Tailings Practice-Trends and Observations. In Proceedings of 14th annual Tailings and Mine Waste Conference, 17-20 October 2010, Vail, Colorado, USA, pp.133-142.

Edraki, M., Baumgartl, T., Manlapig, E., Bradshaw, D., Franks, D.M., and Moran, C.J. (2014). Designing mine tailings for better environmental, social and economic outcomes: a review of alternative approaches. Journal of Cleaner Production, 84: 411-420.

Engels, J. (2002). High density thickened tailings (HDTT) storage. See http://www.tailings.info/disposal/thickened.htm [accessed December 20, 2017].

Fall, M., and Samb, S.S. (2009). Effect of high temperature on strength and microstructural properties of cemented paste backfill. Fire Safety Journal 44 (4): 642-651.

Fall, M., Célestin, J.C., Han F.S. (2009). Potential use of bentonite-paste tailings mixtures as engineering barrier material for hazardous waste containment facilities: Experimental results. GeoHalifax2009.

Fang, K., Fall, M. (2020). Shear Behaviour of rock–tailings backfill interface: effect of cementation, rock type, and rock surface roughness. Geotechnical and Geological Engineering, 1-18.

Cui, L., Fall, M (2018). Mathematical modeling and analysis of in-situ strength development in cemented paste backfill structure. GeoEdmonton 2018.

Geremew, A.M., and Yanful, E.K. (2013). Dynamic properties and influence of clay mineralogy types on the cyclic strength of mine tailings. International Journal of Geomechanics, 13(4): 441-453.

Ghirian, A., Fall, M. (2016). Influence of curing stress on long-term hydro-mechanical response of cemented paste backfill. Proceedings tailings and mine waste, Keystone, Colorado, USA.

Haruna, S., and Fall, M. (2020). Time-and temperature-dependent rheological properties of cemented paste backfill that contains superplasticizer. Powder Technology, 360: 731-740.

Heidarian, P. (2012). Effect of initial water content and stress history on water-retention behaviour of mine tailings. Master thesis, Department of Civil and Environmental Engineering, Carleton University, Ottawa, Ontario, Canada.

Hu, L., Wu, H., Zhang, L., Zhang, P., and Wen, Q. (2017). Geotechnical properties of mine tailings. Journal of Materials in Civil Engineering, 29(2): 04016220.

James, M., Aubertin, M., and Bussière, B. (2013). On the use of waste rock inclusions to improve the performance of tailings impoundments. In Proceedings of the 18th International Conference on Soil Mechanics and Geotechnical Engineering, 2-6 September 2013, Paris, France, pp. 735-738.

Lyu, Z., Chai, J., Xu, Z., Qin, Y., and Cao, J. (2019). A comprehensive review on reasons for tailings dam failures based on case history. Advances in Civil Engineering, 2019.

Meggyes, T., and Debreczeni, Á. (2006). Paste technology for tailings management. Land Contamination and Reclamation, 14(4): 815-827.

Qiu, Y.X., and Sego, D.C. (2001). Laboratory properties of mine tailings. Canadian Geotechnical Journal, 38(1): 183-190.

Rico, M., Benito, G., Salgueiro, A.R., Díez-Herrero, A., and Pereira, H.G. (2008). Reported tailings dam failures: a review of the European incidents in the worldwide context. Journal of Hazardous Materials, 152(2): 846-852.

Robinsky, E., Barbour, S.L., Wilson, G.W., Bordin, D., and Fredlund, D.G. (1991). Thickened sloped tailings disposal-an evaluation of seepage and abatement of acid drainage. In Proceedings of the Second International Conference on the Abatement of Acidic Drainage, Invited Lecture, 16-18 September 1991, Montreal, Quebec, Canada, pp. 529-549.

Robinsky, E.I. (1975). Thickened discharge-a new approach to tailings disposal. Canadian Mining and Metallurgical Bulletin, 68(764): 47-53.

Roshani, A., Fall, M., and Kennedy, K. (2017). Drying behavior of mature fine tailings pre-dewatered with super-absorbent polymer (SAP): Column Experiments. Geotechnical Testing Journal, 40(2): 210-220.

Roshani, A., Fall, M., and Kennedy, K. (2018). Microstructural, hydraulic conductivity and geochemical changes of drying mature fine oil sand tailings in column experiments. International Journal of Mining, Reclamation and Environment, 32(4): 239-253.

Theriault, J., Frostiak, J., and Welch, D. (2003). Surface disposal of paste tailings at the Bulyanhulu gold mine, Tanzania. In Proceedings of Mining and the Environment Conference III, 25-28 May 2003, Sudbury, Ontario, Canada, pp. 1-8.

Verburg, R.B.M. (2001). Use of paste technology for tailings disposal: potential environmental benefits and requirements for geochemical characterization. In Proceedings of the International Mine Water Association Symposium, 24-28 April 2001, Belo Horizonte, Brazil, pp. 1-13.

Vick, S.G. (1983). Planning, design and analysis of tailings dams. John Wiley & Sons, New York, USA.

Wickland, B.E., and Wilson, G.W. (2005). Self-weight consolidation of mixtures of mine waste rock and tailings. Canadian Geotechnical Journal, 42(2): 327-339.

Wijewickreme, D., Sanin, M.V., and Greenaway, G.R. (2005). Cyclic shear response of fine-grained mine tailings. Canadian Geotechnical Journal, 42(5):1408-1421.

Xiao, B., Fall, M., Roshani, A. (2020). Towards understanding the rheological properties of slag-cemented paste backfill. International Journal of Mining, Reclamation and Environment, 1-23.

# 3 Chapter 3: Cyclic Liquefaction Behaviour of Natural and Man-Made Fined-Grained Soils

## 3.1. Introduction

An overview of the pertinent literature is considered essential to obtain baseline knowledge from which new research can be conducted. In this chapter, an overview of several aspects of the liquefaction phenomenon is presented. These include the definition of the liquefaction phenomenon and the factors that can affect the liquefaction susceptibility of soils. In addition, the existing screening criteria for the evaluation of the liquefaction susceptibility of sand and fine-grained soils are presented. The findings from previous studies on the seismic or cyclic liquefaction behaviour of natural and man-made fine-grained soils are also reviewed herein. The previous studies on the seismic or cyclic liquefaction behaviour of man-made fine-grained soils include those that were conducted on highly densified tailings and cemented paste backfill (CPB) tailings.

## 3.2. Definition of seismic liquefaction phenomena

The Alaska (1964) and Niigata (1964) earthquakes that caused disastrous failures due to soil liquefaction led the researchers to develop an interest in this type of phenomenon in the active seismic areas around the world (Seed et al., 1976). In the field of geotechnical engineering, the term *liquefaction* has been used to denote different phenomena. For instance, Seed et al. (1976) identified the three phenomena below for which the term *liquefaction* is used.

i. *Liquefaction*: A condition where soil experiences continued deformation at a constant low residual stress or without residual resistance because of the generation of high pore water pressure, which reduces the effective confining pressure to a very low value. The applications of static or cyclic stress can cause the generation of such pore water pressure.
ii. *Initial liquefaction*: A condition where, during the course of cyclic stress applications, the residual pore water pressure after the completion of any full stress cycle becomes equal to the applied confining pressure. The development of initial liquefaction has no implications on the magnitude of the deformation that the soil may subsequently undergo, but it defines a condition that is a useful basis for assessing various possible forms of subsequent soil behaviour.
iii. *Initial liquefaction with limited strain potential or cyclic mobility*: A condition in which cyclic stress applications develop a condition of initial liquefaction, and the subsequent cyclic stress applications cause limited strains to develop either because of the remaining resistance of the soil to deformation or because the soil dilates, the pore pressure drops and the soil stabilises under the applied loads.

In addition, Boulanger and Idriss (2006) recommended the use of the term liquefaction to describe the development of considerable strains or loss of strength in fine-grained soils that display behaviour similar to that of sand (i.e. sand-like behaviour), while they recommended the term cyclic softening to describe a phenomenon similar to that in fine-grained soils, which display behaviour similar to that of clay (i.e. clay-like behaviour). The liquefaction phenomenon is generally known to increase the pore water pressure and diminish the effective stress in soil. This leads to the loss of strength and stiffness of the soil. This phenomenon can result either from monotonic (i.e. static) loading or cyclic (i.e. dynamic) earthquake loading. According to Prakash (1981), once the shear strength of the soil is completely lost, it will manifest a behaviour similar to that of viscous fluid.

The following description related to soil liquefaction is based on the works of Poulos et al. (1985) and Perlea (2000). During the liquefaction of cohesionless soil, the increase of the pore water pressure and the decrease of the effective stress of such soil diminish the contacts between their particles, as shown in Figure 3.1. The loss of shear strength of fine-grained soils is considered not substantial, however, unlike in the case of cohesionless soil. This is because the cohesion of fine-grained soils has the ability to preclude the separation of the particles. Contractive soils (i.e. loose soils), which are subject to volume reduction, are considered susceptible to liquefaction behaviour while dilative soils (i.e. dense soils) are not subject to liquefaction behaviour because their drained strength is lower than their undrained strength. The occurrence of liquefaction basically puts the soil in a steady undrained state of deformation, wherein the soil is subjected to continuous deformation at a constant volume, a constant vertical stress, a constant shear stress and a constant shear strain rate. When the driving shear strength is larger than the steady-state shear strength (i.e. residual shear strength), the soil is susceptible to liquefaction behaviour under either monotonic or cyclic loading, as shown in Figure 3.2. The driving shear strength is termed *shear stress*, which is needed to maintain static equilibrium.

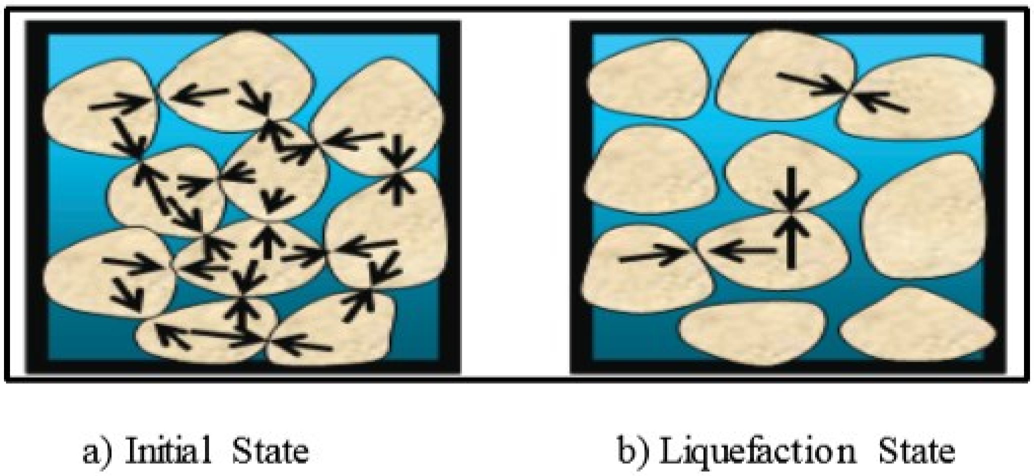


Figure 3.1. Diminishing of the contacts between the soil particles due to an increase in the pore water pressure and a decrease in the effective stress in the liquefaction state (Al-Tarhouni, 2008)

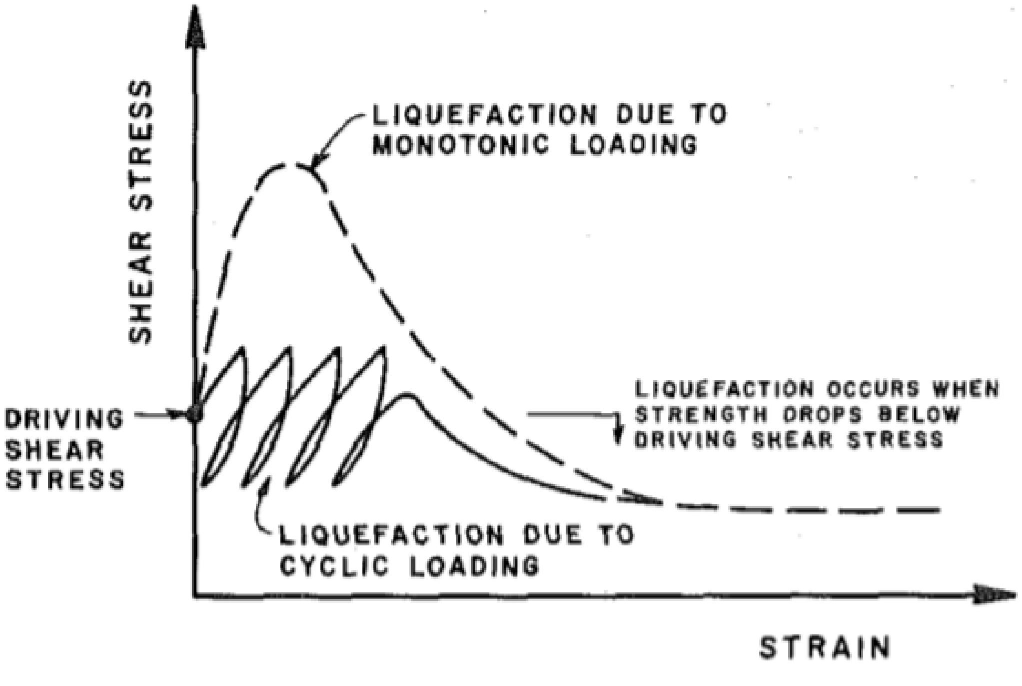


Figure 3.2. Liquefaction due to monotonic or cyclic loading (Poulos et al., 1985)

## 3.3. **Factors that can affect the liquefaction susceptibility of soils**

Numerous previous studies have reported that the susceptibility of soils to liquefaction can be affected by different factors (Seed and Peacock, 1971; Ladd, 1974; De Alba et al., 1976; Mulilis et al., 1977; Seed et al., 1977; Campanella and Lim, 1981; Ishihara et al., 1981; Tokimatsu and Yoshimi, 1983; Puri, 1984; Prakash and Sandoval, 1992; Guo and Prakash, 1999; Crowder, 2004; Kim et al., 2011; Varghese and Latha, 2014; Cui et al., 2020), such as the relative density, grain size distribution, the specimen preparation method used, aging, previous strain history (seismic history), coefficient of lateral earth pressure at rest ($K_o$), overconsolidation ratio (OCR), plasticity index (PI) and effective confining stress.

To study the effect of the relative density of sand on its cyclic stress ratio (CSR), which causes initial liquefaction, De Alba et al. (1976) conducted laboratory tests on samples of Monterey No. 0 sand at different relative densities (54%, 68%, 82% and 90%). They used a one-direction shaking table for inducing cyclic shear stress in the sand samples. They found that a larger relative density requires a larger CSR to cause initial liquefaction. This means that soil with larger relative density had more resistance to initial liquefaction as illustrated in Figure 3.3. Because of the effect of the small volume changes that occurred in the testing system, the researchers applied correction factors ranging from 0.7 to 0.8 to correct the cyclic shear stress ($\tau_h$), which is based on the number of cycles. Similarly, Varghese and Latha (2014) conducted shaking-table tests to understand the influence of relative density on the liquefaction potential of sand. The relative density of the sand in their study varied from 43% to 67%, where the acceleration amplitude and frequency of base shaking that were applied were 0.15 g and 1 Hz, respectively. They found that the sand experienced full liquefaction for the relative densities of 43% and 58% while the sand with a relative density of 67% did not liquefy (Figure 3.4). In their study, liquefaction occurred when the $r_u$ reached 1.0.

Tokimatsu and Yoshimi (1983) conducted a review of the field behaviour during the previous numerous earthquakes, together with laboratory tests on undisturbed sand samples, to investigate the influence of the grain size distribution on liquefaction resistance. Their study revealed the following: (i) sands with more than 10% fines have considerably larger liquefaction resistance than clean sands under identical standard penetration test (SPT) N-values; (ii) soils with more than 20% clay may be hardly subject to liquefaction unless they have low PIs; and (iii) soils with gravel particles appear to have lower resistance to liquefaction than clean sand without gravel under identical SPT N-values.

Ladd (1974) investigated the effect of specimen preparation methods on the liquefaction behaviour of sand samples. He prepared the samples using two methods: dry vibration and wet tamping. The triaxial apparatus was used to induce cyclic stresses in the samples. It was found that the samples prepared through wet tamping had higher resistance to liquefaction than the samples prepared through dry vibration. In addition, it was noticed that the cyclic strength of the samples prepared through wet tamping was almost twice that of the samples prepared through dry vibration. He attributed the difference in liquefaction resistance to the structures of the sand samples prepared using two different methods. Mulilis et al. (1977) studied the effect of the specimen preparation method on the liquefaction behaviour of saturated sand samples using the triaxial apparatus under an undrained condition. They used the following specimen preparation methods, with a comparable relative density of 50%: (i) soil pluviation through air; (ii) soil pluviation through water; (iii) high-frequency (120 Hz) vibration application on dry samples; (iv) high-frequency (120 Hz) vibration application on moist samples; (v) low-frequency (20 Hz) vibration application on dry samples; (vi) moist tamping; (vii) moist rodding and (viii) dry-soil rodding. They observed that, as illustrated in Figure 3.5, the samples prepared using soil pluviation through air had the lowest resistance to soil liquefaction among all the prepared samples, but the samples prepared using high-frequency (120 Hz) vibration application on moist samples had the highest resistance to soil liquefaction among all the prepared samples. The observed differences in the liquefaction resistance of the samples prepared using different methods were due to the differences in the orientation of the contacts between the sand particles and in the packing (i.e. structure/fabric).

Campanella and Lim (1981) carried out undrained cyclic triaxial tests on undisturbed samples of aged and unaged clayey silt to study the effect of aging on liquefaction behaviour. The samples of clayey silt were aged to a maximum of 19 days. As shown in Figure 3.6, the results revealed that the aged clayey silt samples had almost 25% larger resistance to liquefaction than the unaged clayey silt samples.

Seed et al. (1977) studied the effect of previous strain history (seismic history) on the liquefaction of sand samples. For comparison purposes, they also tested the liquefaction of sand samples with no previous strain history (seismic history). A shaking table was used in the study to induce cyclic shear stresses under simple shear conditions. It was found that the previous strain history led to an increase in the sand samples' resistance to liquefaction, as shown in Figure 3.7, which could have been due to the increase in the $K_o$ due to the previous strain history as well as to the change in the soil structure (i.e. fabric). Moreover, under identical densities, the sand samples with a previous strain history needed stresses approximately 45% greater than those of the sand samples with no previous strain history.

Seed and Peacock (1971) used the simple shear apparatus to investigate the effect of OCR and $K_o$ on the liquefaction resistance of saturated sandy soils. Different OCRs (1, 4 and 8) were used in the investigation, and the $K_o$ values were calculated based on the previous OCRs. The results indicated, as shown in Figure 3.8, that as the OCR increased, the $K_o$ also increased, and thus the resistance of the saturated sandy soils to liquefaction likewise increased. Campanella and Lim (1981) carried out undrained cyclic triaxial tests on undisturbed silty clay and clayey silt samples to examine the effect of OCR on such samples' liquefaction behaviour. OCRs of 1, 2 and 4 were used in the study. It was found that the 2 and 4 OCRs increased the resistance of the soil samples to liquefaction by almost 75% and 150%, respectively. Similar results were obtained by Puri (1984), who performed a laboratory study using the cyclic triaxial apparatus to examine the effect of different OCRs (i.e. 1, 2 and 4) on the liquefaction resistance of undisturbed and reconstituted specimens of loessial (silty) soils. On the basis of the relationship between the CSR and the number of cycles that induced initial liquefaction for the tested specimens shown in Figure 3.9, the researcher concluded that as the OCR increased, the resistance of the specimens to liquefaction also increased. Kim et al. (2011) conducted cyclic direct simple shear testing (NGI-type) on low-plasticity thickened gold tailings with a void ratio ranging from ~0.60 to 0.68. The results indicated that the susceptibility of the low-plasticity thickened gold tailings to liquefaction decreased as the OCR increased.

Ishihara et al. (1981) conducted cyclic triaxial tests on undisturbed specimens of fine-grained tailings with PIs ranging from 10 to 40 and found that the resistance of the specimens to liquefaction tended to somewhat increase with increasing PI. Puri (1984) studied the effect of PI on the liquefaction resistance of reconstituted specimens of silt and silt−clay mixtures with PIs ranging from 10% to 20% using the cyclic triaxial apparatus. He found that the resistance of the tested soils to liquefaction increased with increasing PI (in the tested plasticity range), as shown in Figure 3.10. Prakash and Sandoval (1992) investigated the effect of PI on the liquefaction resistance of low-plasticity pure silt (PI = 1.7), 95% silt with 5% clay (PI = 2.6) and 90% silt with 10% clay (PI = 3.4) by conducting cyclic triaxial tests. The results indicated that the resistance of the tested soils to liquefaction diminished with increasing PI (in the low plasticity range), as shown in Figure 3.11. Guo and Prakash (1999) combined the results of the works conducted by Puri (1984) and Prakash and Sandoval (1992) in one graph to present the effect of PI on the liquefaction resistance of silt−silty clay mixtures, as shown in Figure 3.12. On the basis of the data presented in Figure 3.12, Guo and Prakash (1999) stated that there was a critical PI that divided the behaviour of the liquefaction resistance of silt−silty clay mixture into low and high plasticity ranges. In the case of the PIs below the critical PI, the addition of clay grains led to a decrease in the mixture's coefficient of permeability, which then led to the larger generation of pore water pressure and consequently diminished the resistance to liquefaction. In the case of the PIs above the critical PI, the addition of clay grains provided some cohesion to the mixture, which consequently increased the mixture's resistance to liquefaction.

Campanella and Lim (1981) performed undrained cyclic triaxial tests on undisturbed specimens of fine sandy silt soils to study the effect of consolidation stress on such soils' liquefaction resistance. The specimens were normally subjected to 980, 1,470 and 1,960 kPa consolidation stress before the cyclic-loading stage. The results indicated that the liquefaction resistance of the fine-sandy-silt-soil specimens was not affected by the consolidation stress. Similar results were obtained by Puri (1984), who carried out cyclic triaxial tests on undisturbed and reconstituted specimens of loessial (silty) soils to examine their resistance to liquefaction under different effective-confining-stress values (10, 15 and 20 psi). For a given CSR, the researcher noticed that the number of cycles for inducing initial liquefaction for the tested soils was somewhat independent of the initial effective confining stress, as shown in Figure 3.13. Crowder (2004) performed cyclic triaxial tests on the Bulyanhulu tailings (i.e. non-paste tailings) to investigate such tailings' resistance to liquefaction under the two effective confining stress values of 50 and 150 kPa. He concluded that there was no difference between the values obtained from the tests that were performed at 50 kPa and at 150 kPa.

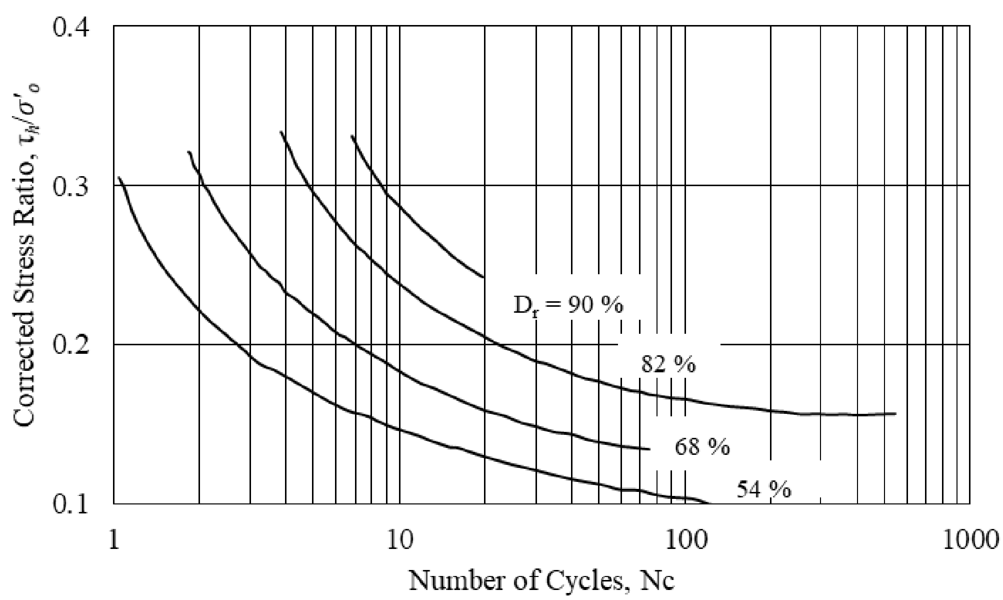


Figure 3.3. Effect of relative density on the corrected cyclic stress ratio that caused initial liquefaction of Monterey No. 0 sand (De Alba et al., 1976)

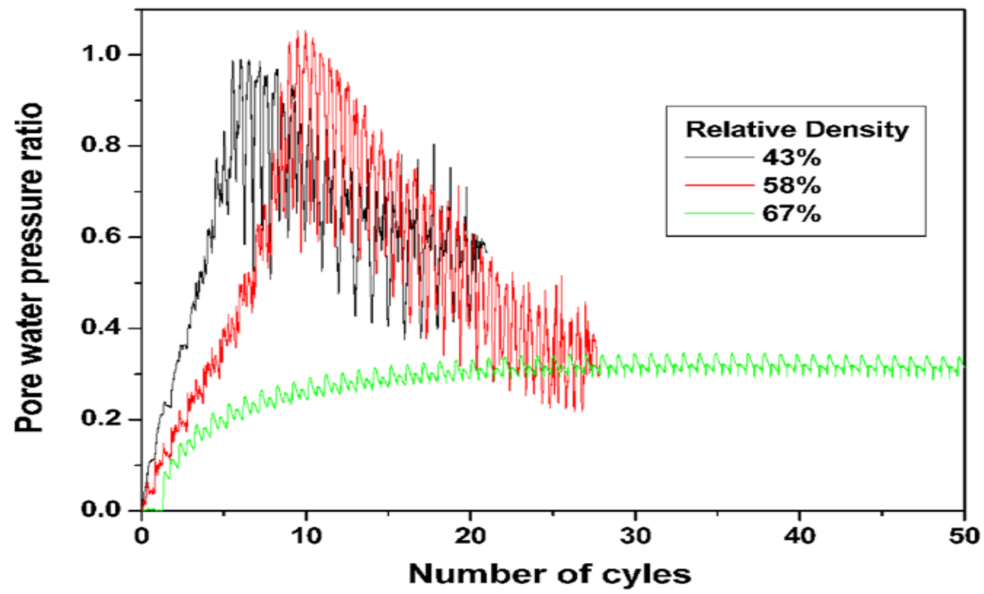


Figure 3.4. Generation of pore water pressure in sand with different relative densities (Varghese and Latha, 2014)

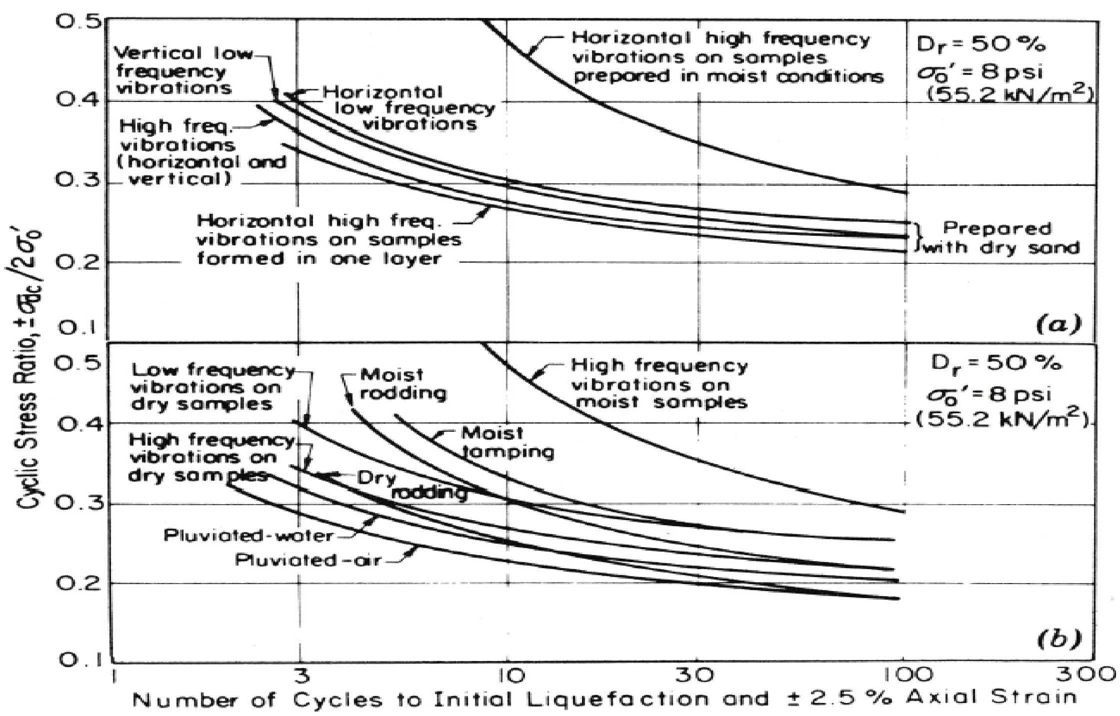


Figure 3.5. Effect of the sample preparation method on the liquefaction resistance of saturated sandy soil (Mulilis et al., 1977)

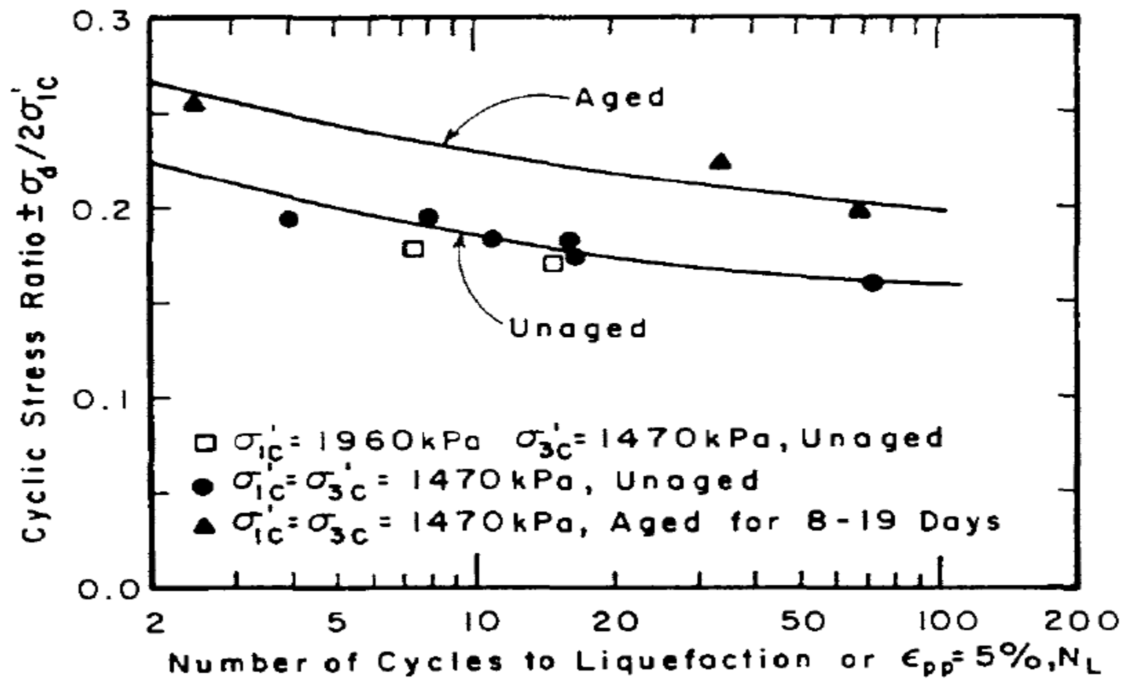


Figure 3.6. Comparison of the liquefaction resistance values of aged and unaged clayey silt samples (Campanella and Lim, 1981)

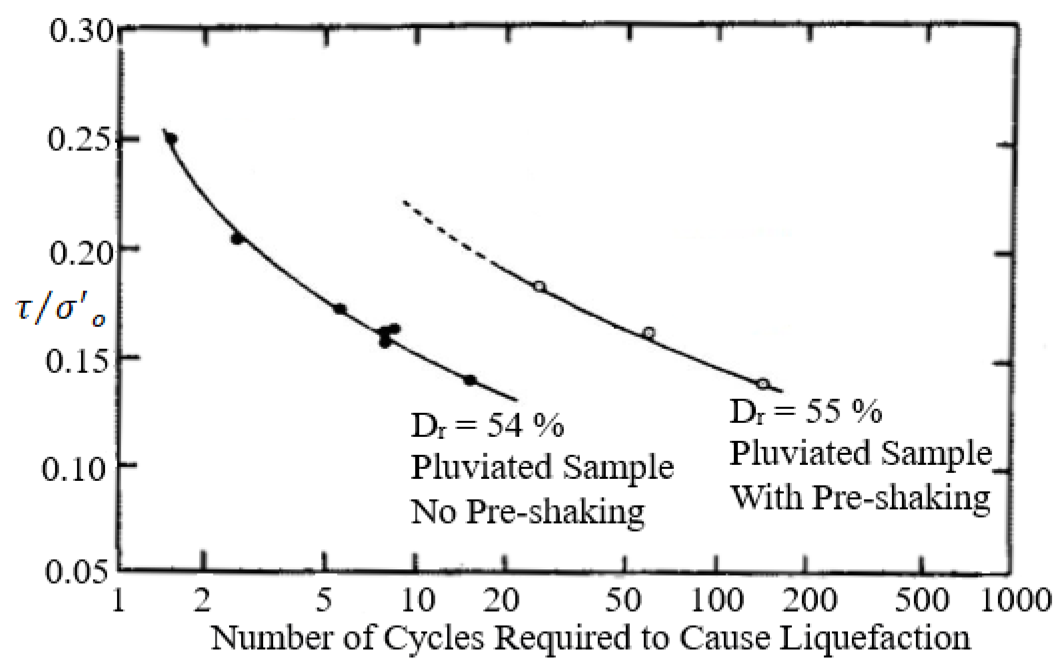


Figure 3.7. Effect of previous strain history on the liquefaction of sands (Seed et al., 1977)

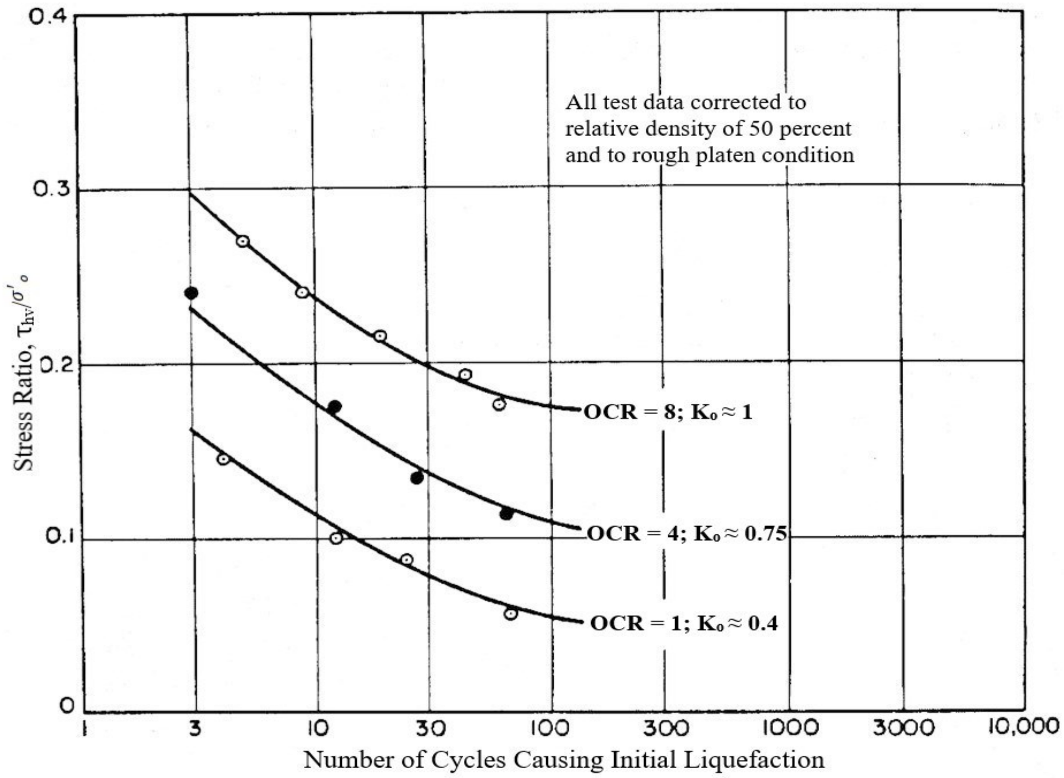


Figure 3.8. Effect of overconsolidation ratio (OCR) on the cyclic stress ratio (CSR) causing liquefaction of saturated sands (Seed and Peacock, 1971)

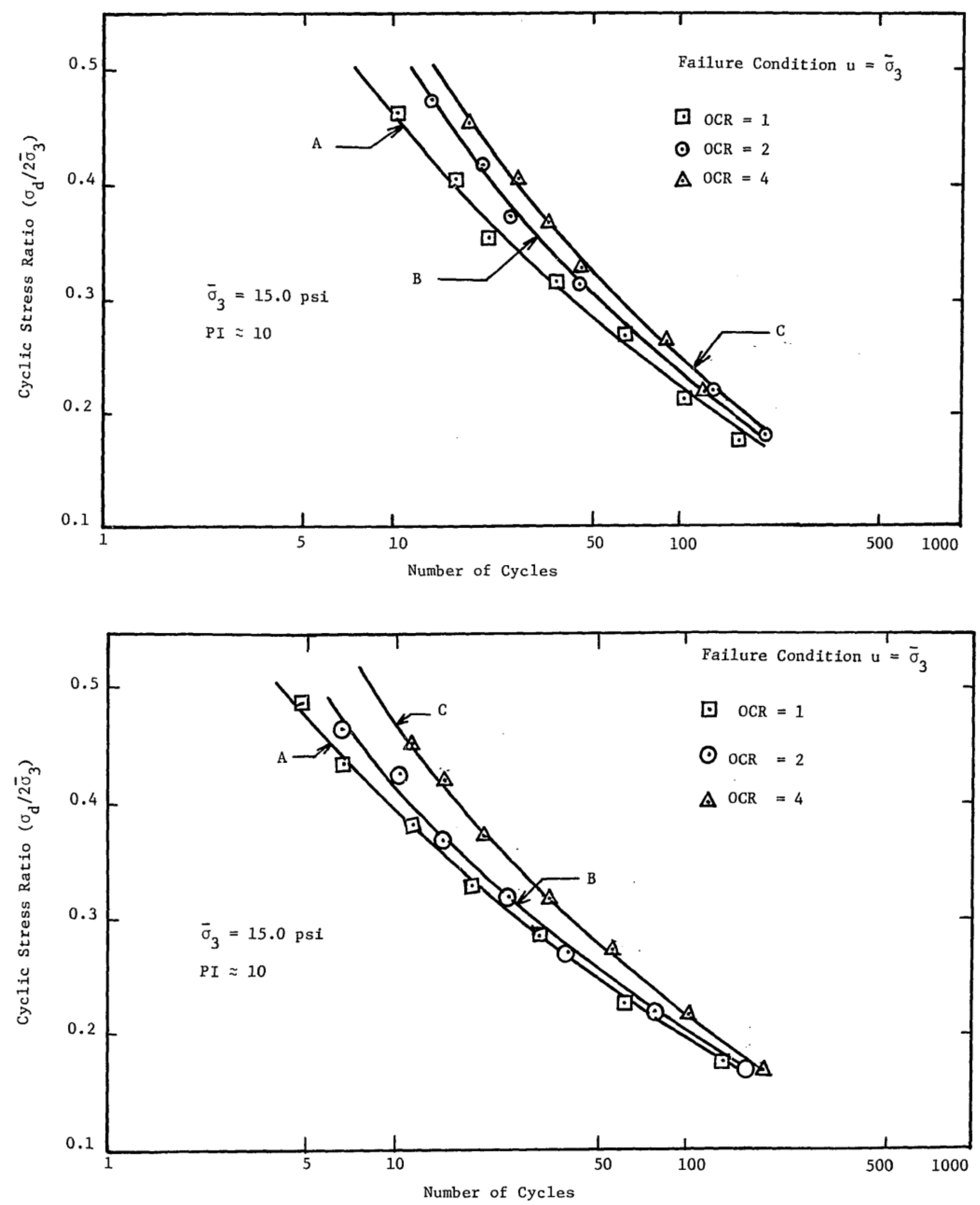


Figure 3.9. Relationship between cyclic stress ratio (CSR) and the number of cycles for inducing initial liquefaction in undisturbed and reconstituted specimens of loessial (silty) soils under different overconsolidation ratios (OCRs) (Puri, 1984)

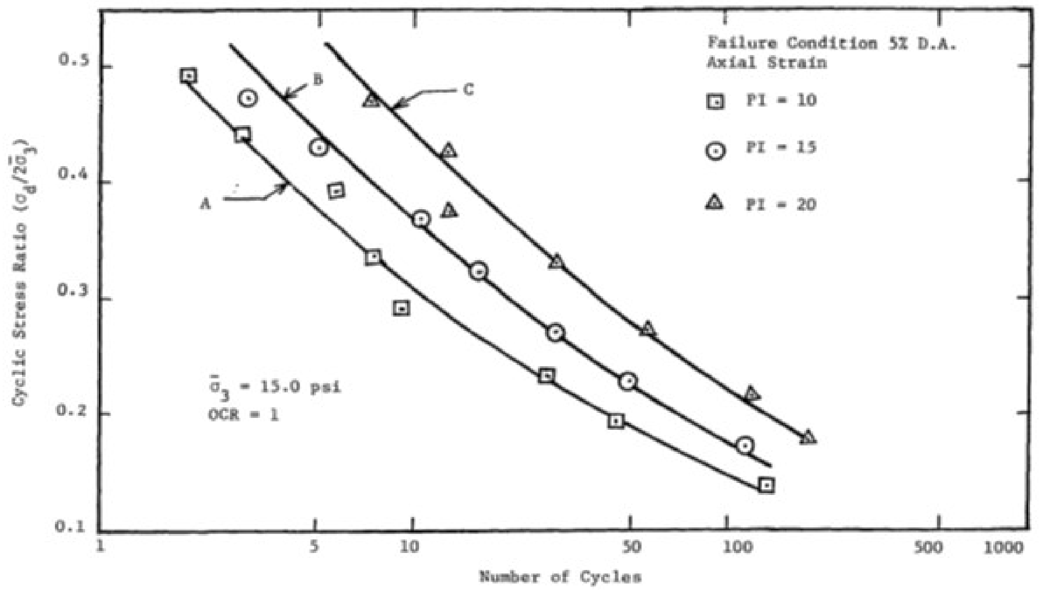


Figure 3.10. Cyclic stress ratio (CSR) vs. number of cycles for inducing initial liquefaction in reconstructed saturated specimens for different plasticity index (PI) values (10−20%) causing 5% double-amplitude (DA) axial strain (Puri, 1984)

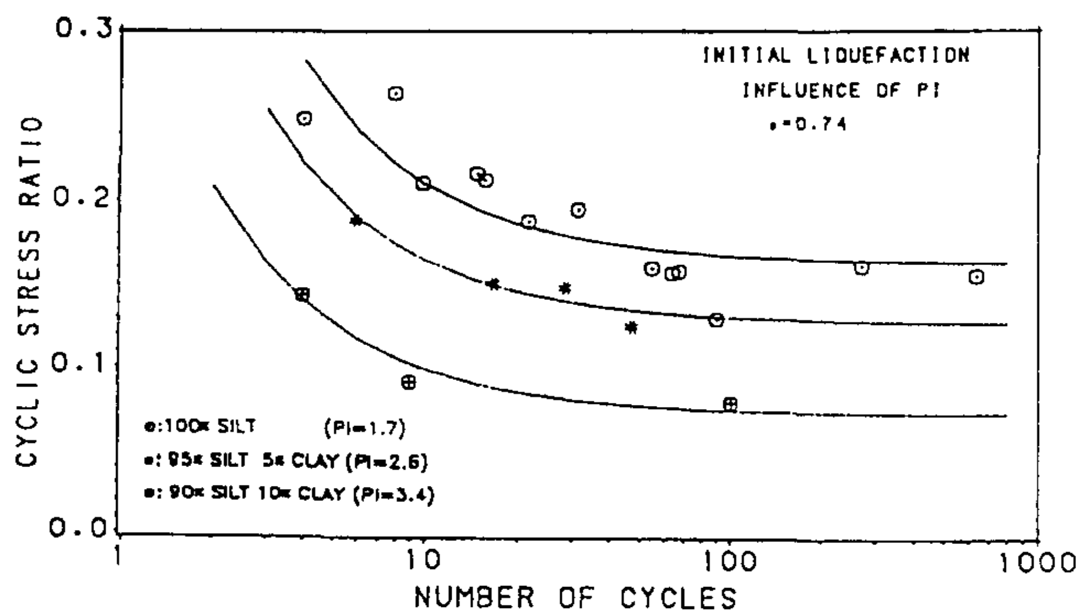


Figure 3.11. Cyclic stress ratio (CSR) vs. number of cycles for inducing initial liquefaction in low-plasticity pure silt (plasticity index [PI] = 1.7), 95% silt with 5% clay (PI = 2.6) and 90% silt with 10% clay (PI = 3.4) (Prakash and Sandoval, 1992)

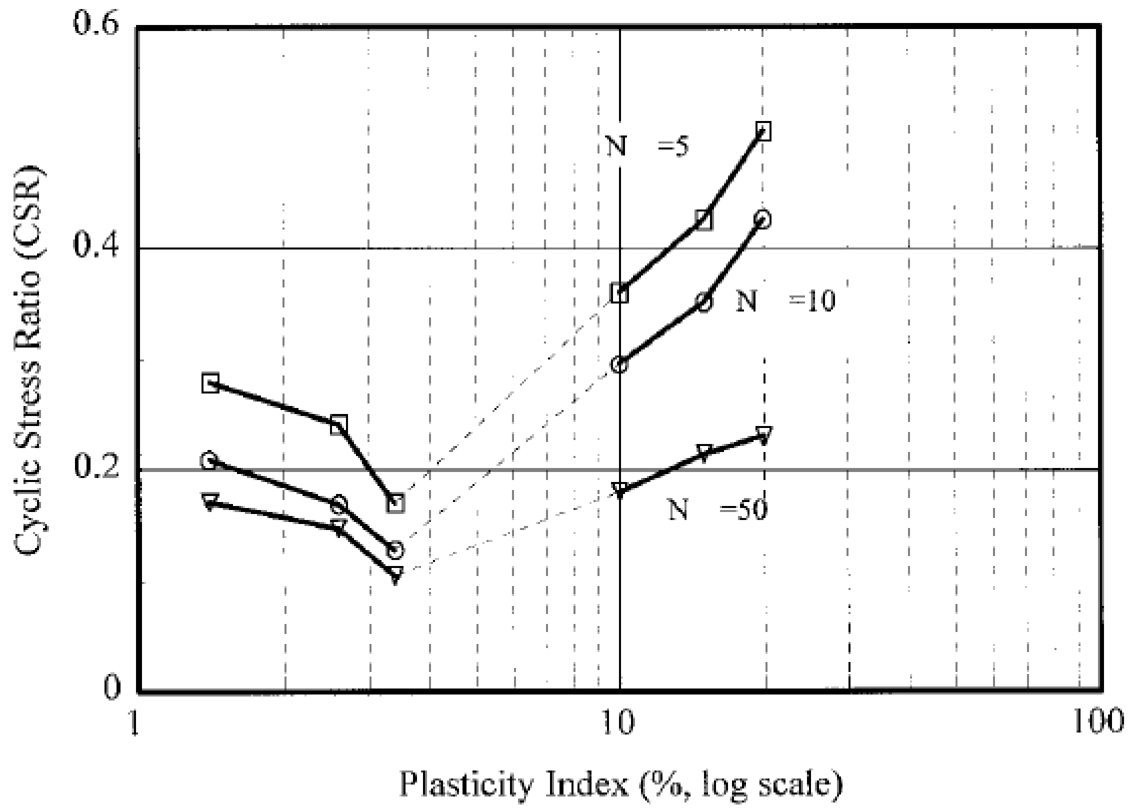


Figure 3.12. Cyclic stress ratio (CSR) vs. plasticity index (PI) for silt−clay mixtures (CSR normalised to initial void ratio = 0.74) (Guo and Prakash, 1999)

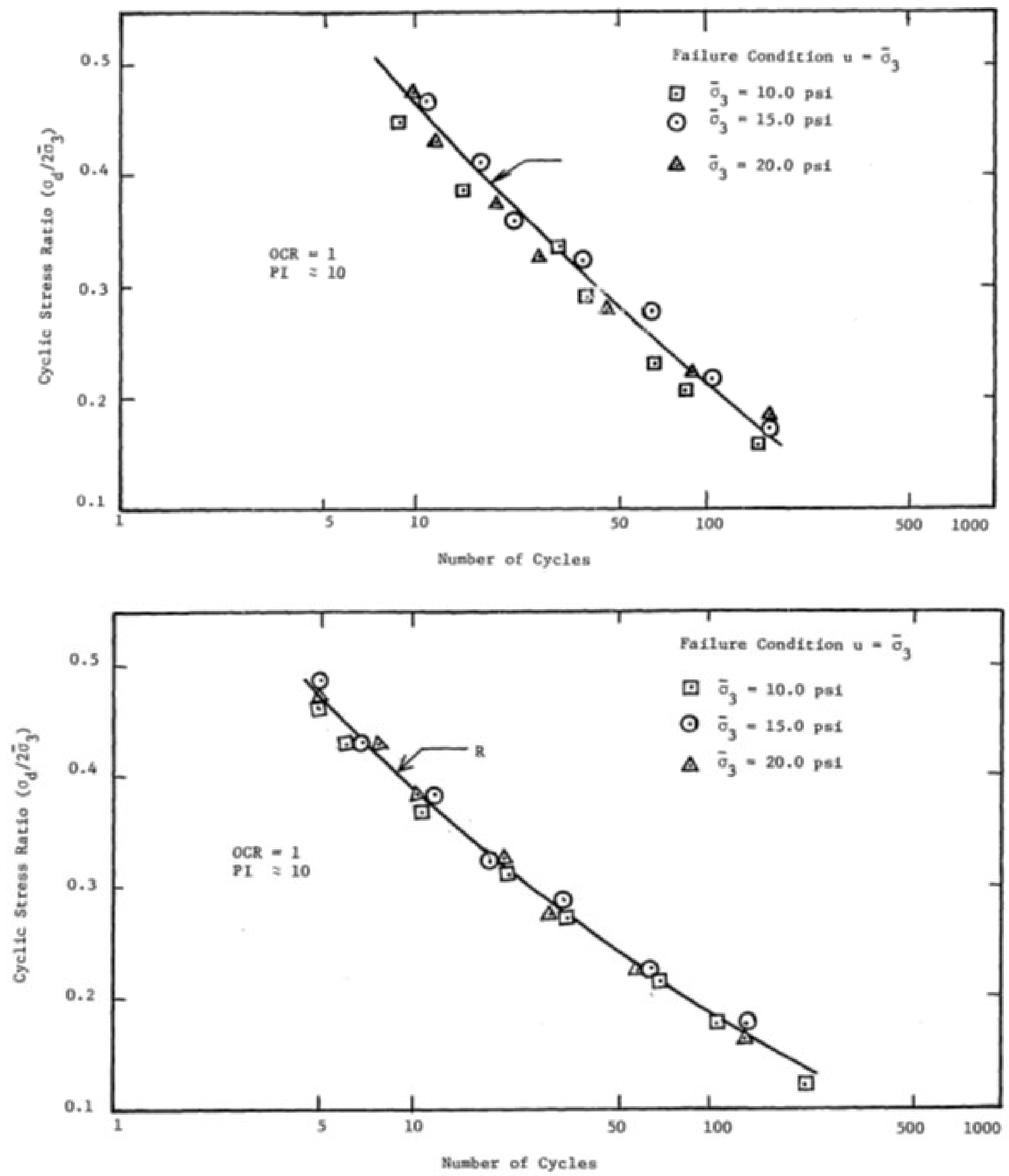


Figure 3.13. Relationship between cyclic stress ratio (CSR) and the number of cycles for inducing initial liquefaction in undisturbed and reconstituted specimens of loessial (silty) soils for different effective confining stress values (Puri, 1984)

## 3.4. Liquefaction criteria for soils

### 3.4.1. Liquefaction criteria for sand soil based on field testing techniques

Several studies were performed to predict the liquefaction susceptibility of sandy soil through laboratory testing using different apparatuses (i.e. cyclic triaxial apparatus, cyclic simple shear apparatus and shaking table) (Prakash and Puri, 2010). The difficulty in obtaining undisturbed specimens of sand and the related cost of carrying out the laboratory tests prompted the investigators to use several common empirical methods based on different field test techniques, such as the standard penetration resistance (SPT), the cone penetration test (CPT), shear wave velocity ($V_s$) and the Becker penetration test (BPT), to predict the liquefaction susceptibility of sandy soil (Zhang et al., 2002; Prakash and Puri, 2010).

Following the catastrophic earthquakes in Alaska, USA and Niigata, Japan in 1964, the term *simplified procedure* based on the SPT blow counts was proposed by Seed and Idriss in 1971 for use as a criterion for assessing the liquefaction resistance of sand (Youd et al., 2001). As the simplified procedure of Seed and Idriss (1971) is considered valid only for a magnitude 7.5 earthquake, however, Seed and Idriss (1982) added a scaling factor known as the magnitude scaling factor (MSF) to make the simplified procedure valid for all earthquake magnitudes. The recommended value of MSF can be found in the paper of Youd et al. (2001).

To assess the liquefaction resistance of soils using the aforementioned simplified procedure, two parameters are required: (i) CSR, which represents the seismic loading on a soil layer induced by an earthquake; and (ii) cyclic resistance ratio (CRR), which represents the capacity of soil to resist liquefaction (Youd et al., 2001). As per the modified simplified procedure of Seed and Idriss (1982), the CSR of the field test methods (SPT, CPT and $V_s$) can be calculated for a given earthquake at a specific soil depth using the following equation:

$$\mathbf{CSR} = \mathbf{0.65}\left(\frac{\boldsymbol{a_{max}}}{\boldsymbol{g}}\right)\left(\frac{\boldsymbol{\sigma_{vo}}}{\boldsymbol{\sigma'_{vo}}}\right)\left(\frac{\boldsymbol{r}_{\mathbf{d}}}{\mathbf{MSF}}\right) \qquad \textbf{(3.1.)}$$

where $a_{max}$ is the peak horizontal acceleration at the ground surface generated by the earthquake, $g$ is the gravity acceleration, $\sigma_{vo}$ is the total vertical overburden stress, $\sigma'_{vo}$ is the effective vertical overburden stress, MSF is the magnitude scaling factor and $r_d$ is the stress reduction coefficient related to soil flexibility. According to Youd et al. (2001), this stress reduction coefficient can be found from a graph or can be calculated using the equations below.

$$\boldsymbol{r_d} = \mathbf{1.0} - \mathbf{0.00765}\boldsymbol{z} \qquad \textbf{for } \boldsymbol{z} \leq \textbf{9.15 m} \qquad \textbf{(3.2.)}$$

$$\boldsymbol{r_d} = \mathbf{1.174} - \mathbf{0.0267}\boldsymbol{z} \qquad \textbf{for 9.15 m} < \boldsymbol{z} \leq \textbf{23 m} \qquad \textbf{(3.3.)}$$

where $\boldsymbol{z}$ is the depth below ground surface in meters. To use the SPT criterion for determining the CRR of soils, the corrected blow count $(N_1)_{60}$ needs to be calculated first using the following equation:

$$(\boldsymbol{N_1})_{\mathbf{60}} = \boldsymbol{N_m C_N C_E C_B C_R C_S} \qquad \textbf{(3.4.)}$$

where $N_m$ is the measured standard penetration resistance, $C_N$ is a factor for normalising $N_m$ to a common reference effective overburden stress, $C_E$ is the correction for the hammer energy ratio, $C_B$ is the correction factor for the borehole diameter, $C_R$ is the correction factor for the rod length and $C_S$ is the correction factor for the samples with or without liners. How to calculate such factors can be found in the paper of Youd et al. (2001). Then Figure 3.14, which was introduced by Seed et al. in 1983 and was updated by Youd et al. in 2001, can be used to determine the CRR of sandy soil.

The alternative field test method that can be used for assessing the resistance of sand to liquefaction is based on the field CPT data. One of the main advantages of CPT is that a continuous profile of penetration resistance is established for stratigraphic interpretation (Youd et al., 2001). The CRR of sand is determined from Figure 3.15, which was introduced by Robertson and Wride in 1998, after calculating the corrected cone tip resistance ($q_{c1N}$) using the following equation:

$$q_{c1N} = C_Q \left(\frac{q_c}{P_a}\right) \quad (3.5.)$$

where $C_Q$ is the normalising factor for cone penetration resistance, whose calculation method can be found in the paper of Youd et al. (2001); $P_a$ is the 1 standard atmosphere of pressure in the same unit used for $\sigma'_{vo}$ and $q_c$ is the field cone penetration resistance measured at the tip.

An alternative tool to the SPT and CPT procedures that can be used as a criterion for assessing the liquefaction resistance of sand is $V_s$, which was developed by Andrus and Stokoe (2000). As $V_s$ and liquefaction resistance (CRR) are similarly affected by the same factors (e.g. void ratio, effective confining stresses, stress history and geologic age), using $V_s$ as an index of liquefaction resistance is considered appropriate (Andrus and Stokoe, 2000; Youd et al., 2001). The use of $V_s$ measurement for liquefaction resistance evaluation is preferable in soils that are not easy to penetrate and that may thus pose problems for SPT and CPT measurements (Andrus and Stokoe, 2000; Youd et al., 2001). However, one of the drawbacks of using $V_s$ to assess liquefaction resistance is that seismic wave velocity measurements are made at small strains whereas pore water pressure build-up and liquefaction are medium- to high-strain phenomena (Andrus and Stokoe, 2000; Youd et al., 2001). The criteria for the assessment of liquefaction resistance (CRR) based on the overburden-stress-corrected $V_s$ ($V_{s1}$), which were suggested by Andrus and Stokoe (2000) and Youd et al. (2001), are shown in Figure 3.16. $V_{s1}$ can be calculated using the following equation:

$$V_{s1} = V_s \left(\frac{P_a}{\sigma'_{vo}}\right)^{0.25} \quad (3.6.)$$

where $P_a$ is the atmospheric pressure approximated by 100 kPa and $\sigma'_{vo}$ is the initial effective vertical stress in the same units as $P_a$.

As both the SPT and CPT measurements are not typically reliable for gravelly soils, BPT was established in Canada in the late 1950s (Youd et al., 2001). Youd et al. (2001) reported that BPT could not be directly used to determine correlations with field behaviour due to the very limited liquefaction sites from which the data of BPT can be obtained. As such, Harder and Seed (1986) established a correlation between BPT and SPT, in which the equivalent values of SPT are calculated from the data of BPT, and then the same assessment procedures used in SPT are applied in BPT (Youd et al., 2001).

To calculate the factor of safety (FS = CRR/CSR) against liquefaction of soil, the determined CRR from Figure 3.14 for SPT data, that from Figure 3.15 for CPT data and that from Figure 3.16 for $V_{s1}$ data were compared with the calculated CSR based on equation (3.1). Liquefaction is predicted to occur when FS $\leq$ 1 while no liquefaction is predicted to occur when FS > 1.

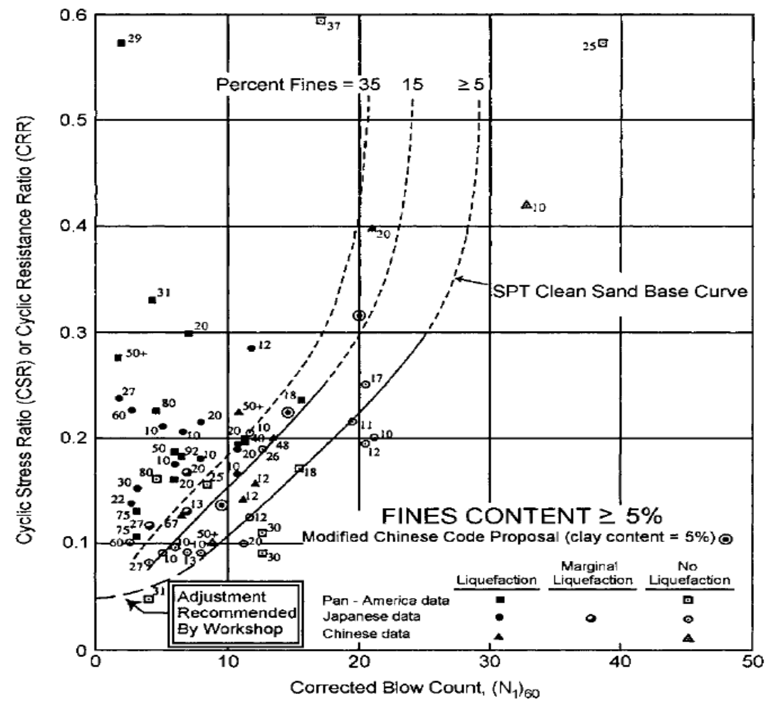


Figure 3.14. Plot used to calculate the cyclic resistance ratio (CRR) for clean and silty sands for magnitude 7.5 earthquakes (Youd et al., 2001)

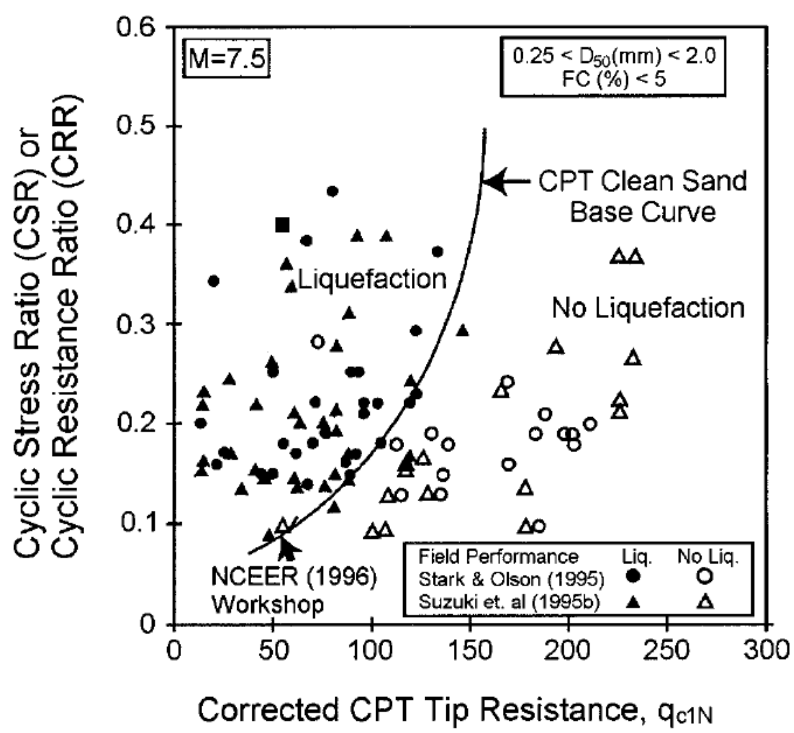


Figure 3.15. Plot recommended for determining the cyclic resistance ratio (CRR) for clean sands (fines content ≤ 5%) for magnitude 7.5 earthquakes from cone penetration test (CPT) data (Robertson and Wride, 1998)

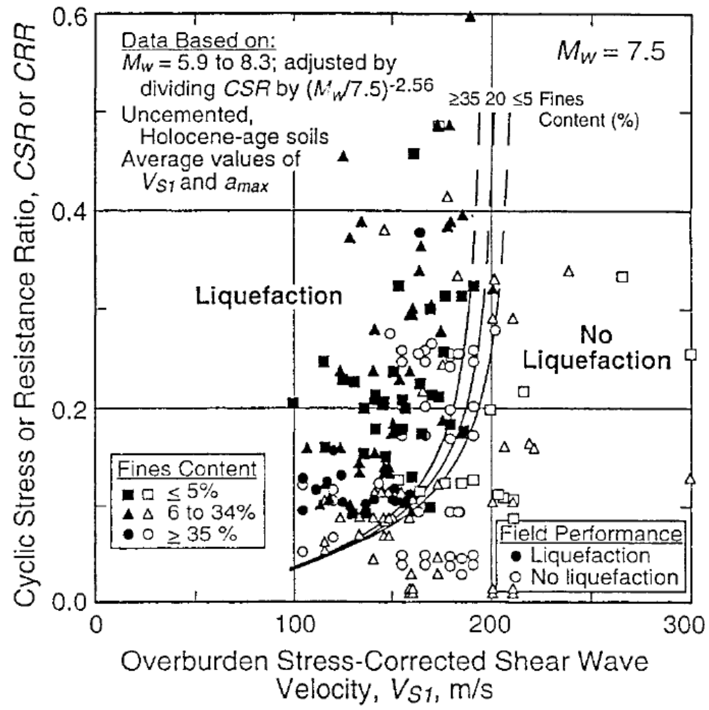


Figure 3.16. Plot recommended for determining the cyclic resistance ratio (CRR) from overburden-stress-corrected shear wave velocity ($V_{s1}$) measurements for clean and silty sands for magnitude 7.5 earthquakes (Andrus and Stokoe, 2000)

### 3.4.2. **Liquefaction criteria for fine-grained soils**

Fine-grained soils (i.e. silt and clay) were characterised as non-liquefiable soils in the recent past until the recent earthquakes occurred in different parts of the world, which shows that these soils may be subject to liquefaction behaviour, as sandy soils are. For instance, Seed et al. (2003) reported that the fine-grained soils in the city of Adapazari, Turkey were liquefied during the 1999 Kocaeli earthquake, and that the fine-grained soils in four cities in Taiwan were liquefied during the 1999 Chi-Chi earthquake. A review of the liquefaction criteria for fine-grained soils proposed by several researchers is presented below.

The Chinese criteria are commonly used for assessing the liquefaction susceptibility of fine-grained soils resulting from earthquakes. These criteria, which were proposed by Wang (1979), were based on previous earthquakes in China, where liquefaction was detected in some fine-grained soils and was not detected in others. These Chinese criteria indicated that silty soil containing less than 15−20% clay particles (less than 5 µm size as per the Chinese definition of clay) and with a PI larger than 3% may be susceptible to liquefaction during the occurrence of a strong earthquake if its $w_c$ is larger than 0.9 of its liquid limit (LL).

Seed and Idriss (1982) modified the Chinese criteria that were introduced by Wang (1979) and reported that clayey soils are susceptible to liquefaction when the following characteristics are satisfied: (i) percent finer less than 5 µm < 15%; (ii) LL < 35% and (iii) $w_c$ > 0.9 LL.

Finn (1991) adjusted the Chinese criteria since their determination of liquid limit was based on the fall cone apparatus instead of the Casagrande cup that is mostly used in North America. These adjustments include the following: decrease the fines content by 5%, increase the liquid limit (LL) by 1% and increase the water content ($w_c$) by 2%.

Koester (1992) pointed out that LL values determined using the fall cone penetrometer apparatus (used in the Chinese criteria) produce LL values that are approximately 4 points larger than the LL values determined using the Casagrande-type percussion apparatus (U.S. standard practices). Accordingly, he suggested that the LL in the Chinese criteria be reduced when the Casagrande-type percussion apparatus (U.S. standard practices) is used for testing soils.

Based on a review of different case histories, Andrews and Martin (2000) recently suggested criteria for determining the liquefaction susceptibility of fine-grained soils. Unlike the Chinese criteria, they used the Casagrande apparatus for LL determination and defined the clay content as particles finer than 2 μm. Table 3.1 shows the modified Chinese criteria as reported by Andrews and Martin (2000).

Seed et al. (2003) recommended new criteria for determining the liquefaction susceptibility of fine-grained soils, which can be defined through three zones (i.e. Zone A, B and C), as shown in Figure 3.17. Zone A includes soils considered potentially susceptible to 'classic' cyclically induced liquefaction when they have the following characteristics: LL ≤ 37, PI ≤ 12 and $w_c > 0.8$ LL. Zone B includes soils that may be liquefiable when they have the following characteristics: LL ≤ 47, PI ≤ 20 and $w_c \geq 0.85$ LL. Zone C includes soils that are typically not susceptible to 'classic' cyclically induced liquefaction when their LL > 20 or PI > 47, even though the soils in this zone should be checked for potential sensitivity.

From the observations of ground failure in the fine-grained soils in Adapazari, Turkey during the 1999 Kocaeli earthquake, and from the results of the laboratory cyclic triaxial tests on the samples obtained from such site, Bray et al. (2004) found that the Chinese criteria are not trustworthy for determining the liquefaction susceptibility of fine-grained soils. Generally, this was because the clay size condition did not satisfy the Chinese criteria. Therefore, the following criteria were suggested for determining the liquefaction susceptibility of fine-grained soils: (i) fine soils with $w_c$/LL ≥ 0.85 and PI ≤ 12 are considered susceptible to liquefaction or cyclic mobility; (ii) fine soils with 12 < PI ≤ 20 and $w_c$/LL ≥ 0.8 may be moderately susceptible to liquefaction or cyclic mobility and need to be tested in the laboratory to evaluate their liquefaction susceptibility under the loading conditions in the field and (iii) fine soils with PI > 20 are considered not susceptible to liquefaction. In addition, Bray and Sancio (2006) proposed criteria generally similar to those proposed by Bray et al. (2004).

On the basis of various case histories and experiment data, Boulanger and Idrisss (2006) proposed that the CRR of cohesive soils to liquefaction must be decided based on their behaviour: whether sand-like or clay-like behaviour. They recommend that soils with PI > 7 be considered 'having clay-like behaviour' and that soils with PI < 7 be considered 'having sand-like behaviour' for determining the liquefaction potential for engineering practice. However, for soils classified as CL-ML, the PI criterion may be reduced to PI = 5. The criterion was simplified, as shown in Figure 3.18. According to the aforementioned researchers, soils defined as 'having clay-like behaviour' should be checked for cyclic liquefaction using laboratory testing and/or the empirical correlations developed for clay materials. On the other hand, fine-grained soils that behave like sand may be examined for liquefaction using the framework of existing SPT- or CPT-based correlations.

Table 3.1. Liquefaction susceptibility of fine-grained soils (Andrews and Martin, 2000)

| | **Liquid Limit < 32%** | **Liquid Limit ≥ 32%** |
|---|---|---|
| **Clay Content < 10%** | Susceptible to liquefaction | Further studies required<br><br>(Consider plastic non-clay sized particles – such as Mica) |
| **Clay Content ≥ 10%** | Further studies required<br><br>(Consider non-plastic clay sized particles – such as mine and quarry tailings) | Non-susceptible to liquefaction |

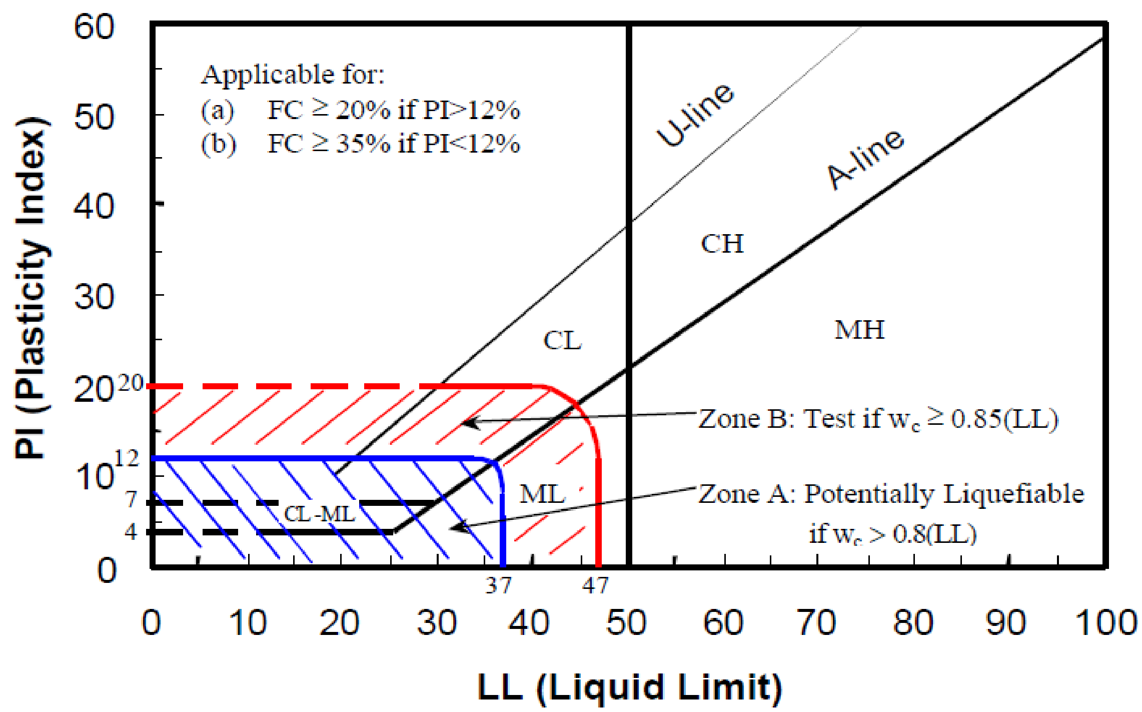


Figure 3.17. Recommendations regarding the assessment of 'liquefiable' soil types (Seed et al., 2003)

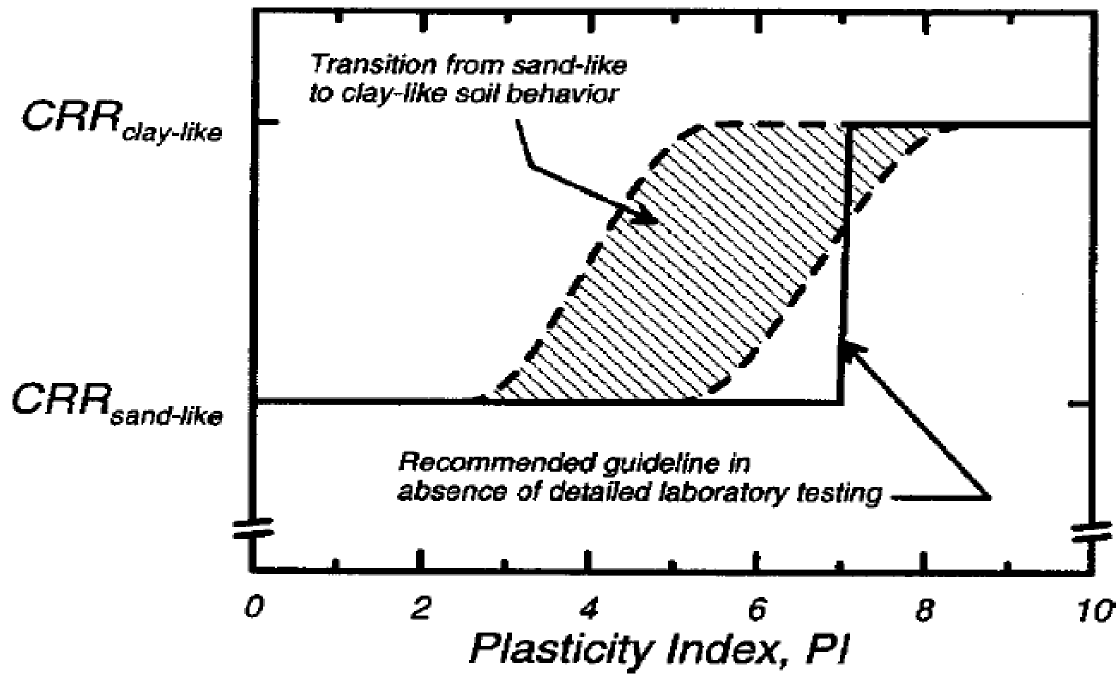


Figure 3.18. Schematic illustration of the transition from sand-like to clay-like behavior for fine-grained soils with increasing PI, and the recommended guideline for practice (Boulanger and Idrisss, 2006)

### 3.4.3. **Liquefaction criteria for soils based on laboratory assessment**

This section presents background information regarding the liquefaction criteria frequently used in geotechnical research and practice to assess soil liquefaction in the laboratory. These criteria are (i) the pore-water-pressure-based criterion; (ii) the strength-based criterion; (iii) the strain/deformation-based criterion and (iv) the energy-based criterion (Wu et al., 2004). The information herein is mainly based on the work of Wu et al. (2004).

According to the pore-water-pressure-based criterion, soil liquefaction is the condition at which $r_u$ is equal to 1.0, where the developed excess pore water pressure ($\Delta u$) is equal to the initial vertical effective stress ($r_u = \Delta u/\sigma'_{vo} = 1$). In the laboratory, this criterion has drawn the attention of geotechnical earthquake engineering experts as it provides essential information about the soil liquefaction mechanism. However, this criterion has some limitations. One major limitation is the uncertainty regarding whether the $r_u$ of unity is actually reachable under many conditions. Previous studies have shown that liquefaction can occur even though the $r_u$ of unity was not attained. For example, Ishihara (1993) reported that the maximum reached $r_u$ for soils, including some amounts of fines (silty sands and sandy silts), is 0.9–0.95. In addition, there is uncertainty regarding whether the $r_u$ of unity in dense clean sand is attainable, as recently reported in the literature. The $r_u$ of unity cannot be reached in soils with initial static 'driving' shear stresses. In multi-directional simple shear experimental testing, Wu et al. (2003) found through tests where the stresses were not fully eliminated during each loading cycle that the $r_u$ values could stay below unity while still developing very large strains. Another limitation of the pore-water-pressure-based criterion is that it does not evaluate the seismic performance of liquefiable soils, specifically denser soils. The parameter of pore pressure alone offers inadequate information regarding soil performance unless the deformations developed are also discussed. In the case of loose sands, the development of the state of initial liquefaction ($r_u \approx 1$) is immediately followed by the accumulation of large shear strains. Conversely, denser sands may produce large pore water pressures under strong dynamic loading conditions, in which the corresponding produced shear strains are considered limited due to the strong dilatative responses associated with such soils. Additionally, in reality, the pore-water-pressure-based criterion is subject to limitations, whereby earthquakes lead to $r_u$'s that have not been widely recorded in the field. For most field liquefaction occurrences, geotechnical engineers depend on liquefaction signs such as ground deformations and sand boil ejecta to indicate the occurrence of liquefaction. Finally, in the laboratory, the pore-water-pressure-based criterion presents a limitation in that the measurement of the excess pore water pressure ($\Delta u$) close to the middle of the soil samples is considered problematic when the loading rate is higher than the rate at which the pore water pressures equalise across the soil sample. This can be problematic specifically in soil samples with low permeability. Accordingly, this led to the implementation of the deformation threshold as a criterion indicating liquefaction occurrence in several laboratory investigations.

The strength-based criterion often requires liquefied soils to transform into viscous liquid. This indicates that these soils must almost entirely lose their shear strength and could not regain their strength. The soils are subjected to full strength loss only when the effective confining stress reaches zero. Thus, this criterion seems to correspond to the pore-water-pressure-based criterion. As such, the strength-based criterion has limitations similar to those of the pore-water-pressure-based criterion.

It used to be that the strain/deformation-based criterion was not as common as the pore-water-pressure- and strength-based criteria partially because soil strain/deformation was considered a result of liquefaction occurrence. Currently, however, the strain/deformation-based criterion is also recognised due to the relationship between deformation and pore water pressure. The strain/deformation-based criterion is recognised as a valid criterion for the evaluation of seismic performance; if liquefaction occurs, such criterion offers key information related to the levels of soil performance. However, this criterion presents some limitations. One key limitation is that the measurement of strain/deformation relies on the deformation mode to which the soil is exposed (e.g. triaxial or simple shear). Another limitation is the difficulty of selecting a unique strain level as the liquefaction criterion. Ishihara (1993) performed cyclic triaxial tests and suggested the use of 5% DA axial strain, equivalent to 3.75% single-amplitude (SA) shear strain under the simple shear condition. Wu et al. (2004) suggested an SA or a DA shear strain of 6% as the failure criterion triggering flow-type deformation. Other investigators used different strain levels, ranging from 2 to 10%. The effect of different strain level selections on the measured liquefaction resistance or cyclic strength varies from fairly non-significant for loose soils to largely vital for dense soils.

With regard to the energy-based criterion, the normalised energy capacity is calculated as the area bounded by the stress-strain hysteresis loops during cyclic loading. This criterion has proven useful in assessing the liquefaction potential of reconstituted laboratory soil samples. However, the implementation of this criterion still needs to be developed.

## 3.5. Review of previous studies on seismic or cyclic liquefaction behaviour of natural and man-made fine-grained soils

### 3.5.1. Review of previous studies on seismic or cyclic liquefaction behaviour of natural fine-grained soils

Many previous studies have been conducted to understand and assess the liquefaction potential of natural fine-grained soils under seismic loading (e.g. Puri, 1984; Prakash and Sandoval, 1992; Atukorala et al., 2000; Adalier et al., 2003; Bray et al., 2004; Sanin and Wijewickreme, 2006; El Takch et al., 2016; Uprety, 2016; Onur, 2018). In this section, a brief review of these studies is provided.

Puri (1984) studied the liquefaction behaviour of undisturbed and reconstituted specimens of loessial (silty) soil using the cyclic triaxial apparatus. He found that this silty soil might or might not undergo initial liquefaction (i.e. $r_u$ generation equal to the initial effective confining pressure). In the case of silty soil with PI ≥ 15, Puri noticed that initial liquefaction was not achieved under the applied cyclic loading conditions. In addition, initial liquefaction was reached after failure defined by 5% and 10% DA strains was reached and before failure defined by 20% DA strain was reached.

Prakash and Sandoval (1992) tested the liquefaction susceptibility of low-plasticity silt and silt with 5% and 10% clay mix under cyclic triaxial loading conditions. The results showed that these soils were susceptible to initial liquefaction (i.e. $r_u$ generation equal to the initial effective confining pressure). According to the researchers, initial liquefaction was achieved at 5% DA axial strain for the tested pure silt. In addition, in the case of silt with 5% clay mix, initial liquefaction was achieved between the 5% and 10% DA axial strains, while for the silt with 10% clay mix, initial liquefaction was achieved between the 10% and 20% DA axial strains.

Atukorala et al. (2000) studied the liquefaction susceptibility of 22 specimens of silty soil under both the cyclic triaxial and cyclic simple shear loading conditions. The results indicated that only nine specimens of silty soil were susceptible to liquefaction as these specimens satisfied either the pore pressure or strain criterion (an SA shear strain of 5% for the simple shear test or a DA axial strain of 5% for the triaxial test).

Adalier et al. (2003) conducted centrifuge testing to evaluate the liquefaction susceptibility of non-plastic silty deposit. This deposit was 7.8 m thick and was tested at a 50 g gravitational acceleration field. It was found that the strength and stiffness of the non-plastic silty deposit was significantly diminished due to liquefaction occurrence. According to the researchers, liquefaction occurrence was indicated through the complete attenuation of the measured soil accelerations and because the soil at all the tested depths reached an $r_u$ of 1.0. Moreover, the study results showed that the maximum settlement of the ground surface was approximately 0.1 m.

Bray et al. (2004) studied the liquefaction potential of undisturbed specimens of fine-grained soils (silty and clayey soils) with PIs ranging from 0 to 25 by carrying out undrained cyclic triaxial tests. The results indicated that the fine-grained soils with PI ≤ 12 and $w_c$/LL > 0.85 were susceptible to liquefaction while the fine-grained soils with 12 < PI < 20 and $w_c$/LL > 0.8 were more resistant to liquefaction but were still considered susceptible to cyclic mobility response. The fine-grained soils that were tested at effective confining stress < 50 kPa and that had PI > 20 were found not susceptible to liquefaction.

Sanin and Wijewickreme (2006) examined the liquefaction susceptibility of low-plasticity silt using an undrained cyclic direct simple shear apparatus. They found that the tested silt exhibited a cyclic-mobility-type response. The study results showed that irrespective of the applied CSR value or the level of generated $r_u$, liquefaction in terms of strain softening associated with loss of shear strength did not occur. According to Sanin and Wijewickreme (2006), this means that the tested silt was likely not susceptible to flow failure or flow liquefaction under seismic loading.

El Takch et al. (2016) investigated the liquefaction potential of non-plastic silts by conducting constant-volume cyclic ring shear tests. They found that non-plastic silts are susceptible to liquefaction in which their cyclic response, in terms of both $r_u$ and strain development, is largely comparable to that of sand.

Uprety (2016) examined the liquefaction susceptibility of specimens of non-plastic clean silt and silt–clay mixture using the cyclic triaxial apparatus. The results indicated that in the case of the non-plastic clean silt specimens whose void ratio varied from 0.74 to 0.76 before the cyclic loading stage, initial liquefaction (i.e. $r_u$ generation equal to the initial effective confining pressure) occurred before the 2.5% and 5% DA strains were reached. However, in the case of the non-plastic clean silt and silt-clay mixture specimens whose void ratio varied from 1.0 to 1.1 before the cyclic loading stage, 2.5% and 5% DA strains were reached before initial liquefaction occurred.

Onur (2018) conducted a laboratory study using a scale shaking table to investigate the liquefaction potential of cohesive silty clay soil specimens with PI = 23. Different accelerations (0.10 and 0.3 m/s$^2$) and number of cycles (5 and 10 cycles) were applied in his investigation. In addition, a 50 kPa vertical stress was applied to the surfaces of the tested specimens using a rigid mass. The test results showed that $r_u$ was not generated under dynamic loading, which indicated that the tested cohesive silty clay soil specimens were not susceptible to liquefaction even though settlement and softening were observed.

### 3.5.2. **Review of previous studies on seismic or cyclic liquefaction behaviour of man-made fine-grained soils**

#### 3.5.2.1. **Review of previous studies on seismic or cyclic liquefaction behaviour of highly densified tailings**

Few studies have been conducted to understand and assess the liquefaction potential of highly densified tailings under seismic loading (Crowder, 2004; Al Tarhouni, 2008; Verdugo and Santos, 2009; Kim et al., 2011; Dalari, 2013; Seidalinova, 2014). All these studies used either the cyclic simple shear or cyclic triaxial apparatus for experimental testing. A brief review of such studies is presented in this section.

Crowder (2004) conducted undrained cyclic triaxial tests to investigate the liquefaction potential of non-plastic paste tailings specimens. The void ratio of these specimens ranged from 0.62 to 0.65. In addition, the applied CSR in his investigation ranged from 0.10 to 0.20. The study results showed that the pore water pressure of all the tested specimens developed until it reached about 100% of the initial confining stress; as such, the specimens had almost zero effective stress. This indicates that the non-plastic paste tailings specimens were susceptible to cyclic liquefaction behaviour. Moreover, the CSR or cyclic strength of the non-plastic paste tailings triggering 5% DA strain at 20 cycles was almost 0.14, similar to the finding of Ishihara et al. (1980) on tailings of the same type.

Al Tarhouni (2008) conducted a laboratory study to examine the liquefaction potential of thickened low-plasticity gold mine tailings specimens under undrained cyclic simple shear loading conditions. The tested specimens had void ratios ranging from 0.537 to 0.620 and CSRs ranging from 0.075 to 0.150. It was found that all the tested tailings specimens were susceptible to cyclic mobility whereas the pore water pressure ratio did not reach unity or the corresponding zero effective stress. It must be mentioned that in such study, 3.75% shear strain ($\gamma$) was used as the liquefaction criterion.

Verdugo and Santos (2009) used the triaxial apparatus to investigate the liquefaction potential of non-plastic reconstituted samples of thickened copper tailings under undrained cyclic loading conditions. They prepared the tested samples through two different methods (i.e. the dried and resaturated method and the slurry method) to simulate the extreme conditions that could occur in situ. According to the researchers, the dried and resaturated method exemplifies the bottom of the thickened-tailings disposal, in which a water table can be established. In this approach, the tailing slurry was deposited in an acrylic box and then left to dry at room temperature until suitable samples were obtained for use in triaxial testing, to which saturation was applied prior to the test. However, the slurry method exemplifies a condition where the climatic conditions do not allow the desiccation of the tailings, for which reason they maintain their saturated phase. In this method, the samples of tailing slurry were prepared following the common testing procedure used for cycling triaxial testing. Generally, it was found that the thickened tailings might have undergone liquefaction during the occurrence of strong seismic events (i.e. earthquakes), even though their density increased through the desiccation or drying process.

Kim et al. (2011) investigated the influence of the mechanical OCR ($OCR_M$) and the OCR due to desiccation ($OCR_D$) on the cyclic resistance of the low-plasticity thickened gold tailings using a direct simple shear apparatus. At all the OCRs (i.e. OCRs ranging from 1 to 8), the results showed that the tested tailings had a cyclic mobility response while $r_u$ did not reach unity or the corresponding zero effective stress. In their investigation, the aforementioned researchers used the developed 3.75% SA shear strain to determine the initiation of liquefaction. In addition, they observed that the non-desiccated low-plasticity thickened gold tailings were subjected to a more rapid development of the pore water pressure compared to the desiccated low-plasticity thickened gold tailings. Even though both $OCR_M$ and $OCR_D$ led to an increase in the CRR of the low-plasticity thickened gold tailings, $OCR_M$ provided a larger CRR to the tailings than did $OCR_D$ (Kim et al., 2011).

Daliri (2013) studied the liquefaction potential of thickened gold tailings specimens under undrained cyclic loading conditions using the simple shear and triaxial apparatuses. The cyclic simple shear and triaxial tests revealed that the non-desiccated and desiccated thickened gold tailings specimens did not achieve zero effective stress (i.e. the $r_u$ was lower than the unity); as such, the tested thickened tailings were considered susceptible to cyclic mobility/liquefaction. In addition, the study results indicated that the resistance of the thickened tailings to liquefaction increased as the degree of desiccation increased. The researcher reported that the resistance of the non-desiccated tailings specimens to liquefaction seemed higher under the cyclic triaxial loading condition than under the simple shear loading condition.

Seidalinova (2014) studied the cyclic shear response of reconstituted thickened fine-grained gold tailings specimens using the constant-volume direct simple shear apparatus. Generally, the results indicated that the behaviour of the reconstituted thickened gold tailings specimens showed a cumulative increase in $r_u$ as the number of loading cycles increased; as such, the shear stiffness was continuously reduced. Even though zero effective stress was not achieved, the effective stress decreased considerably until it reached a small amount near zero, which showed that such material had a cyclic mobility response. The results for the normally consolidated reconstituted thickened gold tailings specimens indicated that the CRR decreased as the initial static shear stress bias increased. Moreover, it was observed that the shear stiffness and CRR of the reconstituted thickened gold tailings specimens increased as the OCR increased. In general, Seidalinova (2014) pointed out that the results that he obtained from his study on the cyclic shear response of normally consolidated reconstituted thickened gold tailings were consistent with those of other investigations performed on different types of tailings. Furthermore, it was found that the reconstituted thickened gold tailings specimens had a CRR similar to that of the Fraser River silt but larger than that of the Fraser River sand and quartz powder.

#### 3.5.2.2. **Review of previous studies on seismic liquefaction behaviour of cemented paste backfill tailings**

Few studies have been conducted to understand and assess the liquefaction potential of the CPB tailings under seismic loading (le Roux, 2004; Saebimoghaddam, 2010; Galaa, 2011; Suazo et al., 2017; Alainachi and Fall, 2019). A brief review of these studies is presented in this section.

In the study by le Roux (2004), cyclic triaxial tests were conducted to investigate the seismic liquefaction potential of Golden Giant CPB with 5% binder content and that had been cured for 3 and 12 h. The tests were conducted with two confining stresses (i.e. 100 and 150 kPa) and with different CSRs ranging from 0.11 to 0.30. In the investigation, cyclic liquefaction was defined in terms of the 5% DA strain that was undergone by the tested specimen. It was found that the cyclic response of Golden Giant CPB with a 5% binder content and that had been cured for 3 h was comparable to that of non-plastic silts. In addition, the study results indicated that even though the 5% CPB with a 3 h curing time was susceptible to cyclic liquefaction, the 5% CPB with a 12 h curing time was not.

Saebimoghaddam (2010) performed cyclic triaxial tests under undrained conditions to investigate the liquefaction potential of 3% CPB using the triaxial apparatus. The CPB specimens were cured for 4 and 12 h before the laboratory testing. The specimens were tested at different CSRs ranging from 0.18 to 0.3 and at three different effective confining stresses (i.e. 30, 50 and 100 kPa). The 5% DA axial strain was used as the liquefaction criterion. The study results showed that liquefaction occurred within the tested CSR range of 0.2−0.3 for the 3% CPB cured for 4 h. Although it was found that the 3% CPB cured for 4 h and tested at a 0.29 CSR was susceptible to liquefaction, it was likewise found that the 3% CPB cured for 12 h and tested at a 0.29 CSR was not susceptible to liquefaction.

In 2011, Galaa studied the liquefaction potential of 4.5% CPB specimens in a series of cyclic triaxial tests. The CPB specimens were cured for 4 and 7 h before laboratory testing. Before the cyclic shearing stage, the specimens were subjected to 100 kPa initial confining stress. The CPB specimens were tested at different CSRs ranging from 0.09 to 0.2. The 5% DA axial strain was used as the liquefaction criterion. The test results indicated that the CPB specimens were susceptible to liquefaction failure of a cyclic-mobility-type response, and that under a similar CSR of 0.2, the 4.5% CPB specimens cured for 7 h had higher cyclic resistance than those cured for 4 h.

More recently, Suazo et al. (2017) used a constant-volume direct simple shear apparatus to examine the liquefaction potential of the CPB under cement contents and curing ages ranging from 1.5 to 5% and 0 to 48 h, respectively. Prior to the cyclic shearing stage, the CPB specimens were subjected to 100 kPa initial confining stress. The 3.0% SA shear strain ($\gamma$) was used as the liquefaction criterion. Regardless of the cement content and curing age, Suazo et al. (2017) observed that the CPB specimens generally exhibited a cyclic-mobility-type response.

Alainachi and Fall (2019) investigated the liquefaction potential of early-aged 4.5% CPB under seismic loading using a shaking table. The CPB specimens were cured for 2.5, 4 and 10 h before shaking was applied to them. These CPB specimens underwent sinusoidal dynamic loading with a 1 Hz frequency and a 0.13g peak horizontal acceleration. The study results indicated that the CPB specimen cured for 2.5 h was susceptible to liquefaction ($r_u \geq 1$), the CPB specimen cured for 4 h was resistant to liquefaction ($r_u < 1$) and the CPB specimen cured for 10 h was highly resistant to liquefaction ($r_u = 0$).

## 3.6. **Conclusion**

The literature review that was conducted on different aspects of the seismic or cyclic liquefaction phenomenon is summarised in this chapter. In such review, the definition of the liquefaction phenomenon, the factors affecting the liquefaction susceptibility of soils and the criteria for evaluating the liquefaction susceptibility of sand and fine-grained soils are discussed. Furthermore, the findings of the previous studies on the seismic liquefaction behaviour of natural and man-made fine-grained soils (i.e. the highly densified and CPB tailings) are summarised in this chapter. Accordingly, the literature review revealed that the seismic liquefaction susceptibility of natural fine-grained soils and CPB tailings has been studied using small-scale equipment (i.e. cyclic simple shear or cyclic triaxial equipment) or large-scale equipment (i.e. centrifugal or shaking table). However, the seismic or cyclically induced liquefaction susceptibility of the highly densified tailings (i.e. thickened and paste tailings) was studied using only small-scale equipment (i.e. cyclic simple shear or cyclic triaxial equipment). Therefore, to reliably evaluate the seismic or cyclic loading-induced liquefaction behaviour of layered and highly densified tailings (i.e. thickened and paste tailings) using large-scale equipment, shaking table tests were conducted in this study. No previous studies have addressed this issue and knowledge gap.

## 3.7. **References**


Adalier, K., Elgamal, A., Meneses, J., and Baez, J.I. (2003). Stone columns as liquefaction countermeasure in non-plastic silty soils. Soil Dynamics and Earthquake Engineering, 23(7): 571-584.

Alainachi, I., and Fall, M. (2019). Liquefaction potential of cementing tailing backfill: shaking table test results. Geotechnical Engineering in the XXI Century: Lessons learned and future challenges. In Proceedings of the XVI Pan-American Conference on Soil Mechanics and Geotechnical Engineering (XVI PCSMGE), 17-20 November 2019, Cancun, Mexico, pp. 1949-1956.

Al-Tarhouni, M.A. (2008). Liquefaction and post-liquefaction behaviour of gold mine tailings under simple shear loading. Master thesis, Department of Civil and Environmental Engineering, Carleton University, Ottawa, Ontario, Canada.

Andrews, D.C.A., and Martin, G.R. (2000). Criteria for liquefaction of silty soils. In Proceedings of the 12th World Conference on Earthquake Engineering, 30 January - 4 February 2000, Auckland, New Zealand, Paper 0312, pp. 1-8.

Andrus, R.D., and Stokoe II, K.H. (2000). Liquefaction resistance of soils from shear-wave velocity. Journal of Geotechnical and Geoenvironmental Engineering, ASCE, 126(11): 1015-1025.

Atukorala, U., Wijewickreme, D., and Mccammon, N. (2000). Some observations related to liquefaction susceptibility of silty soils. In Proceedings of the 12th World Conference on Earthquake Engineering, 30 January - 4 February 2000, Auckland, New Zealand, Paper 1324, pp. 1-8.

Boulanger, R.W., and Idriss, I.M. (2006). Liquefaction susceptibility criteria for silts and clays. Journal of Geotechnical and Geoenvironmental Engineering, ASCE, 132(11): 1413-1426.

Bray, J.D., and Sancio, R.B. (2006). Assessment of the liquefaction susceptibility of fine-grained soils. Journal of Geotechnical and Geoenvironmental Engineering, ASCE, 132(9): 1165-1177.

Bray, J.D., Sancio, R.B., Riemer, M.F., and Durgunoglu, T. (2004). Liquefaction susceptibility of fine-grained soils. In Proceedings of the 11th International Conference on Soil Dynamics and Earthquake Engineering and 3rd International Conference on Earthquake Geotechnical Engineering, 7-9 January 2004, Berkeley, California, USA, Vol. 1, pp. 655-662.

Campanella, R.G., and Lim, B.S. (1981). Liquefaction characteristics of undisturbed soils. In Proceedings of the First International Conference on Recent Advances in Geotechnical Engineering and Soil Dynamics, 26 April - 3 May 1981, St. Louis, Missouri, USA, Vol. 1, pp. 227-230.

Crowder, J.J. (2004). Deposition, consolidation, and strength of a non-plastic tailings paste for surface disposal. PhD thesis, Department of Civil Engineering, University of Toronto, Toronto, Ontario, Canada.

Cui, L., Fall, M., Orbovic, N., Nguyen T.S. (2020). A model for soil-structure interaction-application to small modular reactors. CIGOS 2019, Innovation for Sustainable Infrastructure, 781-786.

Daliri, F. (2013). The influence of desiccation and stress history on monotonic and cyclic shear response of thickened gold tailings. PhD thesis, Department of Civil and Environmental Engineering, Carleton University, Ottawa, Ontario, Canada.

De Alba, P., Seed, H.B., and Chan, C.K. (1976). Sand liquefaction in large-scale simple shear tests. Journal of the Geotechnical Engineering Division, ASCE, 102(GT9): 909-927.

El Takch, A., Sadrekarimi, A., and El Naggar, H. (2016). Cyclic resistance and liquefaction behavior of silt and sandy silt soils. Soil Dynamics and Earthquake Engineering, 83: 98-109.

Finn, W.D. (1991). Assessment of liquefaction potential and post-liquefaction behavior of earth structures: developments 1981-1991. In Proceedings of the Second International Conference on Recent Advances in Geotechnical Earthquake Engineering and Soil Dynamics, 11-15 March 1991, St. Louis, Missouri, USA, Vol. 2, pp. 1833-1850.

Galaa, A.M.M.I.A. (2011). Early age mechanical behavior and stiffness development of cemented paste backfill with sand. PhD thesis, Department of Civil Engineering, University of Toronto, Toronto, Ontario, Canada.

Guo, T., and Prakash, S. (1999). Liquefaction of silts and silt-clay mixtures. Journal of Geotechnical and Geoenvironmental Engineering, ASCE, 125(8): 706-710.

Harder, L.F.Jr., and Seed, H.B. (1986). Determination of penetration resistance for coarse-grained soils using the Becker hammer drill. Report No. UCB/EERC- 86/06, Earthquake Engineering Research Centre, University of California, Berkeley, California, USA.

Ishihara, K. (1993). Liquefaction and flow failure during earthquakes. Géotechnique, 43(3): 351-451.

Ishihara, K., Yasuda, S., and Yokota, K. (1981). Cyclic strength of undisturbed mine tailings. In Proceedings of the First International Conference on Recent Advances in Geotechnical Earthquake Engineering and Soil Dynamics, 26 April - 3 May 1981, St. Louis, Missouri, USA, Vol. 1, pp. 53-58.

Kim, H., Daliri, F., Simms, P., and Sivathayalan, S. (2011). The influence of desiccation and overconsolidation on monotonic and cyclic shear response of thickened gold tailings. In Proceedings of the 64th Canadian Geotechnical Conference (2011 Pan-Am CGS), 2-6 October 2011, Toronto, Ontario, Canada.

Koester, J.P. (1992). The influence of test procedure on correlation of atterberg limits with liquefaction in fine-grained soils. Geotechnical Testing Journal, ASTM, 15(4): 352-361.

Ladd, R.S. (1974). Specimen preparation and liquefaction of sands. Journal of the Geotechnical Engineering Division, ASCE, 100(GT10): 1180-1184.

le Roux, K. (2004). In situ properties and liquefaction potential of cemented paste backfill. PhD thesis, Department of Civil Engineering, University of Toronto, Toronto, Ontario, Canada.

Mulilis, J.P., Seed, H.B., Chan, C.K., Mitchell, J.K., and Arulanandan, K. (1977). Effects of sample preparation on sand liquefaction. Journal of the Geotechnical Engineering Division, ASCE, 103(GT2): 91-108.

Onur, M.I. (2018). Investigation of liquefaction behaviour for cohesive soils. In Proceedings of the 3rd World Congress on Civil, Structural, and Environmental Engineering (CSEE'2018), 8-10 April 2018, Budapest, Hungary, ICGRE 134.

Perlea, V.G. (2000). Liquefaction of cohesive soils. Soil dynamics and liquefaction 2000. In Proceedings of Sessions of Geo-Denver 2000, 5-8 August 2000, Denver, Colorado, USA, ASCE Geotechnical Special Publication, Vol. 107, pp. 58-76.

Poulos, S.J., Castro, G., and France, J.W. (1985). Liquefaction evaluation procedure. Journal of Geotechnical Engineering, ASCE, 111(6): 772-792.

Prakash, S. (1981). Soil dynamics. McGraw-Hill Company, New York, NY, USA.

Prakash, S., and Puri, V.K. (2010). Past and future of liquefaction. In Proceedings of Indian Geotechnical Conference, 16-18 December 2010, GEOtrendz, IIT Bombay, Mumbai, India, pp. 63-72.

Prakash, S., and Sandoval, J.A. (1992). Liquefaction of low plasticity silts. Journal of Soil Dynamics and Earthquake Engineering, 71(7): 373-379.

Puri, V.K. (1984). Liquefaction behavior and dynamic properties of loessial (silty) soils. PhD thesis, Department of Civil and Environmental Engineering, University of Missouri- Rolla, Rolla, Missouri, USA.

Robertson, P.K., and Wride, C.E. (1998). Evaluating cyclic liquefaction potential using the cone penetration test. Canadian Geotechnical Journal, 35(3): 442-459.

Saebimoghaddam, A. (2010). Liquefaction of early age cemented paste backfill. PhD thesis, Department of Civil Engineering, University of Toronto, Toronto, Ontario, Canada.

Sanin, M.V., and Wijewickreme, D. (2006). Cyclic shear response of channel-fill Fraser River Delta silt. Soil Dynamics and Earthquake Engineering, 26(9): 854-869.

Seed, H.B., and Idriss, I.M. (1971). Simplified procedure for evaluating soil liquefaction potential. Journal of the Soil Mechanics and Foundations Division, ASCE, 97(9): 1249-1273.

Seed, H.B., and Idriss, I.M. (1982). Ground motion and soil liquefaction during earthquakes. Monograph Series, Earthquake Engineering Research Institute, Oakland, California, USA.

Seed, H.B., and Peacock, W.H. (1971). Test procedures for measuring soil liquefaction characteristics. Journal of the Soil Mechanics and Foundation Division, ASCE, 97(SM8): 1099-1119.

Seed, H.B., Arango, I., and Chan, C.K. (1976). Evaluation of soil liquefaction potential for level ground during earthquakes. A summary report No. NUREG-0026, Nuclear Regulatory Commission Washington, DC, USA.

Seed, H.B., Idriss, I.M., and Arango, I. (1983). Evaluation of liquefaction potential using field performance data. Journal of Geotechnical Engineering Division, ASCE, 109(3): 458-482.

Seed, H.B., Mori, K., and Chan, C.K. (1977). Influence of seismic history on liquefaction of sands. Journal of the Geotechnical Engineering Division, ASCE, 103(GT4): 257-270.

Seed, R.B., Cetin, K.O., Moss, R.E.S., Kammerer, A., Wu, J., Pestana, J., Riemer, M., Sancio, R.B., Bray, J.D., Kayen, R.E., and Faris, A. (2003). Recent advances in soil liquefaction engineering: a unified and consistent framework. In Proceedings of the 26th Annual ASCE Los Angeles Geotechnical Spring Seminar, Keynote Presentation, 30 April 2003, Long Beach, California, USA, pp. 1-71.

Seidalinova, A. (2014). Monotonic and cyclic shear loading response of fine-grained gold tailings. Master thesis, The University of British Columbia, Vancouver, British Columbia, Canada.

Suazo, G., Fourie, A., and Doherty, J. (2017). Cyclic shear response of cemented paste backfill. Journal of Geotechnical and Geoenvironmental Engineering, ASCE, 143(1): 04016082.

Tokimatsu, K., and Yoshimi, Y. (1983). Empirical correlation of soil liquefaction based on SPT N-value and fines content. Soils and Foundations, 23(4): 56-74.

Uprety, S. (2016). Effects of plasticity on liquefaction characteristics of fine-grained soils. Master thesis, Department of Civil and Environmental Engineering, Southern Illinois University, Carbondale, Illinois, USA.

Varghese, R.M., and Latha, G.M. (2014). Shaking table tests to investigate the influence of various factors on the liquefaction resistance of sands. Natural Hazards, 73(3): 1337-1351.

Verdugo, R., and Santos, E. (2009). Liquefaction resistance of thickened tailings of copper mines. In Proceedings of the 17th International Conference on Soil Mechanics and Geotechnical Engineering (ICSMGE), 5-9 October 2009, Alexandria, Egypt, pp. 295-298.

Wang, W.S. (1979). Some findings in soil liquefaction. Research Report, Water Conservancy and Hydroelectric Power Scientific Research Institute, Beijing, China.

Wu, J., Kammerer, A.M., Riemer, M.F., Seed, R.B., and Pestana, J.M. (2004). Laboratory study of liquefaction triggering criteria. In Proceedings of the 13th World Conference on Earthquake Engineering, 1-6 August 2004, Vancouver, British Columbia, Canada, paper No. 2580.

Wu, J., Seed, R.B., and Pestana, J.M. (2003). Liquefaction Triggering and Post Liquefaction Deformations of Monterey 0/30 Sand under Uni-Directional Cyclic Simple Shear Loading. Geotechnical Engineering Research Report No. UCB/GE-2003/01, University of California, Berkeley, California, USA.

Youd, T.L., Idriss, I.M., Andrus, R.D., Arango, I., Castro, G., Christian, J.T., Dobry, R., Finn, W.D.L., Harder, L.F. Jr., Hynes, M.E., Ishihara, K., Koester, J.P., Liao, S.S.C., Marcuson III, W.F., Martin, G.R., Mitchell, J.K., Moriwaki, Y., Power, M.S., Robertson, P.K., Seed, R.B., and Stokoe, K.H. II. (2001). Liquefaction resistance of soils: summary report from the 1996 NCEER and 1998 NCEER/NSF workshops on evaluation of liquefaction resistance of soils. Journal of Geotechnical and Geoenvironmental Engineering, ASCE, 127(10): 817-833.

Zhang, G., Robertson, P.K., and Brachman, R.W. (2002). Estimating liquefaction-induced ground settlements from CPT for level ground. Canadian Geotechnical Journal, 39(5): 1168-1180.

# 4 Chapter 4: Testing of the Geotechnical Response to Cyclic Loadings

## 4.1. Introduction

Nowadays, highly densified tailings technologies such as thickened and paste tailings have been given more attention in the mining industry worldwide. Regardless of thickened and paste tailings offers advantages to mines, such decrease of the dependency on conventional tailings dams with their related jeopardies in terms of the catastrophic geotechnical and environmental failures and the increase in water recovery and recycling, an evaluation of the cyclic loading-induced liquefaction potential of these technologies is considered crucial, particularly in areas that are prone to earthquake shaking. The behaviour and liquefaction susceptibility of thickened and paste tailings subjected to cyclic loading is not fully understood until now. Furthermore, previous studies have focused only on the behaviour and liquefaction susceptibility of thickened and paste tailings under dynamic (seismic or cyclic) loading by means of the simple shear or triaxial equipment. Yet, there are no research on the behaviour and liquefaction susceptibility of layered thickened and paste tailings under cyclic loading by means of shaking table equipment.

This chapter mainly addresses the results of an experimental investigation on behaviour and liquefaction susceptibility of thickened tailings (Section 4.2) and paste tailings (Section 4.3) by using shaking table testing techniques. The objectives of this current chapter are to evaluate the behaviour and liquefaction susceptibility of layered thickened and paste tailings, in terms of the response of accelerations, displacements and pore water pressures, to cyclic loading by using a shaking table equipment in order to have a better understanding of these technologies from a geotechnical standpoint. The obtained test results from these investigations are discussed and compared with the other available investigations.

## 4.2. Technical Paper #1: Shaking Table Testing of Geotechnical Response of Thickened Tailings to Cyclic Loadings

Fahad Alshawmar, Mamadou Fall
Department of Civil Engineering, University of Ottawa, Ottawa, Ontario, Canada K1N 6N5
Submitted to the Journal of Geotechnical and Geological Engineering

### Abstract

Numerous earthquake-induced catastrophic failures (liquefaction) of conventional (slurry) tailings dams because of the liquefaction occurrence have repeatedly occurred in different seismic areas around the world. Thickened tailings technology is one of the new forms or techniques of the highly densified tailings that has been introduced in the past decades to reduce or eliminate the concerns about such issue, specifically in areas with high seismic activity. Unfortunately, the behaviour and the liquefaction susceptibility of thickened tailings subjected to cyclic loading is poorly understood. Moreover, there are no technical information or data and understandings regarding the behaviour and susceptibility of the layered thickened tailings to cyclic loading-induced liquefaction by using shaking table equipment. Accordingly, this experimental investigation aims to evaluate the behaviour and liquefaction susceptibility of the layered thickened tailings to cyclic loading by using a shaking table equipment. The thickened tailings were deposited subsequently in three thin layers in a flexible laminar shear box mounted on top of the shaking table. Cyclic loading with a peak horizontal acceleration of 0.13g and a frequency of 1 Hz was applied to the layered tailings deposit. Different types of sensors were placed to monitor the accelerations, displacements, volumetric water content and pore water pressures at the intermediate depth of each layer. Results indicated that the acceleration for the bottom and middle layers were similar to that of the base of the shaking table; but, this was not the case for the top layer. The measurements of vertical displacements indicated that all layers of thickened tailings experienced initially contraction and subsequently dilation during the shaking. The excess pore water pressure ratios were found to exceed unity through all layers of thickened tailings when the shaking ended. In other words, the results showed that the layered thickened tailings are susceptible to liquefaction after the cyclic loading under the considered testing conditions. It is also found that upward pore water migration to the top layer and downward pore water flow to the bottom layer occurred in the thickened tailings deposit. This water migration generated additional pore water pressure and also impacted the vertical displacement and liquefaction susceptibility of the thickened tailings material. The results of this study give a better understanding of the behaviour and liquefaction susceptibility of thickened tailings subjected to cyclic loadings, which is crucial for the safety of thickened tailings systems as well as sustainable mining.

**Keywords:** Tailings; Mine; Earthquake; Liquefaction; Tailings dam; Thickened tailings

### 4.2.1. **Introduction**

Mining operations globally generate large quantities of tailings materials every year. Jones and Boger (2012) reported that the mining operations generated 51 billion tons of waste rock and 14 billion tons of tailings in 2010. Tailings materials are considered ground rock particles in which the valuable minerals are recovered (Rankine et al., 2006; Bussière, 2007; Hassani et al., 2008; Ghirian and Fall, 2013, 2014; Lu et al., 2017; Li et al., 2018), where the size of tailings is generally ranged from silt to sand (Highter and Vallee, 1980). Tailings are deposited conventionally as a slurry in a structure called tailings dam (Hassani et al., 2008; Ahmed and Siddiqua 2014; Fall et al., 2010, 2013; Wu et al., 2012; Paul and Azam 2013; Zhang et al., 2015). The deposited slurry tailings in the dam are considered typically soft, loose and constantly saturated. Consequently, they are susceptible to liquefaction phenomenon when subjected to any strong earthquake shaking or seismic loadings (Ishihara, 1984). Tailings dam failures induced by earthquakes have been reported since the early 1900's (e.g., Ke et al., 2019). In the event of a liquefaction, the tailings may be released through a breach in the retaining embankment. The result is comparable to a landslide, with the consequences frequently being the fast release of large quantities of toxic slurry tailings.

The term of liquefaction phenomena has been defined as "a condition where a soil will undergo continued deformation at a constant low residual stress or with no residual resistance, due to the buildup and maintenance of high pore-water pressures which reduce the effective confining pressure to very low value" (Prakash, 1981). Even though the historical events have indicated that the mine tailings dams have experienced more static liquefaction than seismic liquefaction, the liquefaction phenomenon is mostly related to the seismic loading conditions (Davies et al., 2002). The liquefaction due to earthquake events is considered the second cause of tailings dam failures around the world whilst it is not the case in Europe (Rico et al., 2008). Severe consequences such as the loss of life, injuries, and environmental damage from the previous tailings dam failures, due to the liquefaction during the earthquake, have been reported in the literature (e.g. Highter and Vallee, 1980; Ishihara et al., 1980; Bray and Frost, 2010; Verdugon and González, 2015; WISE, 2017). The attention of the society, scholars, and government has been attracted as a result of such seismic failure. Thus, dewatering the slurry tailings before the deposition on the surface is considered an appropriate approach/method to prevent or diminish such consequences that might be resulted from the failures of tailings dams induced by liquefaction. Thickened tailings (TTs) technology is one of the novel dewatering techniques that can be used to significantly dewater low solids concentrated slurry tailings. This is usually accomplished by means of compression thickeners or by combined thickeners and filter presses.

The thickened tailings (TTs) are defined as tailings from which a considerable amount of process water has been removed to reach solids contents of higher than 50% and discharged out through spigot (Robinsky et al., 1991; Davies and Rice, 2001; Edraki et al., 2014). In addition, such thickened tailings material usually displays non-Newtonian flow behaviour (Sofrá and Boger, 2002). Robinsky (1975) is considered to be the pioneer of this technology which was initially implemented at the facility of the Kidd Creek Mine in Ontario, Canada. TTs have more solids content by weight compared with the slurry tailings as well as can be pumped as in the case of slurry tailings (Davies and Rice, 2001). The solid content in thickened tailings ranges between 50% and 70% with a yield stress of between 30 and 100 Pa (Hamade, 2013; Sofrá, 2017). Unlike slurry tailings during the deposition, the segregation of thickened tailings does not occur since the mass of thickened tailings has a homogenous behaviour with low permeability (Robinsky et al., 1991). The high-density thickened tailings will flow up to stop generally at slope beaches ranging from 2% to 10% (Engels, 2002). Thickened tailings disposal method has several advantages. It enables to (i) reduce or eliminate the risk and consequences of tailings dam failure, (ii) increase the amount of water available for reuse, (iii) decrease the footprint of the tailings storage facility, (iv) provide an option for progressive closure, and (iv) reduce the leachate seepage risk (Robinsky 1975, 1991; Edraki et al., 2014; Daliri 2013).

There have been numerous available laboratory studies on the seismic or cyclic behaviour of tailings in the literature which were carried out by different researchers (Ishihara et al., 1981; Crowder, 2004; Wijewickreme et al., 2005; Al-Tarhouni et al., 2011; James et al., 2011; Geremew and Yanful, 2013; Daliri, 2013; Seidalinova, 2014; Antonaki et al., 2019). However, most of these studies were conducted on conventional slurry tailings. Moreover, almost all the past laboratory seismic or cyclic studies were based on either cyclic direct simple shear or triaxial apparatuses. Yet, to the best knowledge of the authors, there is only one study that used shaking table testing technique to investigate the cyclic behaviour of tailings. Indeed, Pépin et al. (2012a, 2012b) have investigated the cyclic behaviour of "conventional" or slurry tailings (hard rock tailings) by using shaking table equipment. However, the results of this study cannot be applied to TTs because TTs are different than "conventional" tailings. However, no studies have been conducted on the cyclic behaviour of layered thickened tailings (TTs) by using shaking table testing technique. The liquefaction susceptibility of TTs is not well-known. An understanding and evaluation of the cyclic behaviour and liquefaction susceptibility of TTs is required before the use or implementation of this TTs deposition technique in earthquake-prone areas. Regulators are concerned with potential liquefaction of TTs deposits in those regions. There is a need to address this research gap.

The main objective of this study is to evaluate the behaviour, particularly liquefaction potential, of layered thickened tailings under cyclic loading conditions using a shaking table. Three different layers of thickened tailings were deposited in the flexible laminar shear box (FLSB). This paper presents and discuss the experimental results including the acceleration and horizontal displacement, pore water pressure, vertical displacement/settlement, and liquefaction responses.

### 4.2.2. **Materials and equipment used in the experiments**

#### 4.2.2.1. **Materials**

The thickened tailings (TTs) were created from mixing natural tailings (NTs) and industrial silica tailings (STs) with municipal water. The usage of these types of tailings together as a mixture allowed the accurate control of the mineralogical and chemical compositions of the tailings materials, thereby reducing uncertainties in the results obtained to a minimal level. Indeed, natural tailings can contain numerous reactive minerals, such as sulphide minerals. The latter, when exposed to air during the preparation and/or deposition of the tailings, can be oxidized. This oxidation can change the initial chemical or mineralogical composition of the thickened tailings and/or result in the precipitation of reaction products, which may cement some tailings particles together.

NTs were sampled from a mine that is located in eastern Canada. STs contain 99.8 wt% silicon dioxide ($SiO_2$). The key physical properties and mineral compositions of the used tailings (NTs; STs) are listed in Tables 4.1 and 4.2. NTs, STs, and their mixture show a particle size distribution (Figure 4.1) close to the average of 9 mine tailings that are coming from eastern Canada (Orejarena and Fall, 2008, 2010; Pokharel and Fall, 2013). From this figure, it can be said that NTs and STs include almost 37% and 45% particles finer than 20 μm, respectively. Based on the classification of tailings, these used tailings are considered as medium tailings (Landriault, 2001). Following the experimental procedure as in the ASTM D4318-17e1 (ASTM, 2017), it was found that the Atterberg limits (liquid and plastic limits) of the used tailings can not be determined in the laboratory. This indicated that the used tailings did not have plasticity. According to the Unified Soil Classification System (USCS), the used tailings are categorized as sandy silts of low plasticity (ML). Therefore, under the conditions of the seismic loading, the anticipation for this mixture of tailings (i.e. TTs) to be subject to liquefaction phenomena can be considered very likely with the absence of plasticity in the tailings (Pépin et al., 2012a).

Table 4.1. Physical properties of the tailings used and the coarse-grained sand

| Material | Physical Properties | | | | | | |
|---|---|---|---|---|---|---|---|
| | $G_s$ | $D_{10}$ (μm) | $D_{30}$ (μm) | $D_{50}$ (μm) | $D_{60}$ (μm) | $C_u$ | $C_c$ |
| STs | 2.7 | 1.9 | 9.0 | 22.5 | 31.5 | - | - |
| NTs | 3.1 | 3.2 | 15.8 | 35.5 | 49.5 | - | - |
| Sand | 2.7 | 700.0 | 740.0 | 880.0 | 1000.0 | 1.4 | 0.8 |

STs: silica tailings; NTs: natural tailings; $G_s$: specific gravity; $C_u$: coefficient of uniformity; $C_c$: coefficient of curvature

Table 4.2. Mineralogical composition of the tailings used

| Tailings | Mineral | | | | | | | | | | |
|---|---|---|---|---|---|---|---|---|---|---|---|
| | Quartz | Albite | Dolomite | Calcite | Chlorite | Magnetite | Pyrite | Talc | Pyrrhotite | Spinel | Others | Total |
| STs (wt.%) | 99.8 | - | - | - | - | - | - | - | - | - | 0.2 | 100.0 |
| NTs (wt.%) | 15.0 | 32.8 | 15.0 | 4.2 | 16.1 | 2.4 | 1.0 | 7.0 | 1.8 | 1.8 | 2.9 | 100.0 |

STs: silica tailings; NTs: natural tailings

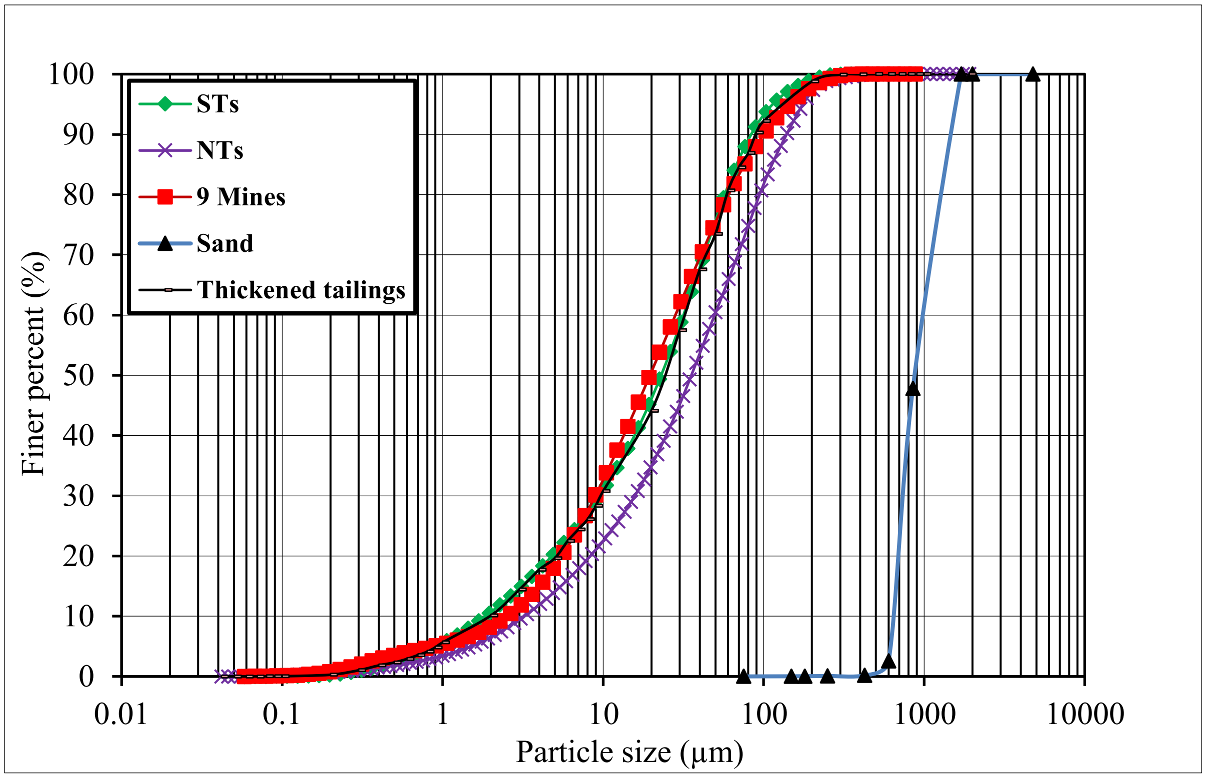


Figure 4.1. Particle size distribution of the tailings and coarse-grained sand used in this work compared with the average of 9 eastern Canadian mine tailings

4.2.2.2. **Preparation of the thickened tailings**

The mixture of 10 % of NTs and 90 % of STs with sufficient municipal water was prepared to reach the consistency of the thickened tailings. In the preparation stage, a large concrete mixer was used to mix the thickened tailings material until reaching homogeneity or obtaining a homogeneous material. The mixing time for all mixes was lasted for about 10 minutes. Wykeham-Ferrance laboratory vane shear apparatus was used for the workability evaluation and the yield stress measurement of this prepared thickened tailings material. From a single-point measurement (the maximum torque), the yield stress of the prepared thickened tailings can be determined (Dzuy and Boger, 1985). It was found that the yield stress was about 63 Pa which is considered related to the characteristic of the thickened tailings as stated, for example, by Sofrá (2017). This amount of yield stress was equivalent to a solid content of about 70 %. The degree of saturation of the prepared thickened tailings was determined to be equal to 100 %.

4.2.2.3. **Shaking table test**

The behaviour of soils under seismic or cylic loading conditions has been often investigated through the physical modeling tests (i.e. 1-g shaking table or centrifuge testes). These physical modeling tests have certain advantages and limitations (Ecemis, 2013). The well-controlled large amplitude, easier experimental measurements, and understanding the basic mechanisms of failure are considered advantages of the shaking table tests as compared with the centrifuge tests. However, the centrifuge tests can be used for measurements under field stress conditions which is not the case for the shaking table tests. Moreover, there are two issues, which associated with the centrifuge tests, that include all laws of scaling can not be fulfilled instantaneously and the response of whole soil can not be measured through a dense sensor set.

In this paper, the shaking table equipment was used to simulate the cyclic behaviour of the thickened tailings under the one direction of shaking loading. This used shaking table equipment belongs to the University of Ottawa, Canada, as illustrated in Figure 4.2. As shown in the figure, this equipment has dimensions of 1000 mm×1000 mm as a top aluminum platform capable of carrying a maximum payload of 1000 kg. A hydraulic actuator (model 244) with its capacity of 25 kN (Figure 4.2) can move the shaking table horizontally up to a frequency of 17 Hz with a maximum allowable peak to peak displacement in the longitudinal direction is 0.12 m.

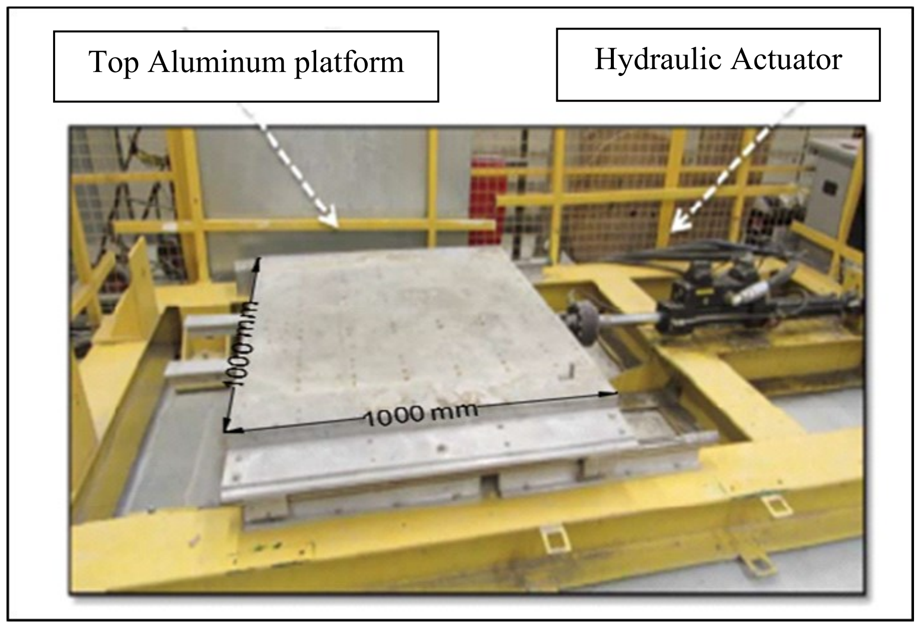


Figure 4.2. Shaking table equipment at the University of Ottawa used for this research (photo from Barakati, 2015)

4.2.2.4. **Model construction, setup and instrumentation**

A flexible laminar shear box (FLSB) is adopted to be used in this research work instead of a rigid box since the flexible laminar shear box (FLSB) permits the shear deformation of the tested specimen while providing enough confinement (Cheung et. al., 2013). Therefore, this leads to more simulation of the free-field boundary conditions when compared with the rigid box.

The FLSB was made-up to be suitable for the shaking table equipment at the civil engineering laboratory at the University of Ottawa. Designing of this FLSB was performed by Alainachi and Fall (2019) while it was constructed in the machine shop at the University of Ottawa. In addition, the design of the used flexible laminar shear box (FLSB) herein is considered to be like the design of those used by other researchers (Turan et al., 2009; Mohamed, 2014). A snapshot of the FLSB is given in Figure 4.3. The volume of this FLSB is about ~ 0.422 $m^3$ (i.e., dimensions: 750 mm in length, 750 mm in width, and 750 mm in height) which was formed by staking a set of 22 horizontal laminae on top of each other with a small distance (i.e. 2 mm) between each one of them to permit for the relative movement. Aluminum material was used to construct these laminae (i.e. box sections 31.65 mm x 31.65 mm) since it has somewhat lightweight and, at the same time, can provide enough confinement. The laminae were individually supported through linear bearings and stainless-steel guide roads in which connected to an external frame. These stainless-steel guide roads (two with 15 mm as diameter) were connected to the exterior wall of each lamina by stiff aluminum brackets. Six ball bearings with low friction, per lamina, were installed to feed these guide roads through them in which were fixed in four vertical bearings brackets. The vertical bearings brackets were then connected to the external frame. In general, the used external frame herein is considered to be like those available in the literature (Turan et al., 2009; Mohamed, 2014). The effect of inertia that can occur due to the mass of the empty FLSB (~ 132 kg) can be removed by transferring the total mass to the external frame. The mass on the external frame is carried then by big steel beams and consequently to the ground of the test site.

In thickened tailings technology, the tailings are subject to the dewatering process, where then they flow away from single or different deposition points to form gently sloped self-supporting stacks (Mizani, 2010). To simulate such slopes in this experimental work, a layer of sand material was, used underneath the thickened tailings deposit, placed inside the FLSB to form a slope with an angle of approximately 5.6% as shown in Figure 4.4. This selected slope angle herein was within the range that is reported in the literature as well as applied in the mining industry (Engels, 2002c; Robinsky, 1982). It should be underlined that, in practice, the slope angle in the field is a function of several factors, such as reclamation and climatic conditions, solid content, grain size distribution and pH of the TTs, and the rate of discharge per spigot (Robinsky, 1982). The used sand is categorized as a poorly graded sand (SP) based on the Unified Soil Classification System (USCS). Table 4.1 illustrates the physical characteristics of this sand layer while Figure 4.1 presents the particle size distribution curve for this sand layer.

A number of sensors were used to monitor the behaviour of the thickened tailings deposit during and after the shaking test. Figure 4.4 illustrates the positions of the sensors along with the FLSB. Three accelerometers (numbered as A1 to A3) were used for monitoring the acceleration behaviour of the tailings (i.e. at the intermediate depth of each layer) and were placed along the left external wall of the FLSB, on the same direction of shaking. To measure the motion of shaking, one accelerometer (numbered as A4) was also placed on the shaking table. These accelerometers (type 7593A) are from Endevco Company and have an acceleration range of ±2g. Three cable displacement transducers (numbered as HD1 to HD3) were used for monitoring the horizontal displacement behaviour of the tailings (i.e., at the intermediate depth of each layer) which were installed on a steel pole and then stretched to the left external wall of the lamina on the same direction of shaking. Additional three cable displacement transducers (numbered as VD1 to VD3) were used for monitoring the settlement of the tailings (i.e. at the intermediate depth of each layer) which were hanged on a steel bridge that was attached on the top middle of the FLSB. These cable displacement transducers (numbered as VD1 to VD3) were then tied on the upper section of steel rods while the lower section of these steel rods was then connected to perforated plastic plates which their settlement lead to pull the cables down. Mesh cylinders (made from light steel) with open holes were used to keep the steel rods from falling during the shaking. Such a way was used previously by Alainachi and Fall (2019). All cable displacement transducers (type SM2-12) are manufactured by Measurement Specialties Company and have a range of ±318 mm. Other sensors were embedded in the tailings deposit (i.e. at the intermediate depth of each layer) on the normal direction of shaking which include three pressure transducers (numbered as P1 to P3) for pore water pressures monitoring and three 5TE sensors (numbered as 5TE1 to 5TE3) for volumetric water content monitoring. These pressure transducers (type PX309-015CG5V series) are manufactured by the Omega Company and have a pressure range of ±103.42 kPa. The 5TE sensors are manufactured by Decagon Devices Inc. and monitor the volumetric water content within the range of 0–80%. These embedded sensors and their cables are in small size, water resistance, and durable.

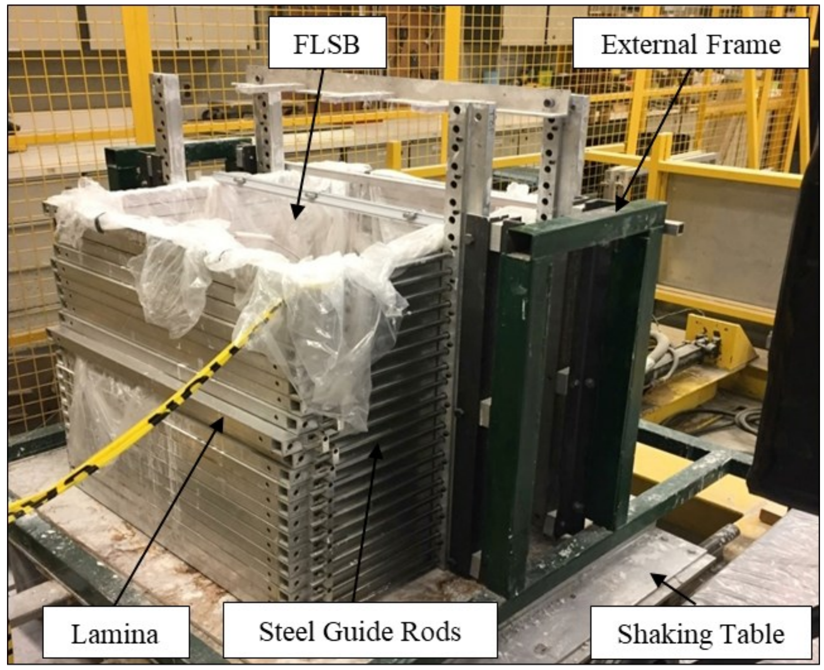


Figure 4.3. Snapshot of the University of Ottawa's FLSB

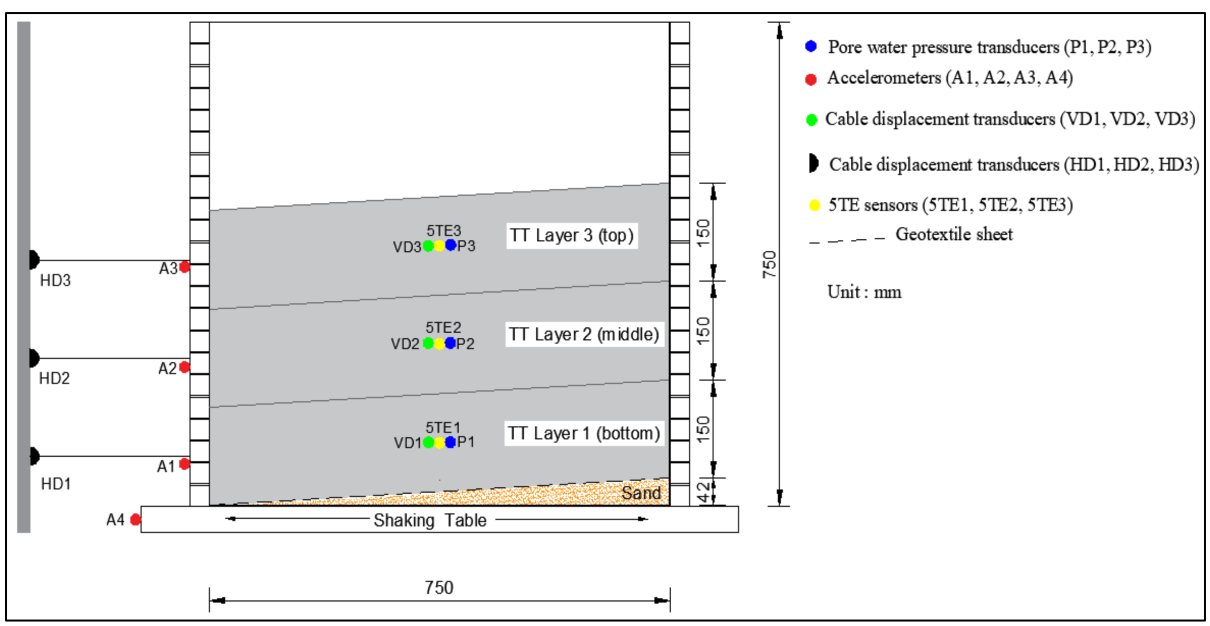


Figure 4.4. The used Flexible Laminar Shear Box (FLSB) on the shaking table with the positions of sensors

### 4.2.3. **Thickened tailings deposition, testing program and procedure**

The deposition process of the thickened tailings in the FLSB was performed in three thin layers (i.e. each layer had a thickness of 150 mm) to simulate the field deposition or field layer thicknesses as in the in-situ (Raposo et al., 2014), as shown in Figure 4.4. These layers were named in the order according to their deposition in the FLSB (Figure 4.4.). The deposition time between the first layer (bottom layer) and the second layer (middle layer) was three days while it was two days between the second layer (middle layer) and the third layer (top layer). Deposition of thin layers and desiccation (drying) are key in order to increase the strength of the tailings prior to pouring the next fresh layer (Li et al., 2009). Although thin-layer deposition method and desiccation promote strength development, which, in turn, enhances the mechanical stability of the thickened tailings structure, an excessive drying could lead to the oxidation of sulphide minerals (e.g., pyrite) in sulphidic tailings. This oxidation can result in the generation of acid mine drainage, thereby jeopardizing the environmental safety of the thickened tailings disposal technique.

In the deposition of the aforementioned thin layers, a concrete bucket that hanged by a crane was used. This concrete bucket has an opening at its bottom for pouring the thickened tailings in the FLSB as shown in Figure 4.5a. The surface of the fresh thickened tailings deposit can be shown in Figure 4.5b. A temperature and humidity sensor was used in the laboratory and showed that the average temperature and relative humidity were 20.4°C and 57%, respectively.

The experimental program of this study comprised from testing of the thickened tailings deposit at early deposition by using the shaking table. It should be pointed out that the goal of this study is to evaluate the cyclic behaviour of thickened tailings at early ages, i.e. when the deposition of the first layers of thickened tailings has been completed. This approach enables to appropriately scale down the parameters of the model experiment based on the similitude laws. Thus, a thickened tailings structure after the deposition of three 150 mm-thin layers of thickened tailings was considered in this testing program. In practice, this will correspond to the early ages (first week) of the deposition of thickened tailings. Though only three layers of thickened tailings or the thickened tailings during early deposition were tested in this research, gaining insight into the response of 3 layers of thickened tailings or thickened tailings at early ages to earthquake-induced dynamic loading will permit to gain a deeper understanding of the cyclic behaviour of thickened tailings deposits at advanced or mature ages, i.e. when the deposit is made of over 30 layers. Moreover, considering a thickened tailings deposit with 3 layers enabled to meet the key similitude requirements between the physical model and prototype. Hence, a geometric scaling factor (N) of 1:1 was adopted for the experimental shaking table tests on the scale model in this study. The geometry and configuration of the models were designed based on the similitude theories associated with the 1 g shaking table test for the soil-fluid models proposed by Iai (1989) and Meymand (1998). The scaling factors used in this investigation are given in Table 4.3.

The testing program includes applying a peak acceleration of 0.13g and a frequency of 1 Hz at the bottom of the thickened tailings deposit that contained inside the FLSB for a time of 1800 seconds (30 min). The minimum level of the generated peak accelerations, due to seismic earthquakes shakings, that needed to cause the liquefaction phenomena were reported in the literature to be 0.05–0.10g (Carter, 1988). Accordingly, the mine tailings in several regions in eastern Canada might be susceptible to the liquefaction phenomena under the generated peak accelerations as a result of the seismic earthquakes shakings (James et al., 2003). The amount of acceleration in this investigation was similar to the acceleration that resulted during the earthquake that occurred in Saguenay, Québec, Canada, which had a scale of 5.9 (Tuttle et al., 1990). It should be emphasized that only the peak acceleration corresponds to the peak of Saguenay Earthquake, not the whole time series. The selected applied frequency herein was based on previous liquefaction studies (e.g. Ishihara et al., 1981; James et al., 2003; Ueng et al., 2010; Pépin et al., 2012a, 2012b; Geremew and Yanful, 2013) and compatible with the capability of the used sensors in terms of the monitoring. The instruments used were unable to monitor the dynamic response of the tested thickened tailings or soils under large loading frequencies. Even though the duration of shaking in the actual earthquakes is much shorter than that one used in this study, such a long duration of shaking (e.g. 1800 seconds) will permit the insight into the cyclic behaviour of the tested tailings as well relative comparisons of their behaviour. This is considered vital in terms of the future development of a constitutive model in order to expect and evaluate the dynamic or seismic behaviour of the thickened tailings. Previous authors have used a similar long duration of seismic shaking in their liquefaction studies of hard rock tailings (e.g. Pépin et al., 2012a). It should be emphasized that these selected conditions were not intended to simulate an actual earthquake but instead they gave a general insight into the seismic or cyclic behavior of this type of tailings. The bottom of the thickened tailings deposit was subject to shaking after 24 hours from the deposition of the top layer. The behaviour of the tested tailings was continued to be observed once the shaking was stopped. Once the excess pore water pressure experienced a completed dissipation condition, the measurements through the sensors were stopped.

Table 4.3. Relationship of similarity between the prototype thickened tailings* and thickened tailings shaking table model

| **Parameters** | **Scale factor** |
|---|---|
| Acceleration | 1 |
| Thickened tailings height | N |
| Mass density | 1 |
| Force | $N^3$ |
| Stiffness | $N^2$ |
| Modulus | N |
| Stress | N |
| Strain | 1 |
| Frequency | $N^{-1/2}$ |
| Shear Wave Velocity | $N^{1/2}$ |
| Time | $N^{1/2}$ |
| EI | $N^5$ |

*Thickened tailings deposit at early ages (made of 3 thin layers) was considered

Several procedures were followed prior to the deposition of the thickened tailings deposit in the FLSB. The interior of the FLSB was first covered by a thin flexible plastic bag to pour the materials inside it, as shown in Figure 4.3. This action was done to inhibit the leakage of the poured materials and water. Then, a drainage layer of sand material, with a slope of 5.6%, was poured on top of the plastic bag. A geotextile material was then placed between the sand layer and the tested tailings. This allowed only the water to move from the tailings materials layer to the sand layer without passing the particles of tailings. Finally, the three thin layers of the thickened tailings were deposited sequentially, as described above, in the FLSB with a total height of 450 mm (Figure 4.4).

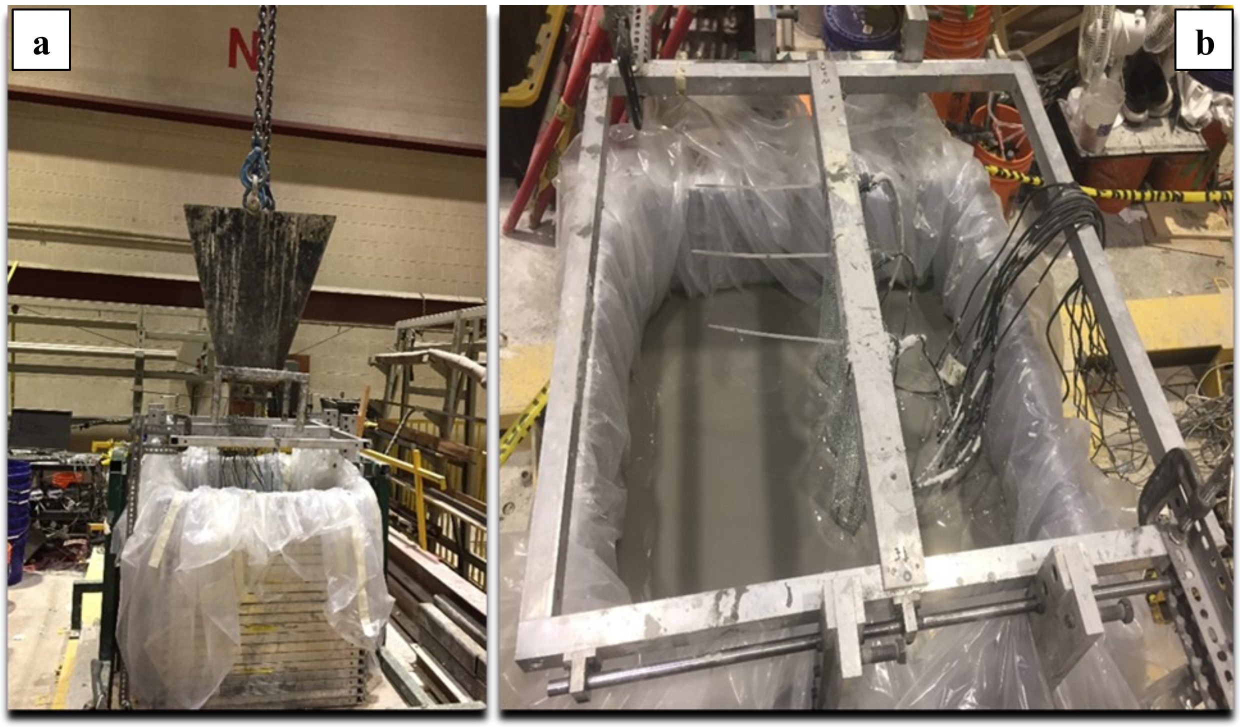


Figure 4.5. (a) Snapshot showing the concrete bucket that was used for deposition of thickened tailings layers. (b) Snapshot of the ground surface of thickened tailings shortly after deposition of the third (top) layer

### 4.2.4. **Results and discussion**

#### 4.2.4.1. **Acceleration and horizontal displacement response**

The acceleration response is considered as one of the ways that can be used as an indication of the liquefaction occurrence (Bahmanpour et al., 2019). For instance, Ueng et al. (2006, 2010) were reported the use of the measured accelerations at different depths of sand as a way for the determination of the liquefaction occurrence. Figure 4.6 reveals the acceleration time histories of measured accelerations at the shaking table and intermediate depth of all layers of the thickened tailings. Similarly, Figure 4.7 shows the horizontal displacement time histories of measured horizontal displacements at the intermediate depth of all layers of the thickened tailings. As depicted in these figures, the termination of shaking loading can be pointed out by the red arrows.

As expected, the measured acceleration at the base of the shaking table increased rapidly and attained almost the sinusoidal input acceleration (0.13g), as shown in Figure 4.6d. This indicated that the system of the shaking table was working well. The results revealed that the measured accelerations, at the intermediate depth of the bottom and middle layers, were seen to be not diminution and somewhat similar to the trend of the measured acceleration at the base of the shaking table (no phase shift was observed in the comparison of the cycles). This means that the applied sinusoidal input acceleration propagated entirely to these two layers. Coelho et al. (2004), who carried out cyclic loading tests on saturated sand using centrifuge apparatus, observed similar behaviour. They stated that the reason for the aforementioned behaviour might be related to the large value of the initial vertical stress at these two layers. However, this Coelho et al.'s explanation may not be valid for this study because of the low vertical effective stress. Future studies should confirm this explanation or clarify the cause of this behaviour. On the other hand, the measured acceleration at the intermediate depth of the top layer found to be not regular and diminution relative to the measured acceleration at the base of the shaking table, as revealed in Figure 4.6a and Figure 4.6d. Such behaviour could be resulted from the occurrence of the liquefaction where this top layer of thickened tailings was experienced nonlinearity, strength and stiffness reduction as a result of the applied shaking loading. However, it should be mentioned that other or additional factors could have caused the observed changes of acceleration in the top layer. These factors could be higher effect of excess pore pressure and reduction in shear resistance as well as increase in damping ratio.

As shown in Figure 4.7, the measured horizontal displacements at the intermediate depth of all layers of the thickened tailings were noticed to be increased rapidly and almost similar to each other. The amount of this displacement was approximately ± 3.1 cm (back and forth motions). Throughout the shaking loading, this behaviour is compatible with the observation of the motion of FLSB by the naked eye.

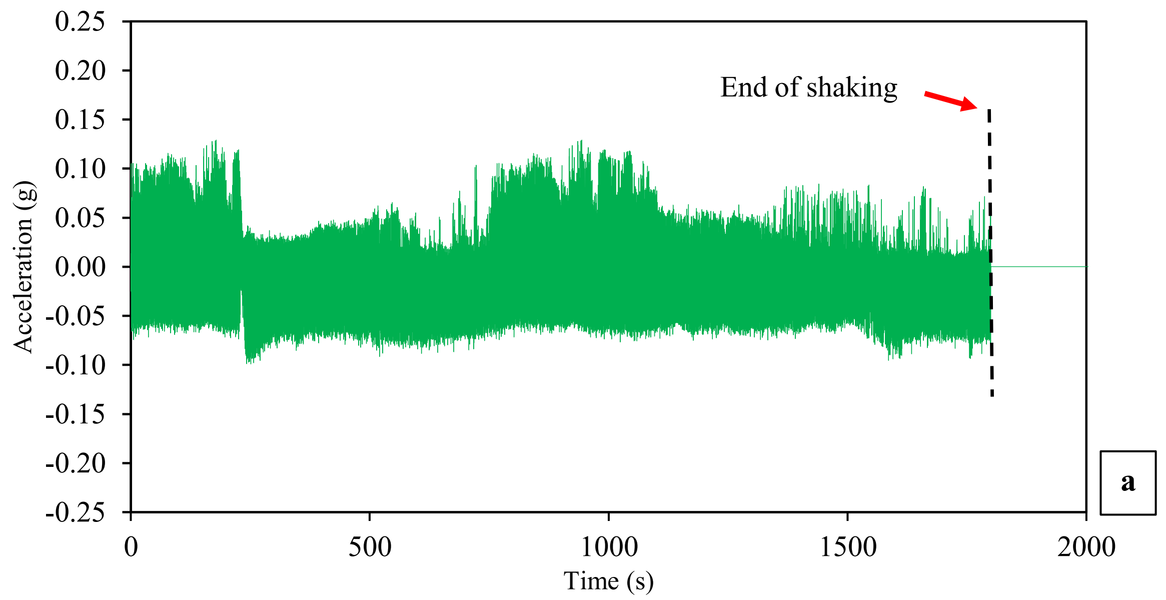


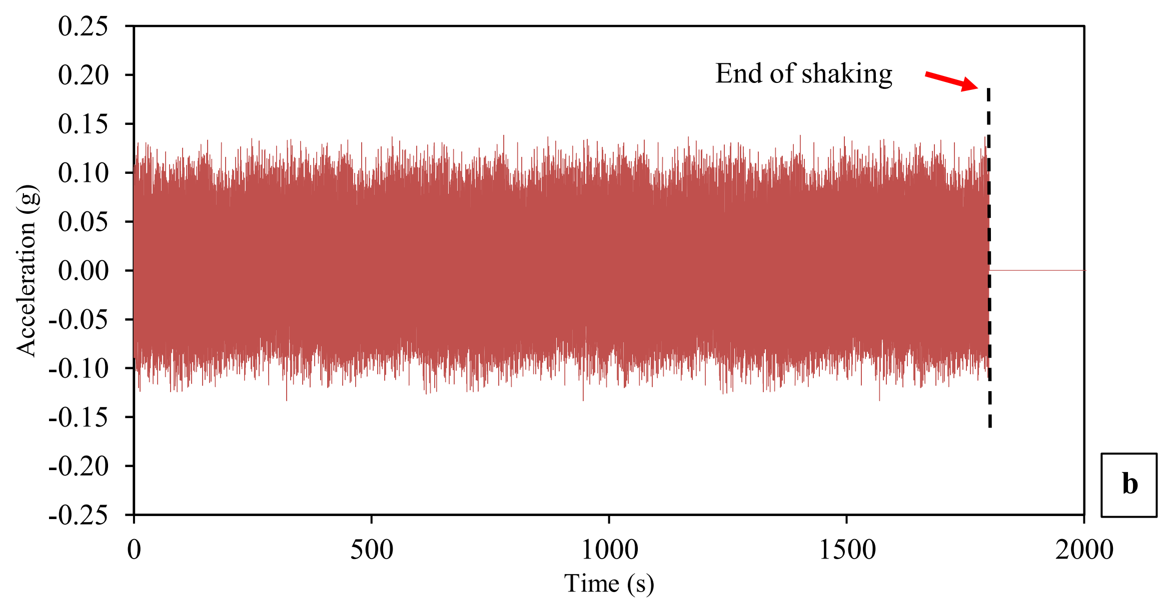

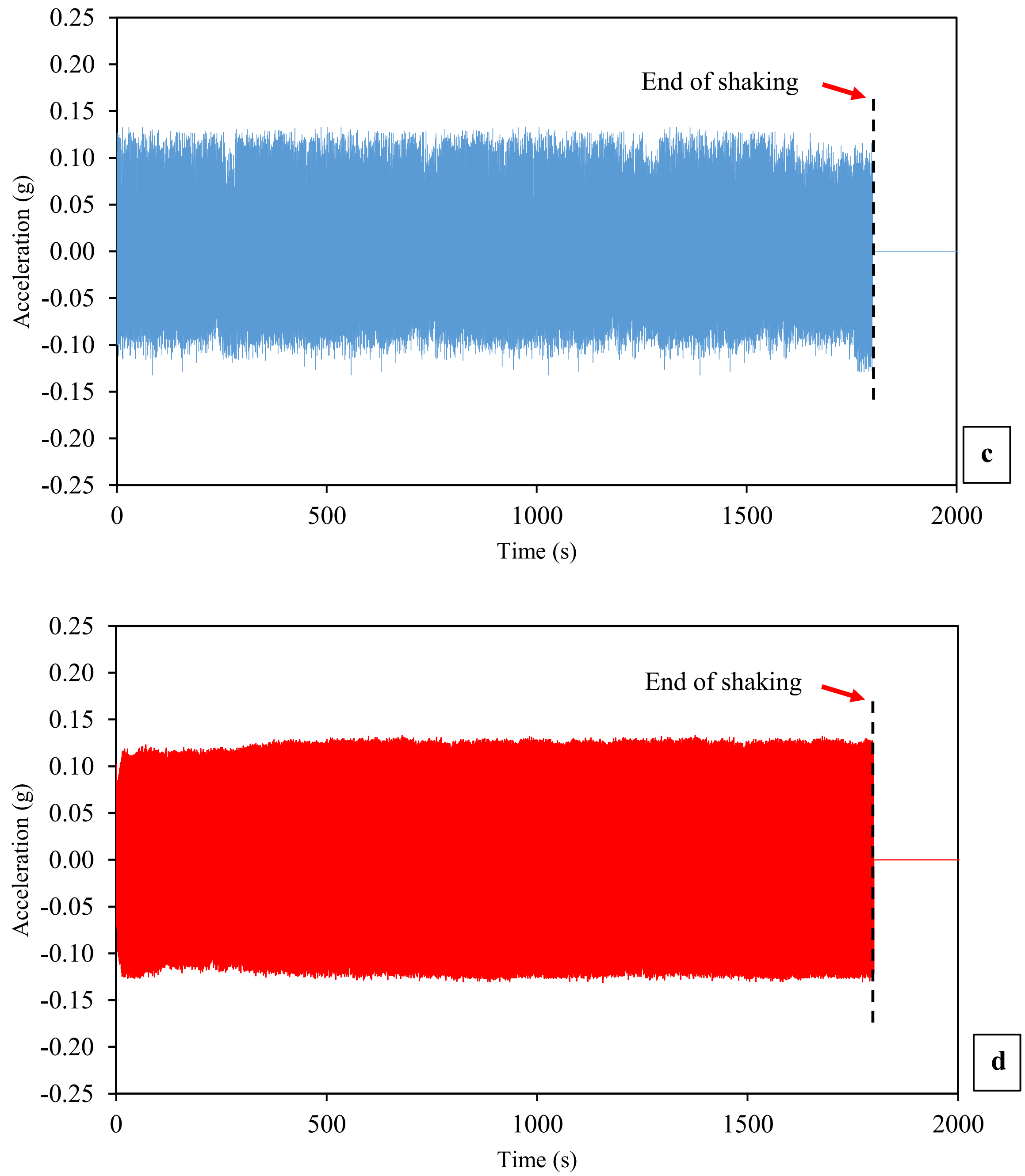


Figure 4.6. Time histories of measured accelerations at the intermediate depth of each layer of thickened tailings deposit and at the base of the shaking table during shaking: (a) Layer 3 (top), (b) Layer 2 (middle), (c) Layer 1 (bottom), (d) shaking table

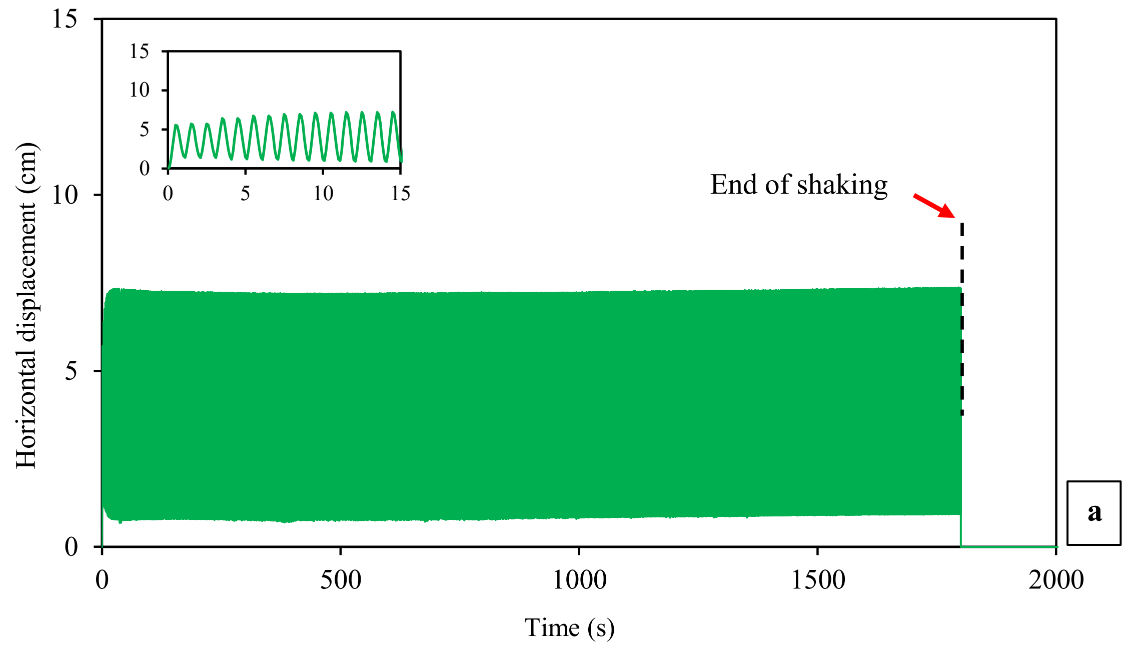

15
10
5
0
0
5
10
15
End of shaking
Horizontal displacement (cm)
0
500
1000
1500
2000
Time (s)
a


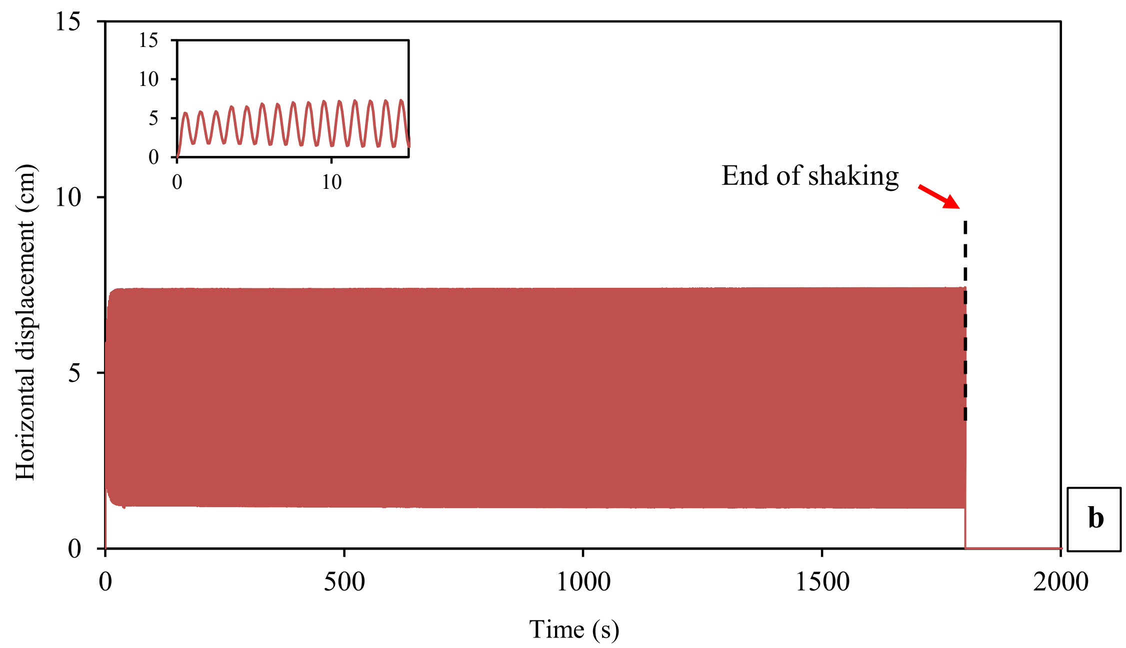

15
10
5
0
0
10
End of shaking
Horizontal displacement (cm)
0
500
1000
1500
2000
Time (s)
b

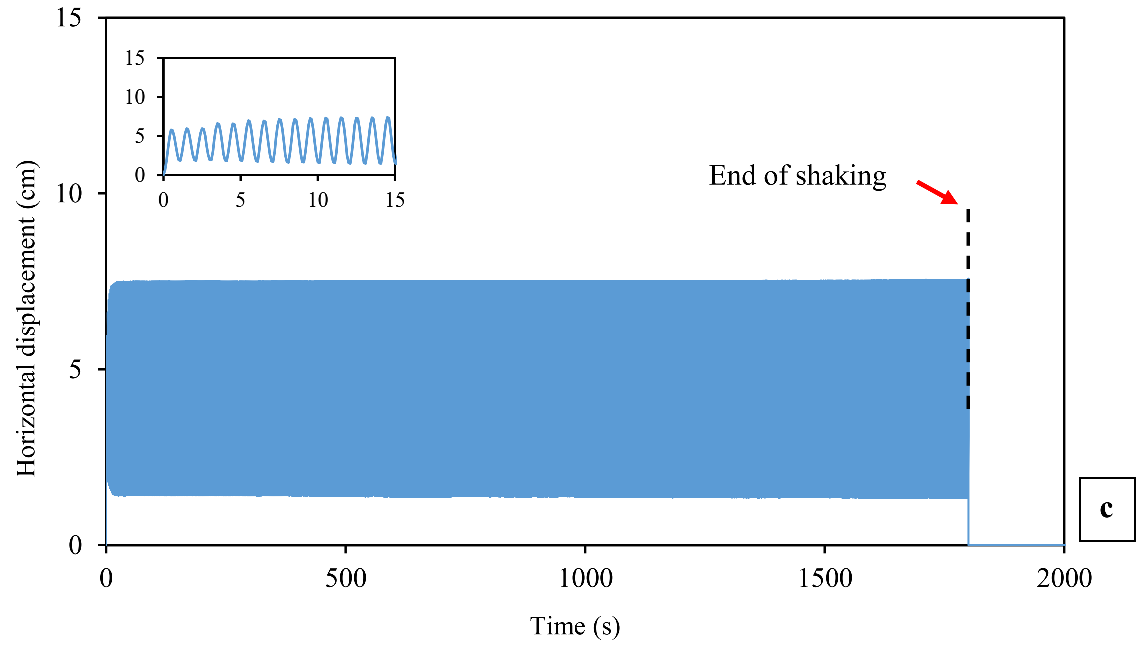


Figure 4.7. Time histories of measured horizontal displacements at the intermediate depth of each layer of thickened tailings deposit during shaking: (a) Layer 3 (top), b) Layer 2 (middle), c) Layer 1 (bottom)

4.2.4.2. **Pore water pressure response and liquefaction analysis**

Numerous liquefaction triggering criteria have been proposed and adopted to describe or determine liquefaction of natural or man-made (tailings) soils. These criteria comprise excess pore pressure-based criteria, strain/deformation-based liquefaction criteria, energy-based liquefaction criteria, and strength-based criteria. Each of these methods has advantages, but also limitations, as described in various previous studies (e.g., Wu et al., 2004).

The excess pore pressure-based criteria are adopted in this study. The development and the dissipation of the excess pore water pressure or the pore pressure-based criteria have been extensively used in evaluating the liquefaction potential of natural and man-made (tailings) in the laboratory, particularly in shaking table tests (e.g., Pépin et al., 2012a; Varghese and Latha, 2013; Lu and Fall, 2018; Wang et al., 2020). The ratio of the excess pore water pressure ($r_u$) is a key parameter that is used as an indication for the liquefaction occurrence. When the ratio of the excess pore water pressure ($r_u$) is larger or equal to 1, the liquefaction occurs (Casagrande, 1936; Ueng et al., 2010; Pépin et al., 2012a, b). However, it has been also shown that the value of $r_u$ at liquefaction triggering is affected by soil densities and loading conditions. Denser soils subjected to larger shear stress ratios generate lower pore pressure ratios $r_u$ at the onset of liquefaction (Wu et al., 2004). This ratio, $r_u$, can be calculated via Equation 4.1.

$$\boldsymbol{r_u} = \Delta \boldsymbol{u}/\boldsymbol{\sigma'}_{\boldsymbol{vo}} \qquad \textbf{4.1.)}$$

In Equation 4.1, $\Delta u$ represents the excess pore water pressure generated during shaking loading and $\sigma'_{vo}$ represents the initial vertical effective stress prior to shaking loading.

The measured time histories of the excess pore water pressure at the intermediate depth of each layer of the tested thickened tailings and the corresponding excess pore water pressure ratio are presented in terms of during and after shaking loadings in Figures 4.8 and 4.9, respectively. The excess pore water pressure at the intermediate depth of each layer of the tested tailings started to build-up immediately once the shaking loading was applied, as shown in Figure 4.8. This excess pore water pressure was continuous to build-up until reaching a peak value which then it did not alter until the shaking loading was terminated. The contraction response of the tested tailings had caused the built-up of this excess pore water pressure, as illustrated in Figures 4.12 and 4.13, which will be discussed later in the next section (section 4.2.4.3). Volume dilation of the tested tailings, as the results of the applied shaking loading at very low vertical effective vertical stress, had led to the somewhat unchanged in the excess pore water pressure beyond this peak value (Pépin et al., 2012a), as evidenced in Figures 4.12 and 4.13. The bottom layer needed the longest time in order to reach the peak value of the excess pore water pressure ($\Delta u$) when compared with the other two layers, as revealed in Figure 4.8. Because of water flow and pressure redistribution takes time, such a delay occurred. Therefore, there is often a delay between the time of seismic shaking and time of attainment the peak excess of pore water pressure or liquefaction failure (Naesgaard and Byrne, 2007; Serafini and Perlea, 2010). Also, it has been observed from this figure that the bottom layer had the highest peak value of the excess pore water pressure ($\Delta u$), which then followed by the middle layer and lastly by the top layer. This means that as the depth increased, the peak value of the excess pore water pressure ($\Delta u$) became larger. Such higher peak value of the excess pore water pressure ($\Delta u$) at the bottom layer might be partly related to the downward flow of pore water that came from the middle layer to the bottom layer (some water is drained through the sand drainage layer) as demonstrated by the results of the volumetric water content as revealed in Figure 4.10 (later will be discussed). This indicated that this pore water pressure in the bottom layer is generated partially by pore pressures generated in the bottom layer and partially by the inflow of pore water from the upper layer. Moreover, from Figure 4.10, it is also noticeable that an upward flow of pore water from the lower part of the thickened tailings deposit to the upper (top) layer took place during shaking. In addition, the observations of Naesgaard and Byrne (2007) on layered soils supported the previous description as they reported that earthquake shaking of layered soils persuades pore water gradients, the inflow of pore water in some areas or layers and outflow of pore water in some areas. Similar behaviour was reported by Tohumcu Özener et al. (2009) who investigated the pore water pressure generation and related liquefaction in layered sand soils under shaking table equipment. Furthermore, the top layer needed longer time to reach the peak value of the excess pore water pressure during shaking in comparison to the middle layer. This can be explained by the fact that water flow and pressure redistribution take time. Accordingly, there is often a delay between time of shaking and time of reaching the maximum excess of pore water pressure (Naesgaard and Byrne 2007; Serafini and Perlea, 2010). The ratio of the excess pore water pressure ($r_u$), during the shaking, was noticed to be greater than 0.95 at all depths of the tested tailings, as revealed in Figure 4.8.

The termination of shaking loading can be pointed out by the red arrows, as displayed in Figure 4.8. An interesting point in this figure is the sudden building-up in the excess pore water pressure ($\Delta u$) that was observed throughout all depths of the tested thickened tailings as soon as the applied shaking loading was terminated. This led the ratio of the excess pore water pressure ($r_u$) to be built-up slightly to be over 1 in general. Based on the above observations, it can be concluded that the tested thickened tailings are potentially liquefiable material under the used input shaking loading conditions. This finding is in agreement with the finding of Antonaki et al. (2019) who have assessed the liquefaction of tailings under the centrifuge testing. It has been seen that as the depth of the tested tailings increased, the amount of this sudden building-up became greater. Such resulted behaviour can be explained by the difference between the three layers in terms of the amount of the vertical total stress where the larger vertical total stress was related to the deeper depth. The termination of the shaking loading is considered to be responsible for the occurrence of such sudden increase, which permitted the volume contraction of partially suspended tailings grains, thus producing further pore water pressure at all depths (Pépin et al., 2012a). The observed responses herein agree with those reported in the literature (Pépin et al., 2012a, 2012b) for hard rock tailings. The process of the upward and downward flow of pore water at the tested thickened tailings deposit could be considered as a further reason that might lead to this sudden increase of excess pore water pressure in the top layer (Layer 3) and bottom layer (layer 1). The pore-water flow upward from the lower part of the thickened tailings deposit to the upper (top) layer while it flows downward from the lower part of the middle layer of the thickened tailings deposit to the bottom layer (Layer 1). This previously explained process is supported through both the evolution of the volumetric water content (VWC), which was observed to be increased in the intermediate of the top and bottom layers during the applied shaking and up to about 40 min after the end of applied shaking as revealed in Figure 4.10, and with the appearance of tailings boils at the ground surface of the top layer of the thickened tailings deposit (Figure 4.11). Such manifestation was observed following the liquefaction of Mailiao silty sand (Ueng et al., 2008) and following the liquefaction of thickened fine mine tailings (Antonaki et al., 2019). This manifestation was attributed to the expel of water together with the grains to the ground surface of the tested tailings. Moreover, Figure 4.10 shows the increase in VWC observed in the bottom layer is higher than that in the top layer. This downward flow of more water to the bottom layer might have been facilitated or enabled by desiccation-induced microcracks that appeared on the surface of the first layer of thickened tailings after 3 days of drying, i.e. before the deposition of the second layer as well as by the sand drainage layer underneath the TTs deposit. It is well acknowledged that cracks increase the permeability of soil or tailings deposits (Roshani et al., 2017a, b).

The value of this sudden increase in excess pore water pressure, at all depths of deposit, stayed stable for a short period of time after the shaking loading was terminated, as revealed in Figure 4.9. Then, the generated pore water pressure started the process of its dissipation, which took a long period of time (approximately 35000–130000 seconds). Pépin et al. (2012a, 2012b) tested the tailings under cyclic loading conditions and found that the tailings needed a long period of time in order to reach the full dissipation of its excess pore water pressure. However, several studied (e.g. Ueng et al., 2010) have indicated that the required time for dissipation of the excess pore water pressure of sandy soil was short. The difference between the tested tailings and the sandy soil, in the period of dissipation, can be due to the relatively lower hydraulic conductivity (~$10^{-5}$ - $10^{-7}$ m/s) that associated with the uncracked thickened tailings (Robinsky et al., 1991; Bussière, 2007) than that in sandy soil (~$10^{-3}$ - $10^{-5}$ m/s). An important observation was noticed in Figure 4.9, where the full dissipation of the excess pore water pressure at the bottom layer needed the greatest period of time when compared with the other two layers. Such observation can be associated with the inflow of pore water as the largest evolution of volumetric water content at the intermediate depth of the bottom layer was noticed after the termination of the applied shaking loading, as revealed in Figure 4.10. The excess pore water pressure at the top layer dissipated slower than that at the middle layer. The reason for that might be related to the transition of water from the middle layer to the top layer which is considered in consistence with the lower evolution of the volumetric water content at the middle layer than at the top layer, as revealed in Figure 4.10, and also with the observations of other researchers (Naesgaard and Byrne, 2007; Serafini and Perlea, 2010) who investigated the seismic liquefaction of layered soils.

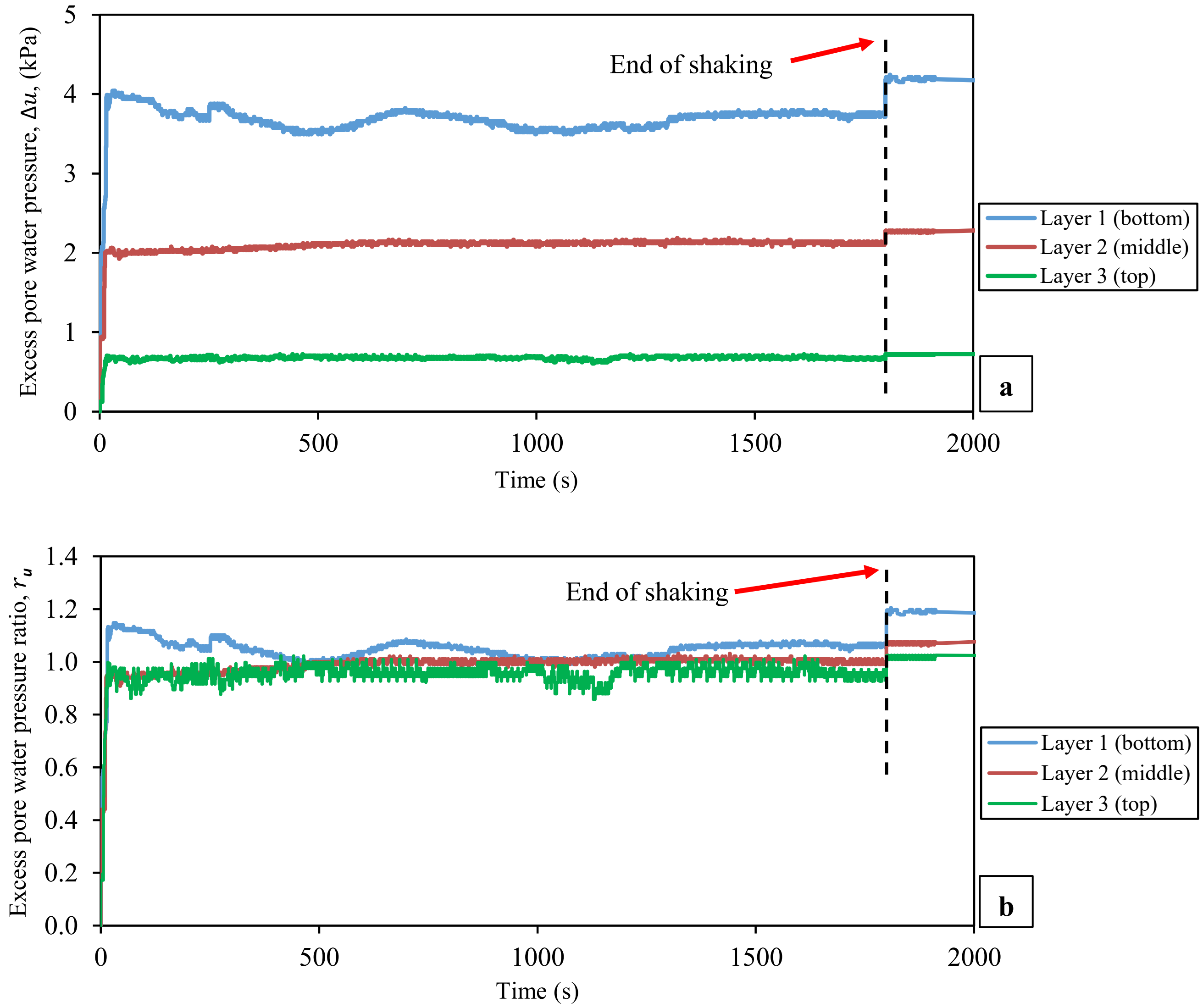


Figure 4.8. Time histories of the excess pore water pressure at the intermediate depth of each layer of the thickened tailings deposit during shaking loading. a) Measured excess pore water pressures ($\Delta u$). b) Excess pore water pressure ratios ($r_u$)

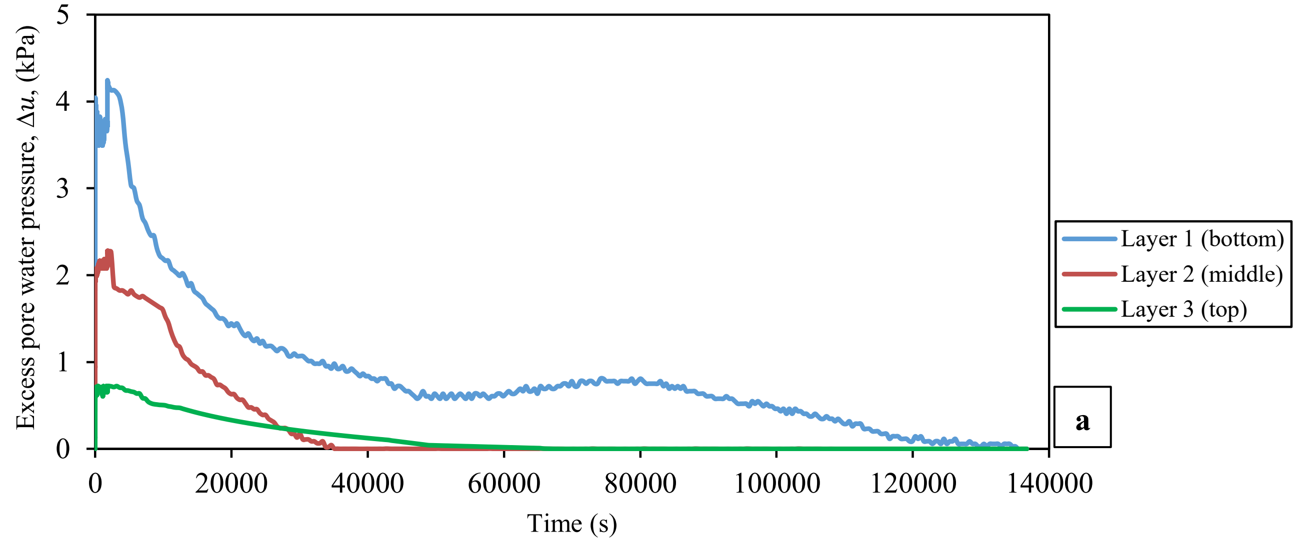


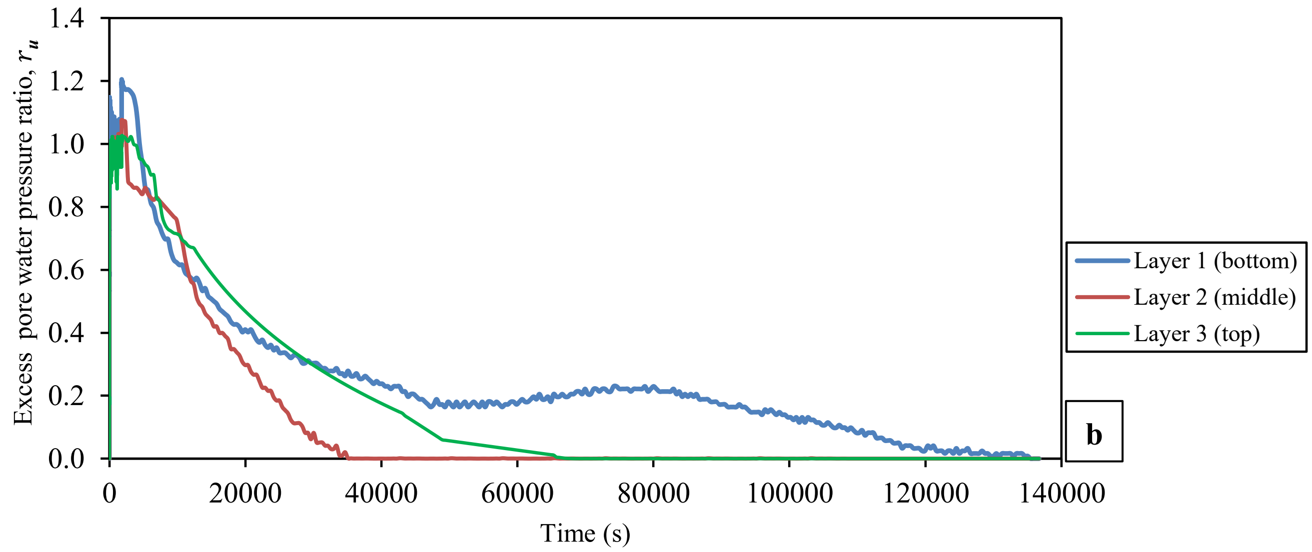


Figure 4.9. Time histories of the excess pore water pressure at the intermediate depth of each layer of the thickened tailings deposit during and after shaking loading. a) Measured excess pore water pressures ($\Delta u$). b) Excess pore water pressure ratios ($r_u$)

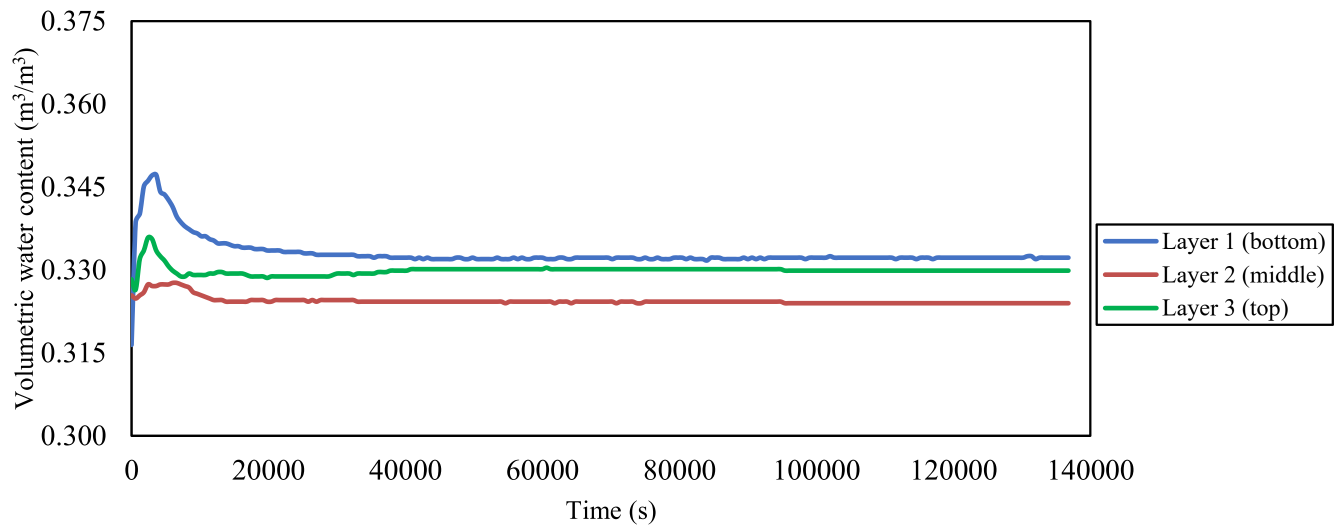


Figure 4.10. Time histories of volumetric water content at the intermediate depth of each layer of thickened tailings deposit during and after shaking

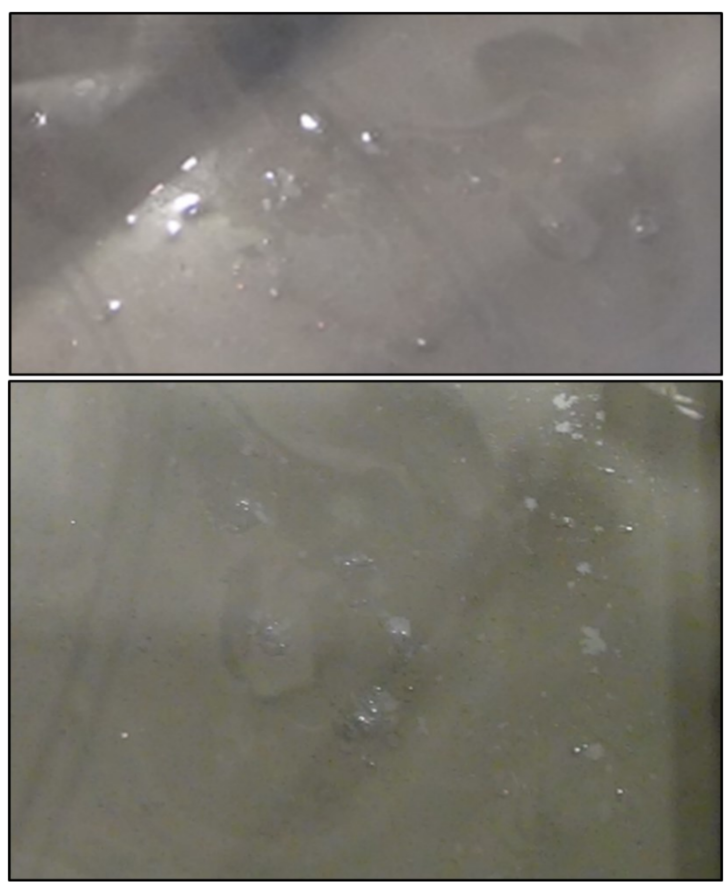

Figure 4.11. Tailings boils observed on the ground surface of the thickened tailings deposit after liquefaction

4.2.4.3. **Vertical displacement/settlement response**

During and after the shaking loadings, the measured time histories of the vertical displacement at the intermediate depth of each layer of the tested thickened tailings are presented in Figures 4.12 and 4.13, respectively. The red arrow in Figure 4.12 depicts the termination of the shaking loading. Two types of responses that the tested tailings passed through during the shaking loading, namely, the volume contraction and dilation, as deduced from Figure 4.12. This figure revealed that all layers of tested tailings were experienced settlement initially (i.e., volume contraction) as soon as the shaking loading was applied. Generally, the value of this settlement was approximately 0.5 mm for the bottom layer, 2.3 mm for the middle layer, and 1.0 mm for the top layer, respectively. This indicates that the deposit at the bottom layer had the lowest settlement as compared with the other two layers. The reason for such a response could be due to the difference in terms of the duration of the drying (desiccation) between these layers as the top and middle layers were experienced a lower duration of drying (desiccation) than that at the bottom layer. The previous investigation conducted by Daliri (2013) revealed that the response of tailings changed from contraction to dilation when they subjected to somewhat degree of drying or desiccation. Following the settlement (i.e., volume contraction) response, the tested deposit transformed to the other response (i.e., volume dilation) which as a result of the uplift of the plastic plates at all layers. The dilation of tested tailings was firstly somewhat developed at the bottom layer then proceeded at the top layer and eventually at the middle layer. The inflow of pore water from the upper portion (middle layer, upper portion of the bottom layer) of tested thickened tailings is considered an additional reason that leads to a lower volume contraction and dilation at the bottom layer. The observation from this current study is considered consistent with that of layered soils as reported in the literature (Naesgaard and Byrne, 2007; Serafini and Perlea, 2010). Following the termination of the shaking loading, it seemed that no substantial difference in the response of the thickened tailings deposit, as revealed in Figure 4.13.

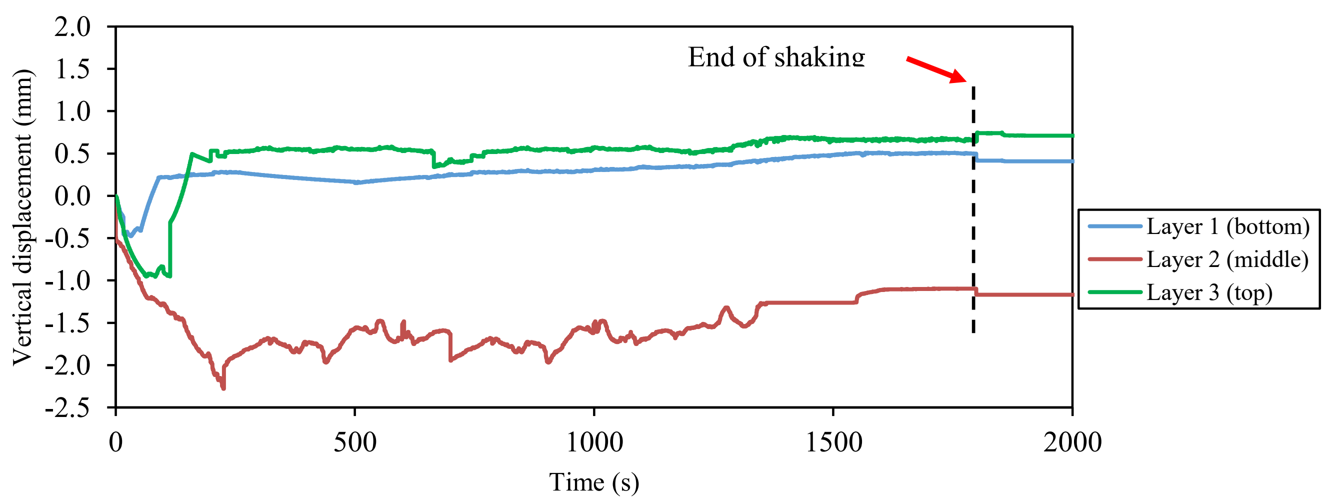


Figure 4.12. Time histories of the vertical displacement at the intermediate depth of each layer of the thickened tailings deposit during shaking loading

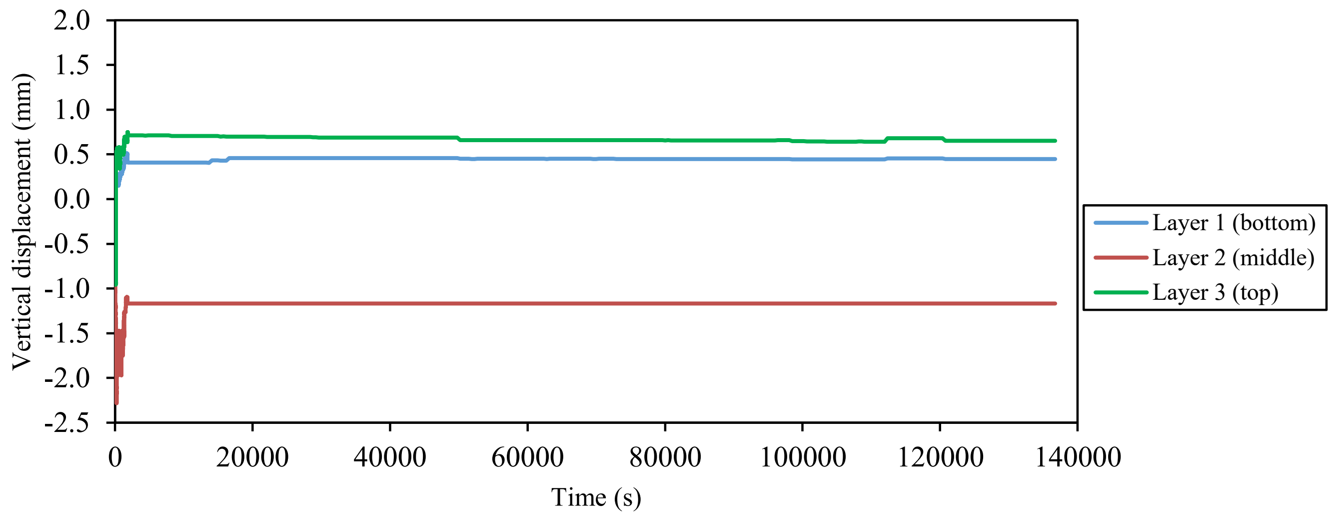


Figure 4.13. Time histories of the vertical displacement at the intermediate depth of each layer of the thickened tailings deposit during and after shaking loading

### 4.2.5. **Conclusions**

In this research work, a shaking table test was conducted on three thin layers of thickened tailings contained within a flexible laminar shear box. This flexible laminar shear box was subjected to a peak horizontal acceleration of 0.13g and a frequency of 1 Hz. Based on these considered testing conditions, the following conclusions can be drawn.

Typically, the results from the measured accelerations indicated that the applied input acceleration propagated completely to the bottom and middle layers except for the top layer, which could be due to its strength and stiffness reduction during shaking. Similar measured horizontal displacements were observed at all depths of the layered thickened tailings.

The flow of water and pressure redistribution in the tested layered of thickened tailings were occurred due to the applied shaking loading. Both the bottom and top layers were subjected to the inflow of water, while the middle layer is influenced by the outflow of water. The behaviour of the tested layered thickened tailings in terms of excess pore water pressure, liquefaction, and vertical displacement significantly influenced by such outflow and inflow of water.

The excess pore water pressure at the intermediate depth of each layer of the thickened tailings deposit was seen to build-up immediately and continuously until attainment a peak value during the applied shaking. Such a built-up was related to the volume contraction of this type of tailings. Additionally, the inflow of pore water into both the bottom and top layers played a role in such a built-up of excess pore water pressure. Once the applied shaking was terminated, there was a sudden building-up in the excess pore water pressure of the layered thickened tailings. Typically, this caused the ratio of the excess pore water pressure to be slightly larger than unity which revealed that the layered thickened tailings liquefied under the considered testing conditions. This sudden building-up in the excess pore water pressure occurred as a result of two factors, namely, (i) the volume contraction of partially suspended tailings grains which producing further pore water pressure; (ii) the movement of upward pore water to the top layer and downward pore water to the bottom layer which leads to produce further pore water pressure. The full dissipation of the excess pore water pressure of the tested layered thickened tailings was seen to be occurred after a long period of time as expected due to the low permeability of such tailings.

During the shaking loading, the layered thickened tailings were observed to be subject to two types of responses, namely, the volume contraction and dilation as per the measurements of the vertical displacements. Since the bottom layer of the deposit was subjected to higher duration of drying (desiccation) than that at the top and middle layers and the more inflow of pore water into the bottom layer of the deposit, the bottom layer of the deposit was experienced less settlement (i.e., volume contraction) than that at the top and middle layers. There was an insignificant difference in the vertical displacements of the layered thickened tailings after the termination of the shaking loading.

Based on the findings mentioned above, alternative disposal methods such as paste tailings and dry stack tailings (filtered tailings) might be considered to increase the resistance to seismic liquefaction, specifically in regions located in high seismic activities. The obtained results in this research work provide valuable knowledge about the cyclic or seismic behaviour and liquefaction potential thickened tailings deposit, under the applied seismic loading conditions, specifically for practitioners and researchers involved in the mining industry and engineering geological or geotechnical research community.

### 4.2.6. **References**

Ahmed, S.I., and Siddiqua, S. (2014). A review on consolidation behavior of tailings. International Journal of Geotechnical Engineering, 8(1): 102-111.

Alainachi, I., and Fall, M. (2019). Seismic induced liquefaction of cemented paste backfill: effect of mixing water. In Proceedings of the 7th International Conference on Earthquake Geotechnical Engineering (VII ICEGE), 17-20 June 2019, Roma, Italy, pp. 1042-1049.

Al-Tarhouni, M., Simms, P., and Sivathayalan, S. (2011). Cyclic behaviour of reconstituted and desiccated-rewet thickened gold tailings in simple shear. Canadian Geotechnical Journal, 48(7): 1044-1060.

Antonaki, N., Abdoun, T., and Sasanakul, I. (2019). Centrifuge tests on liquefaction potential and slope stability of mine tailings. International Journal of Physical Modelling in Geotechnics, 19(2): 104-114.

ASTM. (2017). D4318-17e1: Standard test methods for liquid limit, plastic limit, and plasticity index of soils. ASTM International, West Conshohocken, PA, USA.

Bahmanpour, A., Towhata, I., Sakr, M., Mahmoud, M., Yamamoto, Y., and Yamada, S. (2019). The effect of underground columns on the mitigation of liquefaction in shaking table model experiments. Soil Dynamics and Earthquake Engineering, 116(1): 15-30.

Barakati, A. (2015). Numerical modelling of liquid containing structure under dynamic loading. Master thesis, Department of Civil Engineering, University of Ottawa, Ottawa, Ontario, Canada.

Bray, J., and Frost, D. (2010) Geo-engineering reconnaissance of the 2010 Maule, Chile earthquake. Geo-Engineering Extreme Events Reconnaissance (GEER) Association. GEER association report No. GEER-022, Version 2.

Bussière, B. (2007). Colloquium 2004: hydrogeotechnical properties of hard rock tailings from metal mines and emerging geoenvironmental disposal approaches. Canadian Geotechnical Journal, 44(9): 1019-1052.

Carter, D.P. (1988). Liquefaction potential of sand deposits under low levels of excitation. PhD thesis, Department of Civil and Environmental Engineering, University of California, Berkeley, California, USA.

Casagrande, A. (1936). Characteristics of cohesionless soils affecting the stability of slopes and earth fills. Journal of the Boston Society of Civil Engineers, 23(1): 13-32.

Cheung, W.M., Qin, X., Chouw, N., Larkin, T., and Orense, R. (2013). Experimental and numerical study of soil response in a laminar box. In Proceedings of the Annual New Zealand Society for Earthquake Engineering Conference, 26-28 April 2013, Wellington, New Zealand, pp. 1-7.

Coelho, P.A.L.F., Haigh, S.K., and Madabhushi, S.P.G. (2004). Centrifuge modelling of liquefaction of saturated sand under cyclic loading. In Proceedings of the International Conference on Cyclic Behaviour of Soils and Liquefaction Phenomena, 31 March - 02 April 2004, Bochum, Germany, pp. 349-354.

Crowder, J.J. (2004). Deposition, consolidation, and strength of a non-plastic tailings paste for surface disposal. PhD thesis, Department of Civil Engineering, University of Toronto, Toronto, Ontario, Canada.

Daliri, F. (2013). The influence of desiccation and stress history on monotonic and cyclic shear response of thickened gold tailings. PhD thesis, Department of Civil and Environmental Engineering, Carleton University, Ottawa, Ontario, Canada.

Davies, M.P., and Rice, S. (2001). An alternative to conventional tailings management- “dry stack” filtered tailings. In Proceedings of the 8th International Conference on Tailings and Mine Waste ’01, 15-18 January 2001, Fort Collins, Colorado, USA, pp. 411-420.

Davies, M.P., McRoberts, E.C., and Martin, T.E. (2002). Static liquefaction of tailings-fundamentals and case histories. In the Proceedings of the Joint ASDSO/USSD Speciality Conference on Tailings Dam 2002, Las Vegas, Nevada, USA, pp. 233-255.

Dzuy, N.Q., and Boger, D.V. (1985). Direct yield stress measurement with the vane method. Journal of Rheology, 29(3): 335-347.

Ecemis, N. (2013). Simulation of seismic liquefaction: 1-g model testing system and shaking table tests. European Journal of Environmental and Civil Engineering, 17(10): 899-919.

Edraki, M., Baumgartl, T., Manlapig, E., Bradshaw, D., Franks, D. M., and Moran, C. J. (2014). Designing mine tailings for better environmental, social and economic outcomes: a review of alternative approaches. Journal of Cleaner Production, 84: 411-420.

Engels, J. (2002). Beach Slope Prediction Methods. See http://www.tailings.info/technical/beach-slope.htm [accessed December 20, 2017].

Fall, M., Célestin, J.C., and Han, F.S. (2013). Suitability of bentonite-paste tailings mixtures as engineering barrier material for mine waste containment facilities. Minerals Engineering, 22(9-10): 840-848.

Fall, M., Célestin, J.C., Pokharel, M., and Touré, M. (2010). A contribution to understanding the effects of temperature on the mechanical properties of cemented mine backfill. Engineering Geology, 114(3-4): 397-413.

Geremew, A.M., and Yanful, E.K. (2013). Dynamic properties and influence of clay mineralogy types on the cyclic strength of mine tailings. International Journal of Geomechanics, ASCE, 13(4): 441-453.

Ghirian, A., and Fall, M. (2013). Coupled thermo-hydro-mechanical-chemical behaviour of cemented paste backfill in column experiments. Part I: physical, hydraulic and thermal processes and characteristics. Engineering Geology, 164: 195-207.

Ghirian, A., and Fall, M. (2014). Coupled thermo-hydro-mechanical-chemical behaviour of cemented paste backfill in column experiments. Part II: mechanical, chemical and microstructural processes and characteristics. Engineering Geology, 170: 11-23.

Hamade, T. (2013). Geotechnical design of tailings dams-a stochastic analysis approach. PhD thesis, Department of Mining and Materials Engineering, McGill University, Montreal, Quebec, Canada.

Hassani, F., Mantegh, A., Mohamed, A-M., and Ouellet, J. (2008). Evaluation of flow liquefaction in fine grained tailings using elastic wave velocities. International Journal of Geotechnical Engineering, 2(3): 169-178.

Highter, W.H., and Vallee, R.P. (1980). The liquefaction of different mine tailings under stress-controlled loading. Engineering Geology, 16(1-2): 147-150.

Iai, S. (1989). Similitude for shaking table tests on soil-structure-fluid model in 1-g gravitational field. Soils and Foundations, 29(1): 105-118.

Ishihara, K. (1984). Post-earthquake failure of a tailings dam due to liquefaction of the pond deposit. In Proceedings of the First International Conference on Case Histories in Geotechnical Engineering, 6 May 1984, St. Louis, Missouri, USA, Vol. 3, pp. 1129-1143.

Ishihara, K., Troncoso, J., Kawase, Y., and Takahashi, Y. (1980). Cyclic strength characteristics of tailings materials. Soils and Foundations, 20(4): 127-142.

Ishihara, K., Yasuda, S., and Yokota, K. (1981). Cyclic strength of undisturbed mine tailings. In Proceedings of the First International Conference on Recent Advances in Geotechnical Earthquake Engineering and Soil Dynamics, 26 April - 3 May 1981, St. Louis, Missouri, USA, Vol. 1, pp. 53-58.

James, M., Aubertin, M., Wijewickreme, D., and Wilson, G.W. (2011). A laboratory investigation of the dynamic properties of tailings. Canadian Geotechnical Journal, 48(11): 1587-1600.

James, M., Jolette, D., Aubertin, M., and Bussière, B. (2003). An experimental set-up to investigate tailings liquefaction and control measures. In Proceedings of the International Symposium on Major Challenges in Tailings Dams (ICOLD), 15 June 2003, Montréal, Quebec, Canada, pp. 153-164.

Jones, H., and Boger, D.V. (2012). Sustainability and waste management in the resource industries. Industrial and Engineering Chemistry Research, 51(30): 10057-10065.

Ke, X., Chen, J., and Shan, Y. (2019). A new failure criterion for determining the cyclic resistance of low-plasticity fine-grained tailings. Engineering Geology, 261: 105273.

Landriault, D. (2001). Backfill in underground mining. Underground Mining Methods Engineering Fundamentals and International Case Studies, Hustrulid, W.A., and Bullock, R.L., Eds., Society for Mining, Metallurgy, and Exploration, Inc. (SME), Colorado, USA, pp. 601-614.

Li, A.L., Been, K., Ritchie, R., and Welch, D. (2009). Stability of large, thickened, non-segregating thickened tailings deposits. In Proceedings of the 12th International Seminar on Paste and Thickened Tailings, 21-24 April 2009, Viňa del Mar, Chile, pp. 301-312.

Li, W., Coop, M.R., Senetakis, K., and Schnaid, F. (2018). The mechanics of a silt-sized gold tailing. Engineering Geology, 241: 97-108

Lu, G., and Fall, M. (2018). Simulation of blast induced liquefaction susceptibility of subsurface fill mass. Geotechnical and Geological Engineering, 36(3): 1683-1706.

Lu, G., Fall, M., and Cui, L. (2017). A multiphysics-viscoplastic cap model for simulating blast response of cemented tailings backfill. Journal of Rock Mechanics and Geotechnical Engineering, 9(3): 551-564.

Meymand, P.J. (1998). Shaking table scale model tests of nonlinear soil-pile-superstructure interaction in soft clay. PhD thesis, Department of Civil and Environmental Engineering, University of California, Berkeley, California, USA.

Mizani, S. (2010). Rheology of thickened gold tailings for surface deposition. Master thesis, Department of Civil and Environmental Engineering, Carleton University, Ottawa, Ontario, Canada.

Mohamed, F.M.O. (2014). Bearing capacity and settlement behaviour of footings subjects to static and seismic loading conditions in unsaturated sandy soils. PhD thesis, Department of Civil Engineering, University of Ottawa, Ottawa, Ontario, Canada.

Naesgaard, E., and Byrne, P.M. (2007). Flow liquefaction simulation using a combined effective stress–total stress model. In Proceedings of the 60th Canadian Geotechnical Conference, 21-24 October 2007, Ottawa, Ontario, Canada.

Orejarena, L., and Fall, M. (2008). Mechanical response of a mine composite material to extreme heat. Bulletin of Engineering Geology and the Environment, 67(3): 387-396.

Orejarena, L., and Fall, M. (2010). The use of artificial neural networks to predict the effect of sulphate attack on the strength of cemented paste backfill. Bulletin of Engineering Geology and the Environment, 69(4): 659-670.

Paul, A.C., and Azam, S. (2013). Assessment of slurry consolidation using index properties. International Journal of Geotechnical Engineering, 7(1): 55-61.

Pépin, N., Aubertin, M., and James, M. (2012a). Seismic table investigation of the effect of inclusions on the cyclic behaviour of tailings. Canadian Geotechnical Journal, 49(4): 416-426.

Pépin, N., Aubertin, M., James, M., and Leclerc, M. (2012b). Seismic simulator testing to investigate the cyclic behaviour of tailings in an instrumented rigid box. Geotechnical Testing Journal, 35(3): 469-479.

Pokharel, M., and Fall, M. (2013). Combined influence of sulphate and temperature on the saturated hydraulic conductivity of hardened cemented paste backfill. Cement and Concrete Composites, 38(4): 21-28.

Prakash, S. (1981). Soil dynamics. McGraw-Hill Company, New York, NY, USA.

Rankine, K.J., Sivakugan, N., and Cowling, R. (2006). Emplaced geotechnical characteristics of hydraulic fills in a number of Australian mines. Geotechnical and Geological Engineering, 24: 1-14.

Raposo, N., Bahia, R., Afonso, E., and Topa Gomes, A. (2014). Optimization of thickened tailings deposition. In Proceedings of the 17th International Seminar on Paste and Thickened Tailings, 8-12 June 2014, Vancouver, British Columbia, Canada, pp. 1-14.

Rico, M., Benito, G., Salgueiro, A.R., Díez-Herrero, A., and Pereira, H.G. (2008). Reported tailings dam failures: a review of the European incidents in the worldwide context. Journal of hazardous materials, 152(2): 846-852.

Robinsky, E., Barbour, S.L., Wilson, G.W., Bordin, D., and Fredlund, D.G. (1991). Thickened sloped tailings disposal-an evaluation of seepage and abatement of acid drainage. In Proceedings of the Second International Conference on the Abatement of Acidic Drainage, Invited Lecture, 16-18 September 1991, Montreal, Quebec, Canada, pp. 529-549.

Robinsky, E.I. (1975). Thickened discharge-a new approach to tailings disposal. Canadian Mining and Metallurgical Bulletin, 68(764): 47-53.

Robinsky, E.I. (1982). Thickened tailing disposal in any topography. Essential Readings in Light Metals, Donaldson, D., and Raahauge, B.E., Eds., Springer, Cham, Switzerland, pp. 933-937.

Roshani, A., Fall, M., and Kennedy, K. (2017a). Drying behaviour of mature fine tailings pre-dewatered with super absorbent polymer: column experiments. ASTM Geotechnical Testing Journal, 40(2): 210-220.

Roshani, A., Fall, M., and Kennedy, K. (2017b). Impact of drying on geo-environmental properties of mature fine tailings pre-dewatered with super absorbent polymer. International journal of environmental science and technology, 14 (3): 453-462.

Seidalinova, A. (2014). Monotonic and cyclic shear loading response of fine-grained gold tailings. Master thesis, The University of British Columbia, Vancouver, British Columbia, Canada.

Serafini, D.C., and Perlea, V. (2010). Comparison of liquefaction triggering analysis approaches for an embankment dam and foundation. In Proceedings of the 5th International Conference on Recent Advances in Geotechnical Earthquake Engineering and Soil Dynamics, 24-29 May 2010, San Diego, California, USA, paper No. 4.12b.

Sofrá, F. (2017). Rheological properties of fresh cemented paste tailings. Paste Tailings Management, Yilmaz, E., and Fall, M., Eds., Springer, Cham, Switzerland, pp. 33-57.

Sofrá, F., and Boger, D.V. (2002). Environmental rheology for waste minimisation in the minerals industry. Chemical Engineering Journal 86(3): 319-330.

Tohumcu Özener, P., Özaydın, K., and Berilgen, M.M. (2009). Investigation of liquefaction and pore water pressure development in layered sands. Bulletin of Earthquake Engineering, 7(1): 199-219.

Tuttle, M., Law, K.T., Seeber, L., and Jacob, K. (1990). Liquefaction and ground failure induced by the 1988 Saguenay, Quebec, earthquake. Canadian Geotechnical Journal, 27(5): 580-589.

Ueng, T.S., Chen, C.H., Tsou, C.F., and Chen, Y.C. (2008). Shaking table test on a large specimen of Mailiao silty sand. In Proceedings of the Geotechnical Earthquake Engineering and Soil Dynamics Congress IV, 18-22 May 2008, Sacramento, California, USA, pp. 1-10.

Ueng, T.S., Wang, M.H., Chen, M.H., Chen, C.H., and Peng, L.H. (2006). A large biaxial shear box for shaking table test on saturated sand. Geotechnical Testing Journal, 29(1): 1-8.

Ueng, T.S., Wu, C.W., Cheng, H.W., and Chen, C.H. (2010). Settlements of saturated clean sand deposits in shaking table tests. Soil Dynamics and Earthquake Engineering, 30(1-2): 50-60.

Varghese, R.M., and Latha, G.M. (2013). Effect of overburden stress and surcharge pressure on the liquefaction response of sands. International Journal of Geotechnical Engineering, 7(4): 402-410.

Verdugo, R., and González, J. (2015). Liquefaction-induced ground damages during the 2010 Chile earthquake. Soil Dynamics and Earthquake Engineering, 79: 280-295.

Wang, J., Salam, S., and Xiao, M. (2020). Evaluation of the effects of shaking history on liquefaction and cone penetration resistance using shake table tests. Soil Dynamics and Earthquake Engineering, 131:106025.

Wijewickreme, D., Sanin, M.V., and Greenaway, G.R. (2005). Cyclic shear response of fine-grained mine tailings. Canadian Geotechnical Journal, 42(5):1408-1421.

World Information Service on Energy (WISE). (2017). Chronology of major tailings dam failures. See https://www.wise-uranium.org/mdaf.html [accessed December 10, 2017].

Wu, D., Fall, M., and Cai, S. (2012). Coupled modeling of temperature distribution and evolution in cemented tailings backfill structures that contain mineral admixtures. Geotechnical and Geological Engineering, 30(4): 935-961.

Wu, J., Kammerer, A.M., Riemer, M.F., Seed, R.B., and Pestana, J.M. (2004). Laboratory study of liquefaction triggering criteria. In Proceedings of the 13th World Conference on Earthquake Engineering, 1-6 August 2004, Vancouver, British Columbia, Canada, paper No. 2580.

Zhang, Q., Yin, G., Wei, Z., Fan, X., Wang, W., and Nie, W. (2015). An experimental study of the mechanical features of layered structures in dam tailings from macroscopic and microscopic points of view. Engineering Geology, 195: 142-154.

## 4.3. **Technical Paper #2: Geotechnical Response of Paste Tailings to Cyclic Loading: Shaking Table Tests**

Fahad Alshawmar, Mamadou Fall
Department of Civil Engineering, University of Ottawa, Ottawa, Ontario, Canada K1N 6N5
Submitted to the Journal of Geotechnical Research

### Abstract

A one-dimensional shaking table testing program was performed to assess the behaviour and liquefaction susceptibility of the paste tailings under cyclic loading conditions. The paste tailings were deposited subsequently in three thin layers in a flexible laminar shear box mounted on top of the shaking table, and the response of accelerations, displacements and pore water pressures to cyclic loading was measured at the middle depth of each layer of the tailings. Results showed that the acceleration for the bottom and middle layers were similar to that of the base of the shaking table; however, this was not the case for the top layer. The excess pore water pressure ratios were found to be approaching unity through all layers of paste tailings when the shaking ended. All layers of paste tailings were subjected to contraction and dilation during the shaking. It is also found that upward pore water migration to the top layer and downward pore water flow to the bottom layer occurred in tailings deposit. This water migration produced additional pore water pressure and also influenced the vertical displacement and liquefaction susceptibility of the paste tailings material. The results also indicate that the paste tailings can be susceptible to liquefaction in the post-shaking phase.

**Keywords:** paste tailings; liquefaction; shaking table; layered soils; flexible laminar shear box; excess pore water pressure

### 4.3.1. **Introduction**

The mining industry plays an essential role in the economic and social development of numerous nations around the world, significantly contributing to their gross domestic products (GDPs). For example, the mining industry added C$97 billion to Canada's GDP in 2017 (Marshall, 2018). In Chile, the mining industry contributes to 15% of the Chilean GDP (Stubrin, 2018). However, mining produces an enormous volume of mine waste, such as tailings, worldwide. The volume of mining waste is considerably larger than that of both domestic and industrial waste (ICOLD, 2001).

Tailings are finely ground waste that are left over after the extraction of metal ores (Elberling and Nicholson, 1996). The production of tailings from mining activities grew from tens of thousands of tonnes per day in the 1960s to hundreds of thousands of tonnes per day by 2000 (Jakubick et al., 2003). In 2008, the mining industry in Canada produced 256 million tonnes of waste rock and 217 million tonnes of tailings (Statistics Canada, 2012).

Traditionally, tailings are deposited in a dam in the form of slurry and are allowed to consolidate under their own weight. This can lead the dam becoming highly susceptible to liquefaction. Tailings dam failures have occurred in numerous locations around the world due to liquefaction during an earthquake. For example, a tailings dam failure in Chile occurred on March 28, 1965 at the El Cobre copper mine, which led to the release of about 2.25 million $m^3$ of tailings and killed more than 200 people (Al-Tarhouni et al., 2011; WISE, 2017). Another example of a tailings dam failure was that of the Mochikoshih storage pond during the earthquake near Izu-Ohshima in Japan on January 14, 1978, which led to the release of 80,000 $m^3$ of tailings and killed one person (Ishihara et al., 1980; WISE, 2017). Therefore, paste tailings technology has been proposed to eliminate or diminish the dependence on traditional tailings dams and minimize the risk of tailings dam failure due to seismic loading as well as to increase water recovery.

As man-made fine-grained soils, paste tailings can be defined as dewatered slurry tailings that do not have a critical flow velocity when pumped, are not subject to segregation after deposition and generate an insignificant amount of bleed water when discharged to the surface (Theriault et al., 2003). This form of tailings behaves as a dense viscous mixture of both tailings and water, and it has a consistency comparable to wet concrete and must include at least 15% by mass passing 20 μm to exhibit typical paste flow properties and retain adequate colloidal water to produce a non-segregating mixture (Verburg, 2001). The flow of the paste tailings rests at a slope that usually ranges from 3–10° as long as the underlying material has stabilized (Theriault et al., 2003). The moisture content of paste tailings is commonly 10–25%, which is lower than that of conventional tailings (Meggyes and Debreczeni, 2006). Moreover, the solid content in paste tailings is often 70–85% (Hamade, 2013). The concept of surface paste tailings was first applied at the Bulyanhulu gold mine in Tanzania (Theriault et al., 2003).

The dynamic response of tailings materials has been investigated mainly through the use of small-scale equipment, such as cyclic direct simple shear or triaxial equipment (Ishihara et al., 1981; Crowder, 2004; Wijewickreme et al., 2005; Al-Tarhouni, 2008; Kim et al., 2011; James et al., 2011; Geremew and Yanful, 2012; Daliri, 2013; Seidalinova, 2014; Hu et al., 2017). However, very limited efforts have been made using large-scale equipment (compared to the aforementioned equipment), such as a shaking table, to investigate the dynamic response of tailings materials (Pepin et al., 2012a, 2012b). Pepin et al. (2012a, 2012b) examined the dynamic response of non-plastic hard rock slurry tailings (i.e., conventional tailings) with and without inclusions (i.e., rigid and drainage inclusions) using a rigid box to hold the tailings, which were then placed on a shaking table. They observed that the inclusions generally led to an increase in the resistance of the tested slurry tailings to the dynamic loadings. However, no studies have been conducted to date to assess the behaviour or liquefaction susceptibility of paste tailings to cyclic loadings using a shaking table.

The liquefaction susceptibility of paste tailings is not well-known or understood. An understanding and assessment of the behaviour and liquefaction susceptibility of paste tailings subjected to cyclic loadings is necessary before the use or implementation of this tailings deposition technique in earthquake-prone countries or regions. Regulators are concerned with potential liquefaction of paste tailings deposits in those regions. Therefore, the main objective of this experimental study is to assess the behaviour, particularly liquefaction potential, of the paste tailings under cyclic loading conditions using a shaking table. The paste tailings were deposited in thin layers in a flexible laminar shear box (FLSB) to simulate deposition in the field.

### 4.3.2. **Materials and methods**

#### 4.3.2.1. **Materials**

Tap water and fine-grained tailings were used to prepare the mixture. The tailings used in this research consisted of a mixture of two types, silica tailings (STs) and natural tailings (NTs). STs were used because unlike NTs, which can include reactive materials such as sulfide minerals, their chemical and mineralogical constitutions can be controlled (Cui and Fall, 2016). Sulphide minerals, when exposed to air during the preparation and/or deposition of the paste tailings, can oxidize. This oxidation may change the initial chemical or mineralogical composition of the paste tailings as well as lead to precipitation of reaction products which may cause the cementation of some tailings particles. Therefore, a mixture of the two types of tailings decreased the possible influence of uncertainties on the experimental results.

STs were made from ground silica (U.S. Silica Company, Frederick, Maryland, United States) and consisted of 99.8% silicon dioxide ($SiO_2$). STs are essentially made of quartz, which is the predominant mineral in Canadian hard rock mine tailings. NTs were collected from a Canadian mine at a deposition point and then shipped to the University of Ottawa. Tables 4.4 and 4.5 tabulate the main physical properties and mineral compositions of the STs and NTs. Figure 4.14 presents the grain size distribution of the STs, NTs and their mixture, which were similar to each other and to the average of 9 Canadian mine tailings (Orejarena and Fall, 2008; Pokharel and Fall, 2013). Both types of tailings could be categorized as medium tailings with 37–45wt% fine particles (< 20 µm). Determination of the liquid and plastic limits of the used tailings, as per the ASTM D4318-e1 (ASTM, 2010), was not possible in the laboratory. Based on the laboratory work, the used tailings were non-plastic and could be classified as sandy silts of low plasticity corresponding to ML in the Unified Soil Classification System (USCS).

Table 4.4. Physical properties of the tailings used and the coarse-grained sand

| Material | Physical Properties | | | | | | |
|---|---|---|---|---|---|---|---|
| | $G_s$ | $D_{10}$ (µm) | $D_{30}$ (µm) | $D_{50}$ (µm) | $D_{60}$ (µm) | $C_u$ | $C_c$ |
| STs | 2.7 | 1.9 | 9.0 | 22.5 | 31.5 | - | - |
| NTs | 3.1 | 3.2 | 15.8 | 35.5 | 49.5 | - | - |
| Sand | 2.7 | 700.0 | 740.0 | 880.0 | 1000.0 | 1.4 | 0.8 |

STs: silica tailings; NTs: natural tailings. $G_s$: specific gravity; $C_u$: coefficient of uniformity; $C_c$: coefficient of curvature; $D_{10}$: effective diameter

Table 4.5. Mineralogical composition of the tailings used (obtained by XRD analysis)

| Tailings | Mineral | | | | | | | | | | | |
|---|---|---|---|---|---|---|---|---|---|---|---|---|
| | Quartz | Albite | Dolomite | Calcite | Chlorite | Magnetite | Pyrite | Talc | Pyrrhotite | Spinel | Others | Total |
| STs (wt.%) | 99.8 | - | - | - | - | - | - | - | - | - | 0.2 | 100.0 |
| NTs (wt.%) | 15.0 | 32.8 | 15.0 | 4.2 | 16.1 | 2.4 | 1.0 | 7.0 | 1.8 | 1.8 | 2.9 | 100.0 |

STs: silica tailings; NTs: natural tailings; wt.: weight

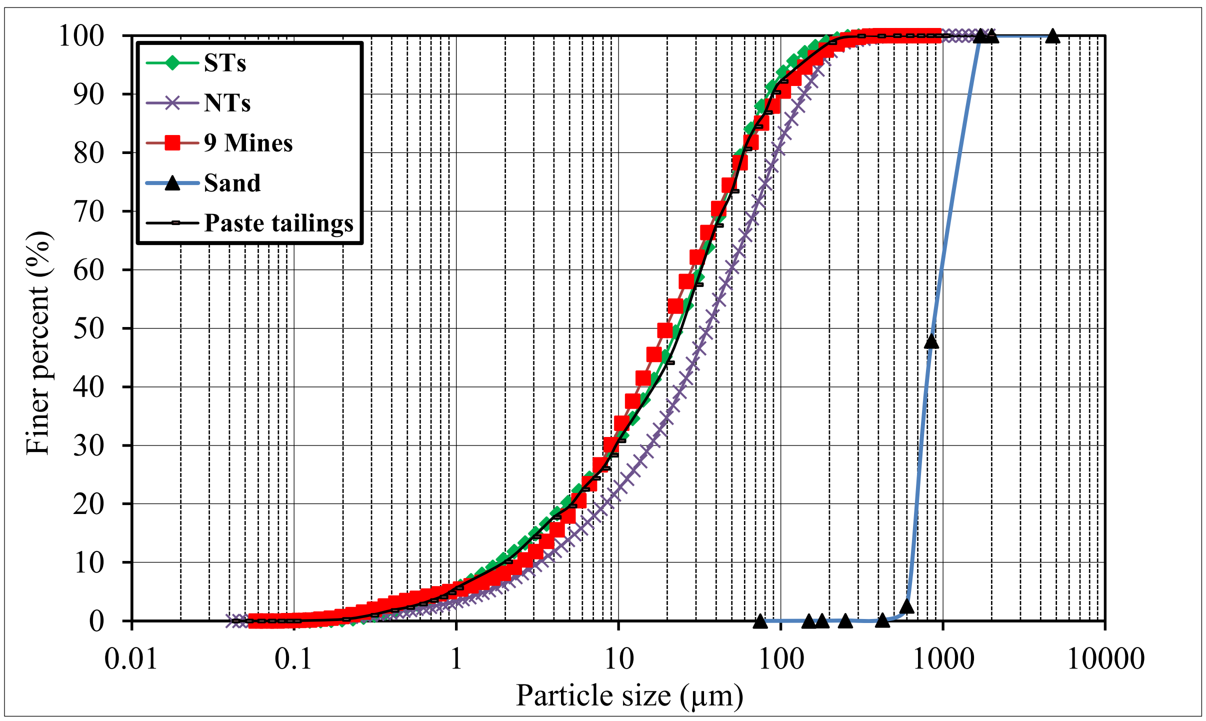


Figure 4.14. Grain size distribution of the tailings and coarse-grained sand used in this research compared with the average of 9 Canadian mine tailings

4.3.2.2. **Preparation of the paste tailings**

The paste tailings were prepared by adding tap water to the tailings material, which was comprised of 90% STs and 10% NTs. A concrete mixer was used to mix the water and tailings thoroughly for a period of about 10 minutes to achieve homogeneity. To assess the flowability or transportability of the prepared paste tailings, vane shear and slump tests (by following ASTM C143/C143M-15a (ASTM, 2015)) were performed to obtain the yield stress value and the slump value of this material, respectively. The results of the vane shear tests showed that the yield stress of this paste tailings was about 139 Pa. This value of yield stress was within the range of other paste tailings' yield stress reported in the literature (Li et al., 2002; Crowder et al., 2002). In addition, the slump value of the prepared paste tailings was 250 mm. This slump value is consistent with the value reported for surface paste disposal conditions in other studies (Newman et al., 2001; Theriault et al., 2003). These measurements corresponded to a solid content of almost 79%.

4.3.2.3. **Shaking table test**

The shaking table test has several advantages. The key advantages of the shaking table test include a large amplitude that can be well controlled, multi-directional input motions, ease of experimental measurements and results that can be used for validating the numerical models or understanding the failure mechanisms (Prasad et al., 2004). However, the shaking table test also has some disadvantages. For example, it cannot produce high gravitational stresses as seen in the field. Furthermore, an electro-hydraulic system is required to replicate a real seismic earthquake.

The shaking table that was used in this research program for testing the paste tailings was located in the civil engineering laboratory at the University of Ottawa. This shaking table consisted of one dimension of horizontal movement (i.e., 1-D) with a plan area of 1000 × 1000 mm as the top aluminum platform of the table (Figure 4.15). The table could be moved horizontally by a mechanical testing and simulation system attached to a hydraulic actuator controlled by a digital control module. The digital control module permitted simulation of different types of dynamic displacement time-histories, which included harmonic spectrum and pre-scored earthquake records. The hydraulic actuator (Model 244) had the ability to move the shaking table back and forth at different frequencies ranging from 1 to 17 Hz with a maximum displacement of ± 120 mm and a 25 kN base shear capacity. The capacity of this shaking table was 1000 kg.

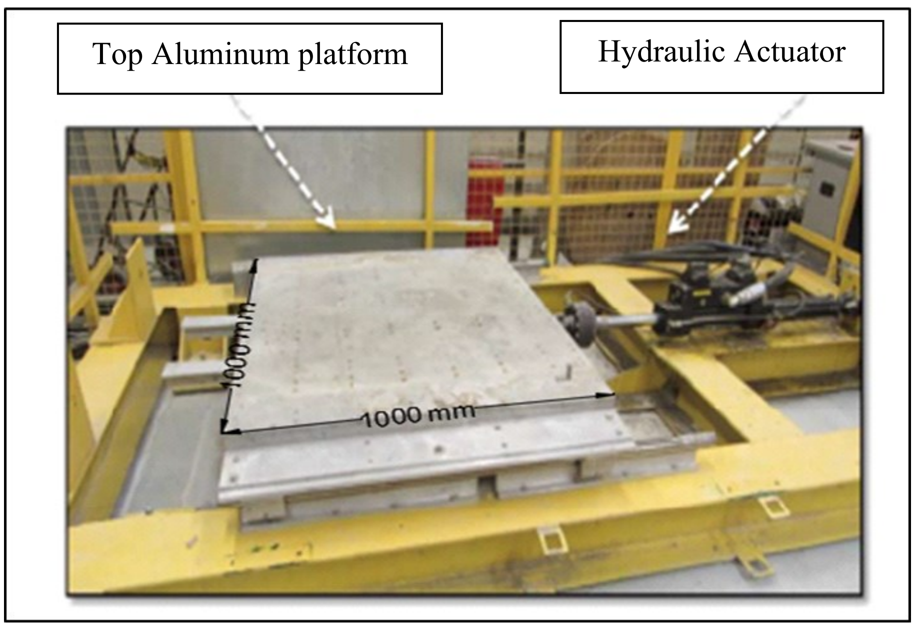


Figure 4.15. Shaking table at the civil engineering laboratory at the University of Ottawa that was used for this research (photo from Barakati, 2015)

4.3.2.4. **Model construction, setup and instrumentation**

A flexible laminar shear box (FLSB), designed by Alainachi and Fall (2019) and fabricated at the University of Ottawa, was attached to the shaking table to simulate the seismic behaviour of the surface paste tailings (Figure 4.16). This FLSB was comprised of 22 horizontal laminae to form a 750 mm high, 750 mm long, and 750 mm wide box. There was a slight gap of 2 mm between each lamina to provide free movement between them. The laminae were made up of solid, high strength aluminum alloy box sections (31.65 × 31.65 mm) fastened together using two adjusting aluminum cubes for each lamina to form the rectangular laminae with a size of 750 × 750 mm as plan dimensions. Every one of these laminae was supported by two 15-mm-diameter stainless steel guide rods attached to the outer edge of the laminae using stiff aluminum brackets. These guide rods fed through six low-friction ball bearings per lamina (three per side), which were housed in four vertical bearing brackets. The system of linear bearing allowed for single-axis motion corresponding to the longitudinal axis of the FLSB. The bearing brackets were then attached to the external support steel frame, made up of channel steel in 50 × 50-mm sections with a thickness of 8 mm, to transfer the weight of the entire FLSB system off the shaking table. The weight carried by the external support steel frame was then transferred to large supporting beams (150-mm flange and 200-mm web) and then finally to the floor of the laboratory. The physical properties of the FLSB and its elements are provided in Table 4.6. The FLSB and external support frame used in this study were similar to those used by Turan et al. (2009) and Mohamed (2014).

In the field, paste tailings commonly flow away from deposition points to form a gentle slope. Thus, the deposition angle of the paste tailings was simulated in this investigation by placing a layer of coarse-grained sand on the base area of the FLSB to form a slope of about 5.6% (Figure 4.17). This amount of slope was within the range associated with the deposition angle of paste tailings (Theriault et al., 2003). It should be underlined that, in practice, the deposition angle achieved in field can be affected by numerous factors, such as temperature variations and shear effects during transport, climatic conditions, deposition rate, and the natural of the ground on which the paste tailings material is deposited (Theriault et al., 2003). This coarse-grained sand layer was placed below the paste tailings deposit to provide drainage. According to the USCS, this type of sand is classified as poorly graded sand (SP). The characteristics of this coarse-grained sand can be seen in Table 4.4, and its grain size distribution can be seen in Figure 4.14.

Different types of instruments or sensors were installed at different depths to monitor the properties and response of the paste tailings (Figure 4.17). Instruments included three pore pressure transducers (Model PX309-015CG5V, Omega Company) for pore water pressure measurements (P1–P3), three cable displacement transducers (Model SM2-12, Measurement Specialties Company) for settlement measurements (VD1–VD3), three 5TE sensors (Decagon Devices Inc.) for volumetric water content (5TE1–5TE3), four accelerometers (Model 7593A, Endevco Company) for acceleration measurements (A1–A4) and three cable displacement transducers (Model SM2-12, Measurement Specialties Company) for horizontal deformation measurements (HD1–HD3).

The pore pressure transducers, cable displacement transducers (VD1–VD3) and 5TE sensors were placed along the center of the FLSB perpendicular to the direction of shaking at the middle depth of each layer of the paste tailings specimen (Figure 4.17). The cable displacement transducers (VD1–VD3) were attached to the top part of thin metal tubes that connected from the bottom to the lightweight perforated circular plastic plates (diameter ≈ 3 cm). When these plates were lowered, the cable displacement transducers (VD1–VD3) were stretched down to measure the settlement. To prevent these thin metal tubes from falling or titling during shaking, they were placed inside mesh cylinders that were attached to a bridge on top of the FLSB. This technique was used successfully by other researchers (e.g., Alainachi and Fall, 2019). The pore pressure transducers had a pressure range of ± 103.42 kPa.

The 5TE instruments measured the volumetric water content within the range of 0–80%. Accelerometers A1–A3 were placed in the same direction as the shaking along the left outer edge of the FLSB near the middle of each layer of paste tailings. However, accelerometer A4 was mounted on the shaking table to measure the actual applied excitation. The accelerometers had an acceleration range of ± 2g. The cable displacement transducers (HD1–HD3) were mounted on a steel rod and then attached along the left outer edge of the FLSB near the middle of each layer of paste tailings. All cable displacement transducers had a range of ± 318 mm. The instruments of pore pressure transducers, cable displacement transducers, and accelerometers were connected to a data acquisition system (Model USB-2416-4AO, Measurement Computing Corporation) to register the readings. However, the 5TE instruments were connected to a data logger (Model Em50, Decagon Devices Inc.) to register the readings.

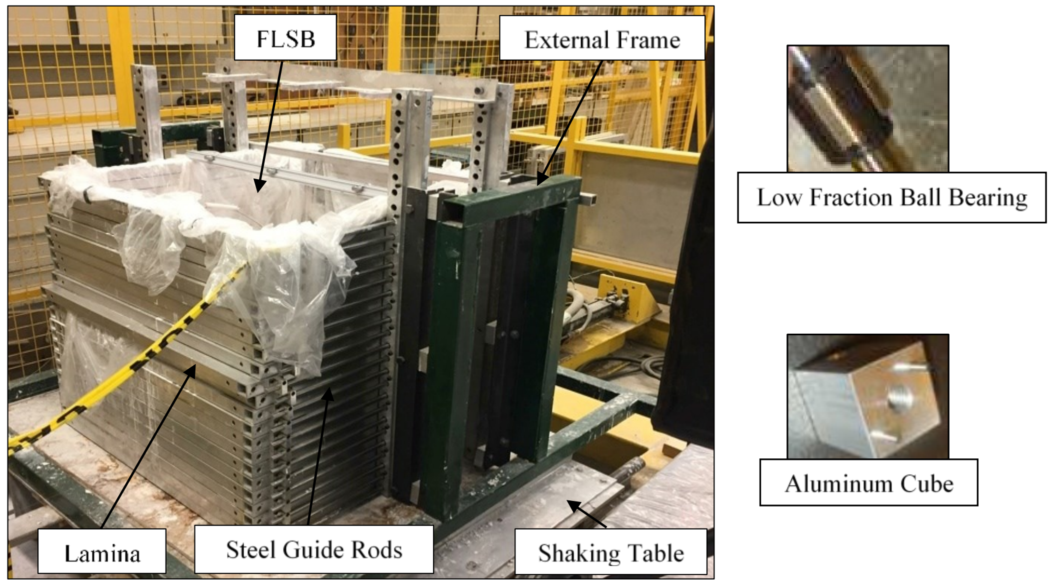


Figure 4.16. Snapshot of the University of Ottawa's FLSB

Table 4.6. The physical properties of the FLSB and its elements

| **Element** | **Property** | **Value** | |
|---|---|---|---|
| Lamina | Number | 22 | |
| | Inside dimensions | 750 mm × 750 mm | |
| | Weight | 2.97 kg | |
| Bearing brackets | Number | 4 External | 2 Internal |
| | Dimensions | 750 mm and 10 mm diameter | |
| | Weight | 3.66 kg external | 2.51 kg internal |
| Guide rods | Number | 44 | |
| | Weight | 0.78 kg | |
| Linear bearings | Number | 88 | |
| | Length | 20 mm | |
| | Diameter | 10 mm | |
| | Weight | 0.02 kg | |
| Bearings | Number | 132 | |
| | Weight | 0.04 kg | |
| Adjusting aluminum cubes | Number | 88 | |
| | Weight | 0.06 kg | |
| Total weight of the empty FLSB = 131.64 kg ~ 132.00 kg | | | |

*Paste tailings deposit at early ages (made of 3 thin layers) was considered

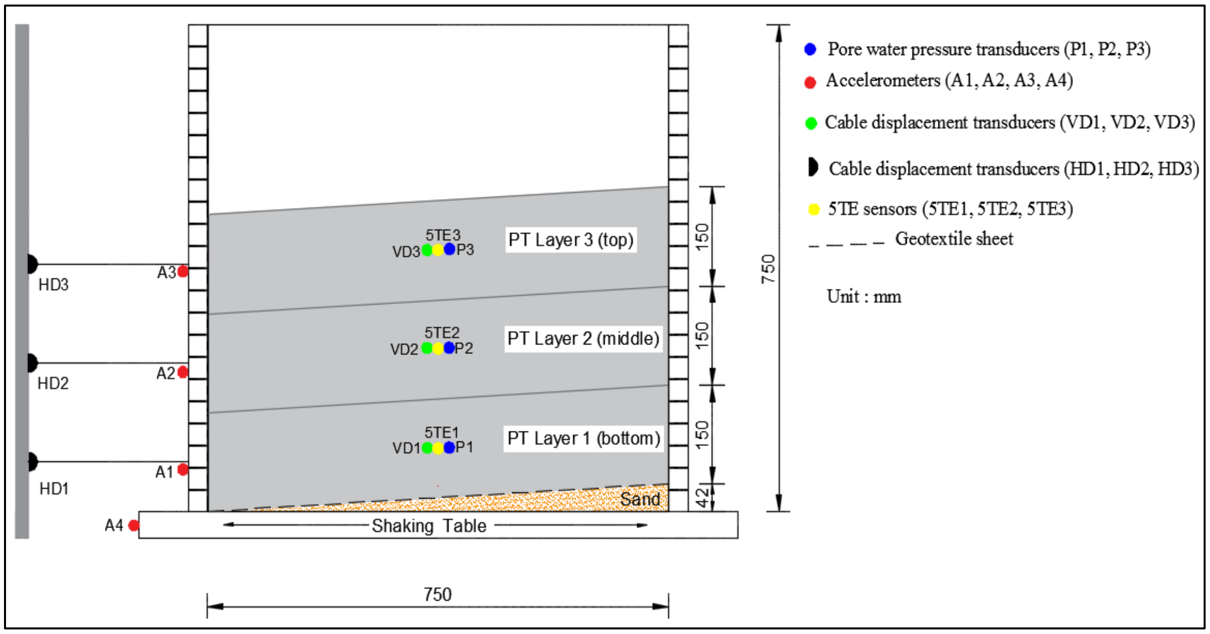


Figure 4.17. Schematic drawing of the instrumented FLSB with different layers of paste tailings situated on the shaking table

4.3.2.5. **Paste tailings deposition, testing program and procedure**

The paste tailings were deposited into the FLSB subsequently in three thin layers, which was similar to the surface disposal of paste tailings at the Bulyanhulu gold mine, Tanzania (Theriault et al., 2003). Thin layer deposition is critical for strength gain through desiccation (Theriault et al., 2003). Each layer of paste tailings had a thickness of 150 mm (Figure 4.17). The time interval between the deposition of the first layer (bottom layer) and the second layer (middle layer) was 3 days, and the interval between the second layer (middle layer) and the third layer (top layer) was 2 days. The deposition of each paste tailings layer was performed by a concrete bucket that hoisted the paste tailings from the concrete mixer to the FLSB (Figure 4.18a). Figure 4.18b shows the surface of the paste tailings just after deposition of the third (top) layer. The average temperature and relative humidity of the laboratory were 20.4°C and 57%, respectively.

It should be underlined that the objective of the present study is not to assess the cyclic behaviour of a paste tailings deposit when its height has reached the top of the deposition towers, but rather to assess its behaviour during the early deposition. The height of paste tailings deposition towers can be between 10 to 15 m (deposition towers at Bulyanhulu gold mine were 12 m high (Theriault et al., 2003)), which is equivalent to the deposition of approximately 65 to 100 (15 cm) thin layers of paste tailings. Simulating the cyclic or seismic response of a 12 m high paste tailings structure by using shaking table testing technique requires the use of large-scale shaking table testing facility to consider the full size (height) of the paste tailings structure or its in situ stress, which is an extremely costly approach, or to properly scale down the parameters of the model experiment based on the similitude laws. However, it is not possible or extremely difficult to ensure that all or key factors meet the similitude laws in the 1-g gravity field, if a prototype model or paste tailings structure of 10 to 15 m high is considered. For the reasons mentioned, a paste tailings structure after the deposition of three 150 mm-thin layers of paste tailings is considered in this study. In practice, this will correspond to the early ages (first week) of the deposition of paste tailings. Although, only three layers of paste tailings or the early age of paste tailings deposition are considered in this study, understanding the geotechnical response of 3 layers of paste tailings or paste tailings at early ages to cyclic loading will enable to gain insight into the seismic behaviour of paste tailings deposits with over 30 layers. Moreover, considering a paste tailings deposit with 3 layers will enable to satisfy key similitude requirements between the physical model and prototype. Thus, a geometric scaling factor (N) of 1:1 was adopted for experimental shaking table tests on the scale model in this study. The geometry and configuration of models were designed based on the similitude theories related to the 1 g shaking table test for the soil-fluid models suggested by Iai (1989) and Meymand (1998). The scaling factors adopted in the present study are summarized in Table 4.7.

The testing program consisted of using shaking table equipment to apply a sinusoidal dynamic loading with a frequency of 1 Hz and peak horizontal acceleration of 0.13g (horizontal displacement amplitude of 32 mm) on the paste tailings deposit. In addition, the deposit was shaken for about 30 min. Typically, the selected loading conditions in this testing program were not meant to represent the identical conditions that occur during a real earthquake, since these loading conditions had a one-dimensional signal, uniform amplitude, constant frequency and long duration (Pepin et al., 2012b). This loading frequency was selected due to the facility limitations. The instruments used were not able to monitor the dynamic response of the tested material under large loading frequencies. Furthermore, similar loading frequencies have been used previously in liquefaction investigations (James et al., 2003; Ueng et al., 2010; Pépin et al., 2012a). The acceleration used in this testing program corresponded to the acceleration of the Saguenay earthquake of 1988 in Québec, Canada, which had a magnitude of 5.9 (Tuttle et al., 1990). It should be underscored that only the peak acceleration corresponds to the peak of Saguenay Earthquake, not the whole time series. The long duration of shaking selected in this investigation was not intended to simulate the real period of earthquakes, which are much shorter. Also, a good observation of the cyclic response of the paste tailings and relative comparisons of their response can be attained through a long duration of shaking (e.g., 30 min). This is important for the future development of a constitutive model to predict and assess the seismic behaviour of paste tailings. A similar duration of shaking was used in an investigation of the liquefaction behaviour of hard rock slurry tailings materials using a shaking table (Pépin et al., 2012a). The shaking was performed 1 day after the deposition of the top layer of paste tailings. After the end of the shaking time, the response of the tailings continued to be monitored until full dissipation of the excess pore water pressure was reached, which took up to 2 days.

Table 4.7. Relationship of similarity between the prototype paste tailings* and paste tailings shaking table model

| Parameters | Scale factor |
|---|---|
| Acceleration | 1 |
| Paste tailings height | N |
| Mass density | 1 |
| Force | $N^3$ |
| Stiffness | $N^2$ |
| Modulus | N |
| Stress | N |
| Strain | 1 |
| Frequency | $N^{-1/2}$ |
| Shear Wave Velocity | $N^{1/2}$ |
| Time | $N^{1/2}$ |
| EI | $N^5$ |

For the testing procedure, a plastic sheet with dimensions of 800 mm × 800 mm × 800 mm and thickness of 0.5 mm was used to hold both the coarse-grained sand and the paste tailings material inside the FLSB (Figure 4.16). This prevented the loss of both solid materials and water. A layer of coarse-grained sand (drainage layer) with a slope of 5.6% and thickness of 42 mm was then placed on the base area of the FLSB. Then, a geotextile sheet was placed on top of the coarse-grained sand. This geotextile sheet acted as a porous barrier between the coarse-grained sand and the tested paste tailings. Following that, the paste tailings were poured in three layers in the FLSB, and each layer had a thickness of 150 mm (Figure 4.17).

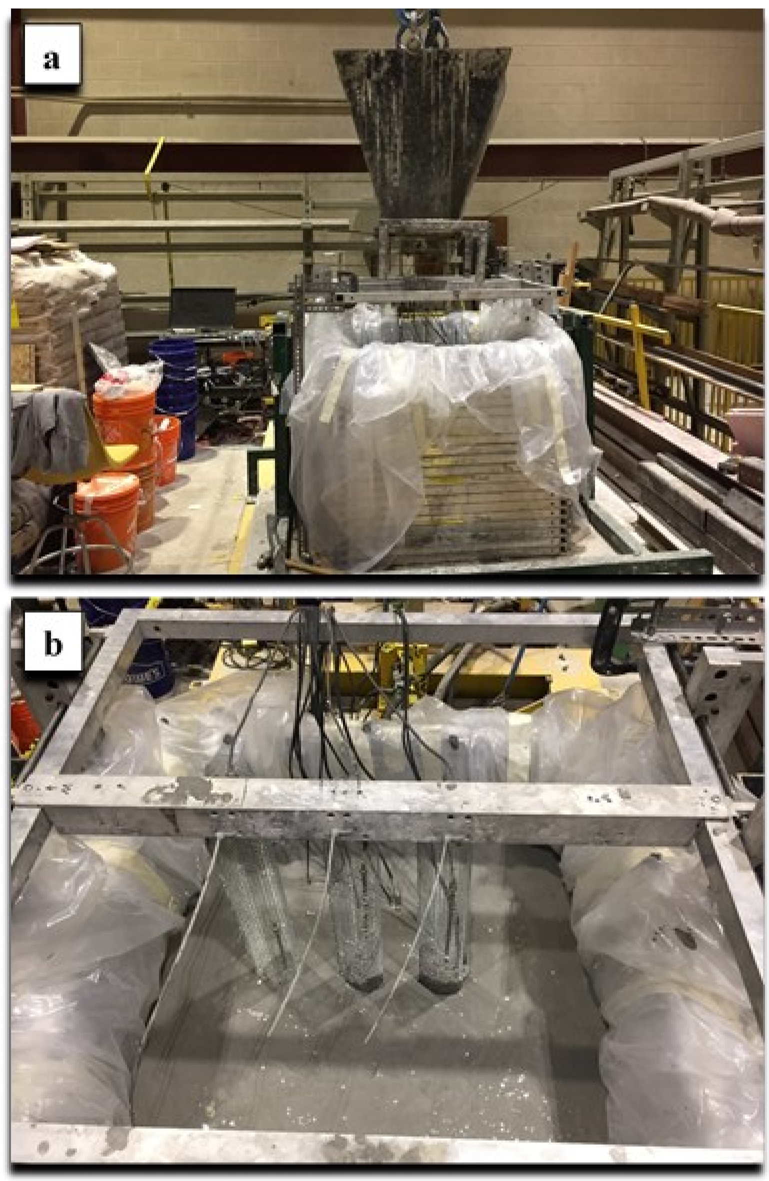


Figure 4.18. (a) Photograph showing the concrete bucket that was used for deposition of paste tailings layers; (b) Photograph of the surface of paste tailings after freshly deposition of the third layer (top layer)

## 4.3.3. **Results and discussion**

### 4.3.3.1. **Acceleration and horizontal displacement response**

The acceleration time histories along the outer edge of the FLSB near the middle depth of each layer of the paste tailings and on the base of the shaking table are shown in Figure 4.19. The red arrows in Figure 4.19 illustrate the end of the shaking duration. It can be observed that the input acceleration reached its full amplitude at about 20 seconds. The attenuation of acceleration at the middle depth of the bottom and middle layers was not observed. Coelho et al. (2004), who conducted cyclic loading tests on saturated sand using centrifuge equipment, made similar observations and attributed this behaviour to the high magnitude of initial vertical effective stress. However, this Coelho et al.'s explanation may not be valid for study due to the low vertical effective stress. Moreover, the measured accelerations at the middle depth of the bottom and middle layers were almost identical to the acceleration on the base of the shaking table.

The response of the horizontal displacements along the outer edge of the FLSB near the middle depth of each layer of paste tailings can be seen in Figure 4.20. The red arrows in Figure 4.20 illustrate the end of the shaking duration. The horizontal displacements of each layer seemed to be relatively steady, with an amplitude of about 3.7 cm, and were found to be somewhat identical to each other. This means that the lateral movement of the paste tailings contained in the FLSB was relatively similar at all depths. This response is consistent with the visual observation of the movement of FLSB during the shaking.

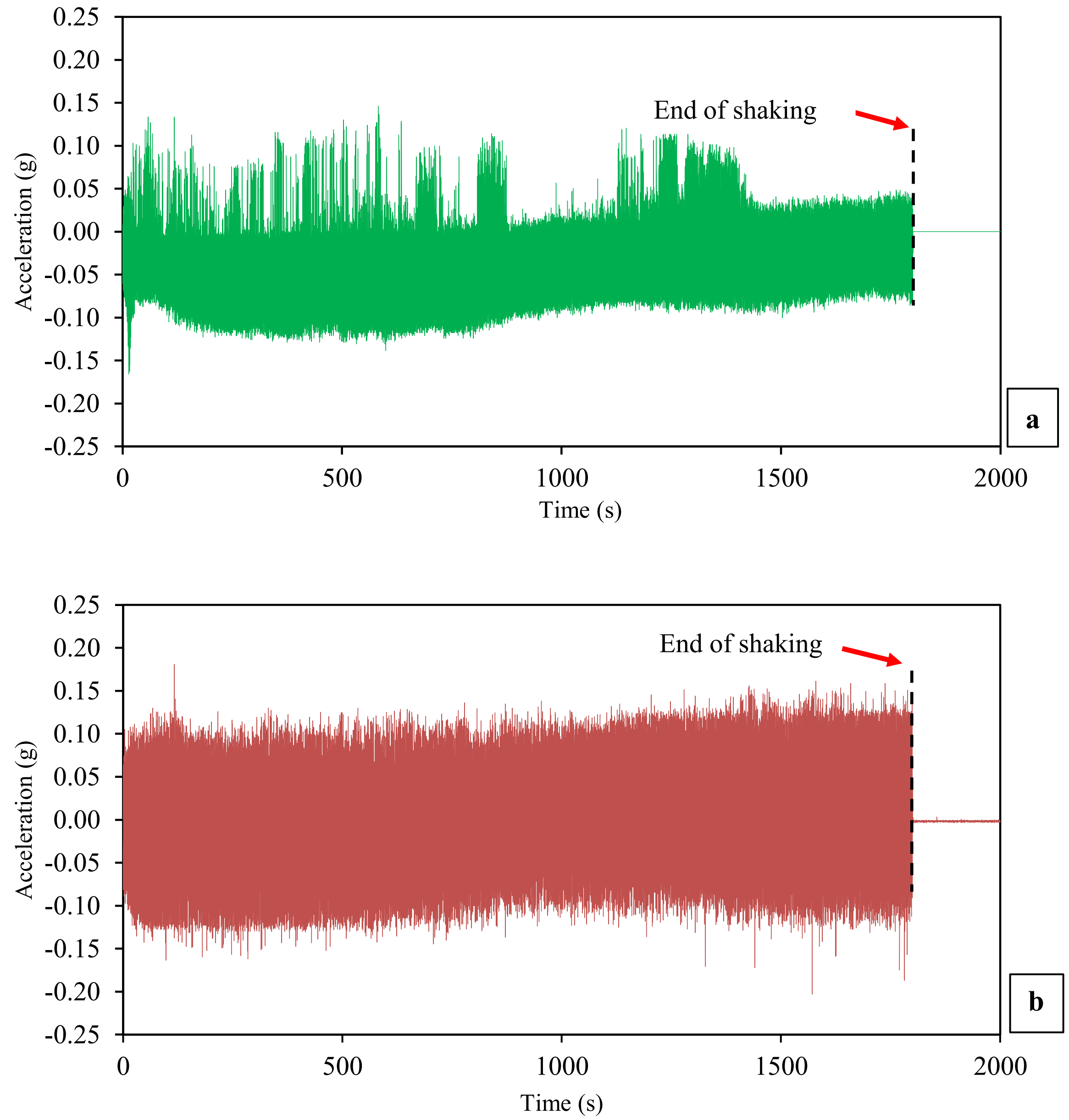
0.25
0.20
0.15
0.10
0.05
0.00
-0.05
-0.10
-0.15
-0.20
-0.25
Acceleration (g)
End of shaking
a
0
500
1000
1500
2000
Time (s)
End of shaking
b
Time (s)

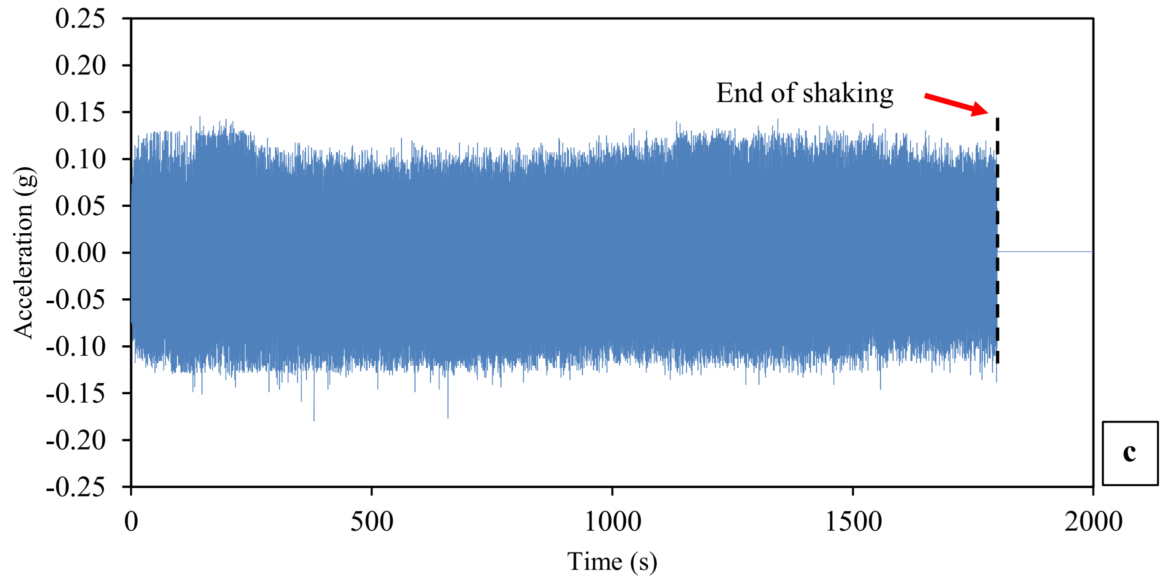


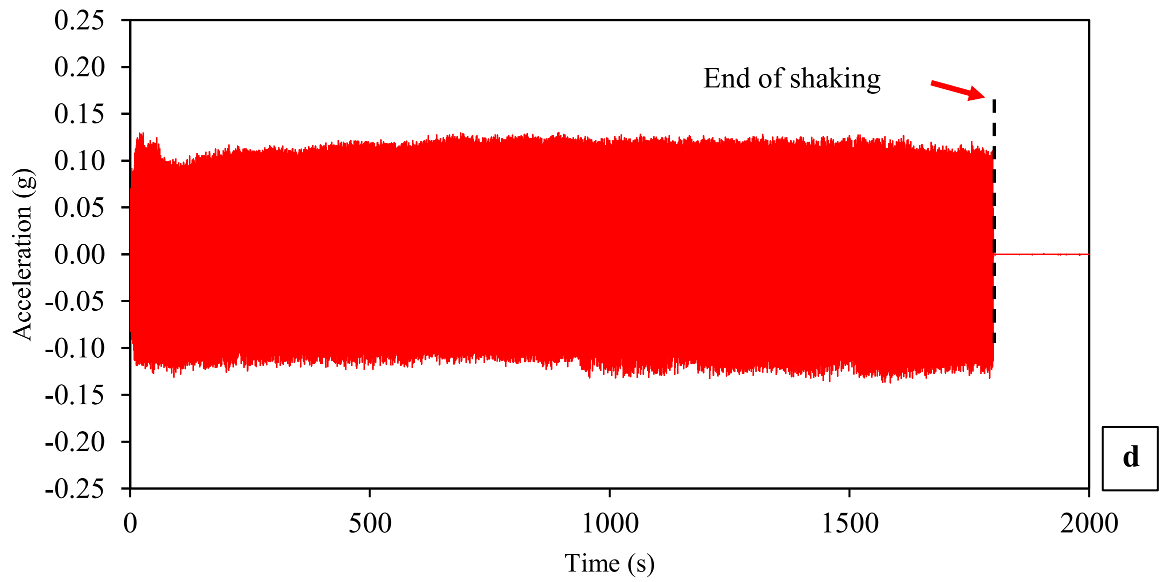


Figure 4.19. Time histories of measured accelerations at the middle depth of each layer of tailings and at the base of the shaking table during shaking: (a) Layer 3 (top), (b) Layer 2 (middle), (c) Layer 1 (bottom), (d) shaking table

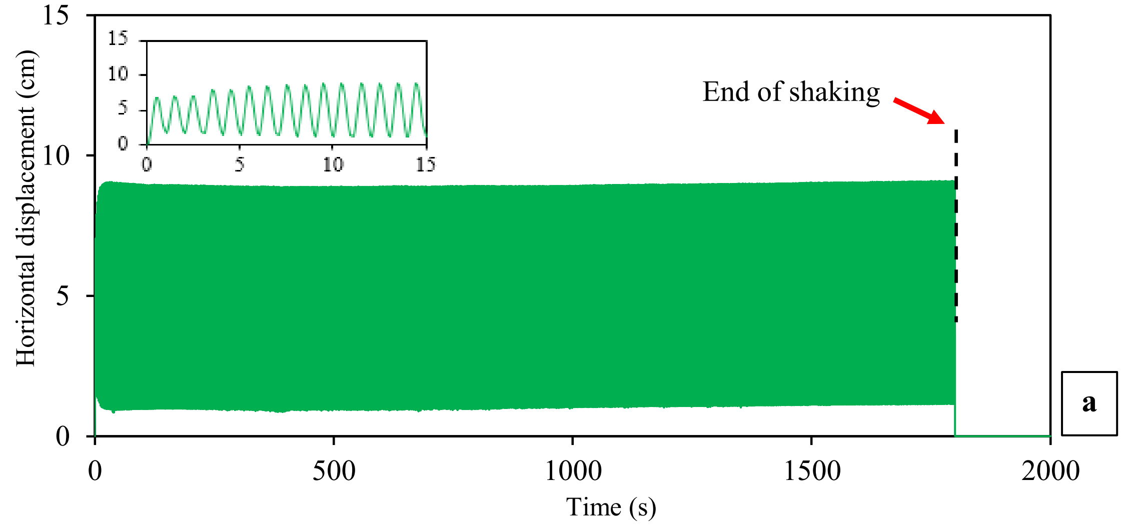
15
10
5
0
Horizontal displacement (cm)
0
500
1000
1500
2000
Time (s)
End of shaking
a

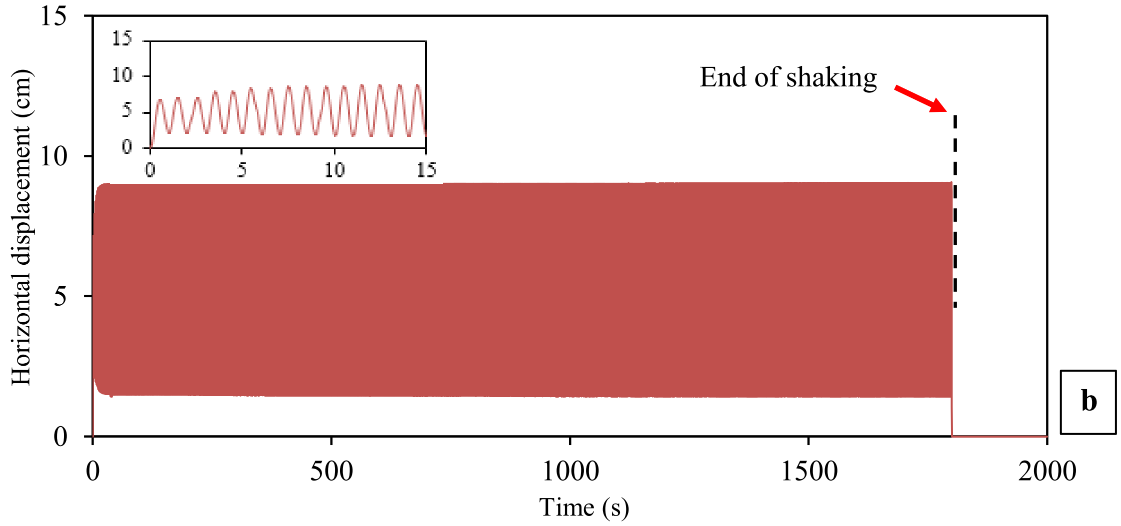
15
10
5
0
Horizontal displacement (cm)
0
500
1000
1500
2000
Time (s)
End of shaking
b

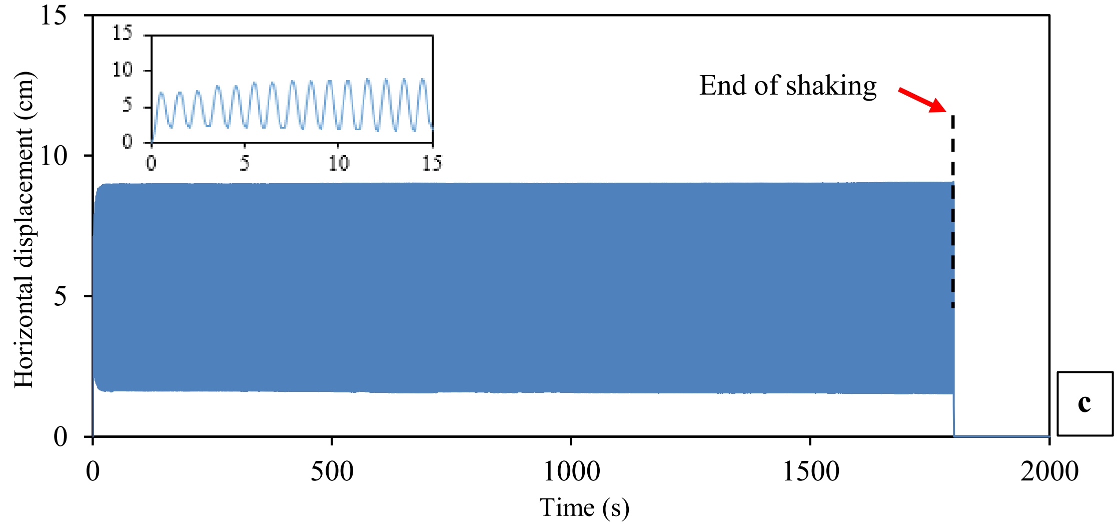


Figure 4.20. Time histories of measured horizontal displacements at the middle depth of each layer of tailings during shaking: (a) Layer 3 (top), b) Layer 2 (middle), c) Layer 1 (bottom)

4.3.3.2. **Pore water pressure response and liquefaction analysis**

Several liquefaction triggering criteria have been proposed and used to define or determine soil liquefaction. These criteria include, strength-based criteria, strain/deformation-based liquefaction criteria, energy-based liquefaction criteria, and (excess) pore pressure-based criteria. Each of these methods or criteria has advantages, but also disadvantages or limitations, as discussed in many previous studies (e.g., Wu et al., 2004). The pore pressure-based criteria are used in this study.

The development and the dissipation of the excess pore water pressure or the pore pressure-based criteria have been extensively used in assessing the liquefaction potential of soils and tailings in the laboratory, particularly in shaking table tests (e.g., Pépin et al., 2012a; Wu et al., 2004). It is most common to assess liquefaction through the excess pore water pressure ratio ($r_u$). This is defined as the ratio between the excess pore water pressure ($\Delta u$) and the initial vertical effective stress ($\sigma'_{vo}$) (i.e., $r_u = \Delta u/\sigma'_{vo}$). Liquefaction is generally defined as $r_u \geq 1$. However, numerous previous studies (e.g., Naesgaard and Byrne, 2007; Serafini and Perlea, 2010; Wu et al., 2004) have shown that soil liquefaction can be triggered with $r_u$ of 0.8 or even lower under certain conditions. The value of $r_u$ at liquefaction triggering is affected by soil densities and loading conditions. Denser soils subjected to larger shear stress ratios generate lower pore pressure ratios $r_u$ at the onset of liquefaction (Wu et al., 2004).

The magnitude of the excess pore water pressure at the middle depth of each layer was calculated by subtracting the final pore water pressure at the end of the test (hydrostatic conditions) from the recorded pore water pressure. In this study, the paste tailings material, which is a highly densified tailings material, is considered to be at a liquefaction state when the criterion of the excess pore water pressure reaches or almost reaches the initial vertical effective stress, which means that the excess pore water pressure ratio equals 1 or is close to 1 (i.e. it is between 1 and 0.9) (Ueng et al., 2010; Pépin et al., 2012a). Figures 4.21 and 4.22 show the time histories of the excess pore water pressure measured at different depths and the corresponding excess pore water pressure ratio during, and after the shaking test, respectively.

From Figure 4.21, it can be deduced that when the shaking began, the pore water pressure or the excess of pore water pressure at the middle depth of each layer increased rapidly until reaching a maximum value; subsequently, it became almost stable until the end of the shaking duration. This rapid and immediate increase in the excess pore water pressure at the start of shaking mainly results from the volume contraction of the tested paste tailings material as shown in Figures 4.25-4.26 (will be discussed later). This relative stabilization of the excess of pore water pressure observed after the maximum value can be attributed to a dilative response of the paste tailings materials to loadings at very low effective stress (Pépin et al., 2012a), as shown in Figure 4.25. Figure 4.21 shows that the maximum values of the excess pore water pressure in the tested tailings during shaking varied between 0.5 kPa and 3.2 kPa. Furthermore, the bottom layer achieved the highest maximum value for the excess pore water pressure, followed by the middle and top layers. A factor that contributes to this higher value of excess pore water pressure in the bottom layer is the downward flow of pore water from the middle layer to the bottom layer as evidenced by Figure 4.23 (will be discussed later). This means that this pore water pressure in the bottom layer is caused partly by pore pressures generated in the bottom layer and partly by inflow of pore water from the upper layer. From Figure 4.23, it is also obvious that an upward flow of pore water from the lower part of the paste tailings deposit to the upper (top) layer took place during shaking, as discussed later. This explanation is also supported by the findings of Naesgaard and Byrne (2007), who concluded that earthquake shaking of layered soils induce pore water gradients, inflow of pore water in some areas or layers and outflow of pore water in some areas. Similar findings were obtained for sand (Tohumcu Özener et al., 2009) using a shaking table. It took longer for the bottom layer to reach the maximum value of the excess pore water pressure during shaking compared to the top and middle layers. Moreover, the top layer required longer time to reach the peak value of the excess pore water pressure during shaking compared to the middle layer. This delay is attributed to the fact that water flow and pressure redistribution takes time. Consequently, there is often a delay between time of shaking and time of reaching the maximum excess of pore water pressure or liquefaction failure (Naesgaard and Byrne, 2007; Serafini and Perlea, 2010). At all layers of the paste tailings deposit, the excess pore water pressure ratio was generally below unity ($r_u < 1$), ranging from 0.7–0.9 during the duration of the shaking. This would indicate that the paste tailings did not liquefy during the applied cyclic loading conditions.

Once the shaking ended (as illustrated by the red arrows), the excess pore water pressure at all layers increased abruptly until reaching a maximum value. At all layers of the tested material, the excess pore water pressure ratios were close to unity ($r_u \approx 1$) due to this abrupt increase in pressure, which indicates that this type of material can be susceptible to liquefaction in the post-cyclic loading phase. The magnitude of this abrupt increase was associated with the depth. The top layer was found to have a lower magnitude compared to the middle and bottom layers. This difference in the magnitude mainly occurred because there was a smaller vertical total stress at the shallower depth. This abrupt increase in excess pore water pressure arose because of the end of the cyclic loading, which enabled the contraction of tailings particles that were partially in suspension, thereby generating additional pore water pressure (Pépin et al., 2012a). Similar responses were reported by Pépin et al. (2012a, 2012b), who tested the susceptibility of hard rock slurry tailings to liquefaction under shaking. An upward flow of pore water from the lower part of the paste tailings sample to the upper (top) layer and a downward flow of water from the lower part of the middle layer of the paste tailings sample to the bottom layer (Layer 1) should be considered as an additional factor that contributed to this abrupt increase of excess pore water pressure in the top layer (Layer 3) and bottom layer, respectively. This downward flow of water to the bottom layer might have been enabled by the sand drainage layer beneath the paste tailing deposit as well as facilitated by desiccation- induced microcracks that appeared on the surface of the first layer after 3 days of drying, i.e. before the deposition of the second layer. Cracks increase the permeability of tailings deposits or soil layers (Roshani et al., 2017). This argument with respect to the aforementioned upward and downward water flow is consistent with the results of the monitoring of the evolution of the volumetric water content (VWC) (Figure 4.23; an increase of the VWC in the middle of the top and bottom layers is observed during shaking and up to 1 hr after the end of shaking) as well as with the tailings boil observed at the surface of the top layer (Figure 4.24). Tailings boils were observed on the surface of the paste tailings deposit after the occurrence of liquefaction (Figure 4.24). This boiling was due to the ejected water with tailings particles rising to the surface of the deposit. A similar observation was also reported after the liquefaction of Mailiao silty sand (Ueng et al., 2008). Moreover, Figure 4.21 shows that the highest value of excess pore water pressure ratios is measured in the bottom layer, which could suggest that this bottom layer is more prone to liquefaction. This can be explained by the aforementioned influx of pore water into the bottom layer.

Following the abrupt increase in the excess pore water pressure at all layers, the pressure began to dissipate gradually until returning to hydrostatic conditions ($r_u = 0$), as shown in Figure 4.22. It should be noted that hydrostatic conditions were reached within 9–40 hours for all layers. The long-term dissipation of the excess pore water pressure of the paste tailings was similar to that of hard rock slurry tailings (Pépin et al., 2012a, 2012b). In contrast, previous investigations found that the excess pore water pressure of sandy soil dissipated rapidly (e.g. Ueng et al., 2010). This is because of the relatively low permeability (~$10^{-5}$ - $10^{-7}$ m/s) of uncracked paste tailings material (Bussière et al., 2007) compared to sandy soil (~$10^{-3}$ - $10^{-5}$ m/s). In terms of the duration of dissipation, the bottom layer took the longest time to completely dissipate its excess pore water pressure. This can be explained by the fact that the bottom layer had the highest value of volumetric water content (Figure 4.23) at the end of shaking due to the inflow of pore water. Furthermore, the dissipation of excess pore water pressure was faster at the middle layer than at the top layer. This can be due to the upward movement of pore water from the middle layer to the top layer. This is agreement with the higher development of the volumetric water content at the top layer than at the middle layer (Figure 4.23) as well as with the findings in other studies on liquefaction or dynamic behaviour of layered soils (Naesgaard and Byrne, 2007; Serafini and Perlea, 2010).

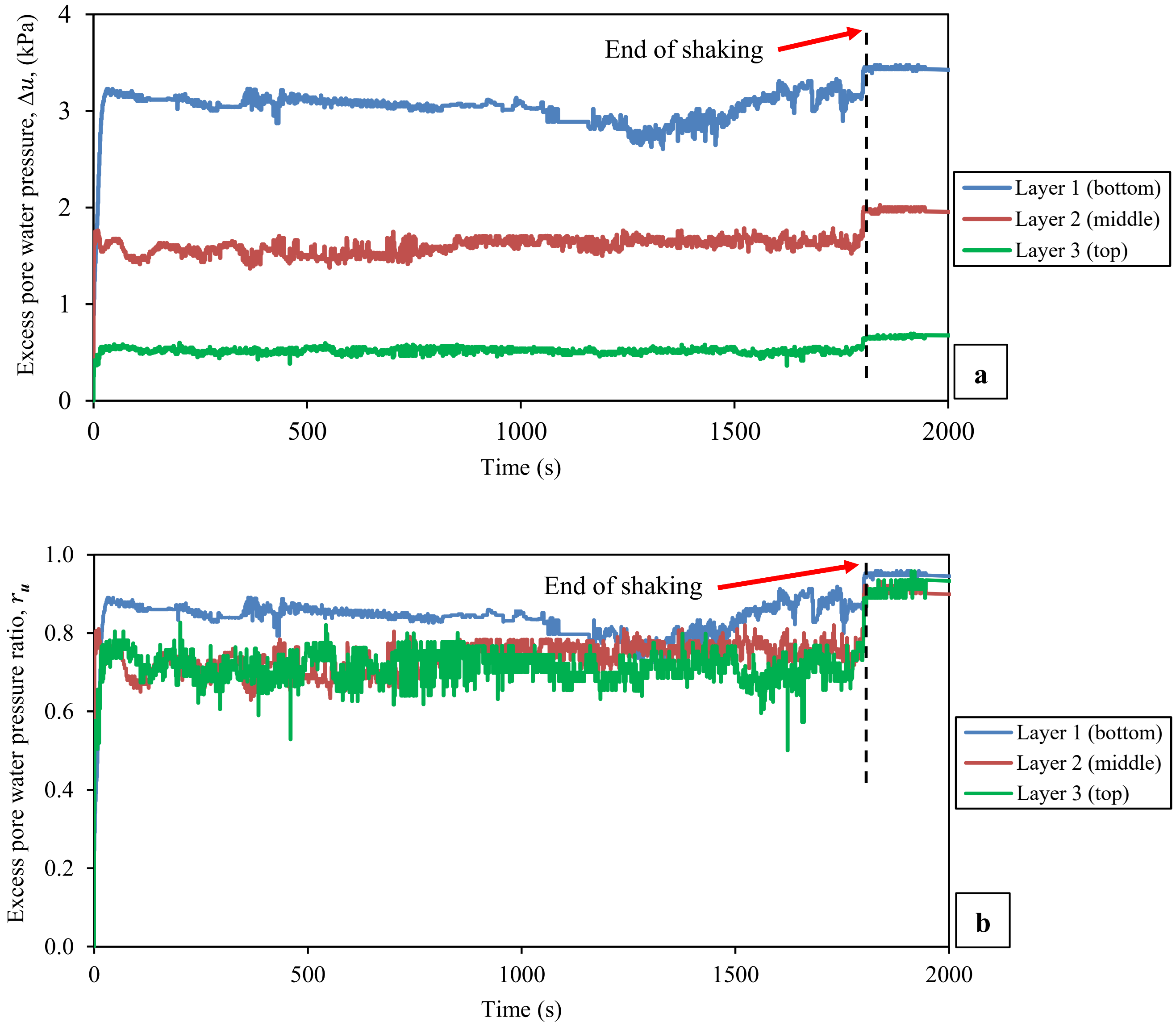


Figure 4.21. Time histories of excess pore water pressures at the middle depth of each layer of tailings during shaking. a) Measured excess pore water pressures ($\Delta u$). b) Excess pore water pressure ratios ($r_u$)

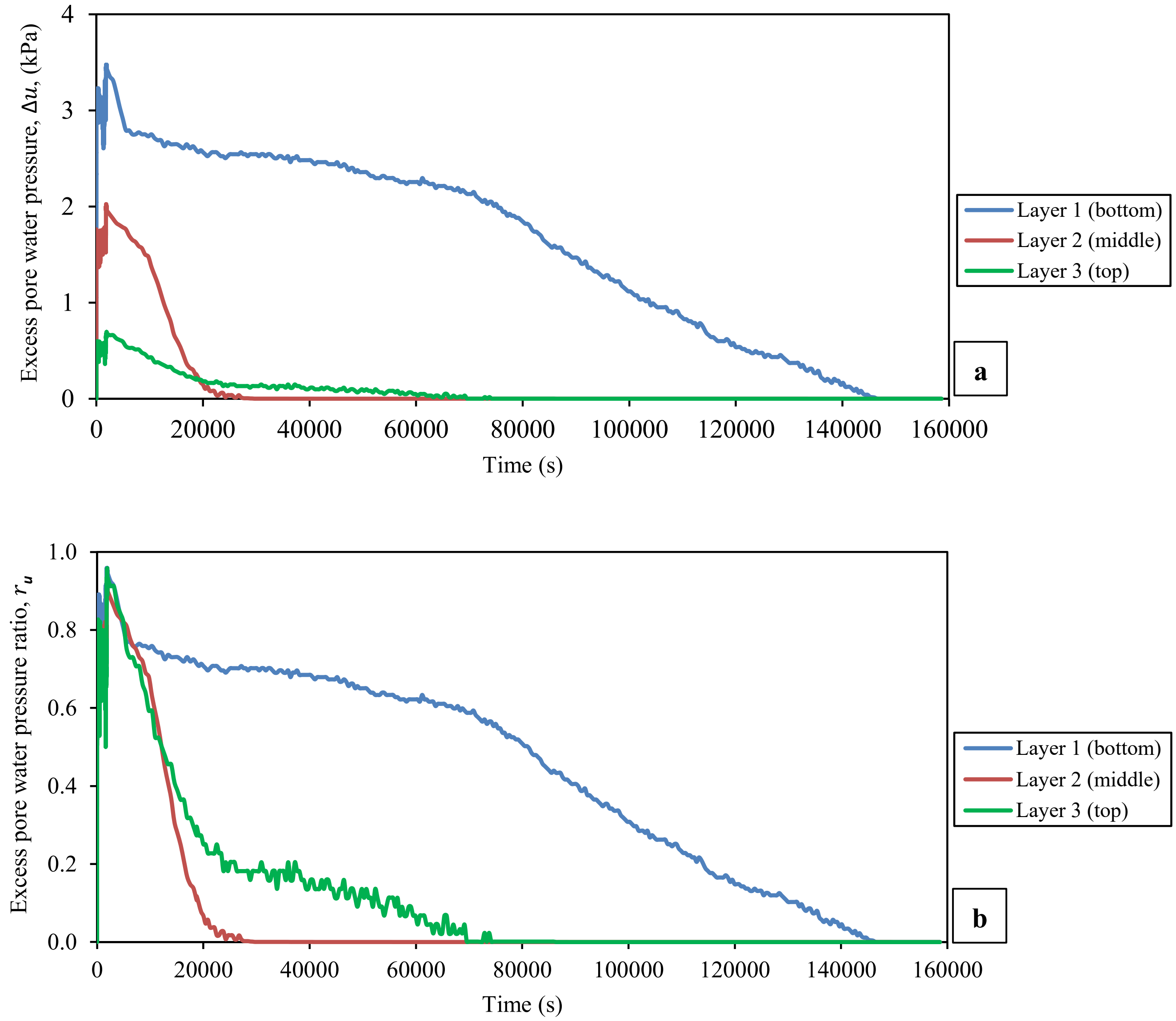


Figure 4.22. Time histories of excess pore water pressures at the middle depth of each layer of tailings during and after shaking. a) Measured excess pore water pressures ($\Delta u$). b) Excess pore water pressure ratios ($r_u$)

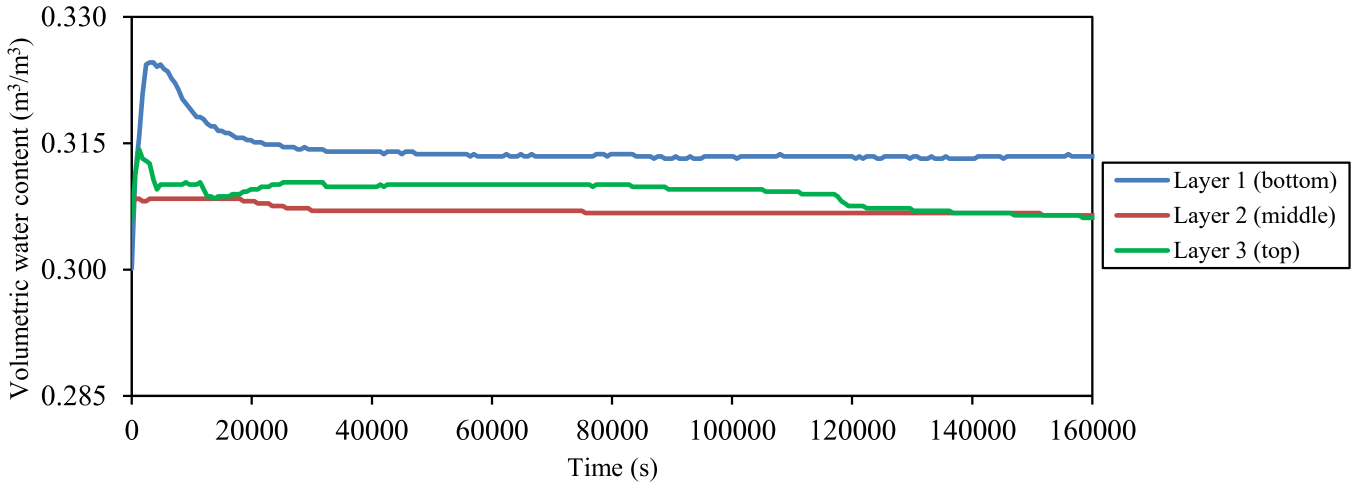


Figure 4.23. Time histories of volumetric water content at the middle depth of each layer of tailings during and after shaking

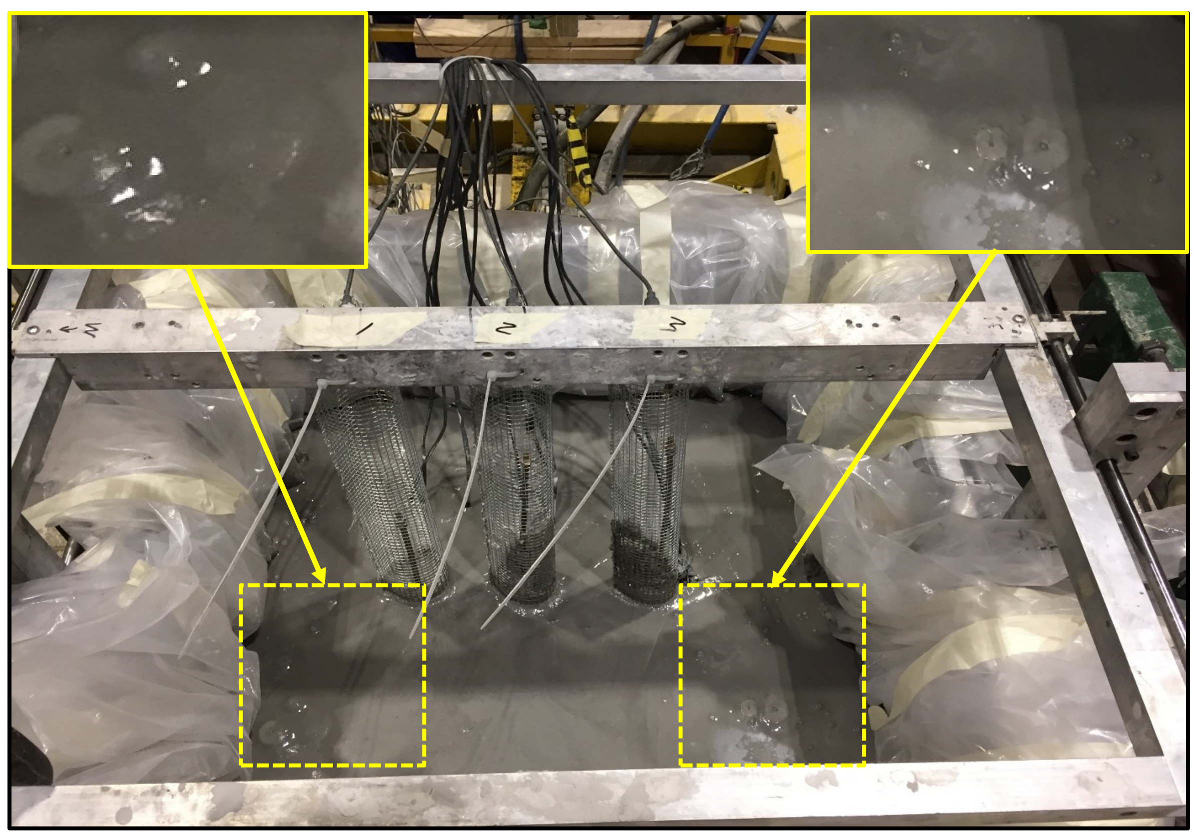

Figure 4.24. Tailings boils on the surface of the deposit after liquefaction

4.3.3.3. **Vertical displacement/settlement response**

The vertical displacement at the middle depth of each layer of paste tailings during and after shaking can be seen in Figures 4.25 and 4.26. Figure 4.25 shows the change in response of the paste tailings from contractive to dilative behaviour. Once the shaking was applied, the tested tailings began to settle for a short duration. This settlement is due to the movement of the plastic plates to a deeper depth, at which the tested tailings are subjected to a contractive response. Moreover, the contractive response was more noticeable at the top and middle layers than at the bottom layer. This is because the bottom layer of the paste tailings experienced a longer period of drying (desiccation), as mentioned in Section 4.3.2.5, than the other two layers. It has been reported that a slight level of drying or desiccation of tailings can transform the response from contractive to dilative (Daliri, 2013). Then, during the shaking, the tested paste tailings began to show a dilative response as the plastic plates moved upward. This dilation occurred first at the bottom layer before the other two layers. An additional factor that contributes to the observed lower contraction and dilative behaviour of the bottom layer is the inflow of pore water from the upper part (middle layer, upper part of the bottom layer) of the paste tailings. The vertical displacement response of the top layer was somewhat different from that of the middle and bottom layers. This different response could be due to the inflow of water, which originated from the middle layer and flowed upward into the top layer during shaking (Figure 4.23). This observation of the paste tailings is in agreement with that of layered soils (Naesgaard and Byrne, 2007; Serafini and Perlea, 2010). Figure 4.26 shows that there were no significant changes in the displacements at the middle depth of each layer of paste tailings after the shaking ended.

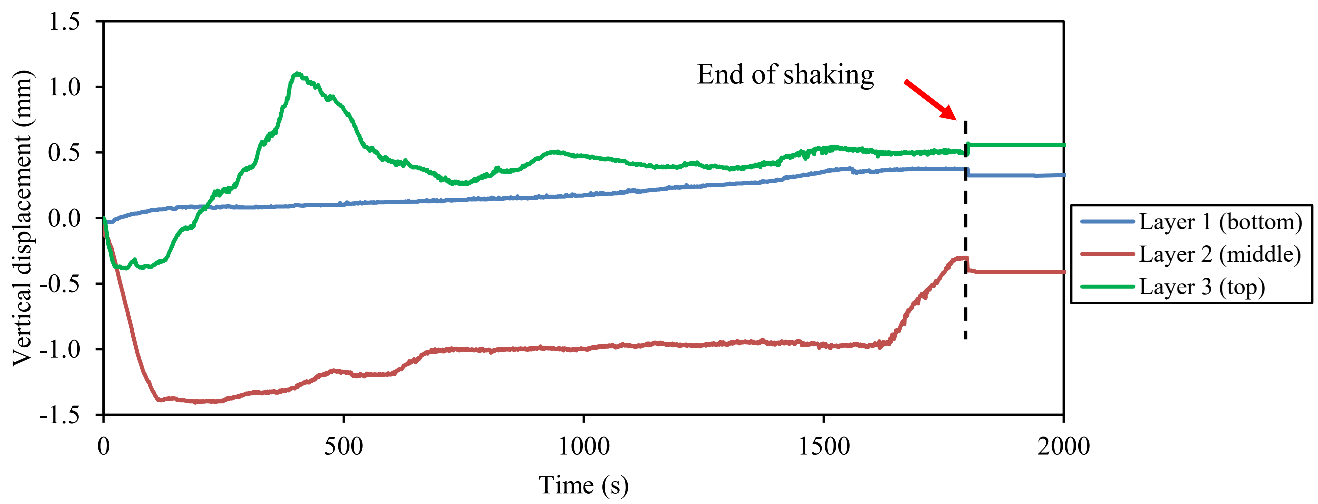


Figure 4.25. Vertical displacements at the middle depth of each layer of tailings during shaking

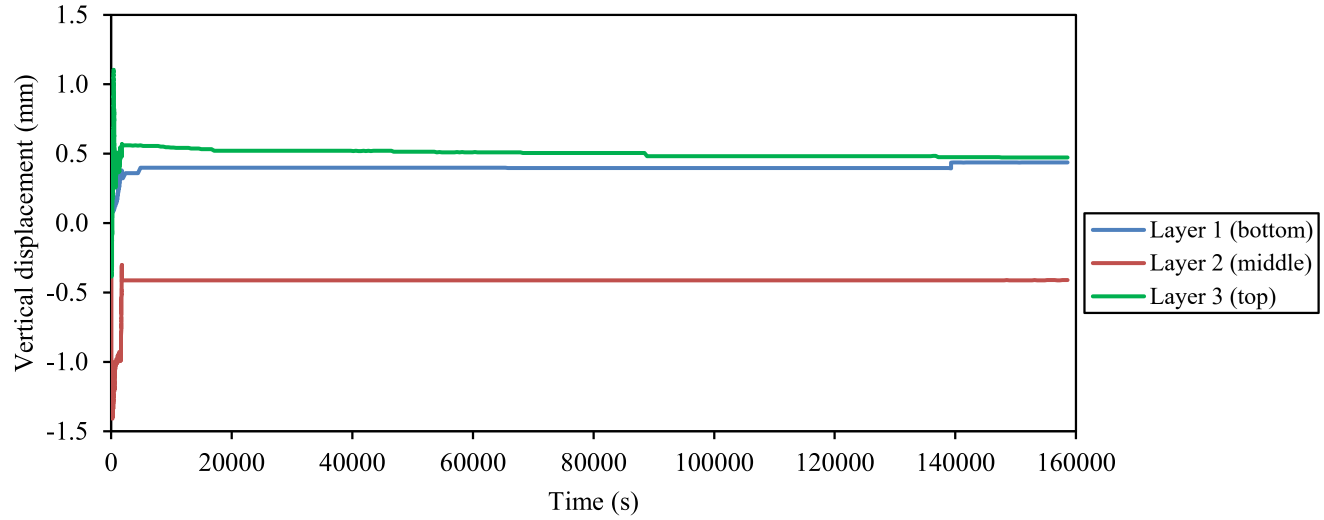


Figure 4.26. Vertical displacements at the middle depth of each layer of tailings during and after shaking

### 4.3.4. **Summary and conclusions**

A shaking table test was performed on layered paste tailings using an FLSB. The paste tailings were deposited into the FLSB in three thin layers. Instruments were installed at the middle depth of each layer of the paste tailings to measure the acceleration, displacement and pore water pressure. In addition, a frequency of 1 Hz and peak horizontal acceleration of 0.13g were used as the loading conditions in this investigation.

The test results generally showed that the accelerations at the middle depth of each layer of paste tailings deposits were not similar. The accelerations at the bottom and middle layers had somewhat similar responses to that of the base of the shaking table. However, the response acceleration at the top layer was different than that of the base of the shaking table. Irregularity and attenuation of the acceleration response at the top layer were observed from the beginning of the shaking loading. Generally, the horizontal displacement at the middle depth of each layer was relatively similar.

It is found that the shaking of the layered paste tailings deposit resulted in pore water flow and pressure redistribution. The bottom and top layers experienced pore water inflow, whereas the middle layer was affected by pore water outflow. This water flow (outflow, inflow) significantly affected the response (excess pore water pressure, liquefaction, vertical displacement) of the paste tailings.

During shaking, the excess pore water pressure at the middle depth of all layers was found to develop quickly until reaching a maximum value, indicating that the paste tailings experienced a contraction response. The pore water inflow into the bottom and top layers also contributed to this increase in excess pore water pressure. However, it was found the excess pore water pressure ratios were less than 0.8 during shaking. This would suggest that all paste tailing layers were resistant to liquefaction during the cyclic loading. At the end of shaking, an abrupt increase in excess pore water pressure was also observed through all layers of paste tailings. Consequently, the excess pore water pressure ratios approached 1 through all layers of paste tailings. Therefore, the studied paste tailings are considered susceptible to liquefaction in the post-cyclic loading stage. Two mechanisms are considered responsible for this abrupt increase in excess pore water pressure: (i) the contraction of tailings particles that were partially in suspension of the tailings that generated additional pore water pressure; (ii) upward pore water migration to the top layer and downward pore water flow to the bottom layer that produced additional pore water pressure. Typically, the dissipation of the excess pore water pressure of tested tailings takes a long period of time, which could be associated with the relatively low permeability of this type of uncracked tailings. The bottom layer of the tested paste tailings took longer to fully dissipate its excess pore water pressure compared with the top and middle layers possibly due to more pore water inflow.

Based on the response of the vertical displacements, the tested tailings experienced both contraction and dilation during the shaking loading. At the beginning of the shaking loading, settlement or contraction was observed at all depths of the tested tailings. Also, the settlement or contraction of the tested tailings was more obvious at the top and middle layers than that at the bottom layer, which could be due to the longer time of drying or desiccation of the bottom layer as well as to more pore water inflow into the bottom layer. The tested tailings did not show substantial changes in vertical displacements following the end of shaking loading.

The outcomes from this study provide a better understanding of the liquefaction susceptibility of this type of tailings material, which is essential for the safety of geotechnical paste tailings structures as well as sustainable mining.

### 4.3.5. **References**


Alainachi, I., and Fall, M. (2019). Seismic induced liquefaction of cemented paste backfill: effect of mixing water. In Proceedings of the 7th International Conference on Earthquake Geotechnical Engineering (VII ICEGE), 17-20 June 2019, Roma, Italy, pp. 1042-1049.

Al-Tarhouni, M., Simms, P., and Sivathayalan, S. (2011). Cyclic behaviour of reconstituted and desiccated-rewet thickened gold tailings in simple shear. Canadian Geotechnical Journal, 48(7): 1044-1060.

Al-Tarhouni, M.A. (2008). Liquefaction and post-liquefaction behaviour of gold mine tailings under simple shear loading. Master thesis, Department of Civil and Environmental Engineering, Carleton University, Ottawa, Ontario, Canada.

ASTM. (2010). D4318-10e1: Standard test methods for liquid limit, plastic limit, and plasticity index of soils. ASTM International, West Conshohocken, PA, USA.

ASTM. (2015). C143/C143M-15a: Standard test method for slump of hydraulic-cement concrete. ASTM International, West Conshohocken, PA, USA.

Barakati, A. (2015). Numerical modelling of liquid containing structure under dynamic loading. Master thesis, Department of Civil Engineering, University of Ottawa, Ottawa, Ontario, Canada.

Bussière, B. (2007). Colloquium 2004: hydrogeotechnical properties of hard rock tailings from metal mines and emerging geoenvironmental disposal approaches. Canadian Geotechnical Journal, 44(9): 1019-1052.

Coelho, P.A.L.F., Haigh, S.K., and Madabhushi, S.P.G. (2004). Centrifuge modelling of liquefaction of saturated sand under cyclic loading. In Proceedings of the International Conference on Cyclic Behaviour of Soils and Liquefaction Phenomena, 31 March - 02 April 2004, Bochum, Germany, pp. 349-354.

Crowder, J.J. (2004). Deposition, consolidation, and strength of a non-plastic tailings paste for surface disposal. PhD thesis, Department of Civil Engineering, University of Toronto, Toronto, Ontario, Canada.

Crowder, J.J., Grabinsky, M.W.F., and Klein, K.A. (2002). Laboratory characterization of tailings paste for surface disposal. In Proceedings of the 55th Canadian geotechnical conference, 20-23 October 2002, Niagara Falls, Ontario, Canada, pp. 401-409.

Cui, L., and Fall, M. (2016). Mechanical and thermal properties of cemented tailings materials at early ages: influence of initial temperature, curing stress and drainage conditions. Construction and Building Materials, 125: 553-563.

Daliri, F. (2013). The influence of desiccation and stress history on monotonic and cyclic shear response of thickened gold tailings. PhD thesis, Department of Civil and Environmental Engineering, Carleton University, Ottawa, Ontario, Canada.

Elberling, B., and Nicholson, R.V. (1996). Field determination of sulphide oxidation rates in mine tailings. Water Resources Research, 32(6): 1773-1784.

Geremew, A.M., and Yanful, E.K. (2012). Laboratory investigation of the resistance of tailings and natural sediments to cyclic loading. Geotechnical Geological Engineering, 30(2): 431-447.

Hamade, T. (2013). Geotechnical design of tailings dams-a stochastic analysis approach. PhD thesis, Department of Mining and Materials Engineering, McGill University, Montreal, Quebec, Canada.

Hu, L., Wu, H., Zhang, L., Zhang, P., and Wen, Q. (2017). Geotechnical properties of mine tailings. Journal of Materials in Civil Engineering, ASCE, 29(2): 04016220.

Iai, S. (1989). Similitude for shaking table tests on soil-structure-fluid model in 1-g gravitational field. Soils and Foundations, 29(1): 105-118.

ICOLD. (2001). Tailings dams–risk of dangerous occurrences–lessons learnt from practical experiences. Bulletin 121, International Commission on Large Dams (ICOLD), Paris, France, pp. 1-144.

Ishihara, K., Troncoso, J., Kawase, Y., and Takahashi, Y. (1980). Cyclic strength characteristics of tailings materials. Soils and Foundations, 20(4): 127-142.

Ishihara, K., Yasuda, S., and Yokota, K. (1981). Cyclic strength of undisturbed mine tailings. In Proceedings of the First International Conference on Recent Advances in Geotechnical Earthquake Engineering and Soil Dynamics, 26 April - 3 May 1981, St. Louis, Missouri, USA, Vol. 1, pp. 53-58.

Jakubick, A.T., McKenna, G., and Robertson, A.M. (2003). Stabilization of tailings deposits: International experience. In Proceedings of Mining and the Environment III, 25-28 May 2003, Sudbury, Ontario, Canada, pp. 1-9.

James, M., Aubertin, M., Wijewickreme, D., and Wilson, G.W. (2011). A laboratory investigation of the dynamic properties of tailings. Canadian Geotechnical Journal, 48(11): 1587-1600.

James, M., Jolette, D., Aubertin, M., and Bussière, B. (2003). An experimental set-up to investigate tailings liquefaction and control measures. In Proceedings of the International Symposium on Major Challenges in Tailings Dams (ICOLD), 15 June 2003, Montréal, Quebec, Canada, pp. 153-164.

Kim, H., Daliri, F., Simms, P., and Sivathayalan, S. (2011). The influence of desiccation and overconsolidation on monotonic and cyclic shear response of thickened gold tailings. In Proceedings of the 64th Canadian Geotechnical Conference (2011 Pan-Am CGS), 2-6 October 2011, Toronto, Ontario, Canada.

Li, M., Bernier, L., and Boucher, J-F. (2002). Rheology of mineral pastes and its implications on underground pipeline delivery. In Proceedings of Symposium 2002 on Environment and Mines, Canadian Institute of Mining, Metallurgy, and Petroleum, 3-5 November 2002, Rouyn-Noranda, Quebec, Canada.

Marshall, B. (2018). Facts and figures of the Canadian mining industry. The Mining Association of Canada (MAC), Ottawa, Ontario, Canada, pp.1-109.

Meggyes, T., and Debreczeni, Á. (2006). Paste technology for tailings management. Land Contamination and Reclamation, 14(4): 815-827.

Meymand, P.J. (1998). Shaking table scale model tests of nonlinear soil-pile-superstructure interaction in soft clay. PhD thesis, Department of Civil and Environmental Engineering, University of California, Berkeley, California, USA.

Mohamed, F.M.O. (2014). Bearing capacity and settlement behaviour of footings subjects to static and seismic loading conditions in unsaturated sandy soils. PhD thesis, Department of Civil Engineering, University of Ottawa, Ottawa, Ontario, Canada.

Naesgaard, E., and Byrne, P.M. (2007). Flow liquefaction simulation using a combined effective stress–total stress model. In Proceedings of the 60th Canadian Geotechnical Conference, 21-24 October 2007, Ottawa, Ontario, Canada.

Newman, P., White, R., and Cadden, A. (2001). Paste–the future of tailings disposal? In Proceedings of the Second International Conference on Mining and the Environment, 27 June - 1 July 2001, Skelleftea, Sweden, pp. 594-603.

Orejarena, L., and Fall, M. (2008). Mechanical response of a mine composite material to extreme heat. Bulletin of Engineering Geology and the Environment, 67(3): 387-396.

Pépin, N., Aubertin, M., and James, M. (2012a). Seismic table investigation of the effect of inclusions on the cyclic behaviour of tailings. Canadian Geotechnical Journal, 49(4): 416-426.

Pépin, N., Aubertin, M., James, M., and Leclerc, M. (2012b). Seismic simulator testing to investigate the cyclic behaviour of tailings in an instrumented rigid box. Geotechnical Testing Journal, 35(3): 469-479.

Pokharel, M., and Fall, M. (2013). Combined influence of sulphate and temperature on the saturated hydraulic conductivity of hardened cemented paste backfill. Cement and Concrete Composites, 38(4): 21-28.

Prasad, S.K., Towhata, I., Chandradhara, G.P., and Nanjundaswamy, P. (2004). Shaking table tests in earthquake geotechnical engineering. Current Science, 87(10): 1398-404.

Roshani, A., Fall, M., and Kennedy, K. (2017). Drying behaviour of mature fine tailings pre-dewatered with super absorbent polymer: column experiments. ASTM Geotechnical Testing Journal, 40(2): 210-220.

Seidalinova, A. (2014). Monotonic and cyclic shear loading response of fine-grained gold tailings. Master thesis, The University of British Columbia, Vancouver, British Columbia, Canada.

Serafini, D.C., and Perlea, V. (2010). Comparison of liquefaction triggering analysis approaches for an embankment dam and foundation. In Proceedings of the 5th International Conference on Recent Advances in Geotechnical Earthquake Engineering and Soil Dynamics, 24-29 May 2010, San Diego, California, USA, paper No. 4.12b.

Statistics Canada. (2012). Human activity and the environment: waste management in Canada, pp. 1-46.

Stubrin, L. (2018). Reprint of: Innovation, learning and competence building in the mining industry. The case of knowledge intensive mining suppliers (KIMS) in Chile. Resources Policy, 58: 62-70.

Theriault, J., Frostiak, J., and Welch, D. (2003). Surface disposal of paste tailings at the Bulyanhulu gold mine, Tanzania. In Proceedings of Mining and the Environment Conference III, 25-28 May 2003, Sudbury, Ontario, Canada, pp. 1-8.

Turan, A., Hinchberger, S.D., and El Naggar, H. (2009). Design and commissioning of a laminar soil container for use on small shaking tables. Soil Dynamics and Earthquake Engineering, 29(2): 404-414.

Tuttle, M., Law, K.T., Seeber, L., and Jacob, K. (1990). Liquefaction and ground failure induced by the 1988 Saguenay, Quebec, earthquake. Canadian Geotechnical Journal, 27(5): 580-589.

Ueng, T.S., Chen, C.H., Tsou, C.F., and Chen, Y.C. (2008). Shaking table test on a large specimen of Mailiao silty sand. In Proceedings of the Geotechnical Earthquake Engineering and Soil Dynamics Congress IV, 18-22 May 2008, Sacramento, California, USA, pp. 1-10.

Ueng, T.S., Wu, C.W., Cheng, H.W., and Chen, C.H. (2010). Settlements of saturated clean sand deposits in shaking table tests. Soil Dynamics and Earthquake Engineering, 30(1-2): 50-60.

Verburg, R.B.M. (2001). Use of paste technology for tailings disposal: potential environmental benefits and requirements for geochemical characterization. In Proceedings of the International Mine Water Association Symposium, 24-28 April 2001, Belo Horizonte, Brazil, pp. 1-13.

Wijewickreme, D., Sanin, M.V., and Greenaway, G.R. (2005). Cyclic shear response of fine-grained mine tailings. Canadian Geotechnical Journal, 42(5):1408-1421.

World Information Service on Energy (WISE). (2017). Chronology of major tailings dam failures. See https://www.wise-uranium.org/mdaf.html [accessed December 10, 2017].

Wu, J., Kammerer, A.M., Riemer, M.F., Seed, R.B., and Pestana, J.M. (2004). Laboratory study of liquefaction triggering criteria. In Proceedings of the 13th World Conference on Earthquake Engineering, 1-6 August 2004, Vancouver, British Columbia, Canada, paper No. 2580.

# 5 Chapter 5: Effect of Environmental Stresses

## 5.1. Introduction

To avoid or minimize geotechnical and environmental issues such as failed tailings dams, acid mine drainage, and surface water contamination related to conventional slurry mine tailings, mine tailings must be stored safely. In this context, a relatively novel technology of mine tailings management known as highly densified tailings (thickened and paste tailings) has been proposed and adopted worldwide as a potential solution. A drying and wetting process can impact the behaviour and liquefaction potential of thickened and paste tailings exposed to cyclic or seismic loading such as an earthquake. Previous research has focused mainly on the behaviour and liquefaction susceptibility of conventional slurry tailings and thickened and paste tailings under cyclic (seismic) loading through laboratory testing, without considering the wetting (heavy rainfall) process' effect. Hence, a research gap exists regarding the effect of heavy rainfall following a drying period on the behaviour and liquefaction susceptibility of thickened and paste tailings under cyclic (seismic) loading using shaking table equipment.

This chapter primarily concentrates on the laboratory test results of an experiment performed using shaking table testing techniques on the cyclic and liquefaction behaviour of layered thickened and paste tailings (Section 5.2). This chapter aims to manually simulate (using the one-dimension shaking table equipment) a heavy rainfall scenario and associated effects on the cyclic liquefaction susceptibility of layered thickened and paste tailings. Liquefaction assessment of these layered tailings is done through the monitoring of several parameters, including pore water pressure, volumetric water content, and horizontal and vertical displacements. This experiment's findings will be discussed and compared with existing published research.

## 5.2. Technical Paper #3: Shaking Table Investigation of Drying and Wetting Effects on Responses of Highly Densified Tailings to Cyclic Loadings

Fahad Alshawmar, Mamadou Fall
Department of Civil Engineering, University of Ottawa, Ottawa, Ontario, Canada K1N 6N5
Journal of Soil Dynamic and Earthquake Engineering

### Abstract

Understanding and evaluating the cyclic liquefaction behaviour of highly densified tailings (thickened and paste tailings) after a heavy rainfall is considered vital in regions that could experience earthquake shaking following a heavy rainfall period. In this technical paper, the layered deposits of thickened and paste tailings were subjected to a period of drying, and rainfall was then applied manually to these tailings. After applying this rainfall, shaking was applied at the bottom of the layered deposits of thickened and paste tailings using one-dimensional shaking table equipment. A sinusoidal dynamic loading with a frequency of 1 Hz and peak horizontal acceleration of 0.13g was applied to these layered tailings deposits. The pore water pressure and displacement responses were monitored at different depths of the layered tailings deposits. The obtained results have shown the excess pore water pressure at the middle depth of each layer of the thickened and paste tailings deposits (initially exposed to a drying and wetting (heavy rainfall) phase or not) was found to be developed instantly until it reached a peak value during the shaking. However, during the shaking or cyclic loadings, the excess pore water pressure ratio was found to be lower than 0.8 in the layered thickened and paste tailings deposits that were initially exposed to a drying and wetting phase. In other words, the layered paste and thickened tailings deposits did not liquefy during the shaking or cycling loadings despite the application of heavy rainfall. Since the excess pore water pressure ratio was found to be lower than 0.85 in the layered paste tailings deposit (not initially exposed to a drying and wetting phase), it can be said that the layered paste tailings deposit did not liquefy during the shaking or cycling loadings. However, the layered thickened tailings deposit (not initially exposed to a drying and wetting phase) liquefied during the shaking or cycling loadings as its excess pore water pressure ratio was found to be larger 1.0. After the shaking or cyclic loadings, the test results revealed that the excess pore water pressure ratio of the layered thickened and paste tailings deposits (initially exposed to a drying and wetting phase) ranged from 0.8–0.9. For the layered thickened and paste tailings deposits (not initially exposed to a drying and wetting phase), the excess pore water pressure ratio was found to be exceed somewhat or approaching 1.0 after the shaking or cyclic loadings. Accordingly, this indicates that the layered thickened and paste tailings deposits (initially exposed to a drying and wetting phase) were resistance to post-shaking liquefaction while the layered thickened and paste tailings deposits (not initially exposed to a drying and wetting phase) were susceptible to post-shaking liquefaction. Contraction and dilation responses were seen in the layered thickened and paste tailings deposits (initially exposed to a drying and wetting (heavy rainfall) phase or not) during the shaking. The layered tailings deposits (initially exposed to a drying and wetting phase) had similar horizontal displacement response to that layered tailings deposits that were not initially exposed to a drying and wetting phase.

**Keywords:** Thickened tailings; Paste tailings; Liquefaction; Shaking table; Flexible laminar shear box; Excess pore water pressure

### 5.2.1. **Introduction**

The mining industry is critically important to modern society; its products are essential components in, for instance, aeroplanes, ceramics, computers, construction materials, metals and paint (Kossoff et al., 2014). In addition, mining provides employment for more than 40 million people on a worldwide scale (Azapagic, 2004). However, the mining industry creates large volumes of mine tailings, which are considered an important type of mine waste and are not economically beneficial. On a worldwide scale, 5–14 billion tons of mine tailings are estimated to be generated annually (Schoenberger, 2016).

The term mine tailings can refer to the fine-grained (1–600 µm) ground-up rock leftover after removing valuable minerals from the mined ore and the related process water (Edraki et al., 2014). Mine tailings are often stored or deposited as a slurry in impoundments behind dams. In this cohesionless, contractive and saturated state, they are susceptible to liquefaction (James et al., 2011) and might fail due to earthquake-induced liquefaction (Hassani et al., 2008; Fall et al., 2010, 2013; Wu et al., 2012; Paul and Azam 2013; Ahmed and Siddiqua 2014; Kossoff et al., 2014; Adiansyah et al., 2015; Zhang et al., 2015). Liquefaction phenomena can be defined as "all phenomena involving excessive deformations arising due to excess pore water pressure generation within saturated particulate media, such as soils and tailings, when subjected to static or dynamic shear (deviatoric) loading under constrained drainage conditions" (James et al., 2011). Historically, the worldwide mining industry sector has been subject to many disastrous tailings dam failures as a result of liquefaction triggered by an earthquake. It has been reported that 14% of tailings dam failures in the previous century were due to seismic liquefaction (Azam and Li, 2010). For instance, tailings dam failures have been reported in the Barahona copper tailings dam (1928, Chile), the two tailings dams in the El Cobre mine (1965, Chile), the Mochikoshi tailings dam (1978, Japan), the Las Palmas tailings dams (2010, Chile) and, most recently, the Fundaõ tailings dam (2015, Brazil) (Ishihara et al., 1980; Verdugo et al., 2012; Verdugo and González, 2015; Miranda and Marques, 2016; Gomes et al., 2017; WISE, 2017). These tailings dam failures have posed serious threats to the environment, public, property and economy, causing concern among society and governments.

The safe storage or deposition of mine tailings is a crucial issue in seismically active regions, so novel dewatering technologies called thickened tailings and paste tailings have lately been adopted to avoid or minimize the threat of tailings dam failures induced by liquefaction. In contrast to slurries, these technologies behave as dense viscous mixtures of tailings and water and do not experience particle segregation when deposited (Robinsky et al., 1991; Verburg, 2001; Theriault et al., 2003; Edraki et al., 2014). For the paste tailings to be flowable, they must comprise at least 15% by mass, passing 20 µm (Verburg, 2001). The solid content in thickened and paste tailings is 50–70% and 70–85%, respectively (Bussière, 2007; Hamade, 2013). Thickened and paste tailings can be transported through pipelines, after which they are stacked by depositing thin layers to create a beach slope ranging from 2–10% (Engels, 2002; Li et al., 2009). Some benefits are associated with adopting these types of technologies, including reclaimed water, reclaimed process reagents, reclaimed energy (heat), maximized density of tailings in storage facilities, decreased footprint of tailings storage facilities, tailings rendered appropriate for mine backfilling, reduced potential for acid rock drainage and reduced risk of dam failure (Jones and Boger, 2012).

Although a number of laboratory studies have been performed to evaluate the seismic or cyclic liquefaction response of conventional (slurry) and highly densified mine tailings (Ishihara et al., 1981; Poulos et al., 1985; Crowder, 2004; Wijewickreme et al., 2005; Verdugo and Santos, 2009; Al-Tarhouni et al., 2011; James et al., 2011; Kim et al., 2011; Geremew and Yanful, 2012; Pépin et al., 2012a, 2012b; Daliri, 2013; Seidalinova, 2014; Suazo et al., 2016; Hu et al., 2017; Antonaki et al., 2019), no research has highlighted the effect of a heavy rainfall (following a period of drying) on the cyclic loading-induced liquefaction of layered, highly densified tailings (thickened and paste tailings) using shaking table equipment. It is thus essential to enhance the knowledge of mining and geotechnical engineers regarding the cyclic behaviour and liquefaction potential of layered thickened and paste tailings following heavy rainfall before applying these technologies, particularly in areas that might experience heavy rainfall and strong earthquake shaking. The main objective of the current study is therefore to evaluate the effect of heavy rainfall on behaviour and the liquefaction potential of layered thickened and paste tailings under seismic or cyclic loading using shaking table equipment. Heavy rainfall was simulated to imitate the extreme rainfall that occurred in the region of Petit Saguenay, Quebec, Canada on July 19, 1996. A flexible laminar shear box (FLSB) mounted on the shaking table equipment and instrumented with different types of sensors (pore pressure transducers, 5TEs and cable displacement transducers) was used to simulate depositing of thin layers in the field.

### 5.2.2. **Materials and Procedures**

#### 5.2.2.1. **Materials tested and preparation of thickened and paste tailings**

Municipal water and medium-grained tailings were used to prepare the thickened tailings and paste tailings. The fine-grained tailings used in this experimental work were made up of a mixture of natural tailings (NTs) and silica tailings (STs). This mixture enabled precise control of the chemical and mineralogical compositions of the tailings, diminishing the possible effect of uncertainties on the test results. Several reactive minerals (such as sulphide minerals) may be available in the natural tailings and can be oxidized when subjected to air during the preparation or depositing of the tailings. Accordingly, this oxidation process can alter the initial chemical or mineralogical composition of the thickened and paste tailings and lead to the precipitation of reaction products, which may result in the cementation of some tailings particles.

The NTs used in this study were collected from a mine in eastern Canada. STs are synthetic tailings made of ground silica (manufactured by U.S. Silica Co.) and include 99.8% silicon dioxide ($SiO2$) by weight. In addition, the mineral composition of STs is essentially quartz, which is the predominant mineral found in Canadian hard rock mine tailings. The main physical properties of the NTs and STs used are given in Table 5.1, while their mineral compositions, as obtained by X-ray diffraction (XRD) analysis, are given in Table 5.2. The grain size distribution of the STs, NTs and their mixture, as determined by laser analysis, are illustrated in Figure 5.1. This figure shows that these tailings had grain size distributions similar to the average of nine Canadian mine tailings (Orejarena and Fall, 2008, 2010; Pokharel and Fall, 2013). With about 37–45% of fine particles by weight (< 20 μm), NTs and STs can be considered medium tailings. Following the testing procedure in the ASTM D4318-17e1 (ASTM, 2017), the results of the test to determine the Atterberg limits (liquid and plastic limits) of these tailings reveal that the tailings used were non-plastic and could be classified as sandy silts of low plasticity and in the ML group of the Unified Soil Classification System (USCS).

The thickened and paste tailing specimens were prepared by mixing municipal water with the medium-grained tailings. The specimens were mixed using an electric cement mixer for 10 min to obtain homogeneity. To evaluate the workability or flowability of the prepared specimens, the Wykeham-Ferrance laboratory vane shear apparatus was used. The results obtained from the vane shear tests revealed that the yield stresses of these thickened and paste tailings specimens were approximately 63 Pa and 139 Pa, respectively. Such yield stress values were within the range of other thickened and paste tailings' yield stress values, as reported in the previous literature (Sofrá, 2017; Li et al., 2002; Crowder et al., 2002). These yield stress values corresponded to a solid content of 70% for the thickened tailings specimen and 79% for the paste tailings specimen.

Table 5.1. Physical properties of the tailings used and the sand

| Material | Physical Properties | | | | | | |
|---|---|---|---|---|---|---|---|
| | $G_s$ | $D_{10}$ (µm) | $D_{30}$ (µm) | $D_{50}$ (µm) | $D_{60}$ (µm) | $C_u$ | $C_c$ |
| **STs** | 2.7 | 1.9 | 9.0 | 22.5 | 31.5 | - | - |
| **NTs** | 3.1 | 3.2 | 15.8 | 35.5 | 49.5 | - | - |
| **Sand** | 2.7 | 700.0 | 740.0 | 880.0 | 1000.0 | 1.4 | 0.8 |

STs: silica tailings; NTs: natural tailings; $G_s$: specific gravity; $C_u$: coefficient of uniformity; $C_c$: coefficient of curvature

Table 5.2. Mineralogical composition of the tailings used

| Tailings | Mineral | | | | | | | | | | | |
|---|---|---|---|---|---|---|---|---|---|---|---|---|
| | Quartz | Albite | Dolomite | Calcite | Chlorite | Magnetite | Pyrite | Talc | Pyrrhotite | Spinel | Others | Total |
| **STs (wt.%)** | 99.8 | - | - | - | - | - | - | - | - | - | 0.2 | 100.0 |
| **NTs (wt.%)** | 15.0 | 32.8 | 15.0 | 4.2 | 16.1 | 2.4 | 1.0 | 7.0 | 1.8 | 1.8 | 2.9 | 100.0 |

STs: silica tailings; NTs: natural tailings

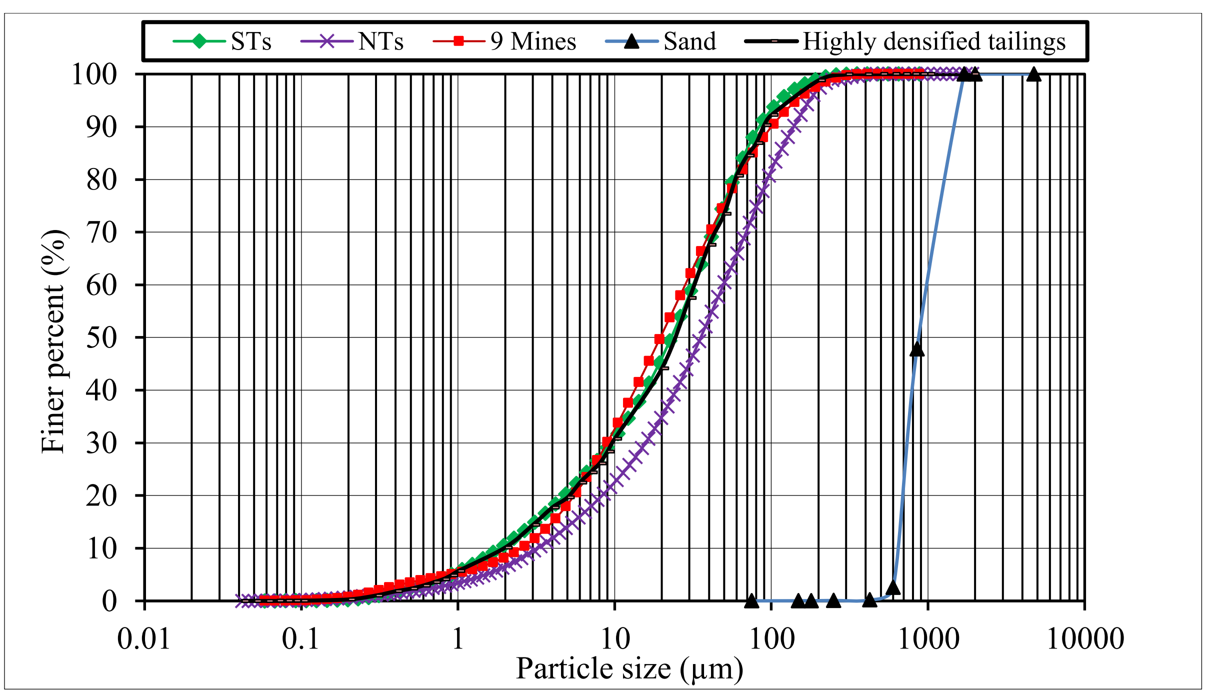


Figure 5.1. Grain size distribution of the tailings and coarse-grained sand used in this experimental work compared with the average of 9 Canadian mine tailings

5.2.2.2. **The shaking simulator**

The seismic or cyclic loading simulator or shaking table test is a powerful tool that can provide vital information related to the seismic or cyclic liquefaction of soils or tailings due to its control of a large amplitude and multi-directional input motions, obtaining laboratory measurements more easily. The obtained results can be used to validate the numerical models or gain a better understanding of the failure mechanisms (Prasad et al., 2004). However, Prasad et al. (2004) reported that the shaking table test has some drawbacks, such as high gravitational stresses as those in the field cannot be generated.

The experimental work in this paper was performed with a shaking table that belongs to the University of Ottawa, Ontario, Canada (Figure 5.2). The equipment comprised of a single degree of horizontal freedom with an aluminum platform and a hydraulic actuator (Model 244) to move the shaking table back and forth horizontally through a hydraulic pump. Table 5.3 shows the key parameters of the shaking table equipment.

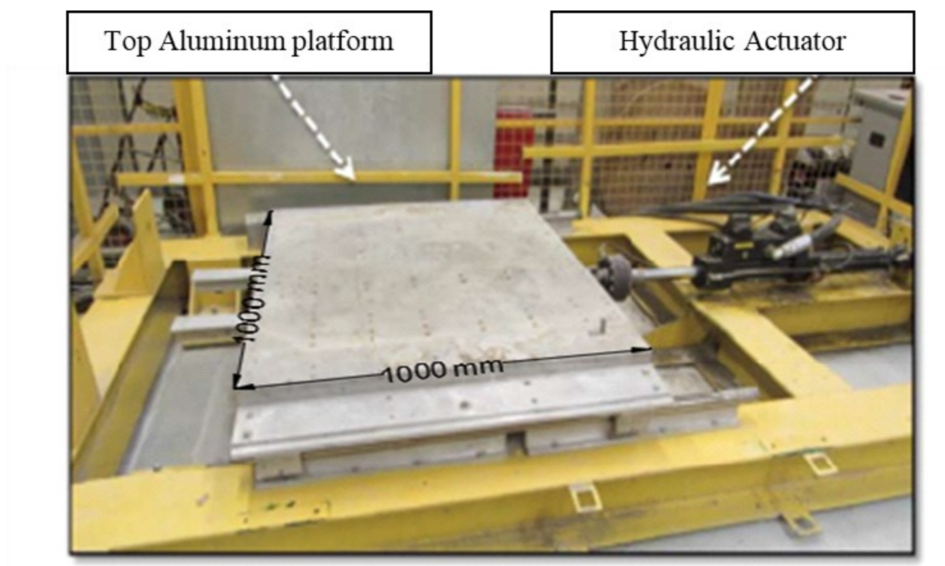


Figure 5.2. Shaking table equipment at the University of Ottawa used for this experimental work (photo from Barakati, 2015)

Table 5.3. Specific key parameters of shaking table equipment

| Size of shaking table platform ($mm^2$) | Maximum payload capacity (kg) | Hydraulic actuator capacity (kN) | Range of frequency (Hz) | Maximum displacement (mm) |
|---|---|---|---|---|
| 1000 × 1000 | 1000 | 25 | 1-17 | ± 120 mm |

5.2.2.3. **Construction of the physical model, experimental setup and instrumentation**

The FLSB used in this experimental work, as shown in Figure 5.3, was designed by Alainachi and Fall (2019) and constructed at the University of Ottawa. This type of FLSB can replicate the deformation of highly densified tailings in the field during cyclic or earthquake shaking. Previous research has used one-dimensional flexible containers for 1-g dynamic investigations on shaking tables

(Gibson, 1997; Prasad et al., 2004; Turan et al., 2009; Mohamed, 2014). This FLSB is composed of 22 horizontal laminae, and its size is 750 mm × 750 mm × 750 mm. There is a 2 mm vertical gap between each of these laminae, so they could move independently during the shaking. These laminae were fabricated of aluminum alloy box sections (31.65 × 31.65 mm) attached to create the laminae with plan dimensions of 750 × 750 mm. They were separately supported by linear bearings and two stainless-steel guide roads attached to an external frame. These stainless-steel guide roads (15 mm as diameter) were attached to the external side of each lamina using stiff aluminum brackets. Six low-friction ball bearings per lamina were mounted to feed these guide roads through them, in which were fixed four vertical bearings brackets. The linear bearing system permitted one direction of movement equivalent to the longitudinal axis of the FLSB. The vertical bearings brackets were then attached to the external frame. Because of the FLSB mass when it is empty (~132 kg), the influence of inertia can be avoided by transferring the total mass to this external frame. The mass carried by this external frame was then transferred to the ground floor of the laboratory.

Thickened and paste tailings create gently sloped, self-supporting stacks when discharged from single or multiple deposition points into the storage area. The in-situ slope associated with these technologies was simulated in this experimental work by pouring a layer of coarse-grained sand on the base area of the FLSB to form a slope of approximately 5.6%, as illustrated in Figure 5.4. This slope falls within the expected range (2–10%) for thickened and paste tailings (Engels, 2002). The slope of the deposited tailings is considered a fundamental parameter in controlling the volume of storage, footprint of the tailings storage facility and susceptibility to liquefaction (Li et al., 2009; Li, 2011). It should be emphasized that, in practice, different factors can influence the slope of the deposited tailings in situ, including reclamation and weather conditions, temperature variations, shear effects through transport, rate of deposition from the discharging point, the nature of the material on which the tailings are deposited and the percentage of solid content, particle size distribution and pH of the tailings (Robinsky, 1982; Theriault et al., 2003). The coarse-grained sand used is classified as poorly graded sand (SP) per the USCS. The physical characteristics of this coarse-grained sand are given in Table 5.1, and its grain size distribution is shown in Figure 5.1.

Several instruments were mounted at different depths to monitor the response of the thickened and paste tailings deposits. A cross-section of the FLSB and the instrumentation arrangement are shown in Figure 5.4. These instruments included three pore pressure transducers (Model PX309-015CG5V, Omega Company, range ± 103.42 kPa) to monitor the pore water pressure (P1–P3), three 5TE instruments (Decagon Devices Inc., range 0–80%) to monitor the volumetric water content (5TE1–5TE3), three cable displacement transducers (Model SM2-12, Measurement Specialties Company, range ± 318 mm) to monitor the settlement (VD1–VD3) and three cable displacement transducers (Model SM2-12, Measurement Specialties Company, range ± 318 mm) to monitor the horizontal deformation (HD1–HD3) of the tailings deposits. The pore pressure transducers (P1–P3), 5TE instruments (5TE1–5TE3) and cable displacement transducers (VD1–VD3) were placed inside the thickened and paste tailings deposits (i.e. at the middle depth of each layer) perpendicular to the direction of the dynamic shaking. The cable displacement transducers (VD1–VD3) were fixed on a steel bridge and then attached to the top part of the thin metal tubes running from the bottom to the lightweight perforated circular plastic plates. These cable displacement transducers (VD1–VD3) stretched down to measure the settlement of tailings once these lightweight perforated circular plastic plates were moved down. The thin metal tubes were placed inside mesh cylinders (fabricated from light steel material), which were fixed to a bridge on top of the FLSB to protect them from falling during the dynamic shaking. Alainachi and Fall (2019) adopted this procedure in their investigation, and it worked very well. The cable displacement transducers (HD1–HD3) were fixed to a steel rod and attached along the left external wall of the FLSB near the middle of each tailings deposit layer.

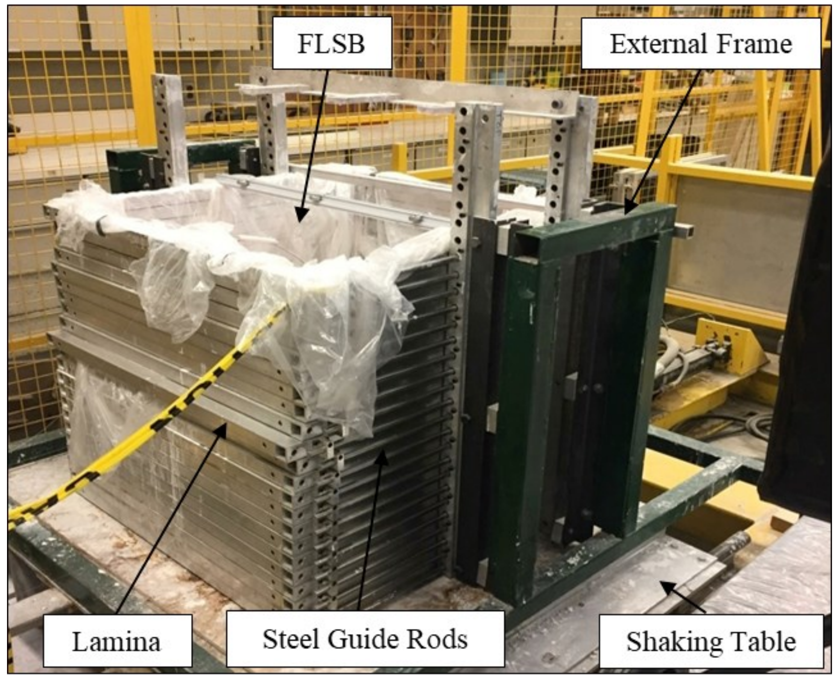


Figure 5.3. Photo of the University of Ottawa's FLSB

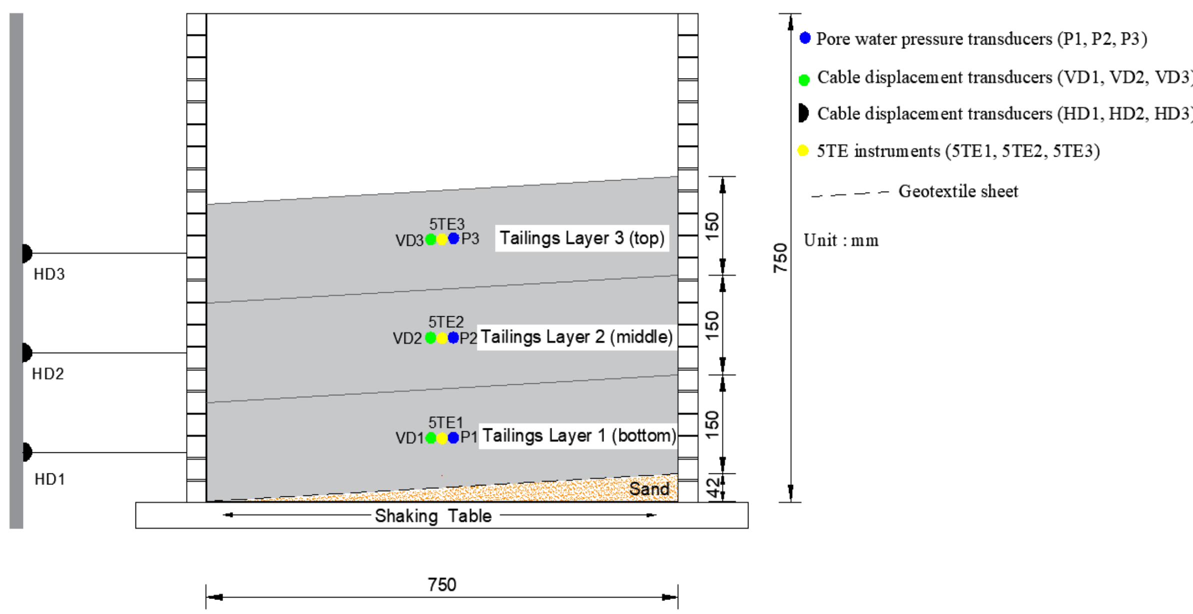


Figure 5.4. Schematic drawing of the instrumented FLSB with three thin layers of (thickened or paste) tailings mounted on the shaking table

5.2.2.4. **Deposition of thickened and paste tailings, experimental testing program and procedure**

The deposition of thickened and paste tailings on the field surface was simulated in this experimental work by depositing layers in the FLSB (Theriault et al., 2003; Li et al., 2009; Raposo et al., 2014). As illustrated in Figure 5.4, there were three of these thin deposited layers, each with a thickness of 150 mm. This figure shows that the layers of these tailings were named as per their pouring or deposition in the FLSB. The time between depositing the first layer (bottom layer) and the second layer (middle layer) was three days, and there were two days between depositing the second layer (middle layer) and the third layer (top layer). Thin-layer deposition and desiccation of thickened and paste tailings are vital to increase their strength before pouring the subsequent layer to prevent flow (Li et al., 2009). However, excessive desiccation could cause the oxidation of sulphide minerals, such as pyrite, in sulphidic tailings, producing acid mine drainage (AMD), which causes serious environmental problems for the mining industry. In the laboratory, the average temperature and relative humidity were 20.4°C and 57%, respectively.

The experimental testing program of the current study comprised two shaking tests. The first shaking test was performed by applying a sinusoidal cyclic loading with a frequency of 1 Hz and a peak horizontal acceleration of 0.13g at the bottom of the thickened tailings deposit contained within the FLSB for a duration of 1800 seconds (30 min). The second shaking test was performed on the paste tailings deposit using test conditions similar to those used in the first shaking test. The frequency applied in this experimental testing program was selected according to earlier cyclic or seismic liquefaction studies (e.g. Ishihara et al., 1981; James et al., 2003; Ueng et al., 2010; Pépin et al., 2012a, 2012b; Geremew and Yanful, 2013) and because of the facility's limitations. Under large loading frequencies, the instruments used in this study were unable to monitor the response of the tested tailings under the cyclic loading condition. The acceleration used in this study was selected based on the acceleration that developed during the earthquake in Saguenay, Québec, Canada in 1988, which had a magnitude of 5.9 (Tuttle et al., 1990). It should be noted that only the peak acceleration was equivalent to the peak of the Saguenay earthquake, not the acceleration for entire time series. The long shaking period selected in this study was not meant to simulate the shaking period of actual earthquakes, which are much shorter. This longer shaking period enables better observation of the cyclic behaviour of the thickened and paste tailings, as well as a comparison of their behaviour. This selected longer shaking period is considered crucial to the future development of a constitutive model to forecast and evaluate the cyclic or seismic behaviour of thickened and paste tailings. Pépin et al. (2012a) have used a similarly long shaking period in their investigations of the cyclic-loading induced liquefaction of conventional slurry tailings. After the deposition of all the thin layers and prior to applying the shaking, the thickened and paste tailings deposits were exposed to heavy rainfall (following a period of drying) to evaluate their cyclic loading-induced liquefaction response. The extreme daily rainfall level of 124.8 mm, which occurred on July 19, 1996 in the region of Petit Saguenay, Quebec, Canada (Government of Canada, 2018), was selected as the heavy rainfall in this study. Since some of this rainfall became surface runoff, a runoff coefficient was adopted to determine the real amount of applied rainfall in this study. This runoff coefficient, which is about 0.5, was selected based on the slope of the deposited tailings (5.6% in this study) and the tailings used (Liu and De Smedt, 2004). Accordingly, the total amount of applied rainfall in this study was 62.4 mm. It should be highlighted that this heavy rainfall was assumed to be last for 5 hours. The bottoms of both the thickened and paste tailings deposits were subjected to shaking one day after the end of this applied heavy rainfall. The monitoring of these tailings' response was terminated following the complete dissipation of excess pore water pressure. It must be noted that two controlled tests, one on the thickened tailings and the other on the paste tailings, were conducted immediately after the deposition all the tailings layers (i.e., without the effects of drying and heavy rainfall).

Numerous experimental testing procedures were followed in this current study to investigate the effect of the drying–wetting (heavy rainfall) process on the cyclic response of the thickened and paste tailings deposits. To hold both the coarse-grained sand and the tailings materials inside the FLSB, it was covered by a thin, flexible plastic bag (Figure 5.3). This was done to prevent the leakage of both the deposited tailings and water. A drainage layer of coarse-grained sand with a slope of 5.6% was then placed on top of this thin, flexible plastic bag. Following that, a geotextile sheet was placed over this layer of coarse-grained sand to work as a porous barrier between the coarse-grained sand and the deposited tailings. Then, the thickened and paste tailings were deposited in three layers (each with a thickness of 150 mm), as described above, in the FLSB. After the deposition of all the layers of these tailings, the period of drying through evaporation started and took approximately 9–11 days. To accelerate this period of dying, commercial fans were mounted on top of the FLSB (Figure 5.5). Then, the heavy rainfall was applied manually to the top surfaces of the thickened and paste tailings deposits, as described above. Following that, rainfall was allowed to infiltrate the thickened and paste tailings deposits for a period of 24 hrs before the shaking was applied. This rainfall water infiltration resulted in the saturation of the thickened and paste tailings, as confirmed by the results of the determination of the degree of saturation (S) of these tailings (S =100%).


Figure 5.5. Pictures of the commercial fans used to dry the tested tailings

### 5.2.3. Results of shaking table tests and discussions

#### 5.2.3.1. Pore water pressure response and liquefaction analysis

To describe or identify the liquefaction potential of natural or man-made tailings soils, some liquefaction triggering criteria have been commonly suggested and used by researchers. These criteria are based on excess pore pressure, strain/deformation-based liquefaction, energy-based liquefaction and strength. Although each of these criteria has advantages, they also have limitations, as described in many earlier studies (e.g., Wu et al., 2004).

In the current study, the excess pore pressure–based criteria are implemented to evaluate the liquefaction potential of the thickened and paste tailings deposits. The development and dissipation of excess pore water pressure and the pore pressure–based criteria have been widely used to evaluate the liquefaction potential of natural and man-made tailings in the laboratory, specifically in the shaking table tests (e.g., Pépin et al., 2012a; Varghese and Latha, 2013; Lu and Fall, 2018; Wang et al., 2020). The parameter of the excess pore water pressure ratio ($r_u$) is most commonly used to evaluate the occurrence of liquefaction, defined as the ratio between the excess pore water pressure ($\Delta u$) and the initial vertical effective stress ($\sigma'_{vo}$) (i.e., $r_u = \Delta u/\sigma'_{vo}$). Liquefaction occurs when the excess pore water pressure ratio ($r_u$) = 1 (Casagrande, 1936; Ueng et al., 2010; Pépin et al., 2012a, b). However, soil liquefaction can be triggered with an $r_u$ of 0.8 or even lower under certain conditions, as reported in earlier literature (e.g., Naesgaard and Byrne 2007; Serafini and Perlea, 2010; Wu et al., 2004). Soil densities and loading conditions can both influence the $r_u$ parameter triggering liquefaction. Denser soils experience larger shear stress ratios and produce lower pore pressure ratios $r_u$ at the onset of liquefaction (Wu et al., 2004).

Figures 5.6 and 5.7 display the measured time histories of the excess pore water pressure values at the middle depth of each layer of the thickened tailings deposit that was initially subjected to a drying and wetting phase and the corresponding excess pore water pressure ratios during and after shaking, respectively. The results for the thickened tailings deposit that was not initially subjected to a drying and wetting phase are shown in Figures 5.6 and 5.7 too. Figures 5.8 and 5.9 display the measured time histories of the excess pore water pressure values at the mid-depth of each layer of the paste tailings deposit that was initially subjected to a drying and wetting phase and the corresponding excess pore water pressure ratios during and after shaking, respectively. The results for the paste tailings deposit that was not initially subjected to a drying and wetting phase are displayed in Figures 5.8 and 5.9 too. As soon as shaking was applied at the bottom of both the thickened and paste tailings deposits, the excess pore water pressure at the middle depth of each layer began to develop instantly regardless whether the tailings deposit was initially exposed to a drying and wetting phase or not, as revealed in Figures 5.6a and 5.8a, respectively. The development of this excess pore water pressure was continuous until reaching a peak value, after which it stayed stable until the shaking was stopped. Such development was associated with the contraction response of the tested tailings, as demonstrated in Figures 5.12 and 5.13, which will be discussed later. The relative stabilization of the excess pore water pressure after the peak value was reached may be due to a dilative response of these tailings deposits to loadings at very low effective stress (Pépin et al., 2012a), as revealed in Figures 5.12 and 5.13.

For the thickened and paste tailings deposits that were initially subjected to a drying and wetting phase, the peak values of the excess pore water pressure were between approximately 0.4 to 2.7 kPa and 0.3 to 2.4 kPa as shown in Figures 5.6a and 5.8a, respectively. For the thickened and paste tailings deposits that were not initially subjected to a drying and wetting phase, the peak values of the excess pore water pressure were between approximately 0.7 to 4.0 kPa and 0.5 to 3.2 kPa as shown in Figures 5.6a and 5.8a, respectively. This means that the tailings that were initially subjected to a drying and wetting phase) were experience lower peak values of the excess pore water pressure compared to the tailings that were not initially subjected to a drying and wetting phase. This could be due to the change into the structure or fabric of the tested tailings that were initially subjected to a drying and wetting phase where the cohesion, strength and density of these tested tailings could be improved as a result of that. Liu et al. (2015) reported that the cyclic shear strength of silty clay increased after drying/wetting phase where soil particles were drawn closer together during this phase and therefore caused variation in the microstructure of soil. The bottom layer of these tailings (initially exposed to a drying and wetting phase or not) attained the highest peak value of excess pore water pressure ($\Delta u$), followed by the middle layer and finally by the top layer. This implies that the peak value of the excess pore water pressure ($\Delta u$) increased as the depth increased. The higher excess pore water pressure ($\Delta u$) value in the bottom layer of these tailings is partially attributed to the downward flow of pore water from the middle layer to the bottom layer (due to the presence of the sand drainage layer), as demonstrated in Figures 5.10 and 5.11, which will be discussed later. This implies that the pore water pressure in the bottom layer of these tailings is produced partially by pore pressures produced in the bottom layer and partially by the inflow of pore water from the upper layer. Furthermore, as shown clearly in Figures 5.10 and 5.11, an upward flow of pore water from the lower part of the thickened and paste tailings deposits to the upper layer took place during shaking, irrespective of whether the tailings deposit was initially exposed to a drying and wetting phase or not. Also, the former explanation is supported by observations on layered soils of Naesgaard and Byrne (2007), who stated that earthquake shaking of layered soils persuades pore water gradients, the inflow of pore water in some areas or layers and outflow of pore water in some areas. Tohumcu Özener et al. (2009) reported similar behaviour after examining pore water pressure generation and related liquefaction in layered sand soils using shaking table equipment. The top layer needed a longer time to reach the peak excess pore water pressure value during shaking than the middle layer. The bottom layer of these tailings required a longer time to reach the peak excess pore water pressure value during shaking than the other two layers. Water flow and pressure redistribution take time, resulting in this delay between time of shaking and the time at which the maximum excess pore water pressure or liquefaction failure are reached (Naesgaard and Byrne 2007; Serafini and Perlea, 2010). During shaking, the excess pore water pressure ratios ($r_u$) at all the layers of the thickened and paste tailings deposits (initially subjected to a drying and wetting phase) were observed to range from 0.7–0.8 and from 0.6–0.7 (see Figures 5.6b and 5.8b), respectively. For the thickened and paste tailings deposits that were not initially subjected to a drying and wetting phase, the excess pore water pressure ratios ($r_u$) (during shaking at all layers) were observed to range from 1–1.05 and from 0.7–0.9 (see Figures 5.6b and 5.8b), respectively. These observations indicated that a wetting (heavy rainfall) after a drying phase of the thickened and paste tailings deposits can increase the liquefaction resistance of the thickened and paste tailings deposits. This drying and wetting phase plays an important role regarding the increase in the liquefaction resistance of the thickened and paste tailings deposits as it alters the structure or fabric of the tested tailings, where the shear strength of these tailings increased due to this phase. This aforementioned explanation can be supported by the findings of Liu et al. (2015) who stated that the microstructure of soil altered and thus the cyclic shear strength of soil increased after drying/wetting phase. In this study, the liquefaction is considered triggered when the excess pore water pressure ratios ($r_u$) ≥ 0.9. Based on the obtained excess pore water pressure ratios ($r_u$), this means that these layers of the thickened and paste tailings deposits (initially exposed to a drying and wetting phase) were resistant to liquefaction during this long shaking phase. Similarly, the paste tailings deposit (not initially exposed to a drying and wetting phase) did not liquefy during the cycling loadings based on the obtained of its excess pore water pressure ratios. However, the thickened tailings deposit (not initially exposed to a drying and wetting phase) liquefied during the cycling loadings based on the obtained of its excess pore water pressure ratios. This finding may have significantly practical implications with respect to the application of thickened and paste tailings disposal technology in seismic and humid regions.

As soon as the shaking was stopped, a sudden development in the excess pore water pressure ($\Delta u$) was noted throughout all the layers of the thickened and paste tailings deposits, as shown in Figures 5.6a and 5.8a, respectively. Typically, this sudden development caused the excess pore water pressure ratio ($r_u$) to be ranging approximately from 0.8–0.9 in the tested thickened and paste tailings deposits (initially subjected to a drying and wetting phase). Similarly, the excess pore water pressure ratio ($r_u$) was seen to be exceed somewhat or approaching unity in case of the tested thickened and paste tailings deposits that were not initially subjected to a drying and wetting phase. This indicates that the tested thickened and paste tailings deposits (initially exposed to a drying and wetting phase) were resistance to post-shaking liquefaction while the tested thickened and paste tailings deposits (not initially exposed to a drying and wetting phase) were susceptible to post-shaking liquefaction. This would mean that the contact between the particles of the tested thickened and paste tailings deposits (initially exposed to a drying and wetting phase) was not completely lost (i.e. effective stress did not reach zero) as in the tested thickened and paste tailings deposits (not initially exposed to a drying and wetting phase). It should be highlighted that the purpose of this post-shaking liquefaction assessment is not to determine that the tested thickened and paste tailings deposits (initially exposed to a drying and wetting phase or not) can or can not liquefy (a 30 min. long shaking duration was selected in this research), but rather to obtain valuable data and information for the development and validation of future constitutive models to describe and predict the seismic behaviour of thickened and paste tailings deposits. The magnitude of this sudden development excess pore water pressure ($\Delta u$) was found to be greater at greater depths of the tailings. Such variance in the magnitude of this sudden development excess pore water pressure ($\Delta u$) arose mainly due to a smaller vertical total stress at shallower depths. The occurrence of this sudden increase in excess pore water pressure ($\Delta u$) is associated with the end of shaking, which allowed the tailings particles that were partially in suspension to contract, thereby generating further pore water pressure at all the layers (Pépin et al., 2012a). An upward flow of pore water from the lower part of these tailings deposits to the upper layer and a downward flow of water (due to the presence of drainage layer at the bottom of the tailings deposit) from the lower part of the middle layer of these tailings deposits to the bottom layer could be an additional reason for such a sudden increase or development of excess pore water pressure in the top and bottom layers. This explanation regarding the upward and downward water flow is in agreement with the results of the volumetric water content's (VWC) evolution, which was observed to have increased in the middle of the top and bottom layers during the application of shaking and up to 40–60 min after the end of the shaking (for example, see Figures 5.10 and 5.11 that related to the tailings deposits that were initially subjected to a drying and wetting phase).

After the sudden increase in the excess pore water pressure at all the layers of the tailings deposits that were initially exposed to a drying and wetting phase or not, the pressure dissipated progressively until it returned to hydrostatic conditions ($r_u = 0$) (Figures 5.7 and 5.9). In general, the hydrostatic conditions were attained within 9–49 hours for all the layers of these deposits (initially exposed to a drying and wetting phase or not). Earlier investigations (e.g., Ueng et al., 2010) have observed that the excess pore water pressure of sandy soil dissipated quickly. This variance regarding the duration of dissipation between the tailings tested in this study and sandy soil may be related to the relatively low hydraulic conductivity (~$10^{-5}$ - $10^{-7}$ m/s) of this study's tailings (Robinsky et al., 1991; Bussière, 2007) compared to sandy soil (~$10^{-3}$ - $10^{-5}$ m/s). The bottom layer required the most time for its excess pore water pressure to dissipate entirely. This finding may be attributed to the inflow of pore water because the greatest increase of volumetric water content at the bottom layer was observed after the application of shaking ended (Figures 5.10 and 5.11). In addition, the dissipation of excess pore water pressure was observed to be quicker in the middle layer of the tailings deposits than in the top layer. The cause of this may be the upward movement of pore water from the middle layer to the top layer. This is supported by the greatest increase of the volumetric water content in the top layer than in the middle layer, as indicated in Figures 5.10 and 5.11, and by the findings of other investigations into the liquefaction of layered soils (Naesgaard and Byrne, 2007; Serafini and Perlea, 2010).

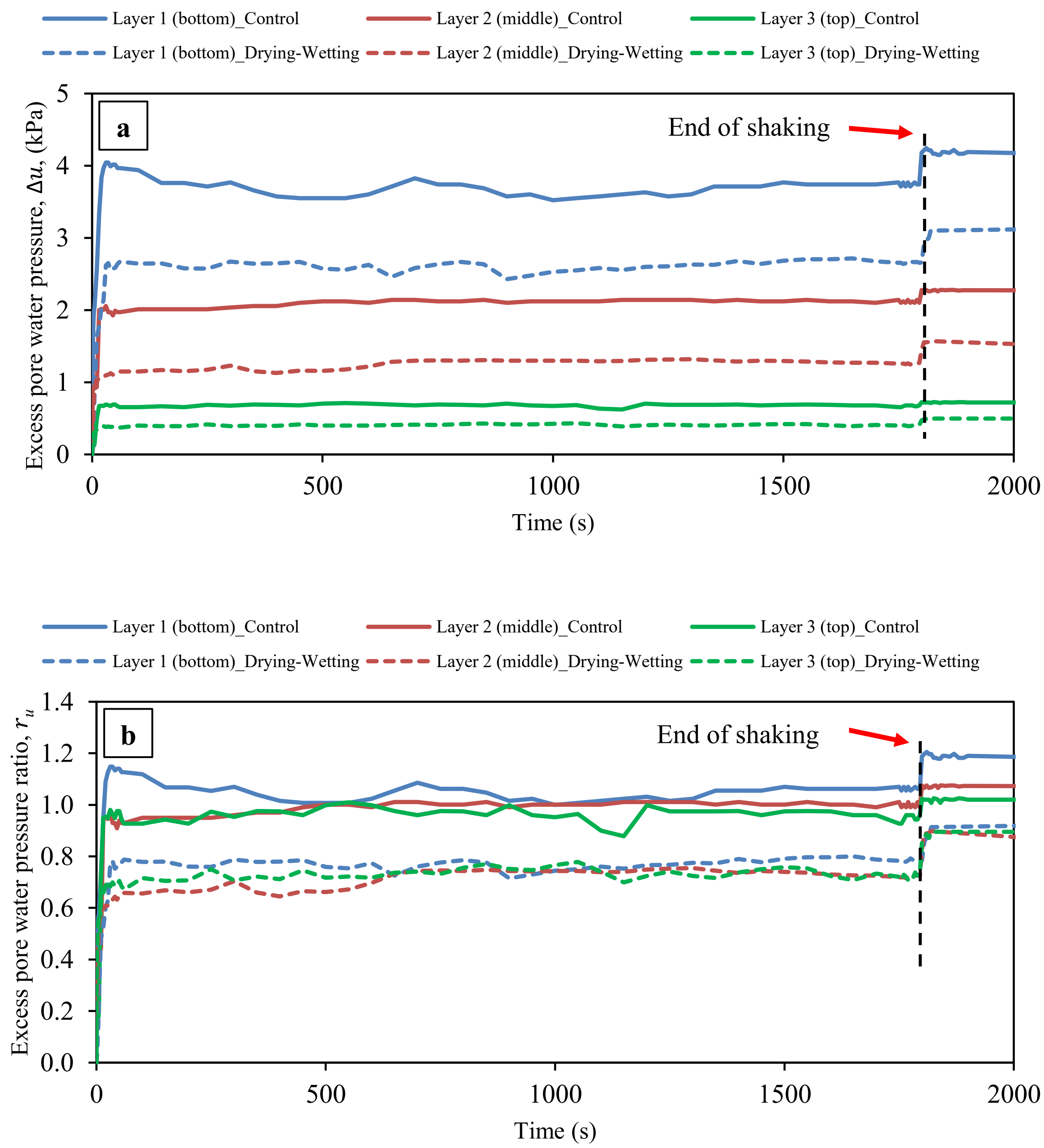


Figure 5.6. Time histories of excess pore water pressures at the middle depth of each layer of the thickened tailings deposit during shaking. a) Measured excess pore water pressures ($\Delta u$). b) Excess pore water pressure ratios ($r_u$)

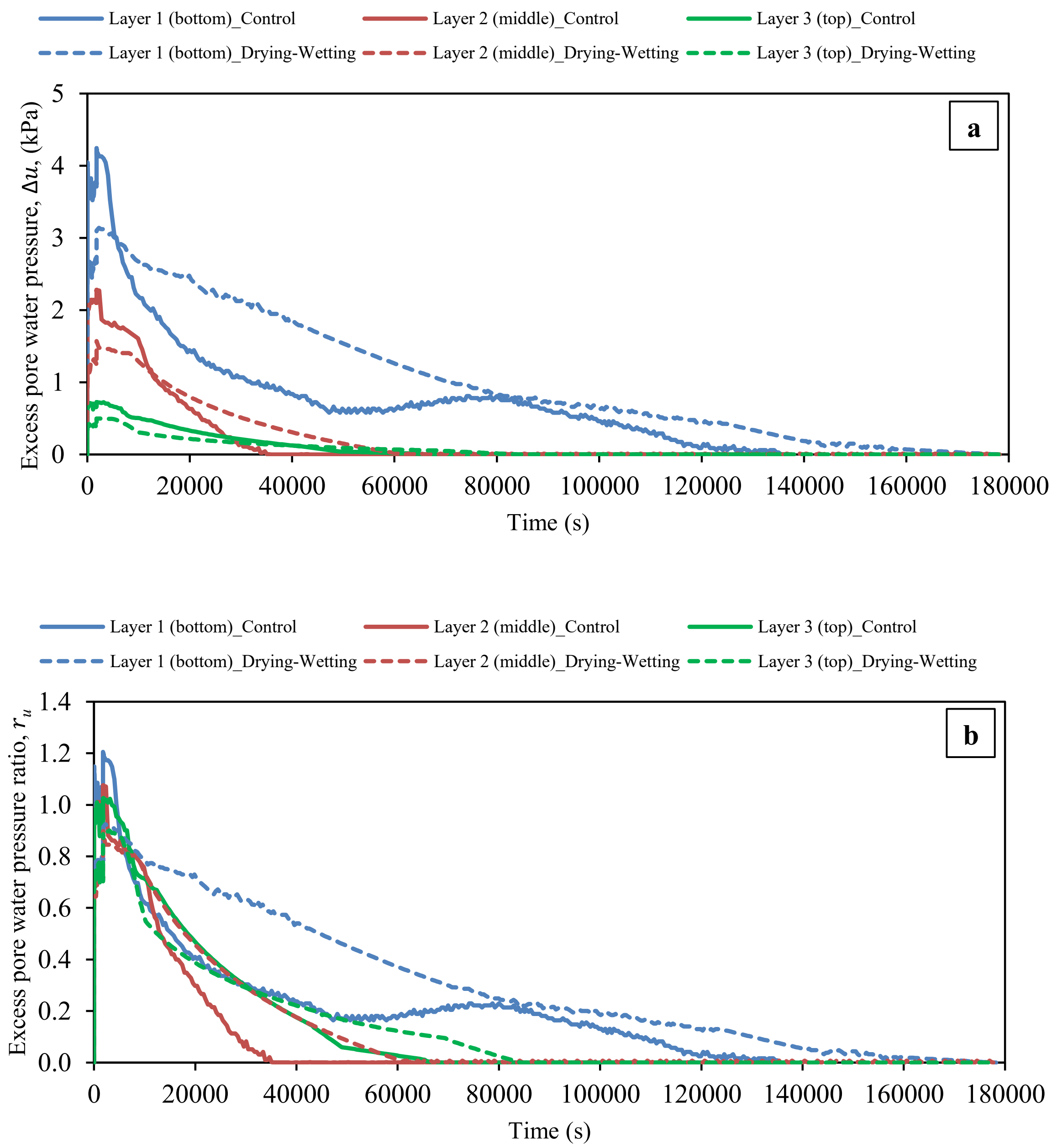


Figure 5.7. Time histories of excess pore water pressures at the middle depth of each layer of the thickened tailings deposit during and after shaking. a) Measured excess pore water pressures ($\Delta u$). b) Excess pore water pressure ratios ($r_u$)

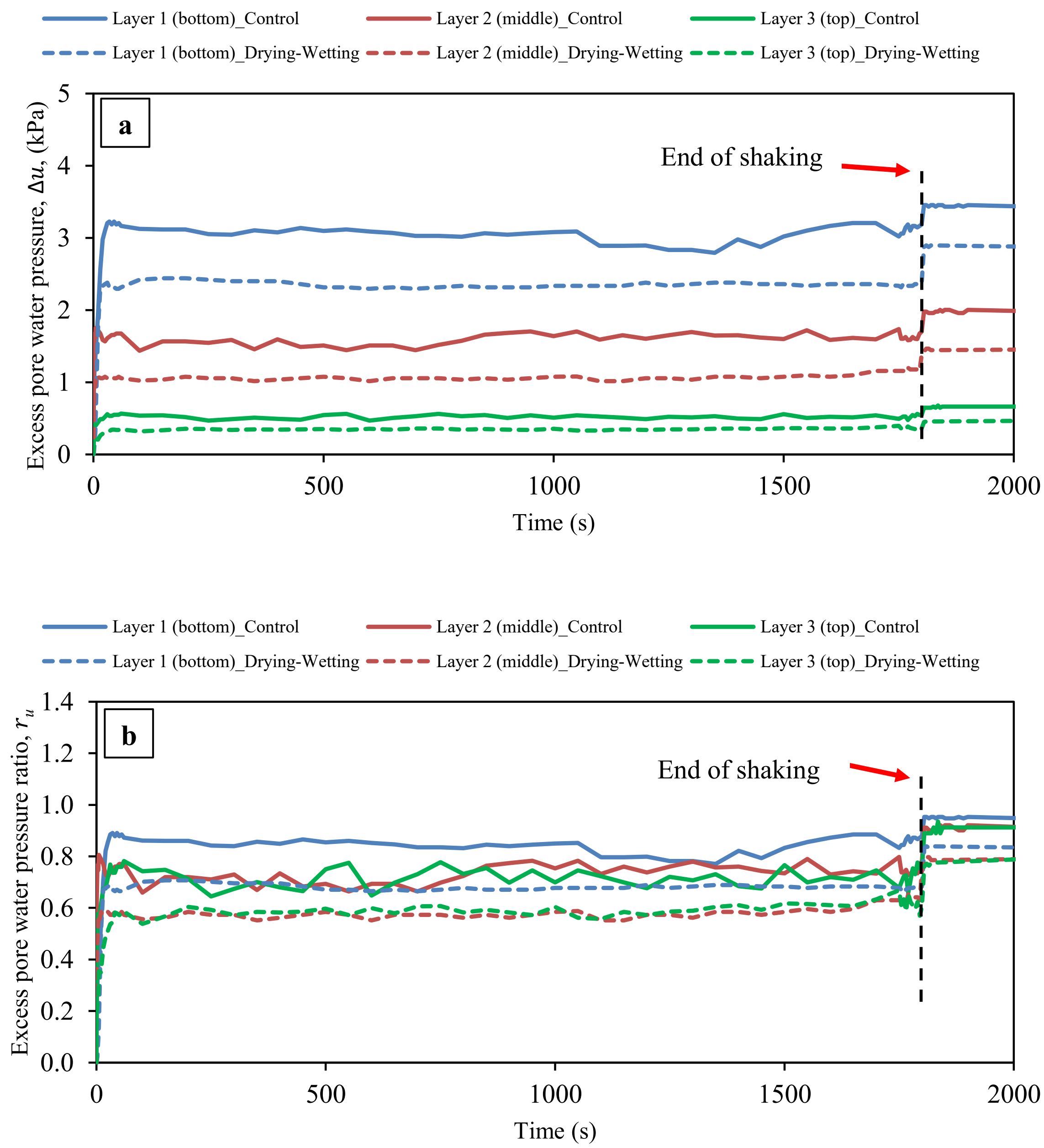


Figure 5.8. Time histories of excess pore water pressures at the middle depth of each layer of the paste tailings deposit during shaking. a) Measured excess pore water pressures ($\Delta u$). b) Excess pore water pressure ratios ($r_u$)

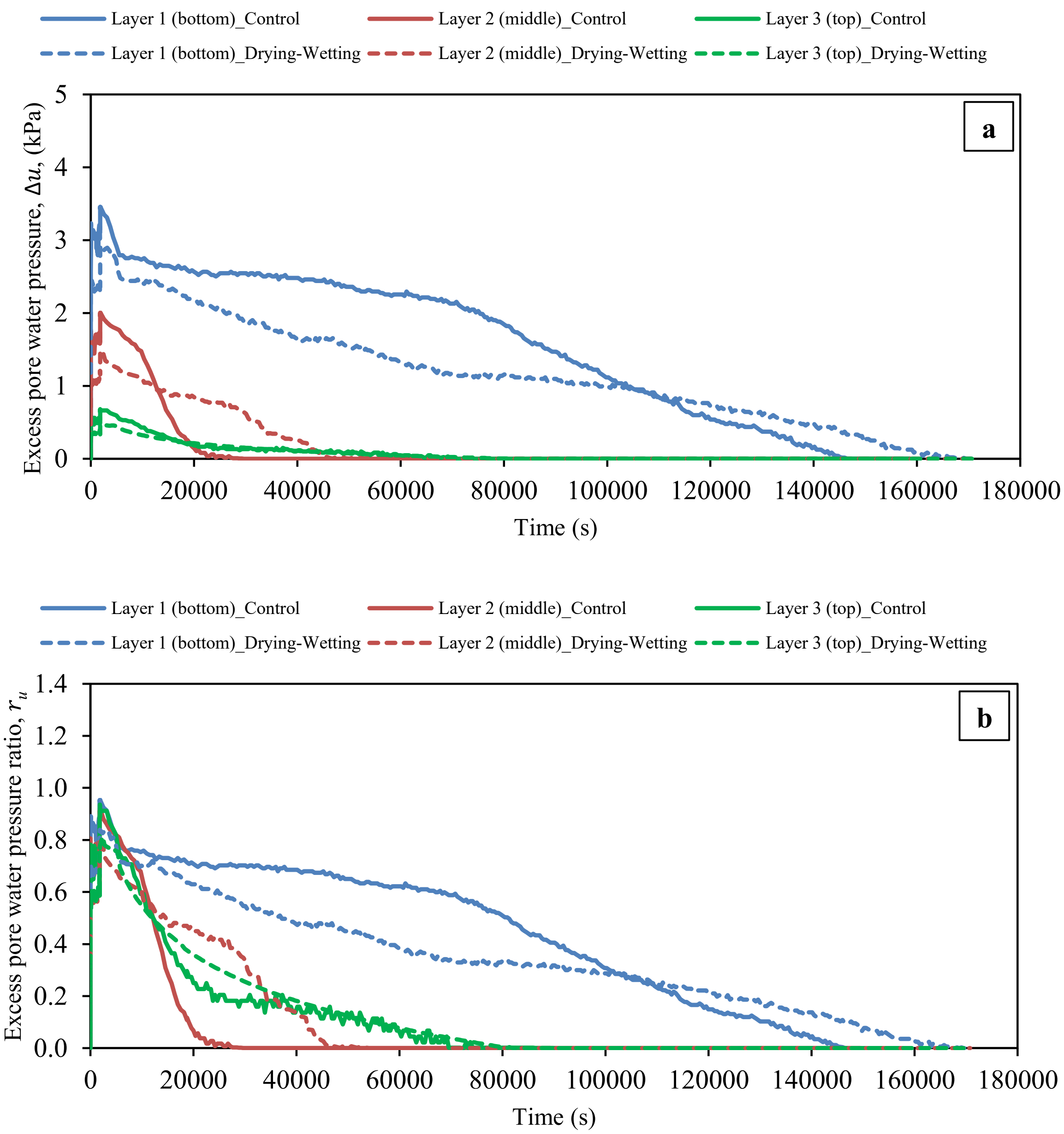


Figure 5.9. Time histories of excess pore water pressures at the middle depth of each layer of the paste tailings deposit during and after shaking. a) Measured excess pore water pressures ($\Delta u$). b) Excess pore water pressure ratios ($r_u$)

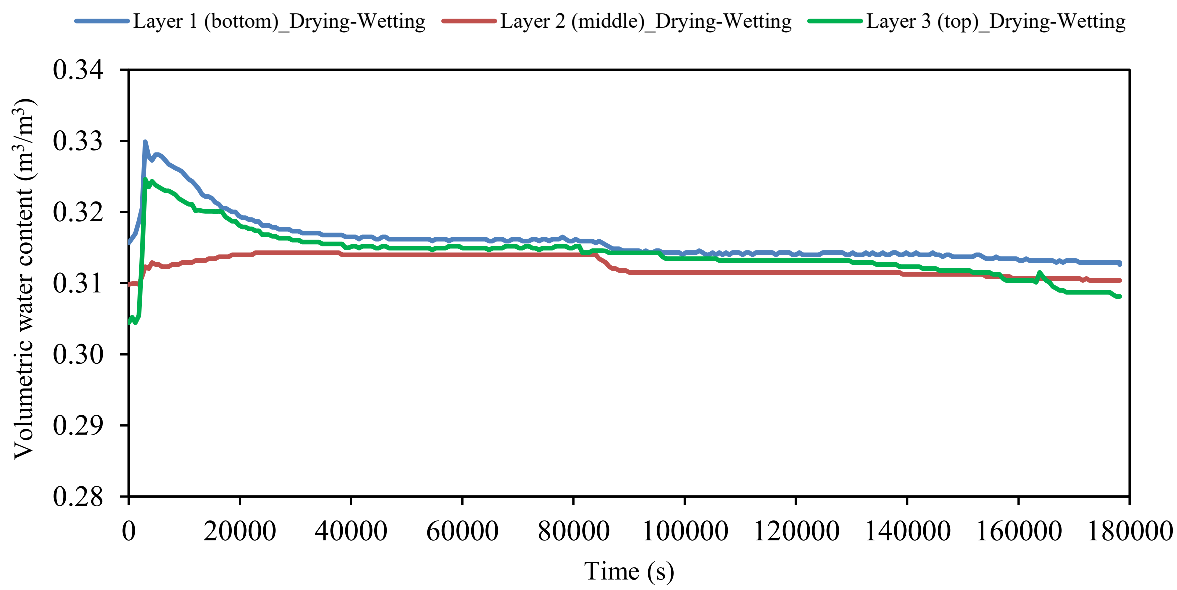


Figure 5.10. Time histories of volumetric water content at the middle depth of each layer of the thickened tailings deposit during and after shaking

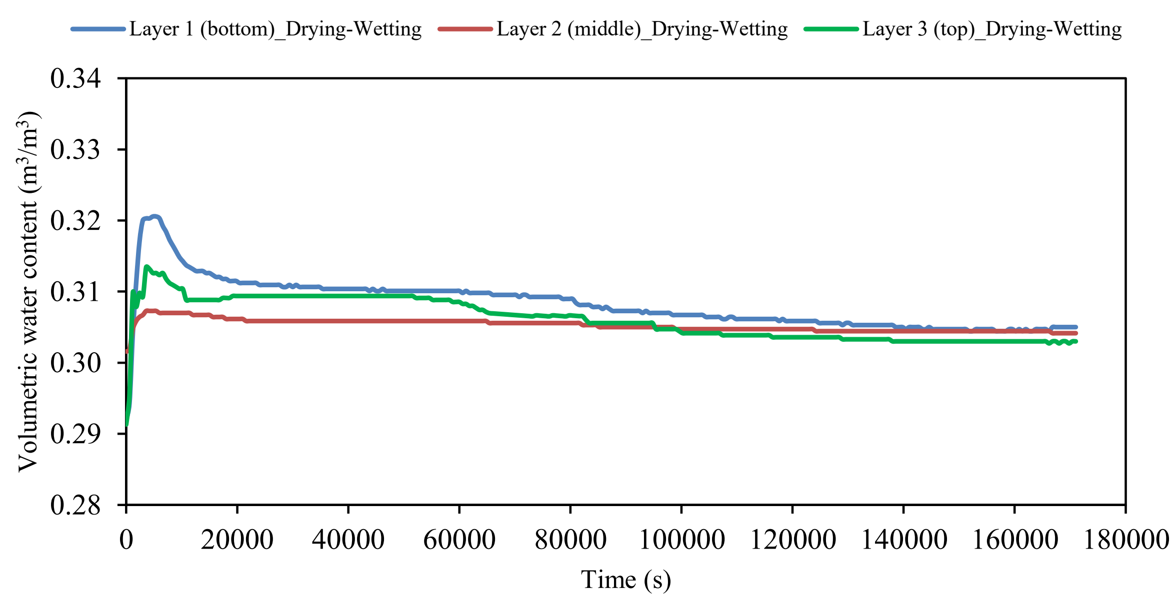


Figure 5.11. Time histories of volumetric water content at the middle depth of each layer of the paste tailings deposit during and after shaking

#### 5.2.3.2. **Vertical and horizontal displacement responses**

##### 5.2.3.2.1. **Vertical displacement response**

The measured time histories of the vertical displacement at the middle depth of each layer of the thickened and paste tailings deposits (initially exposed to a drying and wetting phase or not), during and after shaking, are shown in Figures 5.12 and 5.13, respectively. During shaking, the thickened and paste tailings deposits (initially exposed to a drying and wetting phase or not) were subjected to both contraction and dilative responses, as indicated in Figures 5.12a and 5.13a, respectively. When the shaking was applied, all the layers of the tailings deposits (initially exposed to a drying and wetting phase or not) experienced settlement for a short time (i.e., contraction response) as a result of the downward movement of the plastic plates installed at the middle of these layers. The settlements at all the layers of the thickened and paste tailings deposits (initially subjected to a drying and wetting phase) were observed to range from 0.29–1.05 mm and from 0.20–1.10 mm as indicated in Figures 5.12a and 5.13a, respectively. In addition, the settlements at all the layers of the thickened and paste tailings deposits (not initially subjected to a drying and wetting phase) were observed to range from 0.50–2.30 mm and from 0.05–1.40 mm as indicated in Figures 5.12a and 5.13a, respectively. These observations indicated that the tailings that were initially exposed to a drying and wetting phase experienced smaller settlement. This observation is in agreement with the findings of Liu et al. (2015), who concluded that drying/wetting cycles alter the structure or fabric of soil and the cyclic shear strength of soil increased after drying/wetting phase. The bottom layer of both the thickened and paste tailings deposits (initially exposed to a drying and wetting phase or not) experienced a lower contraction response or settlement than the top and middle layers. After this contraction response, the tailings deposits, which were initially exposed to a drying and wetting phase or not, started to display a dilation response as a result of the upward movement of the plastic plates at all the layers. A slight dilation response was initially observed at the bottom layer and then proceeded to the top layer and finally the middle layer. The lower contraction and dilative responses observed in the bottom layer could be due to the inflow of pore water from the upper part (the middle layer and the upper part of the bottom layer) of the thickened and paste tailings deposits (initially exposed to a drying and wetting phase or not). This observation from the current study is in agreement with that of other researchers regarding layered soils (Naesgaard and Byrne, 2007; Serafini and Perlea, 2010). Figures 5.12b and 5.13b show that there were no substantial changes in the displacements at the middle depth of each layer of the thickened and paste tailings deposits (initially exposed to a drying and wetting phase or not) after the shaking stopped. The displacements at the bottom and top layers of the tailings deposits (initially exposed to a drying and wetting phase) were observed to be almost similar to that at the bottom and top layers of the tailings deposits (not initially exposed to a drying and wetting phase). However, this observation was generally not seen at the middle layer.

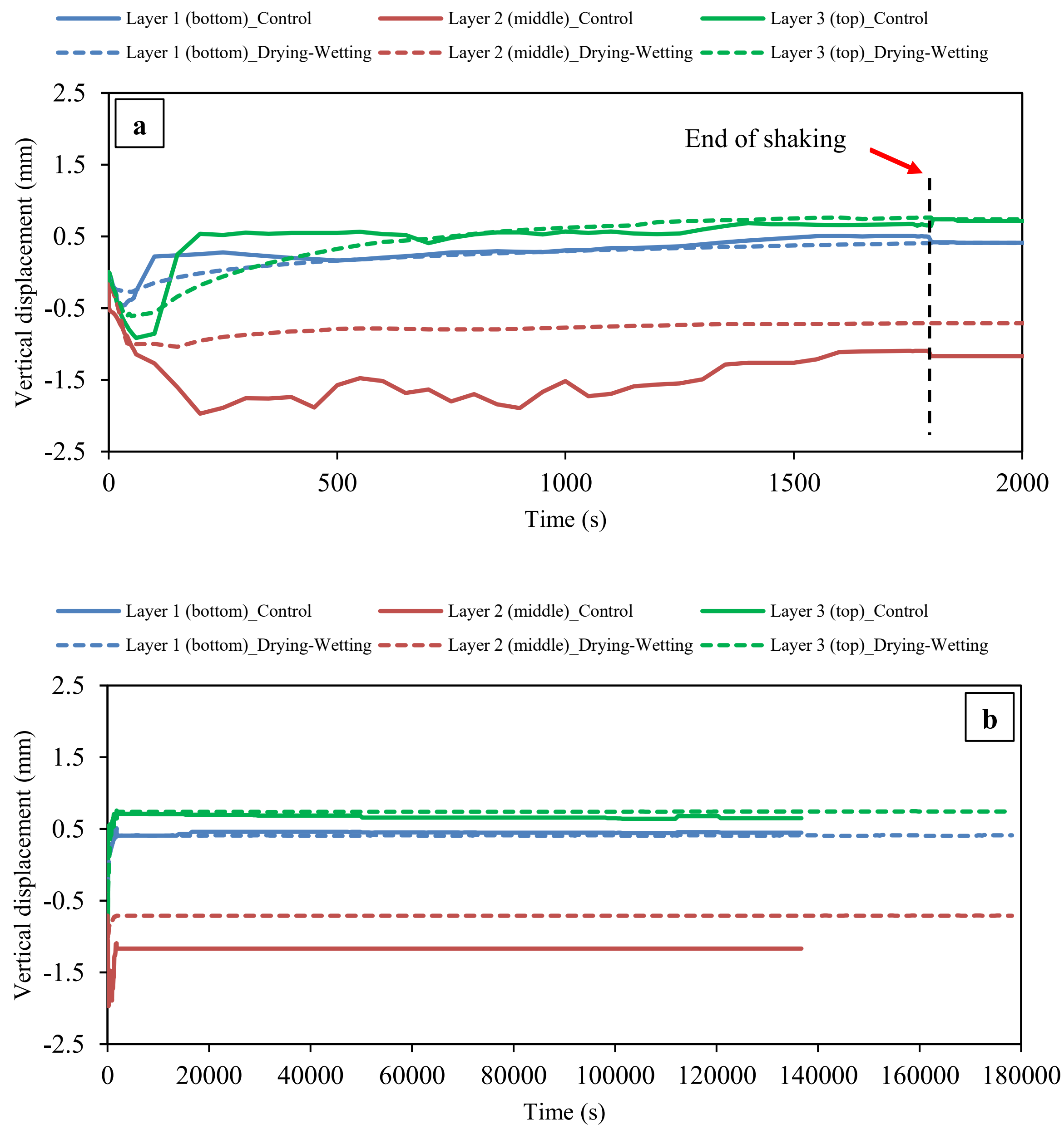


Figure 5.12. Time histories of the vertical displacement at the middle depth of each layer of the thickened tailings deposit. a) during shaking. b) during and after shaking

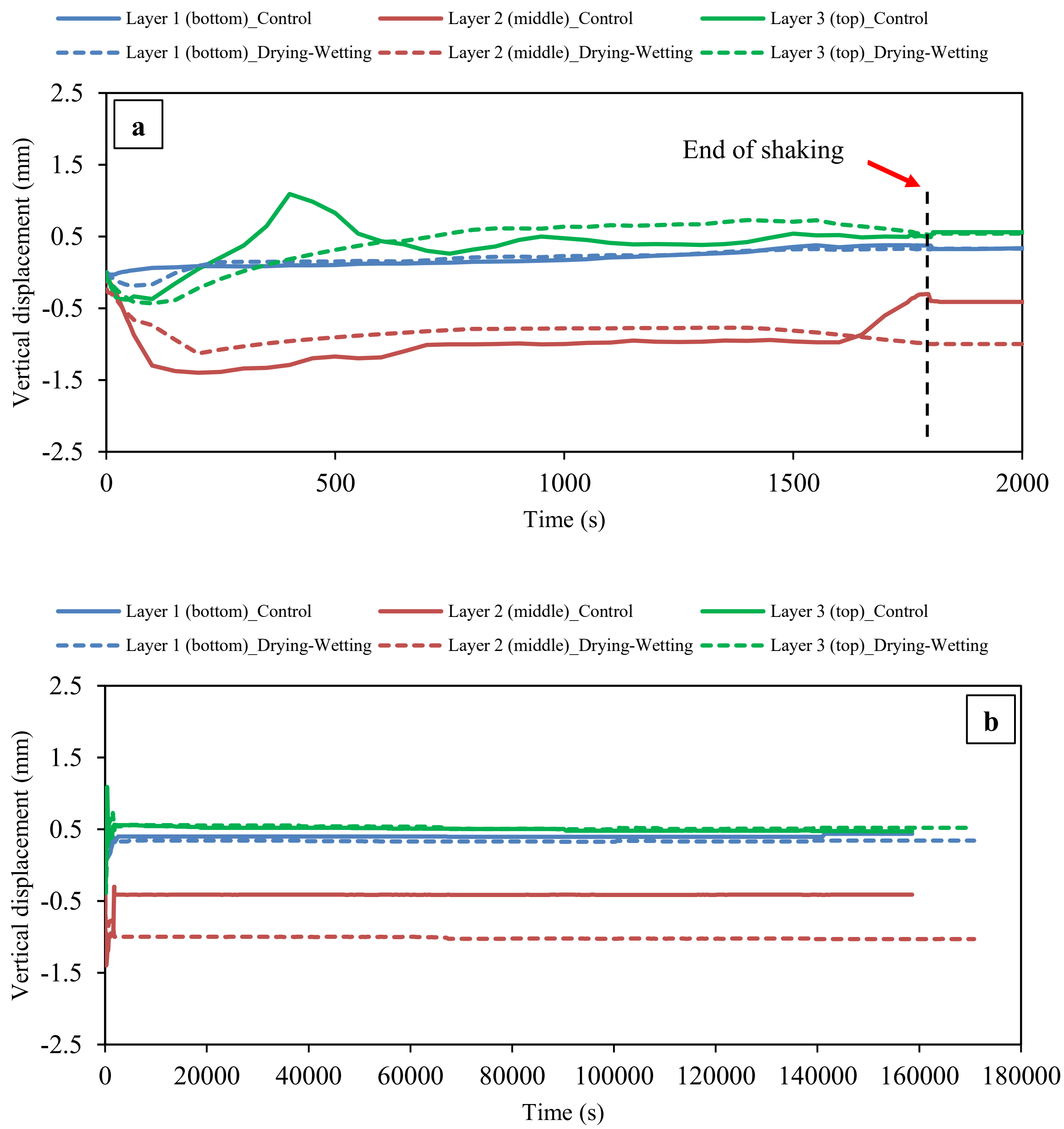


Figure 5.13. Time histories of the vertical displacement at the middle depth of each layer of the paste tailings deposit. a) during shaking. b) during and after shaking

5.2.3.2.2. **Horizontal displacement response**

The measured time histories of the horizontal displacement (during shaking) at the middle depth of each layer of the thickened and paste tailings deposits (initially exposed to a drying and wetting phase) are shown in Figures 5.14 and 5.15, respectively. These figures show that the horizontal displacements at the middle of each layer of these tailings deposits (initially exposed to a drying and wetting phase) were relatively steady and slightly similar to each other in general. The tailings deposits that were not initially exposed to a drying and wetting phase, which were not shown here, had similar horizontal displacement response to that tailings deposits that were initially exposed to a drying and wetting phase. Accordingly, this indicated that the lateral movement of both the thickened and paste tailings deposits (initially exposed to a drying and wetting phase or not) was relatively similar at all depths. Such a response agrees with the visual observation of the movement of the FLSB during shaking. Typically, the tailings deposits that were initially exposed to a drying and wetting phase were experienced slightly higher horizontal displacements than that the tailings deposits that were not initially exposed to a drying and wetting phase. This slight difference in the horizontal displacements can be due to the change into the structure or fabric of tailings as a result of a drying and wetting phase.

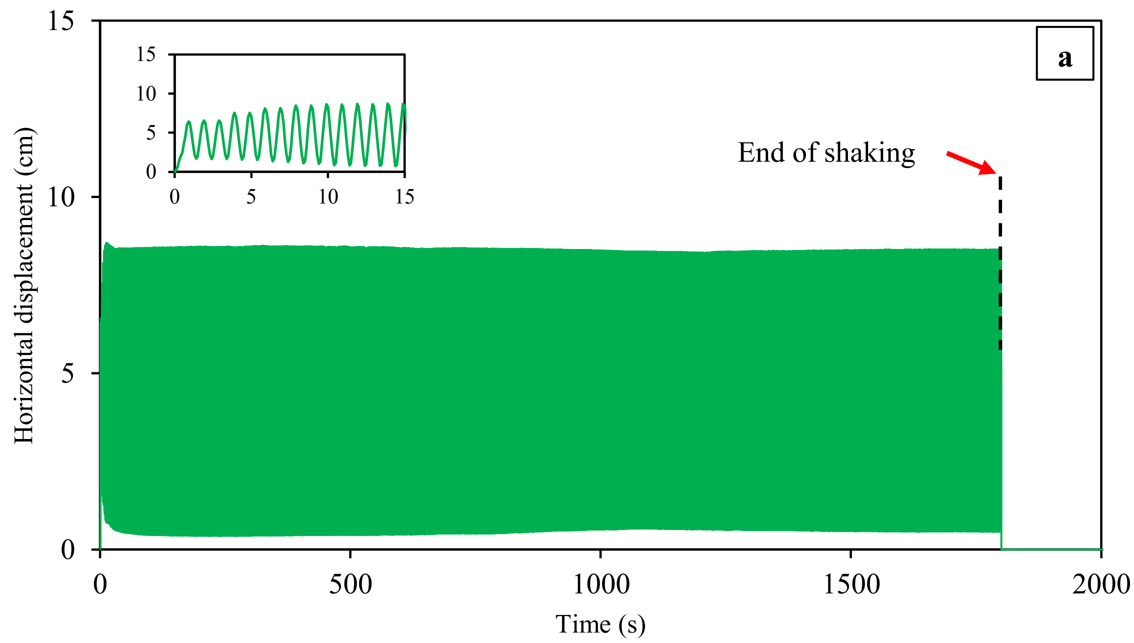

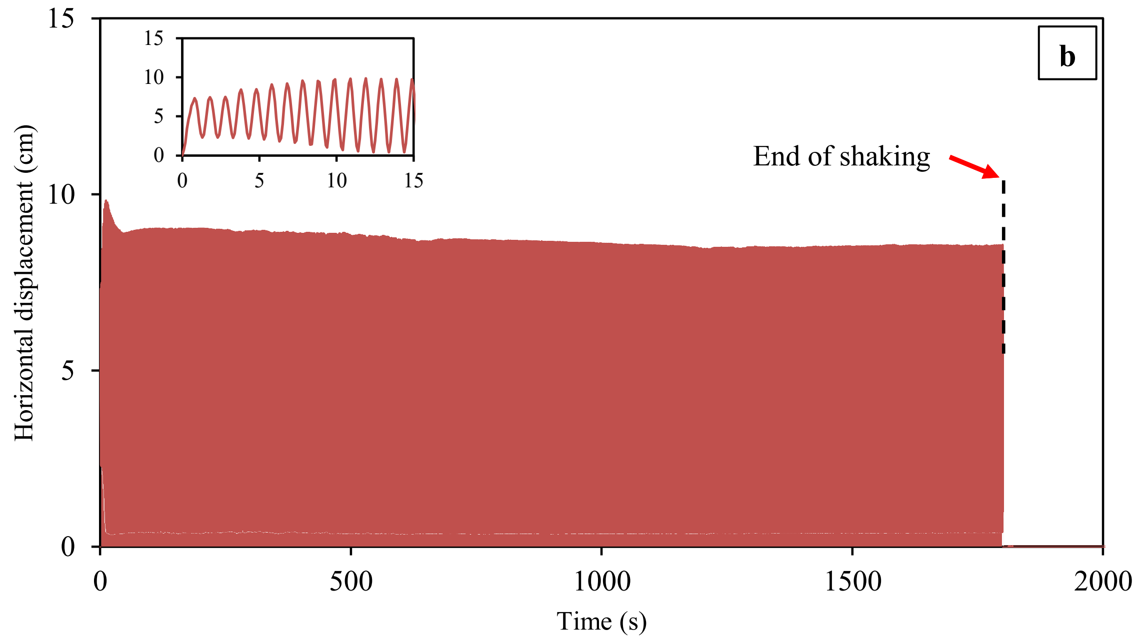


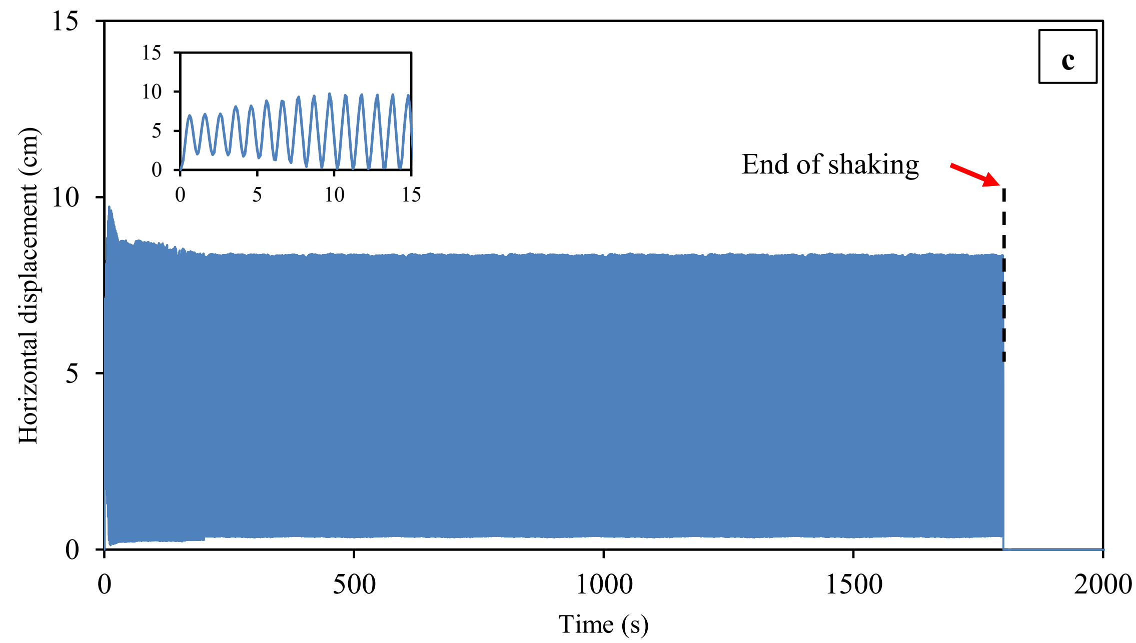


Figure 5.14. Time histories of measured horizontal displacements at the middle depth of each layer of the thickened tailings deposit (drying and wetting phase) during shaking: a) Layer 3 (top), b) Layer 2 (middle), c) Layer 1 (bottom)

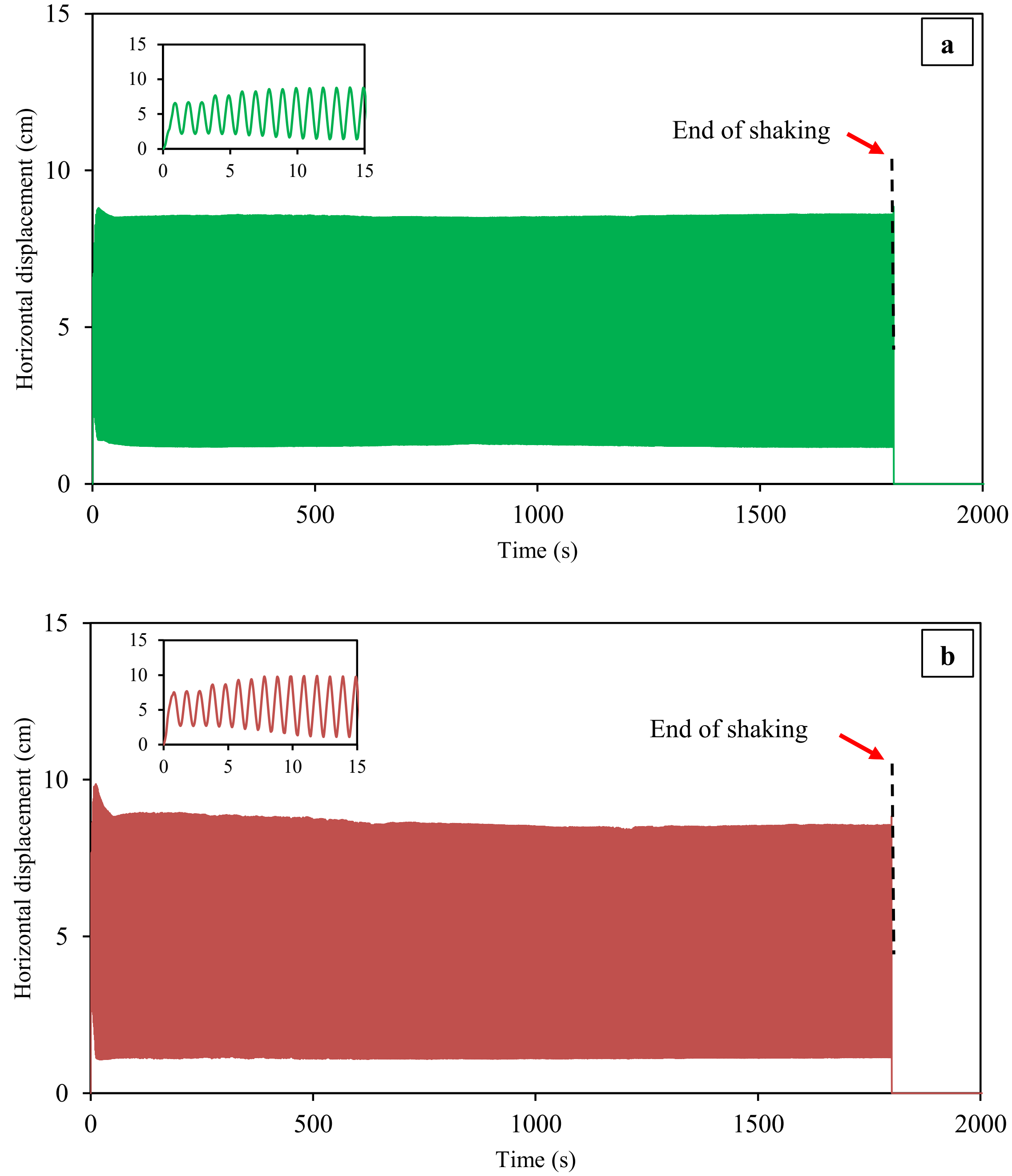
15
10
5
0
Horizontal displacement (cm)
0
500
1000
1500
2000
Time (s)
End of shaking
a
b

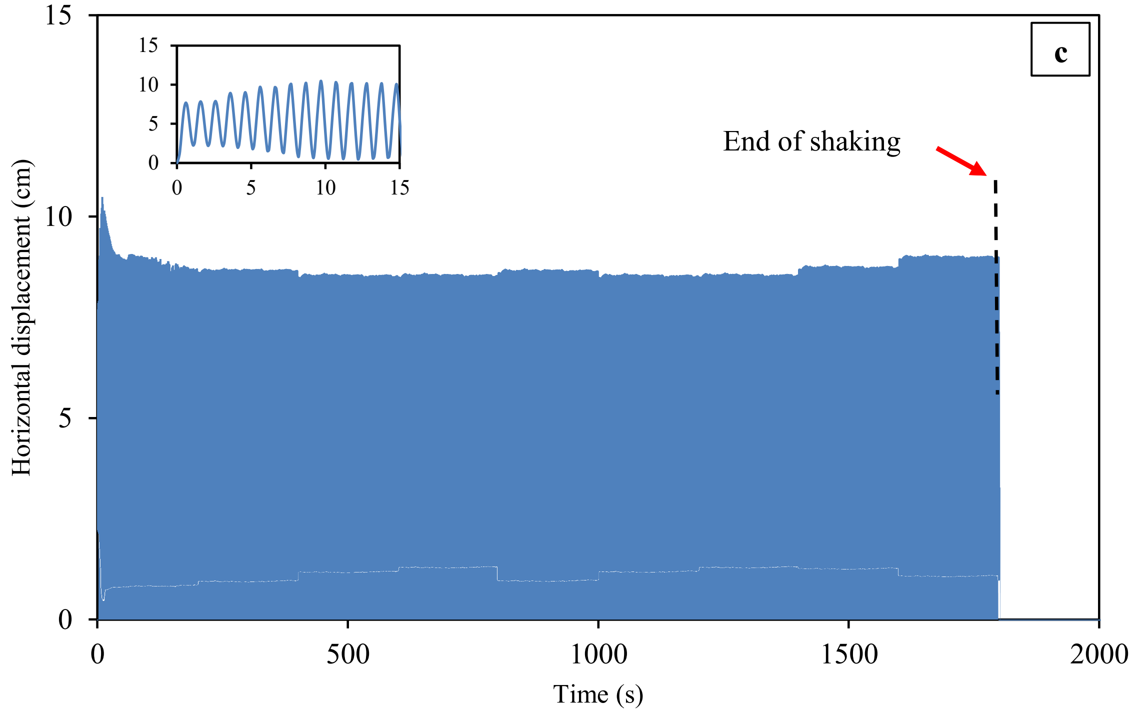


Figure 5.15. Time histories of measured horizontal displacements at the middle depth of each layer of the paste tailings deposit (drying and wetting phase) during shaking: a) Layer 3 (top), b) Layer 2 (middle), c) Layer 1 (bottom)

### 5.2.4. **Conclusions**

In this research paper, the effect of drying-heavy rainfall on the behaviour and cyclic loading-induced liquefaction potential of layered thickened and paste tailings deposits was investigated through a series of shaking table tests. The bottom of these tailings deposits was subjected to loading conditions that included a frequency of 1 Hz and a peak horizontal acceleration of 0.13g. The following conclusions were drawn based on such considered testing conditions.

It was observed that the shaking of the layered thickened and paste tailings deposits (initially exposed to a drying and wetting phase or not) led to water flow and pressure redistribution. Irrespective whether the tailings deposit was initially exposed to a drying and wetting phase or not, the bottom and top layers of these tested tailings were exposed to water inflow, but the middle layer of these tested tailings was impacted by the water outflow. The response of the layered thickened and paste tailings deposits (initially exposed to a drying and wetting phase or not) regarding excess pore water pressure, liquefaction and vertical displacement was largely impacted by this water outflow and inflow.

The excess pore water pressure at the middle depth of each layer of the layered thickened and paste tailings deposits (initially exposed to a drying and wetting phase or not) was found to be developed instantly until it reached a peak value during the shaking. However, the excess pore water pressure ratio was found to be lower than 0.8 in case of the layered thickened and paste tailings deposits (initially exposed to a drying and wetting phase) during the shaking. In other words, the layered paste and thickened tailings deposits did not liquefy during the cycling loadings despite the application of heavy rainfall. Likewise, the layered paste tailings deposit (not initially exposed to a drying and wetting phase) did not liquefy during the cycling loadings as its excess pore water pressure ratio was seen to be lower than 0.85. However, the layered thickened tailings deposit (not initially exposed to a drying and wetting phase) liquefied during the cycling loadings as its excess pore water pressure ratio was seen to be exceed 1.0. The contraction response of these tailings deposits (initially exposed to a drying and wetting phase or not) was responsible for the development of excess pore water pressure. Moreover, the pore water inflow into the bottom and top layers of these tailings deposits (initially exposed to a drying and wetting phase or not) was considered a factor that caused such an increase in the excess pore water pressure. A sudden development in the excess pore water pressure was noticed throughout all layers of these tailings deposits (initially exposed to a drying and wetting phase or not) as soon as the applied shaking stopped. This sudden development led the excess pore water pressure ratio to be ranging approximately from 0.8–0.9 in the layered thickened and paste tailings deposits that were initially exposed to a drying and wetting phase. Also, the excess pore water pressure ratio was seen to be exceed somewhat or approaching unity in the layered thickened and paste tailings deposits that were not initially subjected to a drying and wetting phase. This suggests that the layered thickened and paste tailings deposits (initially exposed to a drying and wetting phase) were resistance to post-shaking liquefaction while the layered thickened and paste tailings deposits (not initially exposed to a drying and wetting phase) were susceptible to post-shaking liquefaction. This sudden development in excess pore water pressure of these tailings deposits (initially exposed to a drying and wetting phase or not) arose for two reasons. First, the stop of the shaking caused the contraction of tailings particles that were partially in suspension, therefore generating further pore water pressure at all thin layers of these tailings deposits. Second, the upward flow of pore water to the top layer and the downward flow of pore water to the bottom layer generated further pore water pressure. The excess pore water pressure of the layered thickened and paste tailings deposits (initially exposed to a drying and wetting phase or not) required a long period of time in order for the water to dissipate entirely as a result of the low permeability associated with such materials.

During the shaking, the layered thickened and paste tailings deposits (initially exposed to a drying and wetting phase or not) initially experienced a contraction response or settlement for a short period of time, and the response altered then to a dilative response. Generally, the settlement of the layered thickened and paste tailings deposits (initially exposed to a drying and wetting phase) was found to be smaller than that settlement of the layered thickened and paste tailings deposits (initially exposed to a drying and wetting phase). Additionally, it was seen that the bottom layer of these tailings deposits (initially exposed to a drying and wetting phase or not) experienced lower contraction and dilative responses than the other two layers. This can be attributed to the pore water inflow from the upper part (middle layer, upper part of the bottom layer) of these tailings deposits. After the shaking stopped, there were no substantial changes regarding the displacements at the layered thickened and paste tailings deposits (initially exposed to a drying and wetting phase or not). Moreover, the displacements at the bottom and top layers of the tailings deposits (initially exposed to a drying and wetting phase) were found to be close to that at the bottom and top layers of the tailings deposits (not initially exposed to a drying and wetting phase). However, this finding was generally not observed at the middle layer. In general, the tailings deposits that were initially exposed to a drying and wetting phase had similar horizontal displacement response to that tailings deposits that were not initially exposed to a drying and wetting phase. The horizontal displacement at the middle of each layer of the thickened and paste tailings deposits (initially exposed to a drying and wetting phase or not) was generally noticed to be quite similar, as confirmed by visual observation.

This experimental study offers a better understanding of the behaviour and liquefaction potential of layered thickened and paste tailings deposits (under cyclic loading) under the effect of drying and heavy rainfall or not.

5.2.5. **References**


Adiansyah, J.S., Rosano, M., Vink, S., and Keir, G. (2015). A framework for a sustainable approach to mine tailings management: disposal strategies. Journal of cleaner production, 108: 1050-1062.

Ahmed, S.I., and Siddiqua, S. (2014). A review on consolidation behavior of tailings. International Journal of Geotechnical Engineering, 8(1): 102-111.

Alainachi, I., and Fall, M. (2019). Seismic induced liquefaction of cemented paste backfill: effect of mixing water. In Proceedings of the 7th International Conference on Earthquake Geotechnical Engineering (VII ICEGE), 17-20 June 2019, Roma, Italy, pp. 1042-1049.

Al-Tarhouni, M., Simms, P., and Sivathayalan, S. (2011). Cyclic behaviour of reconstituted and desiccated-rewet thickened gold tailings in simple shear. Canadian Geotechnical Journal, 48(7): 1044-1060.

Antonaki, N., Abdoun, T., and Sasanakul, I. (2019). Centrifuge tests on liquefaction potential and slope stability of mine tailings. International Journal of Physical Modelling in Geotechnics, 19(2): 104-114.

ASTM. (2017). D4318-17e1: Standard test methods for liquid limit, plastic limit, and plasticity index of soils. ASTM International, West Conshohocken, PA, USA.

Azam, S., and Li, Q. (2010). Tailings dam failures: a review of the last one hundred years. Geotechnical News, 28(4): 50-53.

Azapagic, A. (2004). Developing a framework for sustainable development indicators for the mining and minerals industry. Journal of Cleaner Production, 12(6): 639-662.

Barakati, A. (2015). Numerical modelling of liquid containing structure under dynamic loading. Master thesis, Department of Civil Engineering, University of Ottawa, Ottawa, Ontario, Canada.

Bussière, B. (2007). Colloquium 2004: hydrogeotechnical properties of hard rock tailings from metal mines and emerging geoenvironmental disposal approaches. Canadian Geotechnical Journal, 44(9): 1019-1052.

Casagrande, A. (1936). Characteristics of cohesionless soils affecting the stability of slopes and earth fills. Journal of the Boston Society of Civil Engineers, 23(1): 13-32.

Crowder, J.J. (2004). Deposition, consolidation, and strength of a non-plastic tailings paste for surface disposal. PhD thesis, Department of Civil Engineering, University of Toronto, Toronto, Ontario, Canada.

Crowder, J.J., Grabinsky, M.W.F., and Klein, K.A. (2002). Laboratory characterization of tailings paste for surface disposal. In Proceedings of the 55th Canadian geotechnical conference, 20-23 October 2002, Niagara Falls, Ontario, Canada, pp. 401-409.

Daliri, F. (2013). The influence of desiccation and stress history on monotonic and cyclic shear response of thickened gold tailings. PhD thesis, Department of Civil and Environmental Engineering, Carleton University, Ottawa, Ontario, Canada.

Edraki, M., Baumgartl, T., Manlapig, E., Bradshaw, D., Franks, D.M., and Moran, C.J. (2014). Designing mine tailings for better environmental, social and economic outcomes: a review of alternative approaches. Journal of Cleaner Production, 84: 411-420.

Engels, J. (2002). Beach Slope Prediction Methods. See http://www.tailings.info/technical/beach slope.htm [accessed December 20, 2017].

Fall, M., Célestin, J.C., and Han, F.S. (2013). Suitability of bentonite-paste tailings mixtures as engineering barrier material for mine waste containment facilities. Minerals Engineering, 22(9-10): 840-848.

Fall, M., Célestin, J.C., Pokharel, M., and Touré, M. (2010). A contribution to understanding the effects of temperature on the mechanical properties of cemented mine backfill. Engineering Geology, 114(3-4): 397-413.

Geremew, A.M., and Yanful, E.K. (2012). Laboratory investigation of the resistance of tailings and natural sediments to cyclic loading. Geotechnical Geological Engineering, 30(2): 431-447.

Geremew, A.M., and Yanful, E.K. (2013). Dynamic properties and influence of clay mineralogy types on the cyclic strength of mine tailings. International Journal of Geomechanics, ASCE, 13(4): 441-453.

Gibson, A.D. (1997). Physical scale modeling of geotechnical structures at one-g. PhD thesis, California Institute of Technology, Pasadena, California, USA.

Gomes, L.E.O, Correa L.B., Sá, F., Neto, R.R., and Bernardino, A.F. (2017). The impacts of the Samarco mine tailing spill on the Rio Doce estuary, Eastern Brazil. Marine Pollution Bulletin, 120(1-2): 28-36.

Government of Canada. (2018). Canadian climate normals 1981–2010 station data. Climate normal and averages. Environment and Natural Resources. See https://climate.weather.gc.ca/climate_normals/results_1981_2010_e.html?stnID=5720&autofwd=1 [Accessed March 21, 2018].

Hamade, T. (2013). Geotechnical design of tailings dams-a stochastic analysis approach. PhD thesis, Department of Mining and Materials Engineering, McGill University, Montreal, Quebec, Canada.

Hassani, F., Mantegh, A., Mohamed, A-M., and Ouellet, J. (2008). Evaluation of flow liquefaction in fine grained tailings using elastic wave velocities. International Journal of Geotechnical Engineering, 2(3): 169-178.

Hu, L., Wu, H., Zhang, L., Zhang, P., and Wen, Q. (2017). Geotechnical properties of mine tailings. Journal of Materials in Civil Engineering, ASCE, 29(2): 04016220.

Ishihara, K., Troncoso, J., Kawase, Y., and Takahashi, Y. (1980). Cyclic strength characteristics of tailings materials. Soils and Foundations, 20(4): 127-142.

Ishihara, K., Yasuda, S., and Yokota, K. (1981). Cyclic strength of undisturbed mine tailings. In Proceedings of the First International Conference on Recent Advances in Geotechnical Earthquake Engineering and Soil Dynamics, 26 April - 3 May 1981, St. Louis, Missouri, USA, Vol. 1, pp. 53-58.

James, M., Aubertin, M., Wijewickreme, D., and Wilson, G.W. (2011). A laboratory investigation of the dynamic properties of tailings. Canadian Geotechnical Journal, 48(11): 1587-1600.

James, M., Jolette, D., Aubertin, M., and Bussière, B. (2003). An experimental set-up to investigate tailings liquefaction and control measures. In Proceedings of the International Symposium on Major Challenges in Tailings Dams (ICOLD), 15 June 2003, Montréal, Quebec, Canada, pp. 153-164.

Jones, H., and Boger, D.V. (2012). Sustainability and waste management in the resource industries. Industrial and Engineering Chemistry Research, 51(30): 10057-10065.

Kim, H., Daliri, F., Simms, P., and Sivathayalan, S. (2011). The influence of desiccation and overconsolidation on monotonic and cyclic shear response of thickened gold tailings. In Proceedings of the 64th Canadian Geotechnical Conference (2011 Pan-Am CGS), 2-6 October 2011, Toronto, Ontario, Canada.

Kossoff, D., Dubbin, W.E., Alfredsson, M., Edwards, S.J., Macklin, M.G., and Hudson-Edwards, K.A. (2014). Mine tailings dams: characteristics, failure, environmental impacts, and remediation. Applied Geochemistry, 51: 229-245.

Li, A.L. (2011). Prediction of tailings beach slopes and tailings flow profiles. In Proceedings of the 14th International Seminar on Paste and Thickened Tailings, 5-7 April 2011, Australian Centre for Geomechanics, Perth, Australia, pp. 307-322.

Li, A.L., Been, K., Ritchie, R., and Welch, D. (2009). Stability of large, thickened, non-segregating thickened tailings deposits. In Proceedings of the 12th International Seminar on Paste and Thickened Tailings, 21-24 April 2009, Viňa del Mar, Chile, pp. 301-312.

Li, M., Bernier, L., and Boucher, J-F. (2002). Rheology of mineral pastes and its implications on underground pipeline delivery. In Proceedings of Symposium 2002 on Environment and Mines, Canadian Institute of Mining, Metallurgy, and Petroleum, 3-5 November 2002, Rouyn-Noranda, Quebec, Canada.

Liu, W., Tang, X., Yang, Q., and Li, W. (2015). Influence of drying/wetting cycles on the mechanical cyclic behaviours of silty clay. European Journal of Environmental and Civil Engineering, 19(7): 867-883.

Liu, Y.B., and De Smedt, F. (2004). WetSpa extension, a GIS-based hydrological model for flood prediction and watershed management, documentation and user manual. Department of Hydrology and Hydraulic Engineering, Vrije Universiteit Brussel, Belgium, pp. 1-126.

Lu, G., and Fall, M. (2018). Simulation of blast induced liquefaction susceptibility of subsurface fill mass. Geotechnical and Geological Engineering, 36(3): 1683-1706.

Miranda, L.S., and Marques, A.C. (2016). Hidden impacts of the Samarco mining waste dam collapse to Brazilian marine fauna–an example from the staurozoans (Cnidaria). Biota Neotropica, 16(2): 1-4.

Mohamed, F.M.O. (2014). Bearing capacity and settlement behaviour of footings subjects to static and seismic loading conditions in unsaturated sandy soils. PhD thesis, Department of Civil Engineering, University of Ottawa, Ottawa, Ontario, Canada.

Naesgaard, E., and Byrne, P.M. (2007). Flow liquefaction simulation using a combined effective stress–total stress model. In Proceedings of the 60th Canadian Geotechnical Conference, 21-24 October 2007, Ottawa, Ontario, Canada.

Orejarena, L., and Fall, M. (2008). Mechanical response of a mine composite material to extreme heat. Bulletin of Engineering Geology and the Environment, 67(3): 387-396.

Orejarena, L., and Fall, M. (2010). The use of artificial neural networks to predict the effect of sulphate attack on the strength of cemented paste backfill. Bulletin of Engineering Geology and the Environment, 69(4): 659-670.

Paul, A.C., and Azam, S. (2013). Assessment of slurry consolidation using index properties. International Journal of Geotechnical Engineering, 7(1): 55-61.

Pépin, N., Aubertin, M., and James, M. (2012a). Seismic table investigation of the effect of inclusions on the cyclic behaviour of tailings. Canadian Geotechnical Journal, 49(4): 416-426.

Pépin, N., Aubertin, M., James, M., and Leclerc, M. (2012b). Seismic simulator testing to investigate the cyclic behaviour of tailings in an instrumented rigid box. Geotechnical Testing Journal, 35(3): 469-479.

Pokharel, M., and Fall, M. (2013). Combined influence of sulphate and temperature on the saturated hydraulic conductivity of hardened cemented paste backfill. Cement and Concrete Composites, 38(4): 21-28.

Poulos, S.J., Robinsky, E.I., and Keller, T.O. (1985). Liquefaction resistance of thickened tailings. Journal of Geotechnical Engineering, 111(12): 1380-1394.

Prasad, S.K., Towhata, I., Chandradhara, G.P., and Nanjundaswamy, P. (2004). Shaking table tests in earthquake geotechnical engineering. Current Science, 87(10): 1398-404.

Raposo, N., Bahia, R., Afonso, E., and Topa Gomes, A. (2014). Optimization of thickened tailings deposition. In Proceedings of the 17th International Seminar on Paste and Thickened Tailings, 8-12 June 2014, Vancouver, British Columbia, Canada, pp. 1-14.

Robinsky, E., Barbour, S.L., Wilson, G.W., Bordin, D., and Fredlund, D.G. (1991). Thickened sloped tailings disposal-an evaluation of seepage and abatement of acid drainage. In Proceedings of the Second International Conference on the Abatement of Acidic Drainage, Invited Lecture, 16-18 September 1991, Montreal, Quebec, Canada, pp. 529-549.

Robinsky, E.I. (1982). Thickened tailing disposal in any topography. Essential Readings in Light Metals, Donaldson, D., and Raahauge, B.E., Eds., Springer, Cham, Switzerland, pp. 933-937.

Schoenberger, E. (2016). Environmentally sustainable mining: the case of tailings storage facilities. Resources Policy, 49: 119-128.

Seidalinova, A. (2014). Monotonic and cyclic shear loading response of fine-grained gold tailings. Master thesis, The University of British Columbia, Vancouver, British Columbia, Canada.

Serafini, D.C., and Perlea, V. (2010). Comparison of liquefaction triggering analysis approaches for an embankment dam and foundation. In Proceedings of the 5th International Conference on Recent Advances in Geotechnical Earthquake Engineering and Soil Dynamics, 24-29 May 2010, San Diego, California, USA, paper No. 4.12b.

Sofrá, F. (2017). Rheological properties of fresh cemented paste tailings. Paste Tailings Management, Yilmaz, E., and Fall, M., Eds., Springer, Cham, Switzerland, pp. 33-57.

Suazo, G., Fourie, A., Doherty, J., and Hasan, A. (2016). Effects of confining stress, density and initial static shear stress on the cyclic shear response of fine-grained unclassified tailings. Géotechnique, 66(5): 401-12.

Theriault, J., Frostiak, J., and Welch, D. (2003). Surface disposal of paste tailings at the Bulyanhulu gold mine, Tanzania. In Proceedings of Mining and the Environment Conference III, 25-28 May 2003, Sudbury, Ontario, Canada, pp. 1-8.

Tohumcu Özener, P., Özaydın, K., and Berilgen, M.M. (2009). Investigation of liquefaction and pore water pressure development in layered sands. Bulletin of Earthquake Engineering, 7(1): 199-219.

Turan, A., Hinchberger, S.D., and El Naggar, H. (2009). Design and commissioning of a laminar soil container for use on small shaking tables. Soil Dynamics and Earthquake Engineering, 29(2): 404-414.

Tuttle, M., Law, K.T., Seeber, L., and Jacob, K. (1990). Liquefaction and ground failure induced by the 1988 Saguenay, Quebec, earthquake. Canadian Geotechnical Journal, 27(5): 580-589.

Ueng, T.S., Wu, C.W., Cheng, H.W., and Chen, C.H. (2010). Settlements of saturated clean sand deposits in shaking table tests. Soil Dynamics and Earthquake Engineering, 30(1-2): 50-60.

Varghese, R.M., and Latha, G.M. (2013). Effect of overburden stress and surcharge pressure on the liquefaction response of sands. International Journal of Geotechnical Engineering, 7(4): 402-410.

Verburg, R.B.M. (2001). Use of paste technology for tailings disposal: potential environmental benefits and requirements for geochemical characterization. In Proceedings of the International Mine Water Association Symposium, 24-28 April 2001, Belo Horizonte, Brazil, pp. 1-13.

Verdugo, R., and González, J. (2015). Liquefaction-induced ground damages during the 2010 Chile earthquake. Soil Dynamics and Earthquake Engineering, 79: 280-295.

Verdugo, R., and Santos, E. (2009). Liquefaction resistance of thickened tailings of copper mines. In Proceedings of the 17th International Conference on Soil Mechanics and Geotechnical Engineering (ICSMGE), 5-9 October 2009, Alexandria, Egypt, pp. 295-298.

Verdugo, R., Sitar, N., Frost, J.D., Bray, J.D., Candia, G., Eldridge, T., Hashash, Y., Olson, S., and Urzua, A. (2012). Seismic performance of earth structures during the February 2010 Maule, Chile, earthquake: dams, levees, tailings dams, and retaining walls. Earthquake Spectra, 28(S1): S75-S96.

Wang, J., Salam, S., and Xiao, M. (2020). Evaluation of the effects of shaking history on liquefaction and cone penetration resistance using shake table tests. Soil Dynamics and Earthquake Engineering, 131:106025.

Wijewickreme, D., Sanin, M.V., and Greenaway, G.R. (2005). Cyclic shear response of fine-grained mine tailings. Canadian Geotechnical Journal, 42(5):1408-1421.

World Information Service on Energy (WISE). (2017). Chronology of major tailings dam failures. See https://www.wise-uranium.org/mdaf.html [accessed December 10, 2017].

Wu, D., Fall, M., and Cai, S. (2012). Coupled modeling of temperature distribution and evolution in cemented tailings backfill structures that contain mineral admixtures. Geotechnical and Geological Engineering, 30(4): 935-961.

Wu, J., Kammerer, A.M., Riemer, M.F., Seed, R.B., and Pestana, J.M. (2004). Laboratory study of liquefaction triggering criteria. In Proceedings of the 13th World Conference on Earthquake Engineering, 1-6 August 2004, Vancouver, British Columbia, Canada, paper No. 2580.

Zhang, Q., Yin, G., Wei, Z., Fan, X., Wang, W., and Nie, W. (2015). An experimental study of the mechanical features of layered structures in dam tailings from macroscopic and microscopic points of view. Engineering Geology, 195: 142-154.

# 6 Chapter 6: Synthesis of the Results and Discussion

## 6.1. Introduction

An experimental work has been conducted in this PhD research in order to understand and evaluate the behaviour and liquefaction susceptibility of the highly densified tailings (i.e. thickened tailings and paste tailings) under the dynamic (cyclic) loading condition. A flexible laminar shear box (FLSB) was used to contain the tailings materials which situated on a shaking table equipment that was used to simulate or apply the dynamic (cyclic) loading shaking. In this chapter, the key obtained laboratory test results, which were discussed in detail in Chapters 4 and 5, are synthesized and discussed. A comparison between the obtained laboratory test results of the behaviour and liquefaction response of the thickened tailings with those of the paste tailings is provided in this chapter (Section 6.3). In addition, a comparison between the obtained laboratory test results of the behaviour and liquefaction response of the thickened tailings (initially subjected to a drying and wetting phase) with those of the paste tailings (initially subjected to a drying and wetting phase) is provided in this chapter (Section 6.4). Finally, a comparison between the obtained laboratory test results of the behaviour and liquefaction response of the highly densified tailings (i.e. thickened and paste tailings) with those of the slurry tailings is provided in this chapter (Section 6.5).

## 6.2. Experimental testing conditions

The loading testing conditions or the shaking input parameters (peak horizontal acceleration, frequency and duration of shaking) that employed in this PhD research (as discussed in Chapters 4 and 5) are selected based on actual (field) and laboratory information.

Previous studies have revealed that mine tailings, in different parts of Québec province, might experience liquefaction phenomena due to earthquakes, with a peak horizontal acceleration as a low as 0.05g (Carter, 1988; James et al., 2003). Based on the acceleration of the Saguenay earthquake of 1988 in Québec, Canada, which had a magnitude of 5.9 (Tuttle et al., 1990), the peak horizontal acceleration of 0.13g is adopted in this current research. Previous researchers (e.g. Ishihara et al., 1981; James et al., 2003; Ueng et al., 2010; Pépin et al., 2012a, 2012b; Geremew and Yanful, 2013) have been used a frequency of 1 Hz in their liquefaction investigations, which thereby this frequency is adopted in this current research. The duration of shaking (1800 seconds) adopted in this PhD research is according to earlier liquefaction investigation of tailings (Pépin et al., 2012a). It should be highlighted that these aforementioned loading conditions have the characteristics of a one-dimensional signal, uniform amplitude, constant frequency and long duration, which accordingly do not represent generally the real scenarios of earthquake loading conditions. These loading conditions were not meant to represent the identical conditions that occur during a real earthquake. A good observation of the cyclic response of these highly densified tailings and relative comparisons of their response can be attained through these loading conditions.

## 6.3. Comparison of the behaviour and liquefaction response of the layered thickened tailings with those of the paste tailings

In this section, the main obtained laboratory test results from the technical papers 1 and 2 in Chapter 4 are synthesized and compared. Technical papers 1 and 2 are associated with the behaviour and liquefaction response of the thickened and paste tailings, respectively.

The comparison of the behaviour and liquefaction response of the thickened tailings with those of the paste tailings is mainly based on the pore pressure-based criteria (i.e. $r_u = \Delta u/\sigma'_{vo}$). This is because the pore pressure-based criteria are widely used in evaluating the liquefaction susceptibility of soils and tailings, specifically in shaking table tests (e.g. Pépin et al. 2012a; Varghese and Latha 2013; Lu and Fall, 2018; Wang et al., 2020). In general, liquefaction is defined as $r_u = 1$ (complete liquefaction). It should be emphasized that the tested thickened and paste tailings can experience liquefaction when their $r_u \geq 0.9$, which is considered in this research. The measured time histories of the excess pore water pressure ($\Delta u$) at the middle depth of each layer of the thickened tailings and the corresponding excess pore water pressure ratio ($r_u$) are illustrated in terms of during and after shaking in Figures 6.1 and 6.2, respectively. The results for the paste tailings are illustrated in Figures 6.1 and 6.2 as well. From Figure 6.1, it can be observed that when shaking began, the excess of pore water pressure at the middle depth of each layer of the thickened and paste tailings increased quickly until reaching a peak value; subsequently, it became almost stable until the end of the shaking duration. This instant increase in the excess pore water pressure at the start of shaking mainly results from the contraction response of the thickened and paste tailings. This relative stabilization of the excess of pore water pressure observed after the peak value can be due to a dilative response of the thickened and paste tailings to loadings at very low effective stress (Pépin et al., 2012a). Figure 6.1 indicates that the peak values of the excess pore water pressure in the thickened tailings during shaking varied approximately between 0.7 kPa and 4.0 kPa. In addition, this figure indicates that the peak values of the excess pore water pressure in the paste tailings during shaking varied approximately between 0.5 kPa and 3.2 kPa. This means that the thickened tailings experienced higher peak values of the excess pore water pressure compared to the paste tailings. As illustrated in Figure 6.1, the bottom layer of these tailings (thickened and paste tailings) reached the highest peak value of excess pore water pressure ($\Delta u$), followed by the middle layer and finally by the top layer. This means that as the depth increased, the peak value of the excess pore water pressure ($\Delta u$) in the thickened and paste tailings increased. This higher peak value of the excess pore water pressure ($\Delta u$) at the bottom layer of the thickened and paste tailings may be partially associated with the downward flow of pore water from the middle layer to the bottom layer (some water is drained through the sand drainage layer). This revealed that the pore water pressure in the bottom layer of the thickened and paste tailings is generated in part by pore pressures generated in the bottom layer and in part by the inflow of pore water from the upper layer. In addition, an upward flow of pore water from the lower part of these (thickened and paste) tailings to the upper (top) layer took place during shaking. The bottom layer of the thickened and paste tailings required the longest period of time to reach the peak value of the excess pore water pressure during shaking when compared with the top and middle layers. Moreover, the top layer of the thickened and paste tailings deposits required a longer time to reach the peak value of the excess pore water pressure during shaking in comparison with the middle layer. This delay occurs because water flow and pressure redistribution take time. Thus, there is often a delay between the time of shaking and the time of reaching the peak excess of pore water pressure or a liquefaction failure (Naesgaard and Byrne, 2007; Serafini and Perlea, 2010). During shaking, the excess pore water pressure ratio ($r_u$) was observed to be approximately larger than 0.95 at the thickened tailings, as illustrated in Figure 6.1.; however, during shaking, the excess pore water pressure ratio ($r_u$) was observed to be approximately lower than 0.85 at the paste tailings, as illustrated in Figure 6.1. These findings clearly indicate that the thickened tailings have a tendency to be subjected to cyclic-loading induced liquefaction, while the paste tailings do not have a tendency to be subjected to cyclic-loading induced liquefaction under the considered input loading testing conditions. This suggests that the paste tailings have more resistance to liquefaction than the thickened tailings during shaking. This means that there is still some contact between the particles of the paste tailings, while there is no contact between the particles of the thickened tailings. Therefore, unlike the thickened tailings, the paste tailings still have some effective stress that can lead to a higher resistance to liquefaction. Indeed, this difference between the thickened and paste tailings in terms of resistance to liquefaction can be attributed to the higher dewatering or to the solid content associated with the paste tailings (prior to the deposition in the flexible laminar shear box). These findings might have crucial practical implications in terms of using surface paste tailing disposal techniques rather than using surface thickened tailing disposal techniques in seismic areas or regions.

When the shaking ended, the excess pore water pressure of the thickened and paste tailings increased abruptly until reaching a maximum magnitude. This generally led the excess pore water pressure ratio of the thickened tailings to increase somewhat over unity. For the paste tailings, the excess pore water pressure ratio was generally close to unity due to this abrupt increase in pressure. Based on these observations, both the thickened and paste tailings can be susceptible to liquefaction in the post-cyclic loading phase under the considered input loading testing conditions. Based on the excess pore water pressure ratios during and after cyclic loading or shaking, the thickened tailings reached the liquefaction state faster compared to the paste tailings. Because the thickened tailing particles lose complete contact with each other, this earlier liquefaction state in the thickened tailings occurred during cyclic loading or shaking. The low dewatering or solid content prior to the deposition in the flexible laminar shear box in the thickened tailings could also contribute to this earlier liquefaction state during cyclic loading or shaking. It should be highlighted that the purpose of the assessment of this post-shaking liquefaction is not to reveal that the thickened and paste tailings can liquefy (a long duration of shaking of 1800 seconds was adopted in this research) but rather to attain valuable data and information regarding the development and validation of future constitutive models to describe and to predict the behaviour of the thickened and paste tailings under seismic loading conditions. The magnitude of such an abrupt increase was related to the depth where the top layer of the thickened and paste tailings was found to have a lower magnitude compared to the middle and bottom layers. The difference in this magnitude mainly occurred because there was a smaller vertical total stress at the shallower depth. The end of the shaking is responsible for the occurrence of this abrupt increase in pressure, which allowed the contraction of partially suspended tailing particles, therefore producing further pore water pressure at all depths (Pépin et al., 2012a). The process of the upward and downward flow of pore water at the thickened and paste tailings could be considered an additional cause that may lead to such an abrupt increase of excess pore water pressure in the top layer (Layer 3) and bottom layer (Layer 1). The pore water flows upward from the lower part of the thickened and paste tailings to the upper (top) layer, while it flows downward from the lower part of the middle layer of the thickened and paste tailings to the bottom layer (Layer 1). This downward flow of water to the bottom layer might have been enabled by the sand drainage layer below the thickened and paste tailings, which was facilitated by desiccation-induced microcracks that appeared on the surface of the first layer (bottom layer) after three days of drying, i.e., prior to the deposition of the second layer (middle layer). It has been reported that cracks increase the permeability of the tailings or soil layers (Roshani et al., 2017).

Following the abrupt increase in the excess pore water pressure in the thickened and paste tailings, the pressure began to dissipate gradually until the hydrostatic conditions were returned ($r_u = 0$), as illustrated in Figure 6.2. The thickened tailings needed approximately up to 36 hours to return to the hydrostatic conditions, while the paste tailings needed approximately up to 40 hours to return to the hydrostatic conditions. Typically, this means that the thickened tailings required a slightly lower duration to return to the hydrostatic conditions (i.e. complete dissipation of excess pore water pressure) compared to the paste tailings. This may be because the thickened tailings had a slightly higher permeability compared to the layered thickened tailings deposit. The long durations to return to the hydrostatic conditions (i.e. complete dissipation of excess pore water pressure) could be due to the relatively low permeability (~$10^{-5}$ - $10^{-7}$ m/s) of uncracked thickened and paste tailings (Robinsky et al., 1991; Bussière, 2007). Regarding the duration of dissipation at the thickened and paste tailings, the bottom layer required the longest time to completely dissipate its excess pore water pressure. This is because the bottom layer experienced more inflow of pore water after shaking ended. The dissipation of excess pore water pressure at the thickened and paste tailings was observed to be quicker at the middle layer than at the top layer. The reason for this may be associated with the upward movement of pore water from the middle layer to the top layer. This is considered in line with the findings of other investigations on liquefaction or dynamic behaviours of layered soils (Naesgaard and Byrne, 2007; Serafini and Perlea, 2010).

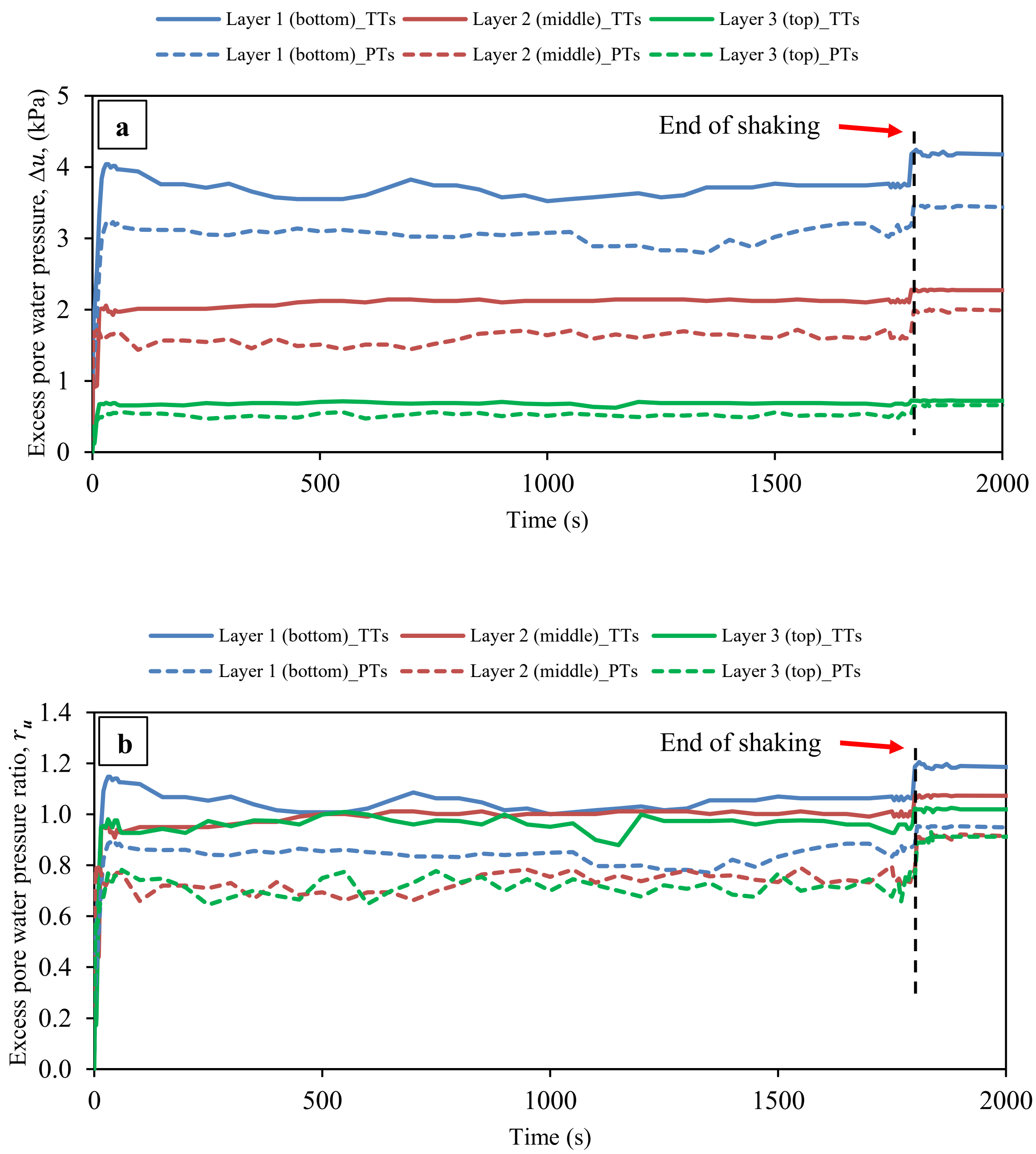


Figure 6.1. Time histories of excess pore water pressures at the middle depth of each layer of the thickened (TTs) and paste (PTs) tailings deposits during shaking. a) Measured excess pore water pressures ($\Delta u$). b) Excess pore water pressure ratios ($r_u$)

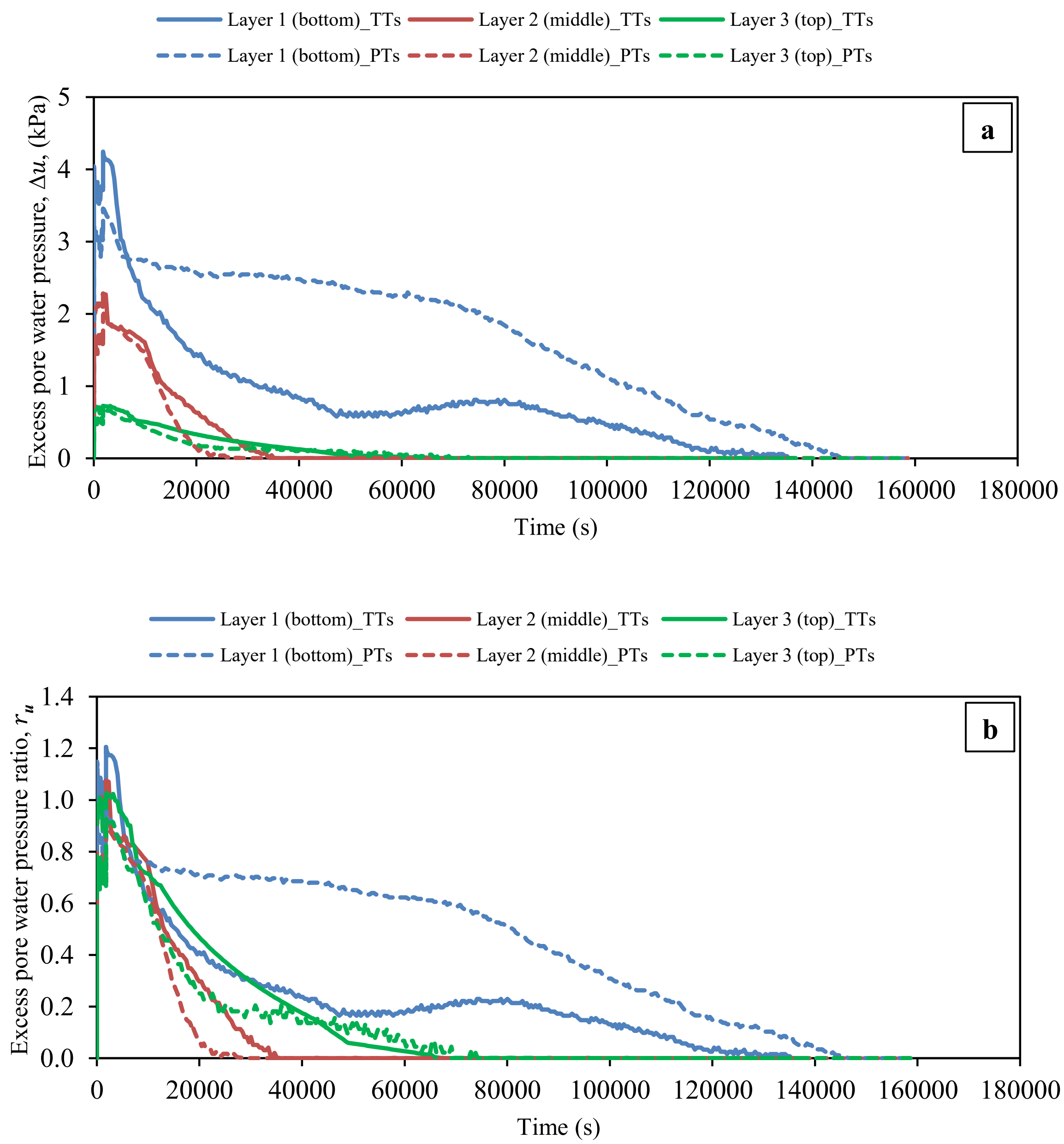


Figure 6.2. Time histories of excess pore water pressures at the middle depth of each layer of the thickened (TTs) and paste (PTs) tailings deposits during and after shaking. a) Measured excess pore water pressures ($\Delta u$). b) Excess pore water pressure ratios ($r_u$)

## 6.4. **Drying-Wetting effects on the behaviour of highly densified tailings subjected to cycling loadings**

In this section, the main obtained laboratory test results from the technical paper 3 in Chapter 5 are synthesized and compared. Technical paper 3 is mainly associated with the behaviour and liquefaction response of the highly densified (thickened and paste) tailings that were initially subjected to a drying and wetting phase.

It should be underlined that the tested thickened and paste tailings (initially subjected to a drying and wetting phase) can be susceptible to liquefaction when their $r_u \geq 0.9$, which is considered in this research. Figures 6.3 and 6.4 show the measured time histories of the excess pore water pressure ($\Delta u$) at the middle depth of each layer of the thickened tailings that were initially subjected to a drying and wetting phase and the corresponding excess pore water pressure ratio ($r_u$) during and after shaking, respectively. The results for the paste tailings that were initially subjected to a drying and wetting phase are shown in Figures 6.3 and 6.4 as well.

As shown in Figure 6.3, the peak values of the excess pore water pressure in the thickened tailings during shaking varied almost between 0.4 kPa and 2.7 kPa. Moreover, this figure shows that the peak values of the excess pore water pressure in the paste tailings during shaking varied almost between 0.3 kPa and 2.4 kPa. Typically, this indicates that both the thickened and paste tailings (initially subjected to a drying and wetting phase) has almost similar peak values of the excess pore water pressure. During shaking, the excess pore water pressure ratios ($r_u$) at the middle depth of each layer of the thickened and paste tailings (initially subjected to a drying and wetting phase) were seen to range from 0.7–0.8 and from 0.6–0.7 (see Figure 6.3), respectively. These findings indicate that both the thickened and paste tailings (initially subjected to a drying and wetting phase) do not tend to be susceptible to liquefaction during cyclic loading under the considered testing conditions. In addition, these findings suggest that the paste tailings are more resistance to liquefaction than the thickened tailings during shaking. This implies that the contact between the particles of the paste tailings is higher than that of the thickened tailings. In other words, the paste tailings have higher effective stress or shear strength compared to the thickened tailings. The difference between the thickened and paste tailings in terms of resistance to liquefaction can be due to the higher dewatering or to the solid content related to the paste tailings (before the deposition in the flexible laminar shear box and starting the drying and wetting phase). As discussed earlier in Section 6.3, during the cycling loadings, the thickened tailings (not initially exposed to a drying and wetting phase) liquefied whereas the paste tailings (not initially exposed to a drying and wetting phase) did not experience liquefaction based on the obtained of its excess pore water pressure ratios. These findings may have significantly practical implications regarding to the application of thickened and paste tailings disposal technology in seismic and humid areas.

Once the shaking terminated, the excess pore water pressure of the thickened and paste tailings increased suddenly until reaching a maximum magnitude. This sudden increase caused the excess pore water pressure ratio to be ranging almost from 0.8–0.9 in the thickened and paste tailings that were initially subjected to a drying and wetting phase. Accordingly, this reveals that the thickened and paste tailings (initially subjected to a drying and wetting phase) were resistance to post-shaking liquefaction whereas the thickened and paste tailings (not initially subjected to a drying and wetting phase) were susceptible to post-shaking liquefaction as discussed earlier in Section 6.3. This suggests that the contact between the solid particles of the thickened and paste tailings (initially subjected to a drying and wetting phase) was not entirely lost (i.e. effective stress did not reach zero) as in the thickened and paste tailings (not initially subjected to a drying and wetting phase).

The excess pore water pressure in the thickened and paste tailings (initially subjected to a drying and wetting phase) required a long duration to return to the hydrostatic conditions ($r_u = 0$), as shown in Figure 6.4. Similar to the thickened and paste tailings (not initially subjected to a drying and wetting phase), the thickened and paste tailings (initially subjected to a drying and wetting phase) required almost similar duration (i.e. up to 49 hours) to return to the hydrostatic conditions. This long duration of the excess pore water pressure dissipation may be attributed to the relatively low hydraulic conductivity (~$10^{-5}$ - $10^{-7}$ m/s) of this study's tailings (Robinsky et al., 1991; Bussière, 2007) as discussed in Chapter 5 (Section 5.2.3.1).

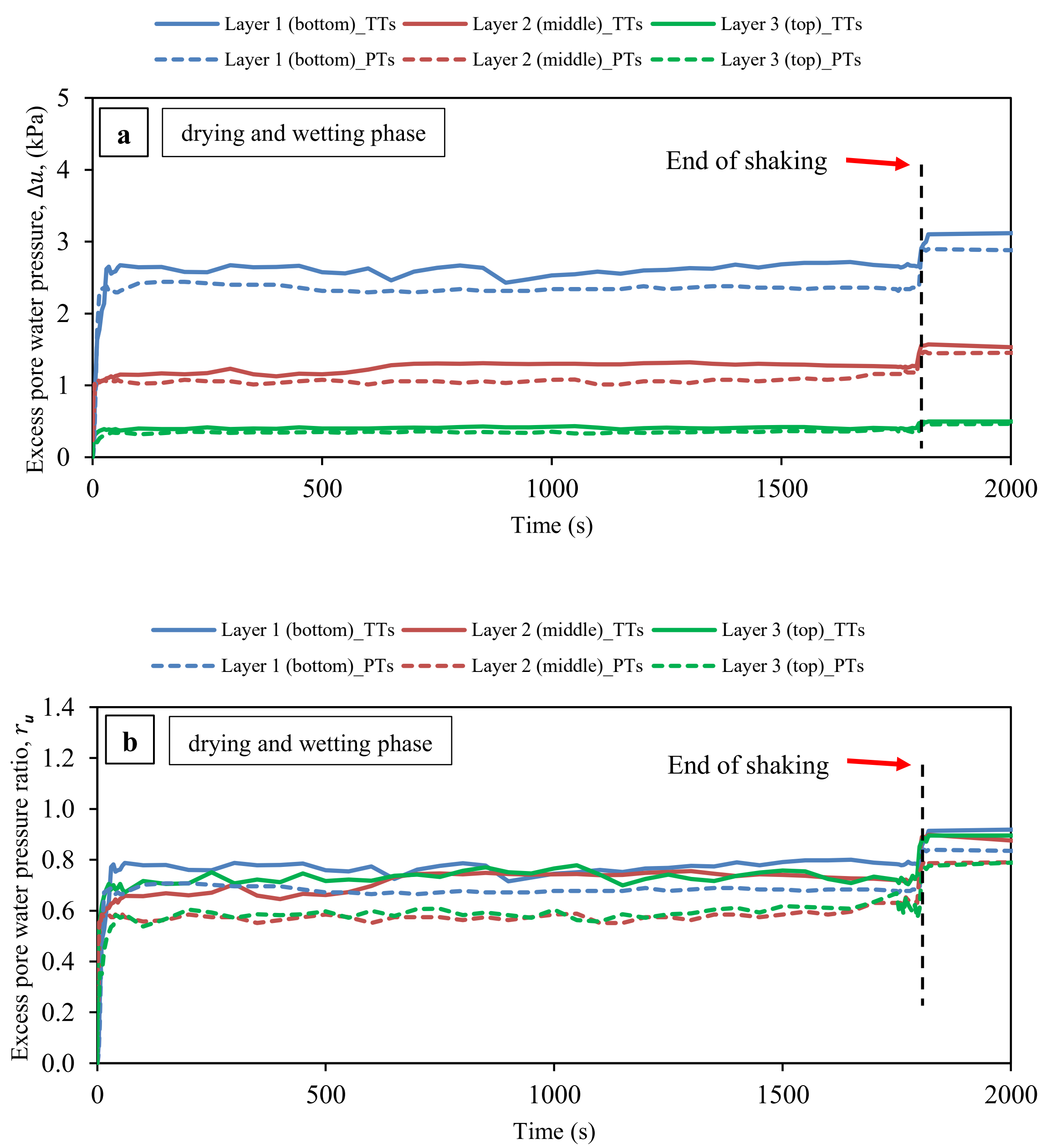


Figure 6.3. Time histories of excess pore water pressures at the middle depth of each layer of the thickened (TTs) and paste (PTs) tailings deposits during shaking. a) Measured excess pore water pressures ($\Delta u$). b) Excess pore water pressure ratios ($r_u$)

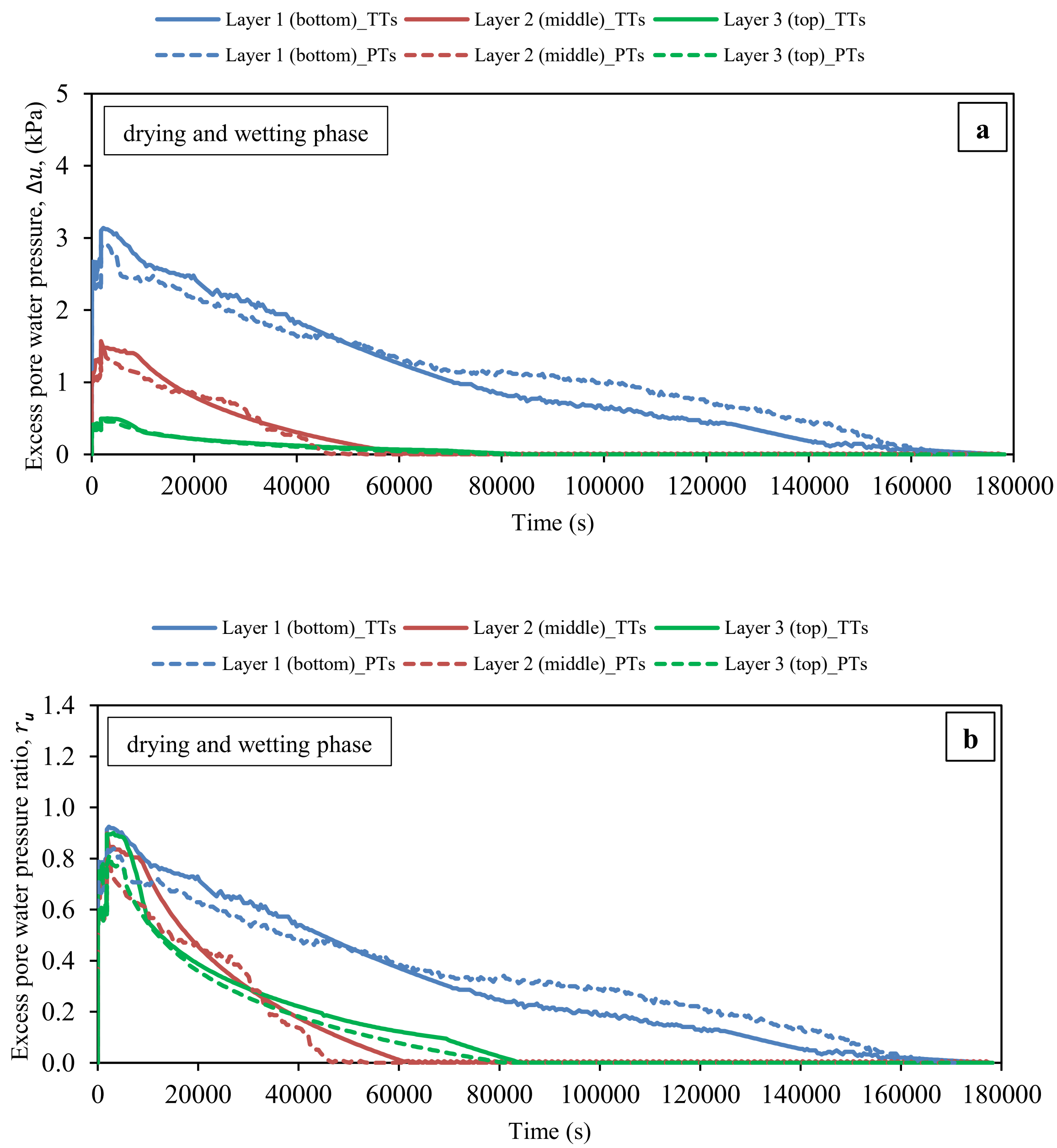


Figure 6.4. Time histories of excess pore water pressures at the middle depth of each layer of the thickened (TTs) and paste (PTs) tailings deposits during and after shaking. a) Measured excess pore water pressures ($\Delta u$). b) Excess pore water pressure ratios ($r_u$)

## 6.5. Comparison of the behaviour and liquefaction response of the highly densified tailings with those of slurry tailings

A comparison of the behaviour and the liquefaction response of highly densified tailings (tests performed for this research) with those of slurry tailings (tests performed by Pepin et al. [2012a, b]) is discussed in this section; however, before discussing this comparison, general background information related to the slurry and highly densified tailings (i.e. thickened and paste tailings) is presented to provide a general overview of these terms.

i. *Slurry tailings*

Tailings are the waste materials that remain after the extraction of valuable minerals from ore. Tailings are deposited hydraulically in slurry form in a loose state in a structure called a tailings dam (Hassani et al., 2008; Wu et al., 2012; Fall et al., 2010, 2013; Paul and Azam 2013; Ahmed and Siddiqua 2014; Zhang et al., 2015; KCB, 2017). It has been reported that about 90% of Canadian mines are handling their tailings in slurry form, which are deposited in conventional tailing facilities (KCB, 2017). Slurry tailings might still experience liquefaction for a significant time after deposition, although they slowly gain strength after deposition (Daliri, 2013; Seidalinova, 2014). Slurry tailings discharge from mills with high water contents and solid contents that range between 20% and 50% ((KCB, 2017; Daliri, 2013; Seidalinova, 2014). The failure of tailing dams may occur as a result of such high-water content in slurry tailings (Daliri, 2013; Seidalinova, 2014). The slurry tailings are usually transported from a mill to a storage area in a pressurized pipe, where a minimal velocity is usually essential to avoid the accumulation of fines in the pipe invert (Mizani, 2010). In general, slurry tailings experience grain size segregation during deposition in which coarse particles settle closer to the point of deposition while fine particles settle further away (Daliri, 2013; Seidalinova, 2014). Typically, slurry tailing deposits have beach slopes of less than 1% (Vick, 1990).

ii. *Thickened tailings*

Thickened tailings are dense, viscous mixtures of tailings and water and are not completely exposed to the process of dewatering (Davies and Rice, 2001; Edraki et al., 2014). Thickened tailings were introduced by Robinsky in 1975, where their first implementation was at the Kidd Creek Mine facility in Ontario, Canada. Thickened tailings can generally be produced by sending slurry tailings to compression thickeners or a combination of thickeners and filter presses (Engels, 2002). Accordingly, the solid content in these produced thickened tailings ranges between 50% and 70% with a yield stress of between 30 and 100 Pa (Bussière, 2007; Hamade, 2013; Sofrá, 2017). Indeed, thickened tailings are discharged from the spigot to form stacks at a gentle slope ranging from 2 to 6% (Robinsky et al., 1991). Unlike slurry tailings, thickened tailings do not experience grain size segregation upon deposition due to the homogenous behaviour of thickened tailings with low permeability (Robinsky et al., 1991; Bussière, 2007). Thickened tailings can significantly reduce the risk associated with the geotechnical instability of dams as no dam construction is needed and no pond of water is formed (Bussière, 2007). Thin layer deposition improves the geotechnical properties of thickened tailings (Bussière, 2007).

iii. *Paste tailings*

Paste tailings can be defined as dewatered slurry tailings that when pumped will not have a critical flow velocity. After deposition, they will not experience grain size segregation, and when discharged into the earth surface, they will not produce a significant amount of bleed water (Theriault et al., 2003). Moreover, paste tailings are a dense, viscous mixture of tailings and water with a consistency similar to that of wet concrete and must contain at least 15% by weight passing a 20 µm to attain a flowable paste material. They should also have sufficient colloidal water to form a mixture with no grain size segregation (Verburg, 2001; Haruna and Fall, 2020). The first mine in the world that implemented the concept of surface paste tailings was the Bulyanhulu gold mine in

Tanzania (Theriault et al., 2003). Paste tailings can be produced by sending slurry tailings to high-density thickeners and/or filters; thereby, the solid content and yield stress of this produced paste range from 70 to 85% and from 100 to 1000 Pa, respectively (Meggyes and Debreczeni, 2006; Bussière, 2007). This means that paste tailings have a higher solid content and yield stress compared to slurry and thickened tailings. Positive displacement pumps are required to transport the paste tailings to the disposal area (Theriault et al., 2003). The flow of paste tailings rests at a beach slope that typically ranges from 3° to 10° (Theriault et al., 2003). Significantly, paste tailings can reduce the risk associated with tailing dam failures, and the construction of a dam is not required (Bussière, 2007). Similar to thickened tailings, thin layer deposition improves the geotechnical properties of paste tailings (Bussière, 2007).

The thickened and paste tailings used for this research were prepared by mixing 10% of natural tailings and 90% of industrial silica tailings with municipal water. The usage of these types of tailings together as a mixture permitted the accurate control of the mineralogical and chemical compositions of the tailings materials, thus reducing uncertainties in the test results obtained to a minimal level. Figure 6.5 illustrates the grain size distribution of the highly densified tailings (i.e. thickened and paste tailings) used for this research. According to the experimental work, the thickened and paste tailings were non-plastic and could be classified as sandy silts of low plasticity corresponding to ML in the Unified Soil Classification System (USCS). The thickened and paste tailings with a sample height of 450 mm were deposited in a flexible laminar shear box (FLSB) (Figure 6.6) to form a 5.6% slope. Using the shaking table with one dimension of horizontal movement, these deposited thickened and paste tailings) were then subjected to sinusoidal loading with a frequency of 1 Hz and a peak horizontal acceleration of 0.13g for a duration of 1800 seconds.

The type of tailings tested by Pépin et al. (2012a, 2012b) was slurry tailings (natural tailings). Figure 6.5 illustrates the grain size distribution of the slurry tailings used in the research of Pépin et al. (2012a, 2012b), which was somewhat similar to the highly densified tailings (i.e. thickened and paste tailings) used for this research. Based on the Unified Soil Classification System (USCS), the slurry tailings used by Pépin et al. (2012a, 2012b) were classified as non-plastic silt (ML). The slurry tailings with an average sample height of 500 mm were deposited in a rigid box (Figure 6.7). Using the shaking table with one dimension of horizontal movement, the slurry tailings were then subjected to sinusoidal loading with a frequency of 1 Hz and a peak horizontal acceleration of 0.12g for a duration of approximately 1000 seconds.

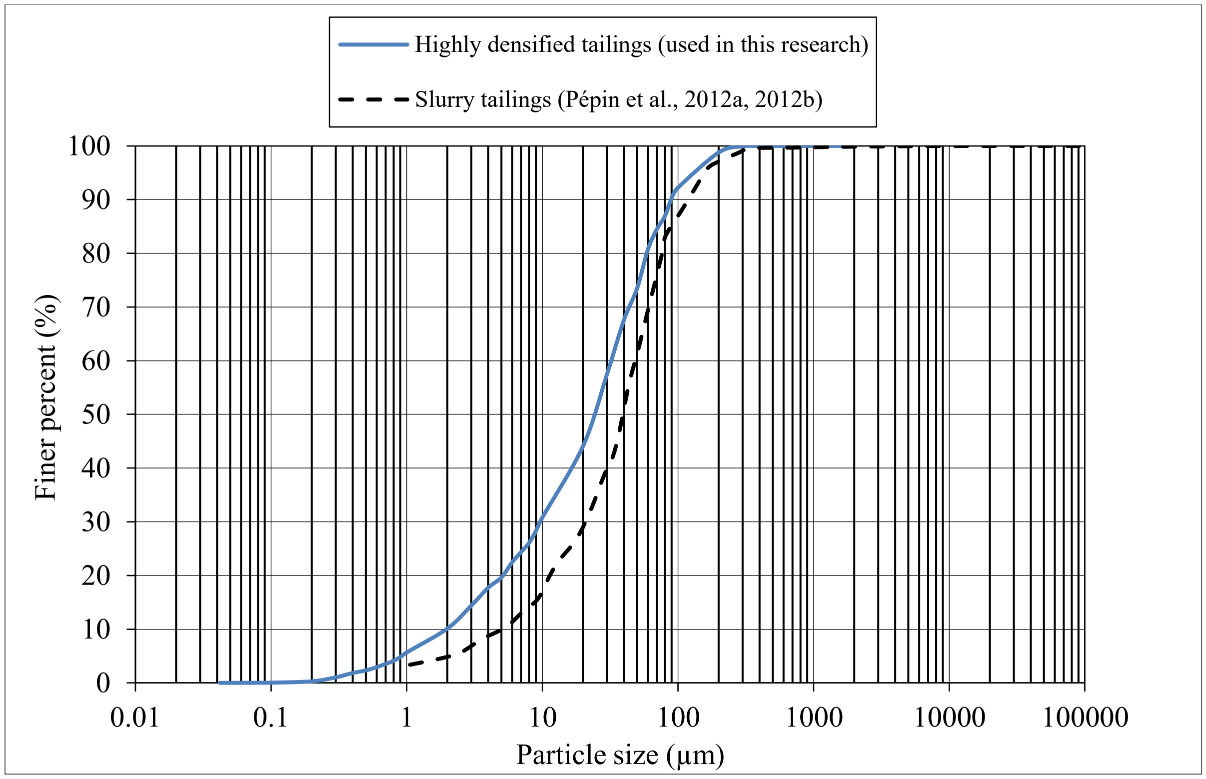


Figure 6.5. Grain size distribution of the highly densified tailings used in this research compared with the slurry tailings


Figure 6.6. Photo of the flexible laminar shear box (FLSB) used in this research

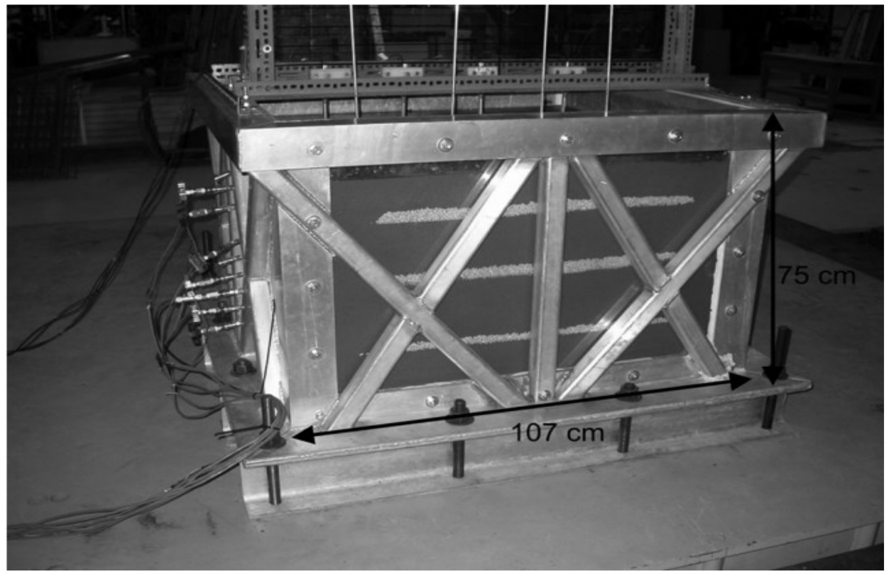


Figure 6.7. Photo of the rigid box used in the research of Pépin et al. (2012a, 2012b)

The comparison of the behaviour and liquefaction response of the highly densified tailings (i.e. thickened and paste tailings) with those of the slurry tailings is based mainly on the pore pressure-based criteria (i.e., $r_u$ = $\Delta u/\sigma'_{vo}$). In general, an excess pore water pressure ratio ($r_u$) of 1.0 indicates complete liquefaction. It should be noted that the highly densified tailings (i.e. thickened and paste tailings) and the slurry tailings can be subjected to liquefaction when their excess pore water pressure ratio ($r_u$) ≥ 0.9, which was considered in this research. This section only focuses on comparing the excess pore water pressure ratio ($r_u$) of the highly densified tailings (i.e. thickened and paste tailings) at a depth of 375 mm (i.e. about the middle depth of the bottom layer) with that of slurry tailings at a depth of 391 mm (tests performed by Pepin et al. [2012a, b]) during and after shaking, as illustrated in Figures 6.8 and 6.9.

For the thickened, paste, and slurry tailings during shaking, the maximum values of the excess pore water pressure ratio ($r_u$) were approximately 1.0, 0.83, and 0.92 respectively, as illustrated in Figure 6.8. These observations indicated that both the thickened and slurry tailings are potentially liquefiable materials during the applied cyclic loading conditions in this research and in the research of Pepin et al. (2012a, b); however, the paste tailings did not liquefy during the applied cyclic loading conditions during this study. This suggests that the paste tailings had more resistance to liquefaction compared to the thickened and slurry tailings due to the higher level of dewatering or densification experienced by the paste tailings compared to the thickened and slurry tailings. Indeed, the higher effective stress (i.e. higher shear strength) in the paste tailings compared to the thickened and slurry tailings leads to a higher resistance to liquefaction during cyclic loading.

The thickened and slurry tailings required a duration of about 40 and 800 seconds to reach the liquefaction state (i.e. $r_u$ ≥ 0.9), respectively. This means that the thickened tailings reached the liquefaction state (i.e. $r_u$ ≥ 0.9) earlier compared to the slurry tailings. Because the input shaking loading conditions used (the peak horizontal acceleration [0.13g]) is different or higher than that used by Pepin et al. (2012a, b) (peak horizontal acceleration [0.12g]), the thickened tailings experienced a faster occurrence of liquefaction compared to the slurry tailings. Moreover, because the thickened tailings were deposited in a flexible laminar shear box while the slurry tailings were deposited in a rigid box, the thickened tailings experienced a faster occurrence of liquefaction compared to the slurry tailings. For example, Jafarian et al. (2020) stated that in saturated sand, lower values of excess pore water pressure were observed during shaking in a rigid box compared to a flexible laminar shear box. The flexible laminar shear box (FLSB) allows for the shear deformation of soils or tailings while providing sufficient confinement (Cheung et. al., 2013). This leads to a better simulation of the free-field boundary conditions when compared with the rigid box. Therefore, careful attention should be exercised when using the rigid box in shaking table studies to interpret the liquefaction results of tailings.

Once the shaking terminated, the excess pore water pressure ratios ($r_u$) of the thickened, paste, and slurry tailings were observed to be slightly increased at 1.20, 0.95, and 1.0, respectively (Figure 6.8). Accordingly, this reveals that the thickened, paste, and slurry tailings were subjected to post-shaking liquefaction ($r_u$ at liquefaction triggering ≥ 0.9 was considered in this research) under the considered testing condition for this current research and in the research of Pepin et al. (2012a, b). The assessment and comparison of post-shaking liquefaction in this section is not to determine that the thickened, paste, and slurry tailings can liquefy (a 1800-second long shaking duration was selected for this research, while a 1000-second long shaking duration was selected for the research of Pepin et al. [2012a, b]) but rather to gain valuable data and information regarding the development and validation of future constitutive models to describe and to predict the seismic behaviours of the thickened, paste, and slurry tailings. In comparison with the thickened and paste tailings, the slurry tailings required a shorter time to return to the hydrostatic conditions ($r_u = 0$), as illustrated in Figure 6.9. The higher permeability of the slurry tailings compared with the thickened and paste tailings is attributed to this short time required to return to the hydrostatic conditions ($r_u = 0$). Based on the aforementioned comparison and discussion, it can be concluded that the densification of the tailings in terms of the paste tailings contributes to increasing the liquefaction resistance of tailings.

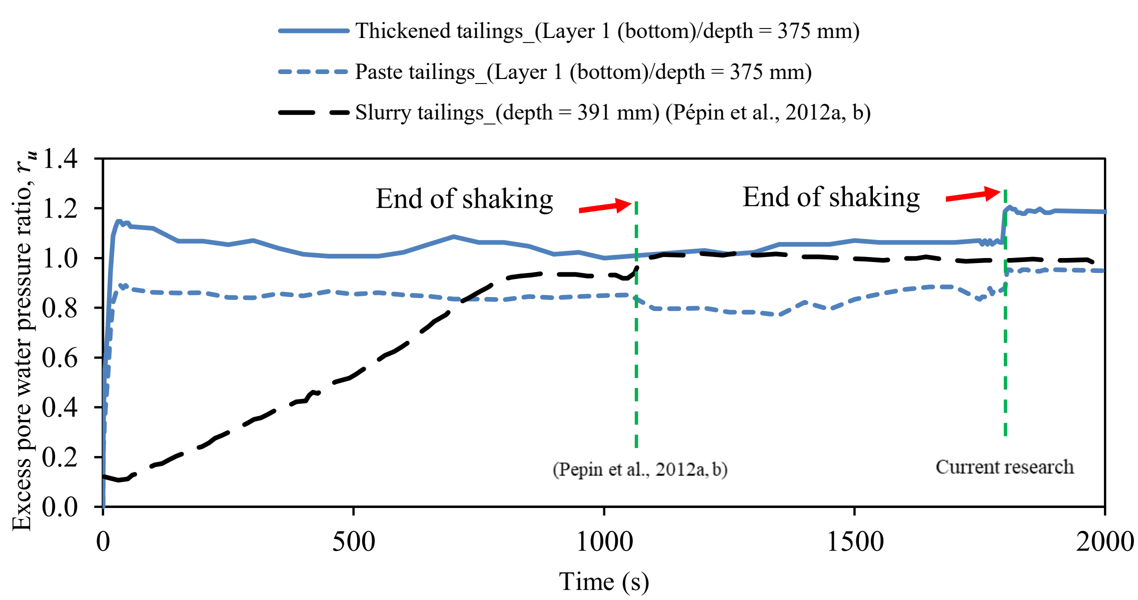


Figure 6.8. Time histories of excess pore water pressure ratios ($r_u$) of the thickened, paste and slurry tailings during shaking

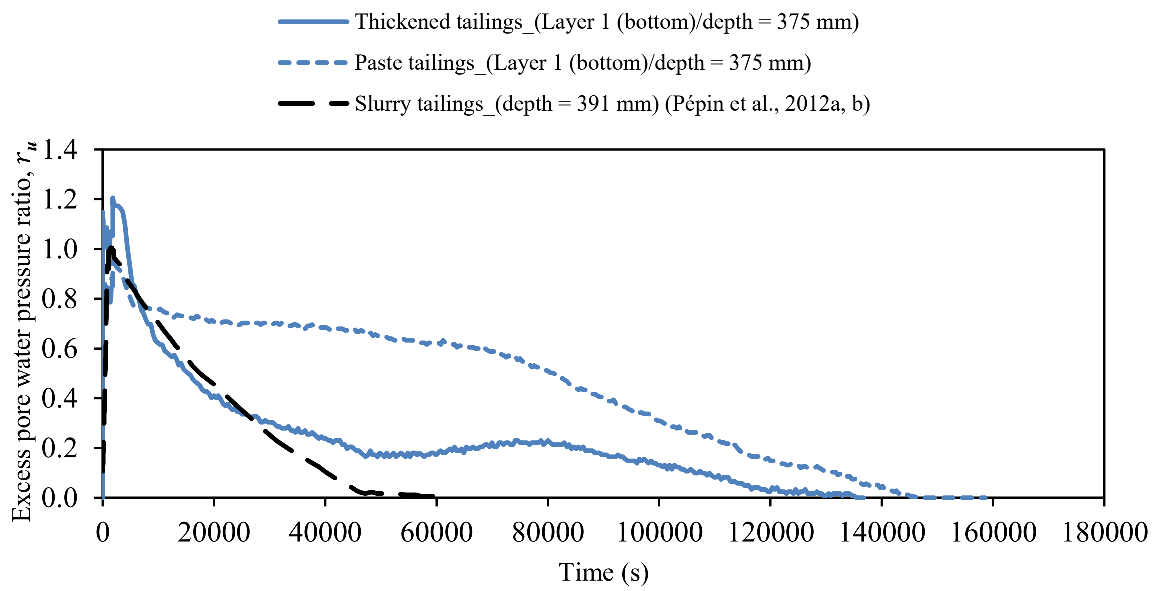


Figure 6.9. Time histories of excess pore water pressure ratios ($r_u$) of the thickened, paste and slurry tailings during and after shaking

## 6.6. **References**


Ahmed, S.I., and Siddiqua, S. (2014). A review on consolidation behavior of tailings. International Journal of Geotechnical Engineering, 8(1): 102-111.

Bussière, B. (2007). Colloquium 2004: hydrogeotechnical properties of hard rock tailings from metal mines and emerging geoenvironmental disposal approaches. Canadian Geotechnical Journal, 44(9): 1019-1052.

Carter, D.P. (1988). Liquefaction potential of sand deposits under low levels of excitation. PhD thesis, Department of Civil and Environmental Engineering, University of California, Berkeley, California, USA.

Cheung, W.M., Qin, X., Chouw, N., Larkin, T., and Orense, R. (2013). Experimental and numerical study of soil response in a laminar box. In Proceedings of the Annual New Zealand Society for Earthquake Engineering Conference, 26-28 April 2013, Wellington, New Zealand, pp. 1-7.

Daliri, F. (2013). The influence of desiccation and stress history on monotonic and cyclic shear response of thickened gold tailings. PhD thesis, Department of Civil and Environmental Engineering, Carleton University, Ottawa, Ontario, Canada.

Davies, M.P., and Rice, S. (2001). An alternative to conventional tailings management- "dry stack" filtered tailings. In Proceedings of the 8th International Conference on Tailings and Mine Waste '01, 15-18 January 2001, Fort Collins, Colorado, USA, pp. 411-420.

Edraki, M., Baumgartl, T., Manlapig, E., Bradshaw, D., Franks, D.M., and Moran, C.J. (2014). Designing mine tailings for better environmental, social and economic outcomes: a review of alternative approaches. Journal of Cleaner Production, 84: 411-420.

Engels, J. (2002). Beach Slope Prediction Methods. See http://www.tailings.info/technical/beach-slope.htm [accessed December 20, 2017].

Fall, M., Célestin, J.C., and Han, F.S. (2013). Suitability of bentonite-paste tailings mixtures as engineering barrier material for mine waste containment facilities. Minerals Engineering, 22(9-10): 840-848.

Fall, M., Célestin, J.C., Pokharel, M., and Touré, M. (2010). A contribution to understanding the effects of temperature on the mechanical properties of cemented mine backfill. Engineering Geology, 114(3-4): 397-413.

Geremew, A.M., and Yanful, E.K. (2013). Dynamic properties and influence of clay mineralogy types on the cyclic strength of mine tailings. International Journal of Geomechanics, ASCE, 13(4): 441-453.

Hamade, T. (2013). Geotechnical design of tailings dams-a stochastic analysis approach. PhD thesis, Department of Mining and Materials Engineering, McGill University, Montreal, Quebec, Canada.

Haruna, S., and Fall, M. (2020). Time-and temperature-dependent rheological properties of cemented paste backfill that contains superplasticizer. Powder Technology, 360: 731-740.

Hassani, F., Mantegh, A., Mohamed, A-M., and Ouellet, J. (2008). Evaluation of flow liquefaction in fine grained tailings using elastic wave velocities. International Journal of Geotechnical Engineering, 2(3): 169-178.

Ishihara, K., Yasuda, S., and Yokota, K. (1981). Cyclic strength of undisturbed mine tailings. In Proceedings of the First International Conference on Recent Advances in Geotechnical Earthquake Engineering and Soil Dynamics, 26 April - 3 May 1981, St. Louis, Missouri, USA, Vol. 1, pp. 53-58.

Jafarian, Y., Taghavizade, H., Rouhi, S., Shojaemehr, S., and Esmaeilpour, P. (2020). Shaking table experiments to evaluate the boundary effects on seismic response of saturated and dry sands in level ground condition. International Journal of Civil Engineering, 18(7): 783-795.

James, M., Jolette, D., Aubertin, M., and Bussière, B. (2003). An experimental set-up to investigate tailings liquefaction and control measures. In Proceedings of the International Symposium on Major Challenges in Tailings Dams (ICOLD), 15 June 2003, Montréal, Quebec, Canada, pp. 153-164.

KCB (Klohn Crippen Berger). (2017). Study of tailings management technologies. MEND Report 2.50.1, pp. 1-164.

Lu, G., and Fall, M. (2018). Simulation of blast induced liquefaction susceptibility of subsurface fill mass. Geotechnical and Geological Engineering, 36(3): 1683-1706.

Meggyes, T., and Debreczeni, Á. (2006). Paste technology for tailings management. Land Contamination and Reclamation, 14(4): 815-827.

Mizani, S. (2010). Rheology of thickened gold tailings for surface deposition. Master thesis, Department of Civil and Environmental Engineering, Carleton University, Ottawa, Ontario, Canada.

Naesgaard, E., and Byrne, P.M. (2007). Flow liquefaction simulation using a combined effective stress–total stress model. In Proceedings of the 60th Canadian Geotechnical Conference, 21-24 October 2007, Ottawa, Ontario, Canada.

Paul, A.C., and Azam, S. (2013). Assessment of slurry consolidation using index properties. International Journal of Geotechnical Engineering, 7(1): 55-61.

Pépin, N., Aubertin, M., and James, M. (2012a). Seismic table investigation of the effect of inclusions on the cyclic behaviour of tailings. Canadian Geotechnical Journal, 49(4): 416-426.

Pépin, N., Aubertin, M., James, M., and Leclerc, M. (2012b). Seismic simulator testing to investigate the cyclic behaviour of tailings in an instrumented rigid box. Geotechnical Testing Journal, 35(3): 469-479.

Robinsky, E., Barbour, S.L., Wilson, G.W., Bordin, D., and Fredlund, D.G. (1991). Thickened sloped tailings disposal–an evaluation of seepage and abatement of acid drainage. In Proceedings of the Second International Conference on the Abatement of Acidic Drainage, Invited Lecture, 16-18 September 1991, Montreal, Quebec, Canada, pp. 529-549.

Robinsky, E.I. (1975). Thickened discharge-a new approach to tailings disposal. Canadian Mining and Metallurgical Bulletin, 68(764): 47-53.

Roshani, A., Fall, M., and Kennedy, K. (2017). Drying behaviour of mature fine tailings pre-dewatered with super absorbent polymer: column experiments. ASTM Geotechnical Testing Journal, 40(2): 210-220.

Seidalinova, A. (2014). Monotonic and cyclic shear loading response of fine-grained gold tailings. Master thesis, The University of British Columbia, Vancouver, British Columbia, Canada.

Serafini, D.C., and Perlea, V. (2010). Comparison of liquefaction triggering analysis approaches for an embankment dam and foundation. In Proceedings of the 5th International Conference on Recent Advances in Geotechnical Earthquake Engineering and Soil Dynamics, 24-29 May 2010, San Diego, California, USA, paper No. 4.12b.

Sofrá, F. (2017). Rheological properties of fresh cemented paste tailings. Paste Tailings Management, Yilmaz, E., and Fall, M., Eds., Springer, Cham, Switzerland, pp. 33-57.

Theriault, J., Frostiak, J., and Welch, D. (2003). Surface disposal of paste tailings at the Bulyanhulu gold mine, Tanzania. In Proceedings of Mining and the Environment Conference III, 25-28 May 2003, Sudbury, Ontario, Canada, pp. 1-8.

Tuttle, M., Law, K.T., Seeber, L., and Jacob, K. (1990). Liquefaction and ground failure induced by the 1988 Saguenay, Quebec, earthquake. Canadian Geotechnical Journal, 27(5): 580-589.

Ueng, T.S., Wu, C.W., Cheng, H.W., and Chen, C.H. (2010). Settlements of saturated clean sand deposits in shaking table tests. Soil Dynamics and Earthquake Engineering, 30(1-2): 50-60.

Varghese, R.M., and Latha, G.M. (2013). Effect of overburden stress and surcharge pressure on the liquefaction response of sands. International Journal of Geotechnical Engineering, 7(4): 402-410.

Verburg, R.B.M. (2001). Use of paste technology for tailings disposal: potential environmental benefits and requirements for geochemical characterization. In Proceedings of the International Mine Water Association Symposium, 24-28 April 2001, Belo Horizonte, Brazil, pp. 1-13.

Vick, S.G. (1990). Planning, design and analysis of tailings dams. John Wiley & Sons, New York, USA.

Wang, J., Salam, S., and Xiao, M. (2020). Evaluation of the effects of shaking history on liquefaction and cone penetration resistance using shake table tests. Soil Dynamics and Earthquake Engineering, 131:106025.

Wu, D., Fall, M., and Cai, S. (2012). Coupled modeling of temperature distribution and evolution in cemented tailings backfill structures that contain mineral admixtures. Geotechnical and Geological Engineering, 30(4): 935-961.

Zhang, Q., Yin, G., Wei, Z., Fan, X., Wang, W., and Nie, W. (2015). An experimental study of the mechanical features of layered structures in dam tailings from macroscopic and microscopic points of view. Engineering Geology, 195: 142-154.

# 7 Chapter 7: Conclusions and Recommendations

The current research includes two key parts; namely, the testing of the geotechnical response of layered thickened and paste tailings to cyclic loadings and the evaluation of drying-rainfall induced changes in geotechnical responses of layered highly densified tailings (thickened and paste tailings) to cyclic loadings. This chapter covers the main conclusions from investigations performed on the testing of the geotechnical response of the layered thickened and paste tailings, with and without the effect of heavy rainfall, to cyclic loadings as well as offers recommendations for future researches.

## 7.1. Conclusions

A series of experimental shaking table tests have been conducted in this PhD research in order to evaluate and predict the behaviour and liquefaction susceptibility of the layered thickened and paste tailings, with and without the effect of heavy rainfall, under cyclic loading conditions. The following conclusions can be derived based on the obtained experimental results.

1. The obtained shaking table results reveal that the response of accelerations at different depths of the layered thickened and paste tailings deposits, without heavy rainfall effect, is not identical in general during shaking. In addition, the accelerations at the bottom and middle layers follow the same pattern of that at the base of the shaking table. However, the acceleration at the top layer is, experience reduction as well as non-regularity, dissimilar to that of the base of the shaking table because of the decreasing in strength and stiffness of tailings at this layer.
2. In general, the response of horizontal displacements at different depths of the layered thickened and paste tailings deposits, with and without heavy rainfall effect, is fairly similar.
3. With and without heavy rainfall effect, the applied shaking leads to the water flow as well as pressure redistribution in the layered thickened and paste tailings deposits. Although the middle layer is impacted by water outflow, the bottom and top layers experience water inflow. Moreover, such water outflow and inflow play a key role in the response of the layered thickened and paste tailings deposits in terms of the parameters of excess pore water pressure, liquefaction, and vertical displacement.
4. Through the applied shaking, the excess pore water pressure at different depths of the layered thickened and paste tailings deposits (with and without the heavy rainfall effect) was generated rapidly until approaching a peak magnitude of excess pore water pressure. This generation was attributed to the contraction behaviour of these tailings. Furthermore, this generation or increase in excess pore water pressure was associated with the water inflow into the bottom and top layers. While shaking was applied, the excess pore water pressure ratios of the layered thickened tailings deposit not exposed to the effect of heavy rainfall prior to shaking were found to exceed 1.0. However, the excess pore water pressure ratios of the layered paste tailings deposit not exposed to heavy rainfall prior to shaking were found to be lower than 0.85 during shaking. This indicates that the layered thickened tailings deposit was susceptible to liquefaction, while the layered paste tailings deposit was resistant to liquefaction during shaking ($r_u$ at liquefaction triggering ≥ 0.9 is considered in this research). The excess pore water pressure ratios of the layered thickened and paste tailings deposits that were exposed to the effect of heavy rainfall prior to shaking were found to be lower than 0.8 during shaking. This indicates that the layered thickened and paste tailings deposits exposed to rainfall were resistant to liquefaction during shaking. As soon as the applied shaking stopped, the excess pore water pressure at different depths of the layered thickened and paste tailings deposits (with and without the heavy rainfall effect) was subjected to a sudden increase. This leads the excess pore water pressure ratios to somewhat exceed or approach unity in the layered thickened and

paste tailings deposits that were not exposed to the effect of heavy rainfall prior to shaking. Additionally, for the layered thickened and paste tailings deposits that were exposed to the effect of heavy rainfall prior to shaking, the excess pore water pressure ratios were found to be approximately within the range of 0.8–0.9. Accordingly, this indicates that the layered thickened and paste tailings deposits (not exposed to the effect of heavy rainfall prior to shaking) were susceptible to post-shaking liquefaction, while the layered thickened and paste tailings deposits (exposed to the effect of heavy rainfall prior to shaking) were not subjected to post-shaking liquefaction after the applied shaking. The sudden increase in the excess pore water pressure arose from two aspects: (i) the contraction behaviour of partially suspended tailings particles in generating further pore water pressure, and (ii) the migration of upward pore water to the top layer and downward pore water flow to the bottom layer, which generated further pore water pressure. The dissipation of the excess pore water pressure of the layered thickened and paste tailings deposits required a long duration of time, and this could be attributed to the low permeability of these tailings. Furthermore, the bottom layer of the thickened and paste tailings deposits needs a longer duration of time to wholly dissipate the excess pore water pressure compared with the top and middle layers because of the greater inflow of pore water.

5. According to the measurements of the vertical displacements during the applied shaking, the layered thickened and paste tailings deposits (with and without heavy rainfall effect) are found to be subject to both contraction and dilatation behaviours. Moreover, the contraction (settlement) behaviour is observed to be more noticeable at the top and middle layers than that at the bottom layer, which can be mainly attributed to the more water inflow into the bottom layer. Following the termination of the applied shaking, no significant change in the behaviour of the vertical displacements of these layered tailings deposits.

## 7.2. Recommendations

Although this PhD research has provided considerable technical information and data related to the cyclic behaviour and liquefaction susceptibility of the layered thickened and paste tailings deposits, there are still some questions that need to be answered. In this section, some recommendations, based on the obtained results of the thickened and paste tailings, are provided for future studies.

1. Effect of some aspects, such as different magnitudes of loading frequencies, different peak horizontal accelerations, different duration of shaking, different duration of drying (desiccation), different thicknesses of layer, different amount of beach slopes and rainfalls, on the seismic liquefaction behaviour of the layered thickened and paste tailings deposits needs to be studied using equipment of a greater scale (i.e., centrifugal or shaking table equipment).
2. Studying the response and liquefaction susceptibility of thickened and paste tailings, with or without heavy rainfalls, to real earthquake-induced seismic loadings was not the scope of this PhD research. Future study should address this technical aspect.
3. The findings in this research were based on a one-dimensional shaking table testing where it is recommended to conduct a two-dimensional shaking table testing in the future. This will provide insight into the liquefaction response of the layered thickened and paste tailings as well as a comparison regarding the one and two-dimensional shaking table testing.
4. It is a good idea to simulate the experimental results for other conditions by using numerical models that are considered very useful tools to predict the seismic liquefaction behaviour of tailings.
5. A novel alternative disposal approaches, such as co-disposal with waste rock, might be considered in order to improve the performance of geotechnical and environmental of surface thickened and paste tailings, particularly in areas with seismic activities and extreme daily rainfall (heavy rainfall).

6. Additives materials such as cement or fly ash can be added to the thicketed and paste tailings to enhance their performance, with and without the effect of heavy rainfall, under seismic loading conditions.